# Singularity formation, existence and regularity for degenerate Cahn-Hilliard equations




Catalina Leticia Pesce Reyes

St Hilda's College

University of Oxford

A thesis submitted for the degree of

*Doctor of Philosophy*

Trinity 2022

# Acknowledgements

This thesis is dedicated to all those who made this work possible. In particular, I want to thank my family for giving me a piece of home every time we talked on the phone. Thanks to Ian, my fiancé, for being there through the good and bad, and for going halfway across the world with me to chase our dreams together. You are my emotional support golden retriever and I love you.

Special thanks to one of my best friends, Maria, just for being herself. I never thought I would find family far from home, but you proved me wrong. Thanks to my Maths friends: Vicki, Eliana, Jeremy and Tommaso. There is no one I would rather party with than you. Vicki and Eliana: you are both amazing (do not forget it!) and a constant source of inspiration to me. And thanks to Brandon Sanderson, one of my favourite authors, for his books. They helped pick me up when the research was not going my way.

In addition, I want to thank Prof. Münch and Prof. Novick-Cohen, as my supervisors, for their continued guidance and patience. Thanks to my examiners, Prof. Süli and Prof. Witelski, who have spent time and effort reading my work. Particularly, I would like to thank Prof. Süli and Prof. Howell for their useful suggestions, which became part of this thesis.

Thank you to all those friends and colleagues, here and there, that have been through this experience with me.

This work was supported by the EPSRC grant EP/L015811/1 and the Chilean National Agency for Research and Development (ANID) / Scholarship Program / DOCTORADO BECAS CHILE / 2018 - 72190029.

# Abstract

Cahn-Hilliard models are central for describing the evolution of interfaces in phase separation processes and free boundary problems. In general, they have non-constant and often degenerate mobilities. However, in the latter case, the spontaneous appearance of regions of vanishing mobility and their impact on the solution are not well understood. In this work, we study the axially symmetric 2-dimensional setting, namely

$$\partial_t u = \frac{1}{r}\partial_r \left( rM(u)\partial_r \left( -\frac{\varepsilon^2}{r}\partial_r \left( r\partial_r u \right) + f'(u) \right) \right),$$

where $f(u) := \frac{(1-u^2)^2}{2}$ and $M(u) := (1-u^2)_+^n$, and develop a singular perturbation theory to identify a range of degenerate mobilities $M$ for which the solution forms a singularity $|u| \to 1$ in infinite time. Moreover, we obtain two different approximate self-similar profiles which divide this range of degeneracies into $\frac{1}{2} < n < 2$ and $2 < n$. We complement this approach by adapting the known theory for degenerate parabolic partial differential equations and Sobolev spaces of radial functions to obtain the existence and regularity of a weak radially symmetric solution. This is an improvement from the weak existence for the degenerate Cahn-Hilliard equation obtained previously in [32], which does not ensure symmetry. Finally, we raise conjectures on the strict boundedness of the solution $|u| < 1$ for $n$ sufficiently large, which would restrict the formation of singularities.

# Contents


**1 Introduction** **1**

**2 Problem formulation** **19**

**3 Preliminary numerical results** **24**

**4 Case $n > 2$** **33**

4.1 Numerical results . . . . . 33

4.1.1 Central region . . . . . 34

4.1.2 Touchdown region . . . . . 38

4.2 Long-time asymptotic analysis . . . . . 42

4.2.1 Central region . . . . . 44

4.2.2 Touchdown region . . . . . 47

4.2.3 Annular region . . . . . 49

4.2.4 Matching . . . . . 53

4.3 Solution in the touchdown region . . . . . 61

4.4 Composite expansion and comparison with numerical results . . . . . 64

**5 Case $n < 2$** **68**

5.1 Numerical Results . . . . . 69

5.1.1 Central region . . . . . 69

5.1.2 Touchdown region . . . . . 73

5.2 Long-time asymptotic expansion . . . 75
5.2.1 Central region . . . 76
5.2.2 Central region: Another method . . . 89
5.2.3 Central region comparison with case $n > 2$ . . . 96
5.2.4 Touchdown region . . . 100
5.2.5 Matching . . . 108
5.3 Solution in the central region . . . 111
5.4 Solution in the touchdown region . . . 113
5.5 Composite expansion and comparison with numerical results . . . 119

**6 Existence and regularity of solutions 122**
6.1 Sobolev spaces of radial functions . . . 125
6.2 Existence and regularity for positive mobilities . . . 129
6.3 Existence and regularity for degenerate mobilities . . . 145

**7 Conclusion 161**

**A Stationary solutions 168**
A.1 Small energy problem . . . 168
A.2 Free boundary problem . . . 170

**B Numerical Method 174**
B.1 Numerical scheme convergence . . . 176
B.2 Initial condition change . . . 178
B.3 Conservation of mass . . . 181
B.4 Epsilon . . . 182
B.5 Grid spacing convergence study . . . 184
B.6 Time tolerance . . . 184
B.7 Comparison with free boundary expansion . . . 184

**C Frobenius method for fourth order ODEs** **188**

**Bibliography** **196**

# Chapter 1

# Introduction

When a binary alloy in a homogeneous state is quenched below its critical temperature, it will decompose into a configuration with two phases, each having a different relative concentration of the two constitutive species, characterised by values between, e.g. $-1$ and $+1$ (after a suitable normalisation). In the simplest case, the process will naturally proceed through two dominant regimes: an initial phase separation stage and a later coarsening stage. During the initial separation, the alloy will rapidly divide into regions with concentrations near $\pm 1$ separated by a diffuse interface, forming a transitional configuration. There are two typical ways in which this can happen: spinodal decomposition or nucleation and growth. In spinodal decomposition, infinitesimal fluctuations between phases will grow spontaneously and exponentially, while in nucleation and growth only perturbations that are above the energetic activation barrier, which is a finite quantity, will grow. Even though these mechanisms are different, they both lead to the formation of patterns, which locally minimise the free energy of the system. The overall shape of the pattern will typically depend on the initial concentration. If the average volume fraction of the two species in the alloy is roughly the same, known as a critical mixture, then the system will separate into mostly connected regions with intricate shapes, see for example the review in [62]; if

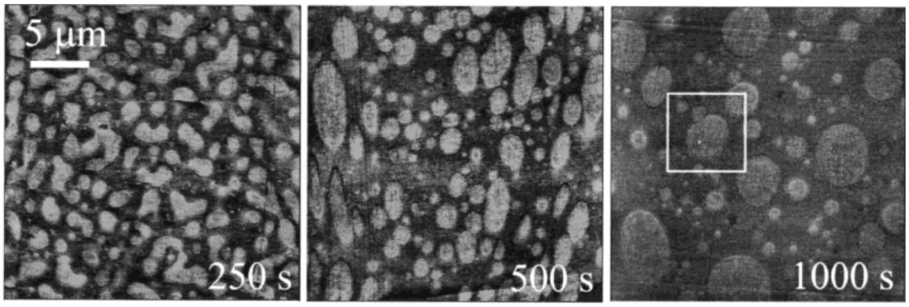



Figure 1.1: Coarsening of an off-critical blend of polymers TMPC/PS at ratio 70/30, annealed at 265°C (deep quench) imaged by $25 \times 25\ \mu m^2$ topography scans with 30 $nm$ height range, for different times. Reprinted with permission from [18]. Copyright 2002 American Chemical Society.

instead one species dominates in volume, called off-critical mixture, then the system evolves into a matrix of small diffuse droplets of one phase surrounded by the other, see [61]. Independently of the shape of the pattern, the outcome of the early phase separation is a domain that has been divided into several regions, each near one of the limit concentrations $\pm 1$, that are separated by diffuse interfacial layers where the concentration changes rapidly but continuously.

The subsequent dynamics are driven by the coarsening of each phase. This is a much slower process in which the geometric configuration becomes increasingly simpler converging to volumes of minimal interface surface area. In each phase, small domains will supply material to larger ones until they have been completely dissipated. This should continue, at least theoretically, until equilibrium is achieved, i.e. when there are typically two pure state regions left, separated by a diffuse interface. This final outcome is rarely seen in physical experiments since coarsening can take a long time. Figure 1.1 shows an experiment done in [18], in which we see the evolution of an off-critical mixture going through coarsening at different times.

A widely used model for spinodal decomposition and coarsening is the Cahn-Hilliard equation. Its stationary version was first derived, using thermodynamics, by Cahn and Hilliard as a way to describe the energy minimisation of a nonuniform system [21]. It was then noted by Cahn [19] that, by introducing time evolution, it

could be used to model spinodal decomposition. A thermodynamical derivation of the equation, as we know it now, was done much later by Gurtin [39]. The Cahn-Hilliard equation has been derived in many different ways through the years, for example, as a gradient flow, as a stochastic problem and even as the singular limit of other phase-field systems, see the reviews [50, 52]. This underscores how important the equation has become, not only in mathematics but in physics and material science.

To introduce the equation we let $N \geq 1$ be the dimension of the spatial domain. Note that, although $N = 2, 3$ are the most physically relevant, we use a general $N \geq 1$ so that we can state more general results from the literature. Let $\Omega \subset \mathbb{R}^N$ be a convex bounded domain representing the region occupied by the alloy, with boundary $\partial\Omega \in C^{1,1}$. Let $x \in \Omega$ be the spatial variable, $t \in \mathbb{R}_+$ the time variable, $\varepsilon > 0$ a small parameter that is related to the width of the diffuse interface during coarsening, and let $u = u(x,t)$ be the order parameter representing a normalised difference between phase concentrations, so that $u = 1$ and $u = -1$ correspond to the two pure states. We say that $u$ satisfies the Cahn-Hilliard equation if

$$\partial_t u = -\nabla \cdot \mathbf{j}, \qquad \text{in } \Omega \times (0, \infty), \tag{1.1}$$

where $\mathbf{j}$, the flux, is defined as

$$\mathbf{j} = -M(u)\nabla\mu, \tag{1.2}$$

and the chemical potential $\mu$ is given by

$$\mu = -\varepsilon^2 \Delta u + f'(u). \tag{1.3}$$

Here, $f(u)$ is the homogeneous part of the free energy of the system and $M(u)$ is the mobility, which reflects how easily the atoms or molecules of the material can move.

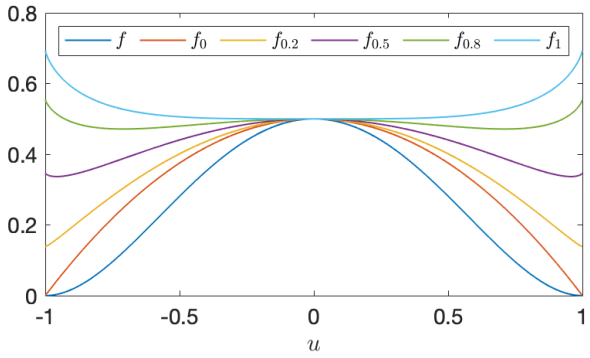



Figure 1.2: Homogeneous free energies $f$ and $f_\theta$ versus $u$ for $\theta = 0,\ 0.2,\ 0.5,\ 0.8,\ 1$.

We will also use Neumann and no-flux boundary conditions, plus an initial condition $u_{init}(x)$, i.e.

$$\nabla u \cdot \mathbf{n} = 0, \qquad \text{on } \partial\Omega \times (0, \infty), \tag{1.4}$$

$$\mathbf{j} \cdot \mathbf{n} = 0, \qquad \text{on } \partial\Omega \times (0, \infty), \tag{1.5}$$

$$u = u_{init}, \qquad \text{on } \Omega \times \{0\} \tag{1.6}$$

where $\mathbf{n}(x)$ is the unit outward normal at the point $x \in \partial\Omega$.

In the literature, the most common choices for the homogeneous free energy are

$$f_\theta(u) := \begin{cases} \frac{\theta}{2}(1-u)\ln(1-u) + \frac{\theta}{2}(1+u)\ln(1+u) + \frac{(1-u^2)}{2}, & \text{for } |u| \le 1 \\ +\infty, & \text{for } |u| > 1 \end{cases}, \tag{1.7}$$

$$f(u) := \frac{(1-u^2)^2}{2}, \tag{1.8}$$

where $\theta \ge 0$ is the normalised temperature of the system and its critical temperature is $\theta_c = 1$. As can be seen in Figure 1.2, for $\theta \ge 1$ the logarithmic free energy (1.7) is smooth and in the interval where it has physical meaning, i.e. $u \in [-1, 1]$, it has a single minimum at $u = 0$. In contrast, for $0 < \theta < 1$, the same energy has two distinct local minima at points $u_\pm := \pm(1 - R(\theta))$, where $R(\theta) \to 0$ as $\theta \to 0$, so that

in the deep quench limit $\theta \to 0$ the minima are achieved at $u_\pm = \pm 1$. The logarithmic terms in the free energy (1.7) arise naturally when deriving the equation using the thermodynamic entropy [19, 21], and it is one of the most widely used energies in the literature.

For the mobility $M(u) = (1 - u^2)$ it is known that the shallow quench limit (i.e. taking the temperature as $\theta \to 1^-$) under an appropriate rescaling is formally the Cahn-Hilliard equation with the quartic polynomial free energy (1.8) and $M(u) = c$, with $c > 0$ constant, see [44]. Thus, a common approach in the literature, see for example [57], is to approximate the logarithmic free energy by the quartic polynomial one. Despite this, the two physical situations are somewhat different. Before scaling and taking the shallow quench limit, the minima of the homogeneous free energy are at $u_\pm$ and the pure phases at $\pm 1$. However, afterwards, the pure phases go to $\pm\infty$ as $\theta \to 1^-$ and the minima of the homogeneous free energy, which is now the quartic polynomial, are at $u = \pm 1$. This means that the new minimal states do not represent the pure phases and thus, are not the ones of the original model, but instead, represent a system that has clearly separated into two distinct types of regions with high or low concentration of one of the phases. This gives physical meaning to concentrations outside $[-1, 1]$ in conjunction with the polynomial free energy (1.8).

Similarly, several types of mobilities have been used to model spinodal decomposition and coarsening. The most relevant are the constant mobility

$$M_0(u) := 1,$$

and the two-sided nonlinear mobility

$$M_n(u) := [(1 - u^2)_+]^n, \tag{1.9}$$

where $()_+$ denotes the positive part, that degenerates at $u = \pm 1$. Here, $n \geq 0$ is

a parameter which we call the degree of degeneracy and $n = 0$ coincides with the constant case. Other variants are also considered in the literature, for example, the one-sided degenerate mobility $M(u) = (1 + u)$ has been used to suppress diffusion to the phase $u = -1$ in [25], the two-sided mobility $M(u) = |1 - u^2|$ has been used to allow solutions with support outside $[-1, 1]$ in [28, 27], and $M(u) = (1 - u^2)$ (which may assume negative values) has been used in coarsening rate studies [44].

With the use of different mobilities and homogeneous free energies, Cahn-Hilliard equations can model a wide range of applications. A common example is pattern formation in biology [54, 55], while more specific instances, in which the quartic polynomial free energy $f$ and the degenerate mobility $M_n$ (for $n = 1, 2$) are used directly (instead of as an approximation of $f_\theta$) to model interface motion and surface tension, are: electromigration in metals [51], heteroepitaxial growth [63], anisotropic fields [67, 68] and phase separation of polymer mixtures [69, 71]. A long list of applications in physics, chemistry and engineering can be found in [50, 49].

For the constant mobility and polynomial free energy, a proof of existence and uniqueness was given by Elliott and Songmu [33]. Later, Elliott and Garcke [32] proved the existence of weak solutions for the degenerate Cahn-Hilliard equation with a general form of free energy and mobility, which includes (1.9) and both homogeneous free energies (1.7) and (1.8). In addition, Elliott and Garcke showed that for bounded initial conditions, namely $|u_{init}| \leq 1$, their weak solution remains inside $[-1, 1]$ for all finite times. In a recent paper, Jihui and Shu [42] improved slightly on the regularity obtained by Elliott and Garcke by strengthening the assumptions on the free homogeneous energy and choosing the specific mobility $M(u) = u^n(1 - u)^n$. These results do not ensure that all solutions to (1.1)-(1.5) with quartic polynomial free energy (1.8) and mobility (1.9) will remain strictly bounded inside $[-1, 1]$, i.e. $|u(x, t)| < 1$ for all $(x, t) \in \Omega \times [0, T]$. Moreover, one could have bounded and non-bounded solutions since non-uniqueness is known to occur for initial value problems

of high order degenerate parabolic partial differential equations, particularly in the context of Cahn-Hilliard and thin film equations, see for example [30, 6]. In addition, for the quartic polynomial potential, mobility $M(u) = |1 - u^2|^n$ with $n > 0$ and starting from an initial condition that is not necessarily bounded within $[-1, 1]$, Dai and Du [28] proved the existence of a weak solution that allows the Gibbs-Thomson effect to occur. This effect, which is a physical result of the bulk free energy caused by the curvature of an interface under tension, is also seen in the stationary case [56] and an important consequence in the present context is that solutions that satisfy it do not necessarily stay bounded inside $[-1, 1]$. In fact, in a computational study, Dai and Du [27] found a numerical solution that, for mobility $M(u) = |1 - u^2|$ and initial profile bounded in $[-1, 1]$, escapes the interval in finite time, evolving into a solution with non-empty set $\{x \in \Omega : M(u(x)) = 0 \text{ and } u(x) > 1\}$.

As it may be guessed from the previous paragraph, one of the most interesting features of Cahn-Hilliard equations is that, while a different mobility does not change the energy landscape, it can strongly affect the kinetics of the process. For constant mobility, for example, the flux $\boldsymbol{j}$ only depends on the gradient of the chemical potential $\mu$ and thus it can freely transport material in the direction of decreasing $\mu$. In contrast, nonlinear mobilities that degenerate at or near the minima of the homogeneous free energy, which is the case for (1.8) and (1.7) in the deep quench limit, reduce or suppress that transport. The differences due to changes in the mobility are extremely important when understanding the kinetics of phase separation, coarsening and their limiting behaviours as $\varepsilon \to 0$.

The sharp-interface models obtained by taking the limit $\varepsilon \to 0$ in the Cahn-Hilliard equation, which brings the width of the diffuse interface to zero, can be investigated using systematic asymptotic techniques as well as rigorous methods. For the constant mobility Cahn-Hilliard equation, Pego [59] showed, via matched asymptotics, that the asymptotic limit is the Mullins-Sekerka problem [53]. This work later

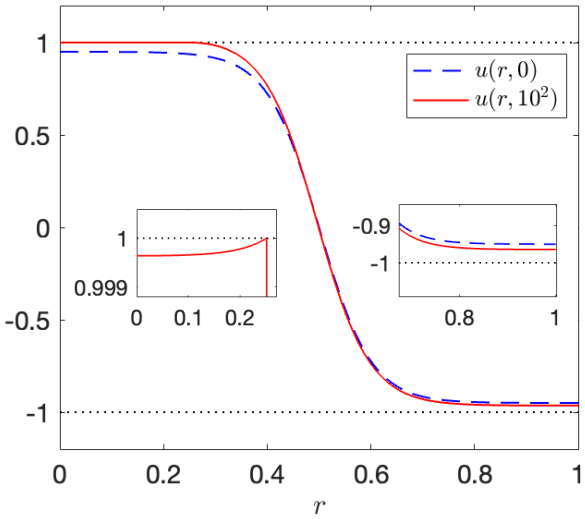



Figure 1.3: Plot of $u$, solution to (1.1)-(1.5) at a long time for $r \in (0,1)$ with mobility $M(u) = (1-u^2)_+$. The solution is bounded between $[-1,1]$. In the left inset, $u$ is below 1 (dotted line in the inset). In the right inset, $u$ is above $-1$.

inspired the rigorous proof by Alikakos, Bates and Chen [2]. On the other hand, for the degenerate mobility $M(u) = 1-u^2$ and the logarithmic homogeneous free energy Cahn, Elliott and Novick-Cohen [20] showed formally, using asymptotic expansions, that the sharp-interface limit was the model for interface motion by surface diffusion. This is why, for the degenerate mobility model with $M(u) = (1-u^2)_+$ and quartic polynomial homogeneous free energy, it was also thought to be motion by surface diffusion, but in the recent paper by Lee, Münch and Süli [49] it was demonstrated via matched asymptotics that the sharp interface limit is given by a generalised Mullins-Sekerka model with both surface and nonlinear bulk diffusion. We note that an earlier and slightly different result was obtained by Dai and Du [26]. The appearance of a generalised model has come as a surprise to some in the community, as by routine application of Pego's asymptotic approach, one can easily miss the contribution from bulk diffusion [47, 48, 70] and obtain the wrong sharp interface model. In fact, the correct computation requires the matching of exponentially small terms which are usually discarded in asymptotic expansions.

In particular, Lee et al. [49] studied the radially symmetric partial differential equation on a circular 2-dimensional domain, which represents a situation where both states, $u = -1$ and $u = 1$, have almost separated into two domains, a circular one centred at the origin and an annular one surrounding it, with a continuous diffuse interface between them. An issue that was barely touched in [49] is that, for initial data $|u_{init}| \leq 1$ and $M(u) = (1 - u^2)_+$, the numerical solution $u$ (as seen in Figure 1.3) developed a maximum near the interface that quickly approached 1, where the mobility, which multiplies the highest order derivative in the equation, vanishes. This is, again, a clear example of how the degeneracy of the mobility can affect the evolution of the solution, and it raises the following questions: Could this "touchdown" to $u = 1$ lead to loss of regularity? And, thus, to singularity formation?

These questions are not new; Elliott and Garcke [32] speculated about which type of singularities could arise in the context of Cahn-Hilliard equations with degenerate mobilities and how the set $\{x \in \Omega : M(u) = 0\}$ could behave as time progresses. Related issues have been studied in numerical simulations. For example, the phenomenon of *pinning*, in which the solution touches down at a point $r \in (0, 1)$ and $u(r, t)$ stays pinned or fixed at its touchdown value (i.e. $-1$ or 1) for all subsequent times. In particular, pinning was observed by Barrett and Blowey in [4] for degenerate Allen-Cahn/Cahn-Hilliard systems in numerical solutions, in contrast to the constant mobility case. Numerical experiments carried out by the same authors and Garcke in [5] demonstrate that the choice of the ratio between the mesh and temporal step sizes yields at least two solutions with very different behaviour. If the mesh sizes are taken to 0 much faster than the step size, the numerical solution becomes stationary and shows pinning at the boundary of the set $\{x \in \Omega : M(u) = 0\}$; if, instead, the mesh and step sizes are taken in a particular distinguished limit, then a different, evolving solution arises. This highlights the role of non-uniqueness, and also prompts questions about the implications for the limiting behaviour: Can pinning

affect long-time pattern formation in numerical simulations? Can it, therefore, alter the interface motion of the sharp-interface limit? Also not understood is the issue of whether or not the phenomena seen in numerical simulations capture only part of the mathematical model, particularly in the case of $n \gg 1$ when the mobility is small or when the solution is near touchdown, since in these cases numerical and machine errors may be amplified and will, therefore, interfere with the solution causing it to exhibit behaviour that disagrees with the analytical model.

A related class of high order parabolic equations that also presents degeneracy is the class of thin liquid films driven by surface tension. These are commonly modelled by the following equation:

$$\partial_t h + \partial_x(h^n \partial_{xxx} h) = 0, \quad \text{in } \mathcal{D} \times (0, \infty), \tag{1.10}$$

$$h(0, \cdot) = h_0, \quad \text{on } \mathcal{D}, \tag{1.11}$$

where $n > 0$, $\mathcal{D} \subset \mathbb{R}$ an interval, $h_0$ is the initial profile and $h \geq 0$ represents the thickness or height of a thin liquid film over a solid surface. The 2D radially symmetric degenerate Cahn-Hilliard equation is related, at least in the highest order derivative, to the 1D thin film equation by considering limits $|1 \pm u| \ll 1$ and letting $h = 1 \pm u$, which is exactly the property of the solution near touchdown, i.e. $|u| \to 1$. Note that under this change of variable the fact that $u \to 1$ can be translated to $h \to 0$, so, instead of talking about touchdown of $u$ to 1 or $u$ remaining strictly bounded $|u| < 1$, we can talk about $h$ vanishing or remaining positive. This link between the two equations allows us to take advantage of the vast literature on thin films and use it to gain insight into degenerate Cahn-Hilliard equations.

Equation (1.10)-(1.11) is usually coupled with one of the following conditions at

the boundary $x \in \partial\mathcal{D}$:

$$\begin{aligned} h(x,\cdot) = 1, \quad \partial_{xx} h(x,\cdot) = p, \quad p \in \mathbb{R}, \qquad & \textit{(fixed pressure)}, \\ h(x,\cdot) = 1, \quad \partial_{xxx} h(x,\cdot) = c, \quad c > 0, \qquad & \textit{(fixed current)}, \\ h_x(x,\cdot) = 0, \quad \partial_{xxx} h(x,\cdot) = 0, \qquad & \textit{(Neumann)}. \end{aligned}$$

The fact that $h^n$ can vanish and induce singularities introduces the need for weak definitions of solutions. For Neumann boundary conditions, Bernis and Friedman [9] proved existence of weak nonnegative solutions of (1.10)-(1.11) in the case of $1 < n < 3$, which was later extended to $0 < n < 3$ by Bernis [8].

For periodic conditions, the existence of classical solutions was demonstrated by Bertozzi and Pugh [14]. The existence of self-similar compactly supported source type solutions for $0 < n < 3$, with $\mathcal{D} = \mathbb{R}$ and polynomial conditions at $x \to \pm\infty$, was proven by Bernis, Peletier and Williams [10] using a shooting technique in combination with asymptotic estimates. Furthermore, they proved that there are no compactly supported spreading source type solutions for $n \geq 3$, i.e. if a point $x_0 \in \mathbb{R}$ starts with $h_0(x_0) = 0$, then it will remain pinned like that for all time, i.e. $h(x_0, t) = 0$ $\forall t > 0$. In other words, the mobility $h^3$ does not allow the modelling of spreading (or receding) droplets. In addition, Bernoff and Witelski [11] proved, using linear stability analysis, that these self-similar compactly supported source type solutions are stable under infinitesimal perturbations.

For pressure boundary conditions, Beretta, Bertsch and Dal Passo [6] proved global existence of classical solutions for $0 < n < 3$. In a Hele-Shaw cell ($n = 1$), Constantin et al. [23] showed that, starting from smooth and positive $h$ on the domain $\mathcal{D} = [-1, 1]$, no singularities can arise up to some positive time $T > 0$. In addition, for fixed pressures with values $p > 2$ and any smooth positive initial condition, the solution must pinch off in either finite or infinite time, i.e. $\inf_{[-1,1]\times[0,T)} h = 0$, for some

$T \in (0, \infty]$. Moreover, any solution that touches 0 in finite time will become singular, in the sense that the integral in time from 0 to $t_*$ ($t_* < \infty$ touchdown time) of $\partial_{xxxx} h$ goes to infinity at the point of touchdown $x_* \in \mathcal{D}$. For the same boundary conditions, Bertozzi, Brenner, Dupont and Kadanoff [13] studied singularity formation for all $n > 0$. They found, using formal matched asymptotics and numerical simulations, that infinite time touchdown was possible for $n > 1/2$, although they call it pinch-off. More specifically, they arrived at two different pinch-off profiles for $1/2 < n < 2$ and $n > 2$, and in both cases, the structure of the leading order could be separated into three regions: central, pinch-off and outer, where the first two are self-similar. They study the self-similar behaviour in detail, obtaining self-similar exponents that depend on the degree of degeneracy $n$. However, they do not address the case $n = 2$ nor carry out the full matching of the asymptotic expansions for $n < 2$.

Finally, Boatto, Kadanoff and Olla [16] catalogued possible qualitative behaviours of travelling wave solutions for (1.10) with $\mathcal{D} = \mathbb{R}$. They expressed the problem as a dynamical system which they were able to reduce to a first order system, where they used asymptotic expansions and phase plane analysis. For more specific details on thin films, see the comprehensive review of Craster and Matar [24] or the very detailed introduction of the paper by Novick-Cohen and Shishkov [58].

Another interesting situation that arises in models of liquid films is when the set of points where $h(x) = 0$ becomes non-empty, which can happen, for example, at the three-phase contact line between a droplet, a flat surface and the air. The spreading of a droplet can be modelled using lubrication theory, which is a simplified form of the Navier-Stokes equations that is appropriate for a thin layer of very viscous fluid. Thus, applying lubrication theory and taking the thickness of the droplet to be much smaller than its radius, one obtains the thin film equation (1.10) with $n = 3$. However, as we will see in what follows, $h^3$ is not the only relevant mobility occurring in thin film and droplet models.

A problem that is passed on from the Navier-Stokes system to the lubrication approximation is that the no-slip condition, which is commonly used at solid-liquid boundaries in the literature, introduces a non-integrable shear stress singularity at the contact line. A natural method for treating this issue is to allow some slippage of the fluid near the contact line which requires the introduction of mobilities $h^n$ with $3 > n > 0$. For example, for the modelling of cell movement, Greenspan [35] introduced a slip condition that led to the regularisation $h^3 + \beta h$ of $h^3$ for $\beta > 0$. Furthermore, with the regular slip approximation $h^3 + \beta h^2$, Lacey [45] obtained an asymptotic expansion of the solution as $\beta \to 0$, i.e. as it approaches the no-slip condition, and found a formula for the speed of the contact line, which goes to 0 as $\ln(1/\beta)^{-1}$ when we take $\beta \to 0$. Haley and Miksis [40] used, instead, a Navier slip condition to get the approximation $h^3 \sim h^3 + \lambda(h)h^2$, with $\lambda(h)$ referred as the slip length, in a more complicated system of equations.

Other models for thin viscous films are also possible by changing the contact angle or adding other forces to treat the stress singularity, as opposed to using a slip condition. For example, Bertozzi et. al. [14] include a porous media diffusion term which suppresses the Van der Waals forces, obtaining

$$\partial_t h = -\partial_x(h^n \partial_{xxx} h - \partial_x h^m), \tag{1.12}$$

for $m > 1$. A version of this but with general space dimension was studied in [31].

In [43], King and Bowen studied the lubrication approximation (1.10) starting from a compactly supported profile, regularised by a smooth cut-off function of length $\varepsilon > 0$. They used matched asymptotics to analyse the limit $\varepsilon \to 0$. For $n \geq 3$, they showed that droplet motion is only possible in this limit for particular time scalings. In contrast, for $n < 3$, boundary movement is possible under certain assumptions on the contact angle and, moreover, for $n < 3/2$, the droplet can either spread or recede.

Even though the physics involved are very different from the ones that model spinodal decomposition and coarsening, the issues arising from lubrication theory and degenerate Cahn-Hilliard equations are intrinsically connected. In particular, the questions about contact lines can be directly translated to how the set $\{x \in \Omega : M(u) = 0\}$, where the equation degenerates, evolves once touchdown has been achieved.

The case where touchdown never occurs is usually referred to as *positivity* in the thin film and lubrication literature. In this sense, Beretta et al. [6] also proved that for $0 < n < 3$ there are weak solutions that after a finite time become positive and, thus, gain regularity which makes them strong solutions. Bertozzi and Pugh [14] proved a similar result for the equation (1.12) for specific sets of the constants $n$, $m > 0$. In fact, it appears that even though the existence of positive solutions has been studied for related lubrication and thin film models, it has not been applied to the problem of finding strictly bounded solutions of degenerate Cahn-Hilliard equations. Novick-Cohen and Shishkov [58] have made some progress in this direction by working with local entropy estimates on the more general equation

$$\partial_t u + \partial_x[u^n(\partial_{xxx}u + \nu u^{m-n}\partial_x u - Au^{M-n}\partial_x u)] = 0,$$

for $\nu = \pm 1$, $n > 0$, $M > m$ and $A \geq 0$. But even though this is close to Cahn-Hilliard models, the direct connection is missing, which means that there is still work to do to fit the Cahn-Hilliard equation into this broader framework.

Let us go back to the Cahn-Hilliard equation stated in (1.1)-(1.5) with non-degenerate mobilities, i.e. $M(u) > b > 0$ for some $b \in \mathbb{R}$. Since the energy of time-dependent solutions strictly decreases over time, these solutions are expected to converge to stationary states as $t \to \infty$. This has been proven at least for the case of constant mobility with logarithmic [1] or quartic polynomial homogeneous

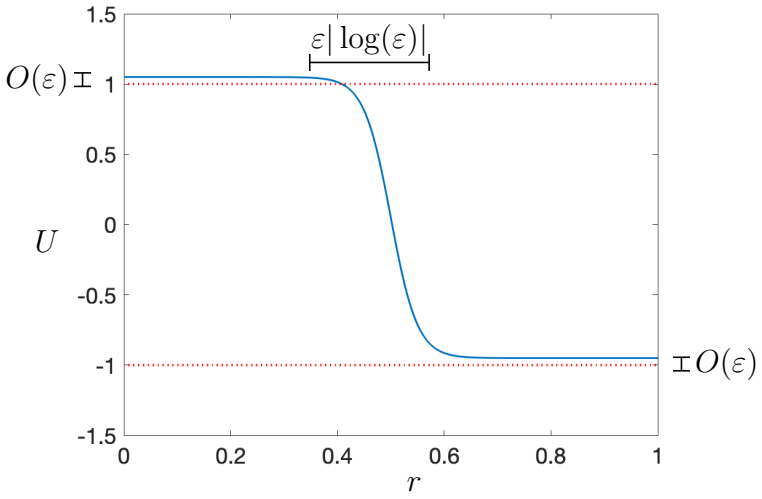



Figure 1.4: Plot of leading order asymptotic approximation to $U$ obtained by Niethammer [56] with order of magnitude of separations with $\pm 1$ and width of interface.

free energy [65]. For the radially symmetric case in the unitary ball in two dimensions, $\Omega = B_1(0) \subset \mathbb{R}^2$, with quartic polynomial homogeneous free energy and non-degenerate mobility, the stationary equation associated with (1.1)-(1.5) for a function $U = U(r)$ is

$$-\varepsilon^2 \Delta U + f'(U) = 0. \tag{1.13}$$

In this setting, Niethammer [56] proved, using rigorous matched asymptotics and a fixed point technique, the existence and uniqueness (up to a $U \to -U$ reflection) of a small energy stationary solutions. Moreover, she found that the solutions have a hyperbolic tangent leading order profile in which the ends of the transition are above (below) $+1$ $(-1)$ by an $O(\varepsilon)$ difference, in order to accommodate the Gibbs-Thomson effect, see Figure 1.4.

Niethammer's result [56] gives us some intuition about how, as $t \to \infty$ in the time-dependent case, the free energy, which acts as the driving force of the dynamics, pushes the solution outside $[-1, 1]$. This implies that the set of points where $|u| \geq 1$ must become non-empty as time goes to infinity, i.e. touchdown must occur. Indeed, since Cahn-Hilliard equations have decreasing energy, if we had a solution that for all

times (including the limit $t \to \infty$) remained strictly bounded $|u| < 1$, then we would have found a stationary solution with small energy (assuming the energy of the initial condition was small) that is not one of the solutions described in [56].

These dynamics pose interesting questions about how the touchdown is approached, such as: Does touchdown happen in finite or infinite time? Do solutions that touch down have any underlying structure (e.g. self-similar profiles, different asymptotic regions)? If touchdown occurs in finite time, can the solutions be continued in some weaker sense? How does the contact line evolve? Will it move or pin the solution at those points? These are all relevant questions and, in this thesis, we will start by answering the first two and we will particularly focus on the issue of infinite time touchdown.

As in Lee et. al. [49], we will work with the radially symmetric version of (1.1)-(1.3) with the quartic polynomial homogeneous free energy (1.8), degenerate mobility (1.9) and boundary conditions (1.4)-(1.5) on the 2-dimensional unit ball $\Omega = \{(x, y); r < 1\}$, where $r = \sqrt{x^2 + y^2}$.

Because we want to study the late stages of the phase separation process we would like the initial condition to be close enough to the profile of a stationary solution but far enough so that we can see the dynamics evolve in a long time. A sensible choice, based on the asymptotic expansions done by Niethammer [56] and Lee et. al. [49], is

$$u_{init}(r) = -0.95 \tanh\left(\frac{r - 0.5}{\varepsilon}\right).$$

We note that initial conditions based on a hyperbolic tangent appear regularly in the literature for Cahn-Hilliard and thin film equations, see for example [2, 27, 38, 68, 67].

We will focus separately on the cases of degeneracy degree $n > 2$ and $n < 2$ because, as it turns out, even though both profiles exhibit infinite time touchdown, the asymptotic structure is different in the two cases. The particular case $n = 2$,

which we do not treat in detail here, does not belong to either of these cases, and we believe that it is a mix of the two cases.

Our numerical results strongly suggest that for the initial condition used here, touchdown is achieved in infinite time for all $n > \frac{1}{2}$, i.e. $u(r,t) \to 1$ as $t \to \infty$ and $r \to r_*$ for some $r_* \in (0,1)$. To investigate this we follow a similar approach as in Bertozzi et. al. [13] for the thin film problem with pressure boundary conditions. We will first obtain key information on the profile of the numerical solution and then use this to carry out a singular perturbation analysis at $(r_*, \infty)$ in terms of a parameter $0 < \delta \ll 1$ which goes to 0 as $t \to \infty$. Here $\varepsilon$, which is usually small, is treated as a fixed parameter and we only expand in terms of $\delta$.

We note that Elliott and Garcke's existence theorem [32] does not ensure that a radially symmetric weak solution exists. By considering Sobolev spaces of radial functions, we prove the existence of a true radially symmetric weak solution to the evolution problem until a time $0 < T < \infty$ such that $|u| \leq 1$ a.e. in $\Omega$ for all times $0 < t < T$. The embeddings between these Sobolev spaces are stronger than in the non-symmetric case, but because we are in dimension $N = 2$ the associated radial Sobolev embedding does not improve the overall regularity of the solution.

A further aim, left as conjectures in the present work, is to use the existence proved here in conjunction with entropy estimates obtained in [42] to ensure that there exists a weak radial solution $u$ that remains strictly bounded $|u| < 1$. These conjectures are informed by the existence and regularity result proved in Chapter 6 and the thin-film literature explored here.

This thesis is divided into seven chapters and three appendices. In Chapter 2 we formulate the radially symmetric degenerate Cahn-Hilliard equation in two dimensions and state the main definitions and properties. In Chapter 3 we extract preliminary information related to the evolution of the solution from numerical simulations. In Chapters 4 and 5 we study the cases $n > 2$ and $n < 2$, respectively,

by examining the numerical solution in more detail to gain information about its long-time profile and use this as an ansatz to obtain asymptotic expansions of the solution. Then, analytically where possible and numerically otherwise, we solve the leading order equations to obtain a composite expansion which we compare to the full numerical solution. It is worth noting that we published the results in Chapter 4 in 2021, see [60]. In Chapter 6 we prove the existence of weak solutions of a non-degenerate radially symmetric problem, and then we use these solutions to obtain the existence of weak solutions for the degenerate problem. We also give a quick overview of known results on the positivity of solutions for the thin-film equation and how they relate to our problem. In Chapter 7 we draw conclusions and give final remarks about the connection between Cahn-Hilliard and thin film equations. Finally, Appendix A is a short literature review of relevant stationary solutions, Appendix B describes and tests the numerical method used in simulations and Appendix C lays out useful cases of the Frobenius method for expanding solutions to fourth-order ordinary differential equations.

# Chapter 2

# Problem formulation

Recall the Cahn-Hilliard equation for $N \geq 1$, $x \in \Omega \subset \mathbb{R}^N$, $t > 0$,

$$\partial_t u = -\nabla \cdot \mathbf{j}, \tag{2.1}$$

$$\mathbf{j} := -M(u)\nabla\mu, \tag{2.2}$$

$$\mu := -\varepsilon^2 \Delta u + f'(u), \tag{2.3}$$

with the quartic polynomial homogeneous free energy and two-sided degenerate mobility

$$f(u) = \frac{(1-u^2)^2}{2}, \quad M(u) = M_n(u) := [(1-u^2)_+]^n,$$

with degree of degeneracy $n \geq 0$ and Neumann and no-flux boundary conditions

$$\nabla u \cdot \mathbf{n} = 0, \quad \text{on } \partial\Omega \times (0,\infty), \tag{2.4}$$

$$\mathbf{j} \cdot \mathbf{n} = 0, \quad \text{on } \partial\Omega \times (0,\infty), \tag{2.5}$$

where $\mathbf{n} = \mathbf{n}(x)$ is the outward unitary normal vector at $x \in \partial\Omega$.

We take $\Omega = \{x \in \mathbb{R}^N : \|x\| = 1\}$ the unit ball on $\mathbb{R}^N$, where $\|x\| = \sqrt{\sum_{i=1}^N x_i^2}$ is the usual Euclidean norm in $\mathbb{R}^N$, and assume our solution to be radially symmetric,

thus $u(r,t)$, where the radius is given by $r = \|x\|$. Then, in the particular case of dimension $N = 2$, the system takes the simpler form

$$\partial_t u = \frac{1}{r}\partial_r \left( r M_n(u) \partial_r \mu \right), \quad \text{in } (0,1) \times (0,\infty), \tag{2.6}$$

$$\mu = -\varepsilon^2 \frac{1}{r}\partial_r \left( r \partial_r u \right) + f'(u), \quad \text{in } (0,1) \times (0,\infty), \tag{2.7}$$

with initial condition $u_{init}(x)$ and boundary conditions, for $t > 0$,

$$\partial_r u(1,t) = 0, \tag{2.8}$$

$$M_n(u(1,t)) \partial_r \mu(1,t) = 0, \tag{2.9}$$

where we have used that $\mathbf{n}(x) = x/\|x\|$.

A sensible choice for our space of solutions, which comes from a variational approach, is to take $u \in L^2((0,\infty); H^2(0,1))$. We will use this when we prove the existence of such solutions in Chapter 6. But for the moment, that is, for Chapters 3, 4 and 5, we will assume our solutions to be sufficiently smooth, i.e. $u \in C^1((0,\infty); C^4(0,1)) \cap C([0,\infty); C^1([0,1]))$, since the weaker regularity does not allow for an asymptotic expansion as we need to evaluate the solution and its derivatives point-wise.

**Remark 2.1.** *We note that the existence of a smooth solution for all time is not guaranteed based on previous results, but we conjecture that for sufficiently smooth initial data that is bounded strictly away from $\pm 1$ we should have existence of sufficiently smooth solutions for sufficiently small times.*

To solve problem (2.6)-(2.9) we also need to set a boundary condition at $r = 0$. A reasonable choice, particularly when considering classical solutions, which must have continuous derivatives up to 4th order in space, is to require the odd derivatives of $u$ at $r = 0$ to vanish, i.e. $\partial_r u(0,t) = 0$ and $\partial_{rrr} u(0,t) = 0$. We note that the

problem is written in terms of $u$ and the chemical potential $\mu$. Moreover, at leading order as $t \to \infty$, one has $\partial_{rrr} u(0,t) \sim \partial_{rrr} \mu(0,t)$. Therefore, we rewrite the boundary conditions at $r = 0$ as

$$\partial_r u(0,t) = 0, \tag{2.10}$$

$$\partial_r \mu(0,t) = 0. \tag{2.11}$$

In addition, to establish a common ground for talking about touchdown and singularity formation we define the following:

**Definition 2.2.** *Let $t_* < +\infty$ (or $t_* = +\infty$). We say that $u \in C^1((0,t_*); C^4(0,1)) \cap C([0,t_*); C^1([0,1]))$ exhibits finite (or infinite) time touchdown if*

$$\lim_{t \to t_*} \sup_{r \in [0,1]} |u(r,t)| = 1.$$

*We also denote as $\bar{r}(t)$ the point where the solution reaches its maximum at time $t$ as*

$$\overline{r}(t) := \operatorname*{argmax}_{r \in [0,1]} |u(r,t)|,$$

*and we denote $r_*$ as its limit in time,*

$$r_* := \lim_{t \to t^*} \overline{r}(t),$$

*where the touchdown is expected to occur.*

**Remark 2.3.** *Note that the definition above applies to functions with less regularity, and for continuous functions, the supremum could be replaced by a maximum.*

In addition, we define the concept of pinning in our context.

**Definition 2.4.** *We say that $u$ exhibits pinning if it has exhibited finite time touchdown at $0 < t_* < \infty$ and the set $\Omega_t := \{r \in (0,1) : |u(r,t)| = 1\}$ does not depend on*

*time* $\forall t \geq t_*$. *In other words, if the solution touches down at a point* $r \in (0,1)$, *then* $u(r,t)$ *stays pinned or fixed at its touchdown value (i.e.* $-1$ *or* $1$*) for all subsequent times.*

An important quantity associated with the Cahn-Hilliard equation is its free energy, which, in polar coordinates, is given by

$$E[u](t) := \int_0^1 \left[\frac{\varepsilon^2}{2}(\partial_r u)^2 + f(u)\right] r dr.$$

This free energy is non-increasing along trajectories, i.e if $u$ satisfies (2.6)-(2.7) then

$$\frac{dE[u]}{dt} = -\int_0^1 M_n(u)(\partial_r \mu)^2 r dr \leq 0.$$

Since $E \geq 0$ is bounded from below, this implies that $E[u](t) \to E_\infty$ as $t \to \infty$ for some $E_\infty \in \mathbb{R}$.

It has been proven that solutions $u$ to (2.6)-(2.11) with constant mobility, i.e. $n = 0$, converge to a stationary solution $U(r)$, see [65]. Thus, $U$ must satisfy (2.6) with $\partial_t u \equiv 0$. By integrating once and using the no-flux condition at the boundary, one obtains

$$-\frac{\varepsilon^2}{r}\frac{d}{dr}\left(r\frac{dU}{dr}\right) + f'(U) = \sigma, \tag{2.12}$$

$$U'(0) = 0, \quad U'(1) = 1, \tag{2.13}$$

where the additional degree of freedom $\sigma \in \mathbb{R}$ is used to include a mass constraint that is inherited from the initial condition. For this, we define the mass as

$$\mathrm{m}(t) := \int_0^1 u(r,t) r dr. \tag{2.14}$$

Applying (2.6) and integrating by parts (using boundary conditions (2.9) and (2.11))

we get

$$\partial_t \mathrm{m}(t) = \int_0^1 \partial_t u(r,t) r dr = \int_0^1 \partial_r (r M_n(u) \partial_r \mu) dr = 0. \tag{2.15}$$

This mass conservation property implies that the stationary solution must satisfy:

$$\int_0^1 U(r) r dr = \mathrm{m}(0) = \int_0^1 u_{init}(r) r dr.$$

It has been shown in [56] that for any $\mathrm{m}(0)$ there exists a pair of solutions to (2.12)-(2.13) with small energy $E[U] = O(\varepsilon)$ which are identical and unique, up to reflection $U \to -U$, and escape the interval $[-1, 1]$, by an $O(\varepsilon)$ amount.

For our discussion, of solutions of (2.6)-(2.11) with $n > 0$, it will turn out to be useful to consider stationary solutions of (2.12) with a free boundary at some point $r_* \in (0, 1)$. More precisely, for $r \in (r_*, 1)$, we look for a stationary solution $U_*(r)$ satisfying

$$-\frac{\varepsilon^2}{r}\frac{d}{dr}\left(r\frac{dU_*}{dr}\right) + f'(U_*) = \sigma, \tag{2.16}$$

$$U_*'(r_*) = 0, \quad U_*'(1) = 0, \tag{2.17}$$

$$U_*(r_*) = 1. \tag{2.18}$$

We extend it to a stationary solution of (2.6)-(2.11) for $n > 0$ by setting $U_* \equiv 1$ in $(0, r_*)$. Note that $r_*$ is a priori unknown and, moreover, depends on $\varepsilon$. An asymptotic approximation to a solution of (2.6)-(2.11) is obtained in [49] and we recall it in section A.2 using notation consistent with our work.

These stationary solutions will be useful for numerical comparisons and asymptotic approximations as $t \to \infty$. Detailed descriptions of both can be found in Appendix A.

# Chapter 3

# Preliminary numerical results

In the present section, we study numerical solutions of the radially symmetric degenerate Cahn-Hilliard system (2.6)-(2.11), which were obtained using the numerical method described in Appendix B.

For the simulations, we set $\varepsilon = 0.1$ and the initial condition

$$u_{init}(r) = -0.95 \tanh\left(\frac{r - 0.5}{\varepsilon}\right).$$

Note that $u_{init}$ is smooth and satisfies the boundary conditions up to exponentially small terms. We have tested the error associated with these terms, see the results in Section B.2 of Appendix B, and found that it does not change the main features of the solution, in particular, its long-time behaviour remains the same.

To simplify our analysis we will plot

$$v(r,t) := 1 - u(r,t), \tag{3.1}$$

instead of $u$. This not only makes the figures clearer near touchdown, as we are looking at $v$ approaching 0 instead of $u$ approaching 1, but it also allows us to draw direct connections with the thin film theory where $v$, in the regions where $v \ll 1$,

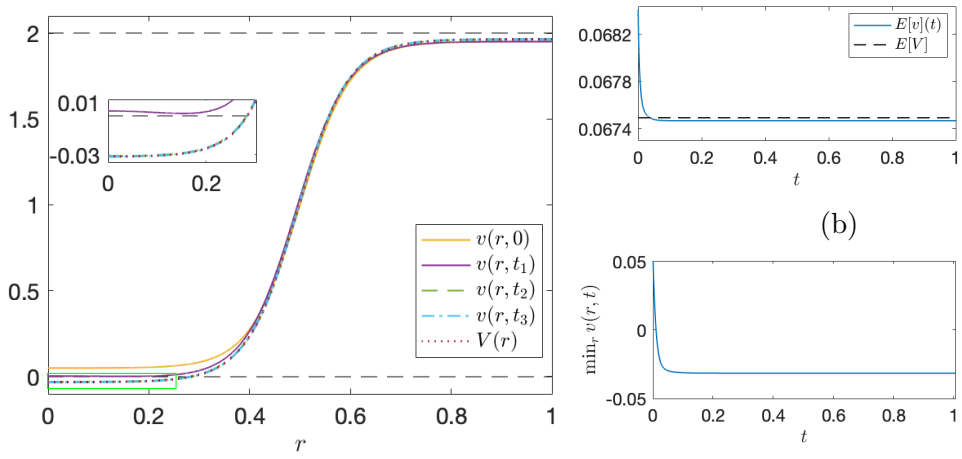



Figure 3.1: (a) Solution $v$ for $n = 0$, for different times $t = 0$, $t_1 = 0.01$, $t_2 = 0.1$, $t_3 = 1$, and function $V = 1 - U$, where $U$ solves (2.12)-(2.13). (b) Evolution of the energy. (c) Evolution of the minimum.

can be translated into the height of a thin layer of liquid. We will look at the cases $n = 0, 1, 2, 4$, which provide good numerical examples of the ranges of interest $n < 2$, $n = 2$ and $2 < n$.

*Constant mobility* $n = 0$. The solution of Figure 3.1 (a) develops a minimum approximately at $r = 0.15$, then quickly crosses $v = 0$ at time $t_* = 0.0106$ and radius $r_* = 0.15$, and settles, more slowly, into a stationary solution $V(r) := 1 - U(r)$, where $U$ solves (2.12)-(2.13), which is exactly the problem from [56]. In Figure 3.1 (a) we see that the agreement between $v$ and $V$ as time increases is excellent.

The fact that the limiting profile as $t \to \infty$ is smaller or equal than 0 at some point in $r$ was expected. Otherwise, because of the decreasing energy, which we denote $E[v](t) := E[1 - u](t)$, we would have found a stationary solution with small energy (since the energy of the initial condition was small) that is not one of the solutions described in [56].

In Figure 3.1 (b) we can see that $E[v]$ goes below the energy $E[V]$ of the stationary solution, with a remaining deviation of $10^{-5}$, which can be explained by numerical errors. We verified this by refining the grid that was used for both $v$ and $V$ and noted

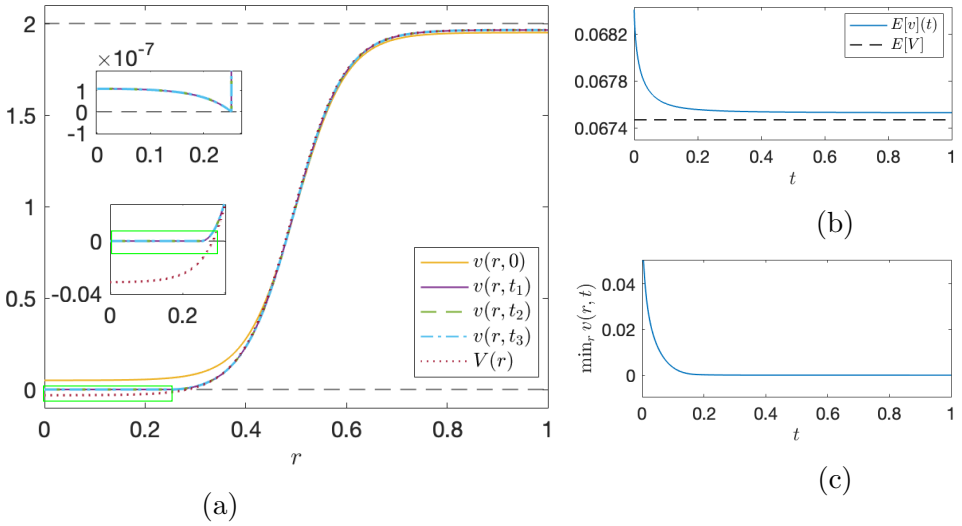



Figure 3.2: (a) Solution $v$ for $n = 1$, for different times $t = 0$, $t_1 = 10^8$, $t_2 = 10^9$, $t_3 = 0.39 \times 10^{10}$, and function $V = 1 - U$, where $U$ solves (2.12)-(2.13). (b) Evolution of the energy. (c) Evolution of the minimum.

| $\Delta r$ | $t_*$ |
|---|---|
| $10^{-3}$ | 1.21 |
| $10^{-4}$ | 3.44 |
| $10^{-5}$ | 10.60 |
| $10^{-6}$ | 222.23 |

Table 3.1: Time exactly before $\min v(r,t)$ crosses 0 for different grid sizes and $n = 1$.

that the deviation decreased accordingly.

*Degenerate mobility* $n = 1$. The numerical solution behaves similarly to the constant mobility case in that $\min_r v$ reaches 0 in finite time, at $t = t_* = 222.23$ for a grid spacing of $\Delta r = 10^{-6}$, see fig. 3.2(a) and the inset. However, we noticed that $t_*$ increases significantly upon decreasing $\Delta r$, see Table 3.1, leaving open the possibility that this finite-time touchdown is a numerical artefact. This means that we could still be approximating a solution that presents infinite-time touchdown, and are only thrown off this trajectory due to numerical errors. Moreover, from Table 3.1 we can infer that $t_* \sim \frac{1}{\sqrt{Deltax}}$, raising questions about how the numerical solution approaches infinite time touchdown, which could be investigated in future work.

An interesting feature that we can see in Figure 3.2 (a) is that the minimum of $v$ approaches zero more rapidly than the segment near $r = 0$ and we also note that the evolution in the region to the right of the minimum is slower than to the left.

Moreover, where the solution achieves a value for which the mobility vanishes, it typically loses regularity. To express this rigorously we let $\overline{v}(t) := v(\overline{r}(t), t)$ be the minimum of $v$ at time $t$. If $u$ satisfies (2.6) and (2.7) then for $(r, t) \in (0, 1) \times (0, \infty)$, the function $v = v(r, t)$ satisfies

$$\partial_t v = -\frac{1}{r}\partial_r \left[ r M_n(v) \partial_r \left( \varepsilon^2 \frac{1}{r} \partial_r \left( r \partial_r v \right) + 2(-v^3 + 3v^2 - 2v) \right) \right], \tag{3.2}$$

$$\partial_r u(1, t) = 0, \quad M_n(u(1, t))\partial_r \mu(1, t) = 0, \quad \forall t \in (0, \infty), \tag{3.3}$$

$$\partial_r u(0, t) = 0, \quad \partial_r \mu(0, t) = 0, \quad \forall t \in (0, \infty) \tag{3.4}$$

where $M_n(v) = v_+^n[(2 - v)_+]^n$ is the mobility for general $n$. Then, finite time touchdown is translated as: There exists $t_* < \infty$ such that

$$\lim_{t \to t_*} \inf_{r \in [0,1]} v(r, t) = 0$$

and we can re-state the loss of regularity as:

**Proposition 3.1.** *Let $0 < t_* < \infty$ and suppose $v \in C^4((0, t_*); (0, 1))$ is a classical solution of (3.2). Let $1 \leq n < \infty$, assume $2 > v(r, t) > 0$ for all $(r, t) \in (0, 1) \times (0, t_*)$ and $\overline{r}(t) \geq k$ for all $t \in (0, t_*)$ for some $1 > k > 0$. If there is touchdown at the finite time $t_*$, then*

$$\int_0^{t_*} \left[ |\partial_{rrrr} v(r, t) + \partial_{rrr} v(r, t) + \partial_{rr} v(r, t)| \right]_{r = \overline{r}(t)} dt = +\infty.$$

*Proof.* We note that the main idea of this proof is similar to the ones used for the thin film equation, see for example Bertozzi et. al. [13] and Constantin et. al. [23].

Assume that $v$ touches down to 0 at time $t_*$ (the same arguments we will use

can be applied to the case where $v$ touches down to 2 at time $t_*$). For $n > 1$, using equation (3.2) and the fact that $\partial_r v(\overline{r}(t), t) = 0$ (because it is a minimum), we get

$$\begin{aligned}
\frac{d}{dt}\left(\overline{v}^{1-n}(t)\right) =& \frac{(1-n)}{\overline{v}^n(t)}\left(\partial_r v(\overline{r}(t),t)\frac{d\overline{r}(t)}{t} + \partial_t v(\overline{r}(t),t)\right), \\
=& \frac{(1-n)}{\overline{v}^n(t)}\partial_t v(\overline{r}(t),t), \\
=& \frac{n-1}{v(\overline{r}(t),t)^n}\frac{1}{\overline{r}(t)}\partial_r\left(\overline{r}(t)v(\overline{r}(t),t)^n[(2-v(\overline{r}(t),t))_+]^n\partial_r\mu(\overline{r}(t),t)\right), \\
=& \frac{(n-1)}{\overline{r}\overline{v}^n}\left[v(r,t)^n[(2-v(r,t))_+]^n\partial_r\mu(r,t)\right. \\
& + rnv(r,t)^{n-1}[(2-v(r,t))_+]^n\partial_r v(r,t)\partial_r\mu(r,t) \\
& - rnv(r,t)^n[(2-v(r,t))_+]^{n+1}\partial_r v(r,t)\partial_r\mu(r,t) \\
& \left. + rv(r,t)^n[(2-v(r,t))_+]^n\partial_{rr}\mu(r,t)\right]_{r=\overline{r}(t)}, \\
=& \frac{(n-1)}{\overline{v}^n}\overline{v}^n[(2-\overline{v})_+]^n\left[\frac{1}{r}\partial_r\mu(r,t) + \partial_{rr}\mu(r,t)\right]_{r=\overline{r}(t)},
\end{aligned}$$

where

$$\begin{aligned}
\partial_r\mu(r,t) =& \partial_r\left(\varepsilon^2\frac{1}{r}\partial_r\left(r\partial_r v\right) + 2(-v^3+3v^2-2v)\right), \\
=& \partial_r\left(\varepsilon^2\left(\partial_{rr}v + \frac{1}{r}\partial_r v\right) + 2(-v^3+3v^2-2v)\right), \\
=& \varepsilon^2\partial_{rrr}v + \frac{\varepsilon^2}{r}\partial_{rr}v - \frac{\varepsilon^2}{r^2}\partial_r v + 2(-3v^2\partial_r v + 6v\partial_r v - 2\partial_r v). \\
\partial_{rr}\mu(r,t) =& \partial_r\left(\varepsilon^2\partial_{rrr}v + \frac{\varepsilon^2}{r}\partial_{rr}v - \frac{\varepsilon^2}{r^2}\partial_r v + 2(-3v^2\partial_r v + 6v\partial_r v - 2\partial_r v)\right), \\
=& \varepsilon^2\partial_{rrrr}v + \frac{\varepsilon^2}{r}\partial_{rrr}v - \frac{\varepsilon^2}{r^2}\partial_{rr}v - \frac{\varepsilon^2}{r^2}\partial_{rr}v + \frac{2\varepsilon^2}{r^2}\partial_r v \\
& + 2(-6v(\partial_r v)^2 + -3v^2\partial_{rr}v + 6(\partial_r v)^2 + 6v\partial_{rr}v - 2\partial_{rr}v).
\end{aligned}$$

At $r = \overline{r}(t)$ we have

$$\left[\partial_r\mu(r,t)\right]_{r=\overline{r}(t)} = \left[\varepsilon^2\partial_{rrr}v + \frac{\varepsilon^2}{r}\partial_{rr}v\right]_{r=\overline{r}(t)}.$$

$$[\partial_{rr}\mu(r,t)]_{r=\overline{r}(t)} = \left[\varepsilon^2\partial_{rrrr}v + \frac{\varepsilon^2}{r}\partial_{rrr}v - \frac{2\varepsilon^2}{r^2}\partial_{rr}v + 2(-3v^2\partial_{rr}v + 6v\partial_{rr}v - 2\partial_{rr}v)\right]_{r=\overline{r}(t)}.$$

Hence,

$$\begin{aligned}\frac{d}{dt}\left(\overline{v}^{1-n}(t)\right) =&(n-1)[(2-\overline{v})_+]^n\left[\varepsilon^2\partial_{rrrr}v(r,t) + \frac{2\varepsilon^2}{r}\partial_{rrr}v(r,t)\right.\\ &\left.+\left(-\frac{\varepsilon^2}{r^2} - 6v(r,t)^2 + 12v(r,t) - 4\right)\partial_{rr}v(r,t)\right]_{r=\overline{r}(t)}.\end{aligned}$$

Integrating from 0 to $0 < s < t_*$ and using the Fundamental Theorem of Calculus we obtain

$$\begin{aligned}\overline{v}^{1-n}(s) - \overline{v}^{1-n}(0) =&(n-1)\int_0^s [(2-\overline{v})_+]^n\left[\varepsilon^2\partial_{rrrr}v(r,t) + \frac{2\varepsilon^2}{r}\partial_{rrr}v(r,t)\right.\\ &\left.+\left(-\frac{\varepsilon^2}{r^2} - 6v(r,t)^2 + 12v(r,t) - 4\right)\partial_{rr}v(r,t)\right]_{r=\overline{r}(t)} dt,\\ \leq&(n-1)\sup_{t\in(0,t_*)}[(2-\overline{v})_+]^n\int_0^s\left[\varepsilon^2\partial_{rrrr}v(r,t) + \frac{2\varepsilon^2}{r}\partial_{rrr}v(r,t)\right.\\ &\left.+\left(-\frac{\varepsilon^2}{r^2} - 6v(r,t)^2 + 12v(r,t) - 4\right)\partial_{rr}v(r,t)\right]_{r=\overline{r}(t)} dt,\\ \leq&(n-1)2^n\max\left\{\varepsilon^2, \frac{2\varepsilon^2}{k}, -\frac{\varepsilon^2}{k^2} + 2\right\}\int_0^s [\partial_{rrrr}v(r,t)\\ &+ \partial_{rrr}v(r,t) + \partial_{rr}v(r,t)]_{r=\overline{r}(t)}\, dt.\end{aligned}$$

To bound the term with the round brackets which accompanies the second derivative we used the following inequality:

$$-\frac{\varepsilon^2}{\overline{r}(t)^2} - 6\overline{v}(t)^2 + 12\overline{v}(t) - 4 \leq -\frac{\varepsilon^2}{k^2} + 2,$$

which is true since, as a function of $\overline{v}$, the left-hand side achieves its maximum at $\overline{v} = 1$. A priori, we also require a bound from below, since the quadratic term can go to $-\infty$. In that case, i.e. when the term multiplying $\partial_{rr}v(\overline{r}(t),t)$ becomes negative, then we can just bound it from above by the second derivative since $\partial_{rr}v(\overline{r}(t),t) > 0$

(because it is a minimum).

Therefore,

$$\overline{v}^{1-n}(s) - \overline{v}^{1-n}(0) \leq C \int_0^s \left[|\partial_{rrrr} v(r,t) + \partial_{rrr} v(r,t) + \partial_{rr} v(r,t)|\right]_{r=\overline{r}(t)} dt,$$

where $C = C(n, \varepsilon, k) > 0$ and we have bounded the integrand by its absolute value.

Taking $s \to t_*$ the left-hand side goes to infinity, since $n > 1$, and using the Monotone Convergence Theorem on the right-hand side integral (since its integrand is positive), we obtain

$$+\infty \leq C \int_0^{t_*} \left[|\partial_{rrrr} v(r,t) + \partial_{rrr} v(r,t) + \partial_{rr} v(r,t)|\right]_{r=\overline{r}(t)} dt.$$

Therefore, the integral must be infinite which means that at least one of the higher derivatives becomes unbounded at $(r_*, t_*)$, thus losing regularity.

The same argument can be adapted for the case $n = 1$ where one must replace $\overline{v}^{1-n}(t)$ by $\log(\overline{v}(t))$ at the beginning. □

**Remark 3.2.** *We note that we have not encountered numerical solutions with finite time touchdown for $n \geq 1$. We have only seen this in the case $n = 0$. It would be interesting to see if there are any conditions between the time and spacial steps that can lead to a finite time touchdown solution for $n \geq 1$. This also raises questions about the potential behaviour of numerical solutions in the case $0 < n < 1/2$, which is out of the scope of our work but would make an interesting problem in the future.*

At this stage one may ask if the vanishing of the mobility can be avoided, so that, for example, the proof of existence of solutions with $|u| \leq 1$ by Elliott and Garcke [32] can be strengthened to $|u| < 1$ which would allow the existence of solutions that remain strictly below 1 even as $t \to \infty$. However, the same argument used for the constant mobility case can be applied here, that is: if $|u(r,t)| < 1$ for all $r \in (0,1)$

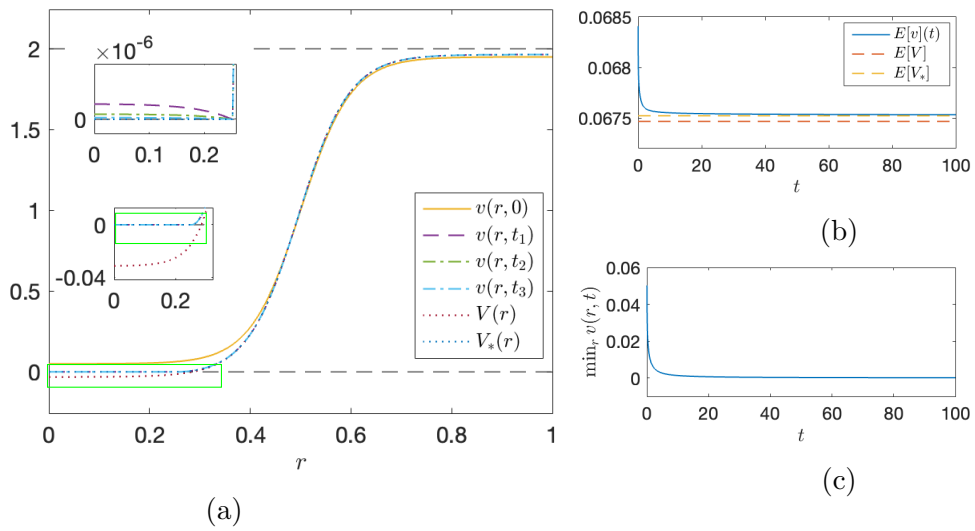



Figure 3.3: (a) Solution $v$ for $n = 2$, for different times $t = 0$, $t_1 = 10^8$, $t_2 = 10^9$, $t_3 = 10^{10}$, and functions $V = 1 - U$, $V_* = 1 - U_*$ where $U$ and $U_*$ solve (2.12)-(2.13) and (2.16)-(2.18), respectively. (b) Evolution of the energy. (c) Evolution of the minimum.

and all $0 < t < \infty$, then $M_n$ does not vanish and the limiting profile as $t \to \infty$ would be a stationary solution of small energy strictly bounded between $-1$ and 1, contradicting the uniqueness result from Niethammer [56]. Thus, the solution must achieve touchdown either in finite or in infinite time. In particular, from now on we will be focusing mostly on studying cases with infinite time touchdown.

*Degenerate mobility* $n = 2$. As in the previous case, the numerical solution $v$ in Figure 3.3 (a) quickly develops a minimum near the interface, but still has not touched 0 at $t = 10^{10}$, which suggests that the singularity is approached in infinite time.

In Figure 3.3 (a), $v$ seems to converge to a stationary solution $V_* := 1 - U_*$, where $U_*$ solves the free boundary stationary equation (2.16)-(2.18). We also note that in Figure 3.3 the energy of $v$ approaches from above $E[V_*]$ more closely than $E[V]$.

*Degenerate mobility* $n = 4$. The evolution is similar to the previous case, only

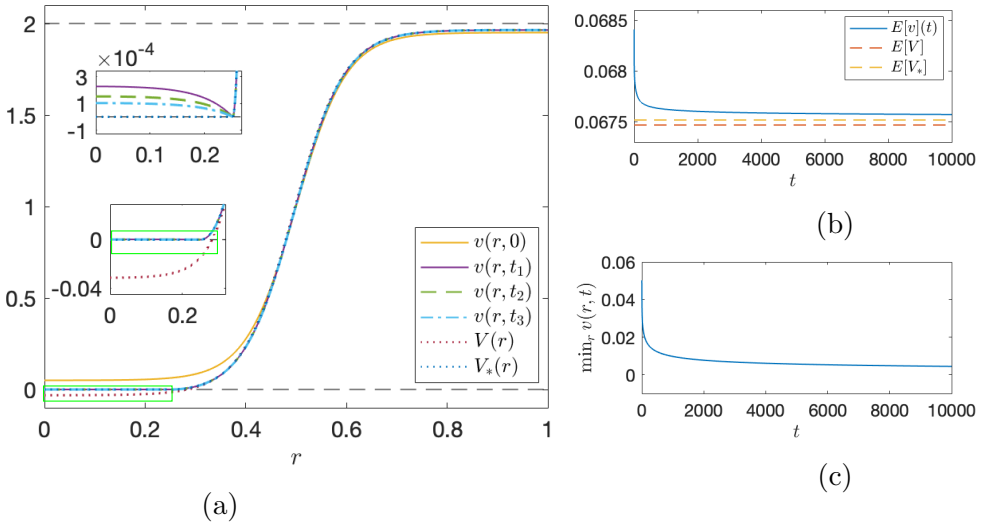



Figure 3.4: (a) Solution $v$ for $n = 4$, for different times $t = 0$, $t_1 = 10^{13}$, $t_2 = 10^{14}$, $t_3 = 10^{15}$, and functions $V = 1 - U$, $V_* = 1 - U_*$ where $U$ and $U_*$ solve (2.12)-(2.13) and (2.16)-(2.18), respectively. (b) Evolution of the energy. (c) Evolution of the minimum.

much slower. In Figure 3.4 (a), we can see that the structure of the solution in the interval $(\overline{r}(t), 1)$ has a similar shape to $V_*$.

We also observe in Figure 3.4 (a) the minimum $\overline{v}(t)$ approaches 0 much faster than $v(0,t)$ as $t \to \infty$. However, the profile of the solution in $(0, \overline{r}(t))$ remains the same, prompting us to seek self-similar solutions with power law scaling factors in time for this region, which we will refer to as the central region. Moreover, from the thin film literature on pinch-off evolution, see for example [13], we can expect the touchdown region to also have a self-similar profile with power law scaling factors in time.

In conclusion, for the cases exhibiting infinite time touchdown, we expect three asymptotic regions when we expand the solution as $t \to \infty$. To leading order the central and touchdown regions are self-similar and the annular region is a steady state.

We will use these insights in the next two chapters, where we discuss the cases $n > 2$ and $n < 2$ separately. It turns out that $n = 2$ is a critical value where the self-similar profiles in the central and touchdown regions change.

# Chapter 4

# Case $n > 2$

In this section we study the problem formulated in Section 2 for the case $n > 2$ numerically and asymptotically as $t \to \infty$. We go over this case first, instead of the whole range including $n < 2$, because touchdown in the numerical simulations happens more slowly for larger $n$, therefore tracking the evolution on a log scale is easier. In Section 4.1 we go over the long-time numerical solution of the degenerate Cahn-Hilliard equation (2.1)-(2.5) to obtain numerical approximations to the self-similarity exponents in the central and touchdown regions. In Section 4.2 we use this information as an ansatz to develop asymptotic expansions for each region, and we solve the leading order equations, analytically where possible and numerically otherwise. The remainder of the section is focused on solving the touchdown region numerically and obtaining a numerical composite solution which we compare to the numerical solution of the partial differential equation. A shorter version of this chapter was published in 2021, see [60].

## 4.1 Numerical results

In the following sub-sections, we will study the evolution of the profiles in the central and touchdown regions for the particular cases $n = 3, 4, 5$, as these provide examples

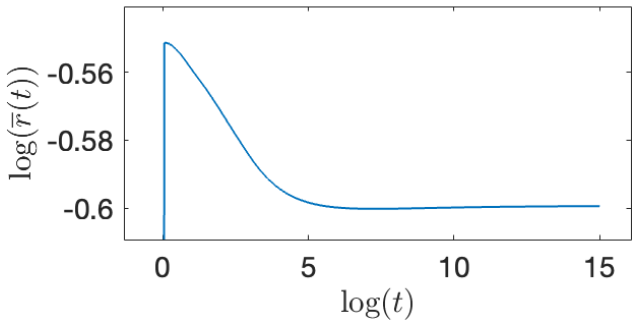



Figure 4.1: $\log(\overline{r}(t))$ versus $\log(t)$, for $n = 4$ and $\varepsilon = 0.1$.

of the touchdown behaviour in the range $n > 2$.

### 4.1.1 Central region

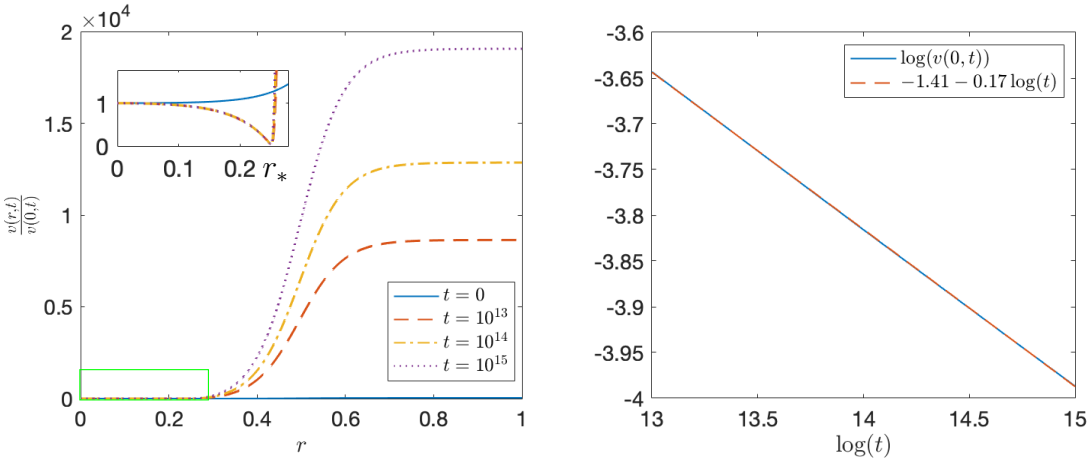
In the central region, using the analysis of the numerical solution for $n = 4$ we make the following general self-similar ansatz:

$$v(r,t) \sim \xi(t)\psi(r), \tag{4.1}$$

where $\psi : r \mapsto \psi(r), \xi : t \mapsto \xi(t)$ are functions to be found. Note that the independent variable is not scaled, since the region it characterises, i.e. $(0, r_*)$ (recall $r_* = \lim_{t\to\infty} \overline{r}(t)$), does not change in long-time. In Figure 4.1 we can see that the location of the minimum of $v$ stabilises at approximately $\log(t) \sim 1$. Moreover, it appears to converge to the limit $r_*$ early on in the evolution of the solution. In this case, $n = 4$ and $r_* = 0.25$ approximately.

Next, suppose that neither $\psi(0)$ nor $v(0,t)$ vanish at time $t$; then (4.1) holds if and only if

$$\frac{v(r,t)}{v(0,t)} \sim \frac{\psi(r)}{\psi(0)},$$




(a) (b)

Figure 4.2: (a) $v(r,t)/v(0,t_k)$ versus $r$ for different times and $n = 4$. (b) Log-log plot of $v(0,t)$.

where the right-hand side does not depend on time. Moreover,

$$\xi(t) \sim \frac{v(0,t)}{\psi(0)} \tag{4.2}$$

for $t > 0$.

For $n = 4$, we plot the function $\frac{v(r,t)}{v(0,t)}$ versus $r$ for several long times until $t = 10^{15}$. We choose this time frame because it is the maximum interval for which it was practical to compute the numerical solution. The grid size needs to be adjusted as the minimum of $v$ gets smaller in the touchdown region, increasing the computational time as time gets large. At $t = 10^{15}$, we already needed a million points to compute a solution.

**Remark 4.1.** *In conversations with past assessors of this work, it was discussed that one way to obtain numerical solutions for longer times was to use an adaptive mesh. This is a promising idea, which we leave for future work. In any case, our current numerical results suffice to give us an ansatz for the asymptotic expansions, which was their main objective.*

Since we expect $\frac{v(r,t)}{v(0,t)}$ to be independent of time near $r = 0$, then all curves should

collapse onto each other in the central region, which is exactly what we see in Figure 4.2 (a).

In Figure 4.2 (b) we observe that the data fits well to a line in the log-log plot for the range $10^{13} < t < 10^{15}$. The mean square error of the linear fitting is $1.3 \times 10^{-7}$ which is very small. This suggests power law behaviour in the outer scaling in equation (4.1). The function $\xi$ has power law behaviour if and only if there exists $\alpha \in \mathbb{R}$ such that

$$\log(v(0,t)) \sim \alpha \log(t) + \log(\psi(0)).$$

Thus, Figure 4.2 (b) suggests that $\xi$ is a power law with negative exponent $\alpha \sim -0.17$, obtained from the fit to the numerical data in Figure 4.2 (b). Hence, we postulate

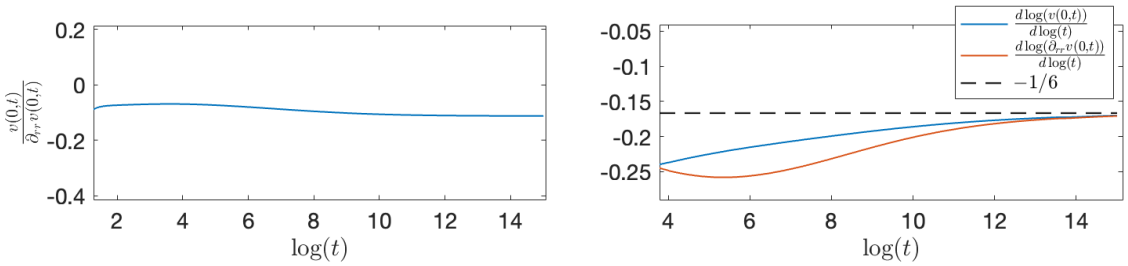
$$v(r,t) \sim t^{\alpha}\psi(r) \quad \text{as } t \to \infty, \tag{4.3}$$

for some $\alpha < 0$. We can now deduce that there cannot be a time scaling of the independent variable $r$ by checking that $v(0,t)$ and $\partial_{rr}v(0,t)$ have the same scaling, since, by applying (4.3) we have

$$v(0,t) \sim t^{\alpha}\psi(0),$$
$$\partial_{rr}v(0,t) \sim t^{\alpha}\partial_{rr}\psi(0).$$

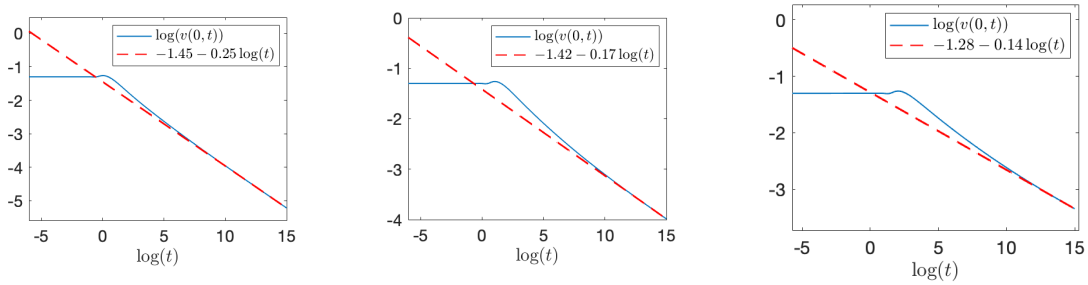
In Figure 4.3 (a) we plot the ratio between both quantities, which seems to converge to a constant in long-time. This implies that they must have the same scaling, at least for longer times. In fact, in Figure 4.3 (b) we confirm that the slopes of the log of these quantities are the same as $t \to 10^{15}$, and, moreover, they approximate the expected value for $\alpha$, obtained from 4.2.

At this stage, the numerical plots provide evidence for the ansatz (4.1) and we can obtain $\alpha$ by doing a linear approximation of $\log(v(0,t))$ for long-time. The result



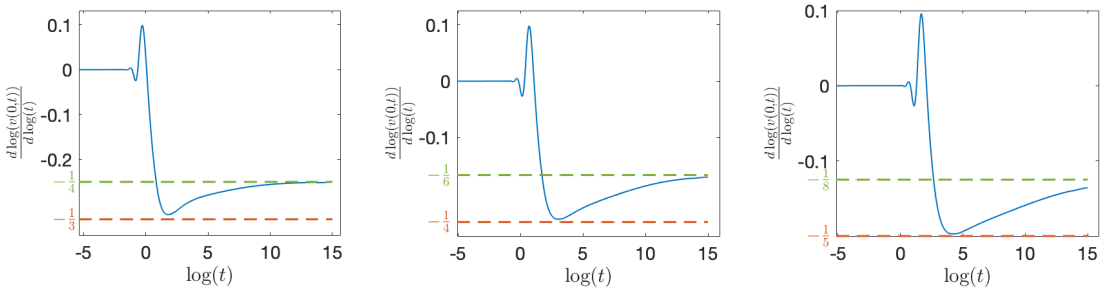

(a) (b)

Figure 4.3: (a) Ratio between $v(0,t)$ and $\partial_{rr}v(0,t)$ versus $\log(t)$, for $n = 4$. (b) Derivatives of the curves $\log(v(0,t))$ and $\log(\partial_{rr}v(0,t))$, dashed line corresponds to the expected value of $\alpha$ according to Figure 4.2.




(a) (b) (c)

Figure 4.4: Linear fitting for $\log(v(0,t))$ versus $\log(t)$ for final time $10^{15}$ and (a) $n = 3$, (b) $n = 4$, (c) $n = 5$.




(a) (b) (c)

Figure 4.5: $\frac{d\log(v(0,t))}{d\log(t)}$ versus $\log(t)$ for final time $10^{15}$ and (a) $n = 3$, (b) $n = 4$, (c) $n = 5$.

is shown in Figure 4.4 for three different $n = 3, 4, 5$. We see that for long times $\log(v(t,0))$ is linear in $\log(t)$, though it appears that two different slopes emerge at different times. To analyse this further we also plot $\frac{d\log(v(0,t)))}{d\log(t)}$ as a function of $\log(t)$ in Figure 4.5 which directly gives the approximate exponent of the power-law behaviour. It is clearly visible that this derivative takes a dip, with the minimum near $-1/3$, $-1/4$ and $-1/5$, or approximately $-\frac{1}{n}$ for $n = 3, 4, 5$ respectively. Then, the derivative moves away from the dip, tending in a longer time to $-1/4$, $-1/6$, $-1/8$ respectively. This is consistent with

$$\alpha = -\frac{1}{2(n-1)}. \tag{4.4}$$

### 4.1.2 Touchdown region

Following similar reasoning as in the central region, we have the following ansatz for the solution near $r = r_*$:

$$v(r,t) \sim \xi_1(t)\varphi(\eta), \tag{4.5}$$

where

$$\eta(r) := \frac{(r - r_*)}{\xi_2(t)},$$

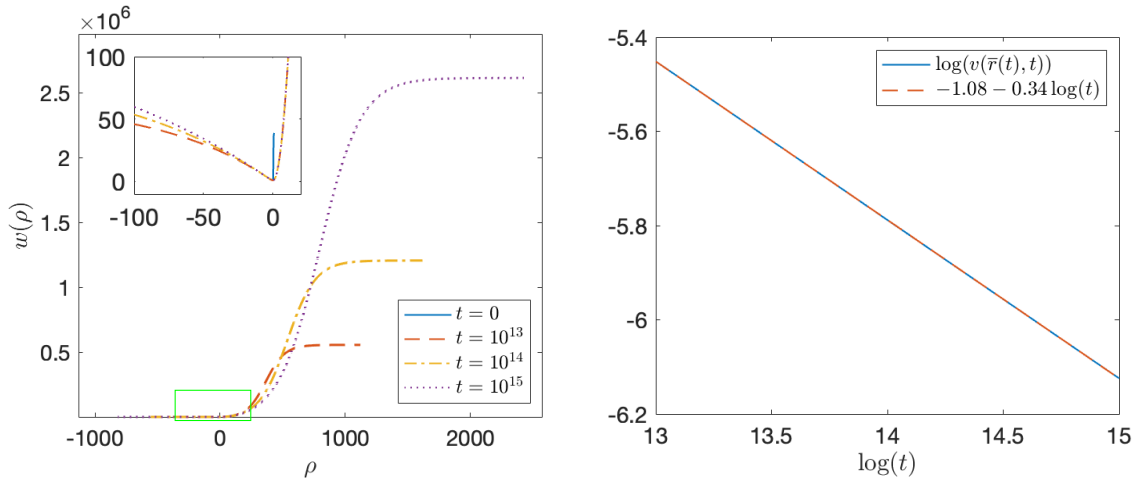
and $\varphi, \xi_1, \xi_2$ are functions to be found. First, note that (4.5) holds if and only if

$$\frac{v(r,t)}{v(r_*,t)} \sim \frac{\varphi(\eta)}{\varphi(0)},$$

where the right-hand side does depend on time through $\eta$. We define

$$w(r,t) := \frac{v(r,t)}{v(\bar{r}(t),t)},$$

where we recall that $\bar{r}(t) = \text{argmin}_{r\in(0,1)} v(r,t)$. Here we assume uniqueness of $\bar{r}$ based on the evidence suggested by simulations. Note that $w$ has minimum 1 and is well




(a) (b)

Figure 4.6: (a) $w(\rho, t)$ versus $\rho$. (b) Log-log plot of $v(\overline{r}(t), t)$. For $n = 4$.

defined because we expect $v(\overline{r}(t), t) > 0$ for all time $t < \infty$. Since we do not know the exact law of how $\xi_2$ behaves, we cannot plot $w$ as a function of $\eta$ directly; instead, we define a rescaled and centred variable

$$\rho := \left( \frac{\partial_{rr} v(r_*, t)}{v(r_*, t)} \right)^{1/2} (r - \overline{r}(t)).$$

If (4.5) holds at long times, then to leading order

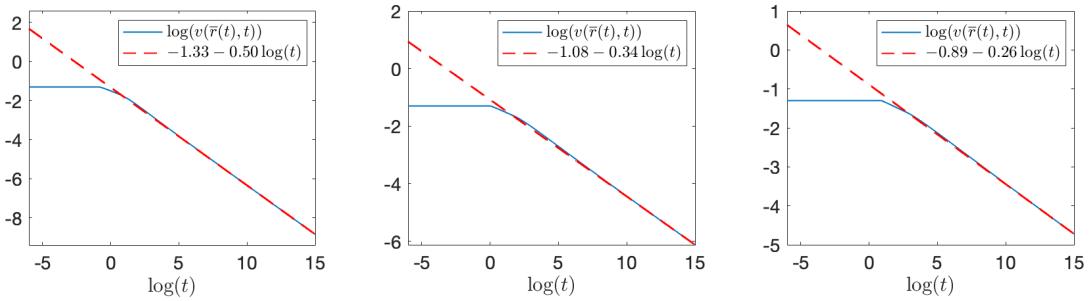
$$\left( \frac{\partial_{rr} v(r_*, t)}{v(r_*, t)} \right)^{-1/2} \sim \left( \frac{\xi_1(t) \partial_{\eta\eta} \varphi_0(0)}{\xi_2^2(t) \xi_1(t) \varphi_0(0)} \right)^{-1/2} \sim \xi_2(t).$$

Plotting $w$ versus $\rho$ in Figure 4.6 (a) allows us to see that the curves collapse nicely around $\rho = 0$, i.e. $r = r_*$, at various long times.

Now, the function $\xi_1$ has power law behaviour if and only if $\log(v(r_*, t)) = \log(\varphi(0)) + \beta \log(t)$, and Fig. 4.6 (b) confirms that $\xi_1$ is a power law with exponent $\beta$ negative, i.e.

$$v(r, t) \sim t^{\beta} \varphi(\eta), \tag{4.6}$$

with $\beta < 0$.




(a) (b) (c)

Figure 4.7: Linear fitting for $\log(v(\overline{r}(t), t))$ versus $\log(t)$ for the final time $10^{15}$ and (a) $n = 3$, (b) $n = 4$, (c) $n = 5$.

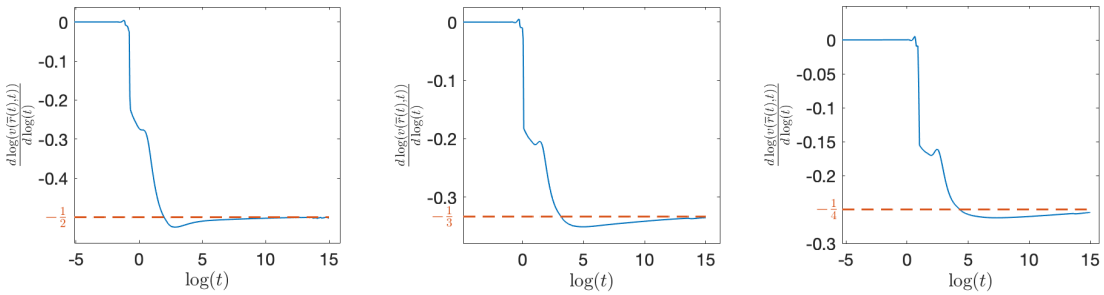
We can obtain $\beta$ in the same way as in the central region. We need to be careful here, as plotting $v(r_*, t)$ at each time step would require knowing $r_*$ at the beginning of each numerical simulation, which would require running each instance of the algorithm twice. We choose a simpler approach by approximating $r_* \sim \overline{r}(t)$, which is valid for long times up to an error of order $O(10^{-4})$ as seen in Figure 4.1 (a) for the central region simulations.

A visible difference between the central and touchdown regions is that the initial dip in Figure 4.8 does not approach a simple constant as in the previous case. This points to a transitional behaviour which might be more complex than in the central region. The rest of the evolution is very similar to the case of the central region. At long times, the curves converge to the values $-1/2$, $-1/3$, $-1/4$ for $n = 3, 4, 5$ respectively. This suggests that a good approximation for the power-law exponent is

$$\beta(n) = -\frac{1}{n-1}. \tag{4.7}$$

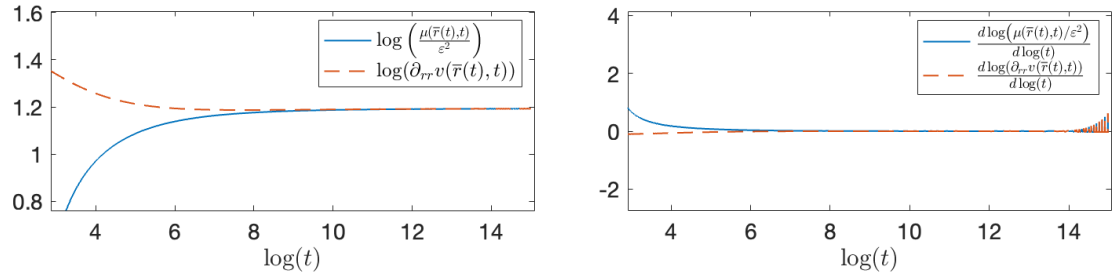
The only part left to characterise is $\xi_2$. To confirm numerically that it also behaves as a power law we note that if $\xi_2(t) = t^\gamma$ for some $\gamma \in \mathbb{R}$, then

$$\partial_{rr} v(r_*, t) \sim t^{\beta - 2\gamma} \partial_{\eta\eta} \varphi(\eta).$$




(a) (b) (c)

Figure 4.8: $\frac{d\log(v(\overline{r}(t),t)))}{d\log(t)}$ versus $\log(t)$ for the final time $10^{15}$ and (a) $n = 3$ , (b) $n = 4$, (c) $n = 5$.




(a) (b)

Figure 4.9: (a) Log-log plot for $\mu(\overline{r}, t)/\varepsilon^2$ and $\partial_{rr}v(\overline{r}, t)$, (b) Derivative of (a) for $n = 4$ and $\varepsilon = 0.05$.

Moreover, when $t$ is large we can roughly approximate the leading order of the chemical potential by

$$\mu(r, t) \sim \varepsilon^2 \partial_{rr} v(r, t).$$

Thus, both functions should behave linearly when we plot their logarithms. Even better, we see in Figure 4.9 that for long times not only both are linear and coincide, but the line they converge to has an approximate slope of 0. This indicates that $\beta - 2\gamma = 0$, and hence $\gamma = \frac{\beta}{2}$, which implies $\alpha = \gamma$. Substituting (4.7) we get that a good approximation of the exponent is

$$\gamma(n) = -\frac{1}{2(n-1)}. \tag{4.8}$$

**Remark 4.2.** *We chose* $\varepsilon = 0.05$ *for Figure 4.9, instead of our standard* $\varepsilon = 0.1$*, because our second-order centered difference approximation of* $\partial_{rr} v(\overline{r}(t), t)$ *breaks down for relatively large* $\varepsilon$ *as* $\log(t) \to 15$*. In choosing a different* $\varepsilon$*, we are assuming that the similarity exponents are independent of* $\varepsilon$*. Some features, like the interface width and the position or* $r_*$*, are, to leading order, expected to depend on* $\varepsilon$*, because of what was seen for the stationary cases in [56] and [49]. However, the simulations done in Section B.4 for different values of* $\varepsilon$ *imply the self-similar profile and its exponents do not change with* $\varepsilon$ *as* $t \to \infty$*.*

## 4.2 Long-time asymptotic analysis

In this section, we carry out a long-time asymptotic analysis of the solution to (2.6)-(2.11) via singular perturbation theory. For this purpose, we introduce the following time scaling

$$t = \frac{\tau}{\delta}, \tag{4.9}$$

where $0 < \delta \ll 1$ is the small parameter on which the asymptotic analysis is based and $\tau$ is an independent variable, which we have introduced because we find it helpful to separate the magnitude $\delta$ from the variable $\tau$.

We first formulate the leading order problem in each of the three regions (central, touchdown and annular) then solve and match them to form a composite solution, which finally we compare with the numerical solution to the partial differential equation. We also note that, while $\varepsilon$ is also small, we will treat it as a fixed parameter. In particular, we will not take advantage of the asymptotic sub-structure of the annular region that was established by Lee et al. [49], although we will make use of their leading order approximations to match the expansion in the touchdown region.

For the central and touchdown regions, it is convenient to formulate the problem in terms of $v = 1 - u$. Substituting this into (2.6)-(2.11) and rescaling time according

to (4.9), we obtain for $v = v(r, \tau)$ that

$$\delta \partial_\tau v = -\frac{1}{r}\partial_r \left( r M_n(v) \partial_r \mu \right), \tag{4.10}$$

$$\mu = \varepsilon^2 \frac{1}{r}\partial_r \left( r \partial_r v \right) + 2(-v^3 + 3v^2 - 2v), \tag{4.11}$$

where $(r, \tau) \in (0, 1) \times \mathbb{R}_+$. From the numerical results from the previous section, we anticipate that the solution will be positive, i.e. $v(r, \tau) > 0$ for all $r \in [0, 1]$ and $\tau < \infty$, and thus we only look for positive solutions, which allows us to take $M_n(v) = v^n[(2 - v)_+]^n$ (without positive part in the first term on the left, $v^n$). We also state the boundary conditions for $v$ as follows:

$$\partial_r v(1, \tau) = 0, \tag{4.12}$$

$$M_n(v(1, \tau))\partial_r \mu(1, \tau) = 0, \tag{4.13}$$

$$\partial_r v(0, \tau) = 0, \tag{4.14}$$

$$\partial_r \mu(0, \tau) = 0. \tag{4.15}$$

We recall that these boundary conditions come from the Neumann (2.8), no-flux (2.9) and smoothness constraints (2.10)-(2.11), respectively.

Notice that we have written the problem as a system of two partial differential equations in terms of $v$ and $\mu$; however, we record the flux for later computations separately as

$$j = -M_n(v)\partial_r \mu. \tag{4.16}$$

### 4.2.1 Central region

We start from (4.10), (4.11) with boundary conditions (4.14), (4.15) and assume, using the insight gained from the numerical results, that $v$ can be expanded as

$$v_{central}(r,\tau) = \delta^{-\alpha}\tau^{\alpha}\psi_0(r) + o(\delta^{-\alpha}), \tag{4.17}$$

for some $\alpha \in \mathbb{R}$ and nonnegative function $\psi_0 : r \mapsto \psi_0(r)$. We focus on the case $\alpha < 0$, since otherwise the solution would either grow unbounded as $\delta \to 0$ or be independent of time.

Substituting (4.17) in (4.10)-(4.11) we get

$$\begin{aligned}\delta^{-\alpha+1}(\alpha\tau^{\alpha-1}\psi_0 + o(\delta^{-\alpha})) =& -\frac{1}{r}\partial_r[r(\delta^{-\alpha}\tau^{\alpha}\psi_0 + o(\delta^{-\alpha}))^n \\ &\cdot [(2 - (\delta^{-\alpha}\tau^{\alpha}\psi_0 + o(\delta^{-\alpha})))_+]^n\partial_r\mu], \qquad (4.18)\\ \mu =& \varepsilon^2\delta^{-\alpha}\tau^{\alpha}\left(\partial_{rr}\psi_0 + \frac{1}{r}\partial_r\psi_0 + o(\delta^{-\alpha})\right) \\ &+ 2[-(\delta^{-\alpha}\tau^{\alpha}\psi_0 + o(\delta^{-\alpha}))^3 + 3(\delta^{-\alpha}\tau^{\alpha}\psi_0 o(\delta^{-\alpha}))^2 \\ &- 2(\delta^{-\alpha}\tau^{\alpha}\psi_0 + o(\delta^{-\alpha}))]. \qquad (4.19)\end{aligned}$$

Expanding the binomials in (4.18)-(4.19) and discarding higher order terms in $\delta$, we obtain the following leading order terms

$$\begin{aligned}\alpha\delta^{-\alpha+1}\tau^{\alpha-1}\psi_0 =& -\frac{1}{r}\partial_r[r\delta^{-n\alpha}\tau^{n\alpha}\psi_0^n 2^n\partial_r\mu] + h.o.t.,\\ \mu =& \varepsilon^2\delta^{-\alpha}\tau^{\alpha}\left(\partial_{rr}\psi_0 + \frac{1}{r}\partial_r\psi_0\right)\\ &+ 2[-\delta^{-3\alpha}\tau^{3\alpha}\psi_0^3 + 3\delta^{-2\alpha}\tau^{2\alpha}\psi_0^2 - 2\delta^{-\alpha}\tau^{\alpha}\psi_0] + h.o.t.,\end{aligned}$$

where h.o.t. means higher order terms, i.e. that they go faster to 0 than the other terms in the equation. Since $\alpha < 0$, the terms in $\mu$ that go to 0 slowest as $\delta \to 0$

must be the ones of order $\delta^{-\alpha}$. Thus, after substituting the chemical potential back into the equation, to leading order the equation is

$$\alpha\delta^{-\alpha+1}\tau^{\alpha-1}\psi_0 = -\delta^{-(n+1)\alpha}\tau^{(n+1)\alpha}\frac{2^n}{r}\partial_r\left[r\psi_0^n\partial_r\left(\varepsilon^2\left(\partial_{rr}\psi_0+\frac{1}{r}\partial_r\psi_0\right)-4\psi_0\right)\right].$$

Balancing the two sides would require $\alpha = -1/n$, but this is not consistent with the numerical results, for which $\alpha$ is clearly larger. In that case, the right-hand side of the equation dominates, which, as $\delta \to 0$, means that the left-hand side (the time derivative) vanishes much faster. Hence, after cancelling constants and $\tau$ terms, we obtain

$$\partial_r\left[r\psi_0^n\partial_r\left(\varepsilon^2\left(\partial_{rr}\psi_0+\frac{1}{r}\partial_r\psi_0\right)-4\psi_0\right)\right] = 0.$$

We integrate twice in $r$, using the no-flux boundary condition at the origin (4.15) to cancel the first integration constant, and we arrive at the leading order central region problem

$$\varepsilon^2\left(\partial_{rr}\psi_0(r)+\frac{1}{r}\partial_r\psi_0(r)\right)-4\psi_0(r) = c_1, \quad r\in(0,r_*) \tag{4.20}$$

$$\partial_r\psi_0(0) = 0, \tag{4.21}$$

where $c_1 \in \mathbb{R}$ is an unknown constant that comes from the second integration. Note that this formulation does not include the boundary condition on $\mu$ at $r = 0$, as it was implicitly used in the derivation of (4.20). Also, notice that this problem does not depend directly on $n$; rather the leading order of $v_{central}$ will only depend on $n$ through $\alpha$.

The general solution of (4.20)-(4.21) can be directly computed as

$$\psi_0(r) = -\frac{c_1}{4}+c_2 I_0\left(\frac{2}{\varepsilon}r\right),$$

where $I_0$ is the modified Bessel function of the first kind and $c_2 \in \mathbb{R}$ is an integration constant.

This solution will be matched to the solution in the touchdown region, which plays the asymptotic role of an inner solution. Moreover, the dependent variable is small (in terms of $\delta \ll 1$) compared to the solution in the central region. Thus $\psi_0$ must match to zero at $r = r_*$, i.e.

$$\psi_0(r_*) = 0. \tag{4.22}$$

In fact, any condition of the type $\psi_0(r_*) = a \neq 0$ will not enter at the leading order of the composite expansion, because any constant translation of $\psi_0$ will match to a correction (and thus higher order) in the touchdown region.

We expand $\psi_0$ around $r_*$ using its Taylor expansion

$$\psi_0(r) = -\frac{c_1}{4} + c_2 I_0\left(\frac{2}{\varepsilon} r_*\right) + \frac{2c_2}{\varepsilon} I_0'\left(\frac{2}{\varepsilon} r_*\right)(r - r_*) + O((r - r_*)^2).$$

Then, condition (4.22) allows us to eliminate $c_1$, obtaining

$$\psi_0(r) = c_2\left(-I_0\left(\frac{2}{\varepsilon} r_*\right) + I_0\left(\frac{2}{\varepsilon} r\right)\right). \tag{4.23}$$

This solution is only valid for $0 \leq r \leq r_*$, and we extend it by setting $\psi_0 \equiv 0$ for $r_* < r \leq 1$ where this is necessary, for example, in the evaluation of the composite expansion in the full domain $0 \leq r \leq 1$ in Section 4.4.

The remaining constant $c_2$ is an unknown parameter that corresponds to a normalisation of the solution. We will obtain an expression for it through the matching to the touchdown region.

For later calculations, we also record the Taylor expansion of $\psi_0$:

$$\psi_0(r) = a_1(r - r_*) + O((r - r_*)^2), \tag{4.24}$$

where

$$a_1 := \frac{2c_2}{\varepsilon} I_0'\left(\frac{2}{\varepsilon} r_*\right) \neq 0, \tag{4.25}$$

which is non-zero since the modified Bessel function has a positive first derivative for positive arguments.

### 4.2.2 Touchdown region

In this region, we introduce the independent variable

$$\eta := \frac{r - r_*}{\delta^{-\gamma}\tau^{\gamma}}, \tag{4.26}$$

where $\gamma \in \mathbb{R}$. We take $\gamma < 0$, since otherwise, in the limit $\delta \to 0$ the domain of $\eta$ would collapse onto a single point.

As suggested by our numerical simulations we expand the solution as

$$v_{touchdown}(\eta, \tau) = \delta^{-\beta}\tau^{\beta}\varphi_0(\eta) + o(\delta^{-\beta}), \tag{4.27}$$

where $\beta < 0$ is negative to guarantee boundedness and $\varphi_0 : \eta \mapsto \varphi_0(\eta)$ is a nonnegative function. Substituting $\eta$ and (4.27) into (4.10)-(4.11), we obtain the leading order terms

$$\delta^{-\beta+1}(-\gamma\eta\tau^{-1}\partial_\eta\varphi_0) = -\frac{\tau^{-2\gamma}\delta^{2\gamma-n\beta}2^n}{\eta\left(\frac{\tau}{\delta}\right)^{\gamma} + r_*}\partial_\eta\left(\left(\eta\left(\frac{\tau}{\delta}\right)^{\gamma} + r_*\right)\varphi_0^n\partial_\eta\mu\right) + h.o.t., \tag{4.28}$$

$$\begin{aligned}\mu =& \varepsilon^2\left(\tau^{-2\gamma}\delta^{2\gamma-\beta}\partial_{\eta\eta}\varphi_0 + \frac{\tau^{-\gamma}\delta^{\gamma-\beta}}{\eta\left(\frac{\tau}{\delta}\right)^{\gamma} + r_*}\partial_\eta\varphi_0\right) \\ &+ 2(-\delta^{-3\beta}\varphi_0^3 + 3\delta^{-2\beta}\varphi_0^2 - 2\delta^{-\beta}\varphi_0) + h.o.t..\end{aligned} \tag{4.29}$$

We use that $\beta, \gamma < 0$ to discard higher order terms and then substitute (4.29) in

(4.28), which gives us the following leading order equation:

$$\delta^{-\beta+1}(-\gamma\eta\tau^{-1}\partial_\eta\varphi_0) = -\,\delta^{4\gamma-(n+1)\beta}\frac{\tau^{-4\gamma}\varepsilon^2 2^n}{\eta\left(\frac{\tau}{\delta}\right)^\gamma + r_*}\partial_\eta\left(\left(\eta\left(\frac{\tau}{\delta}\right)^\gamma + r_*\right)\varphi_0^n\partial_{\eta\eta\eta}\varphi_0\right).$$

Similarly as in the central region, balancing would require $\beta = \frac{4\gamma-1}{n}$, however the numerical simulations in Section 4.1.2 suggest that $\beta$ is larger. Therefore, the equation for the dominant terms, obtained after some simplifications, is

$$0 = \partial_\eta\left(\left(\eta\left(\frac{\tau}{\delta}\right)^\gamma + r_*\right)\varphi_0^n\partial_{\eta\eta\eta}\varphi_0\right).$$

Integrating once and simplifying, we arrive at the leading order touchdown problem

$$\varphi_0^n(\eta)\partial_{\eta\eta\eta}\varphi_0(\eta) = J, \tag{4.30}$$

where the unknown flux $J \in \mathbb{R}$ appears as an integration constant. This third-order problem requires four conditions to fix all degrees of freedom, which need to come from matching to the central region as $\eta \to -\infty$ and to the annular region as $\eta \to +\infty$, where both act as larger/outer regions. We will discuss these expansions in detail later in Section 4.2.4.

Before moving on to the next region there are two useful observations to make. First, to match to a leading order $O(1)$ contribution in the annular region, the leading order term of $\varphi_0$ must be $\sim \eta^{\beta/\gamma}$ for $\eta \to \infty$. Otherwise, rescaling $\eta$ and $\varphi_0$ into the outer variables will not give an $O(1)$ term. From the numerical results, we readily notice that $\gamma < \beta$, hence $\varphi_0$ grows faster than linear. In fact, the data from Figure 4.9 in Section 4.1 suggests that they differ by a factor of two, but the weaker condition is sufficient to select the correct behaviour for the inner expansion of the solution in the annular region. We, therefore, anticipate that to match successfully to the outer

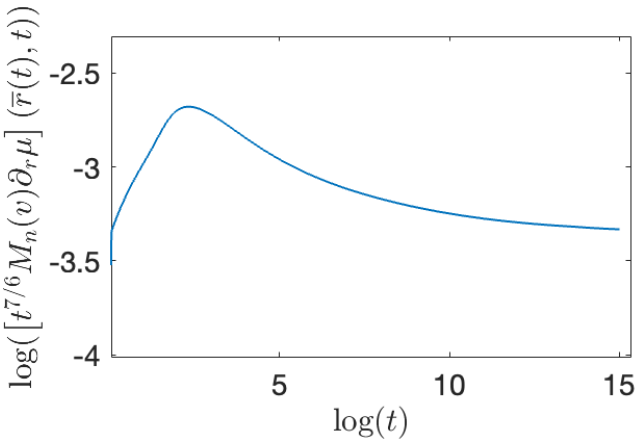



Figure 4.10: Plot of an approximation of flux $J$ over a long-time interval in log-log scale.

region $\varphi_0$ must satisfy

$$\varphi_0(\eta) \gg \eta, \qquad \text{as } \eta \to \infty. \tag{4.31}$$

Second, we remark for later that there is numerical evidence indicating $J > 0$, since, for long times and $r \sim r_*$, $J$ can be approximated as

$$J = \varphi^n \partial_{\eta\eta\eta}\varphi + O(\delta^{-\beta}) \sim t^{3\gamma - n\beta} v^n \partial_{rrr} v \sim \frac{1}{\varepsilon^2} t^{3\gamma - n\beta} M_n(v)\partial_r \mu(v) = \frac{1}{\varepsilon^2} t^{3\gamma - n\beta} j.$$

We can see in Figure 4.10 that, at least for $n = 4$ and using (4.4), (4.7), (4.8), this last quantity is constant and positive.

### 4.2.3 Annular region

In the numerical simulations from Section 4.1, we saw that the solution evolves much slower in the annular interval $(\overline{r}(t), 1)$, at least compared with the central and touch-down regions. We state this by defining

$$v_{annular}(r, \tau) = 1 - U_*(r) + o(1), \tag{4.32}$$

where $U_* = U_*(r)$ is the solution obtained by substituting $\partial_t u \equiv 0$ into (2.6)-(2.11), i.e.

$$0 = \frac{1}{r}\partial_r \left( r M_n(U_*) \partial_r \mu \right), \quad r \in (r_*, 1), \tag{4.33}$$

$$\mu = -\varepsilon^2 \frac{1}{r}\partial_r \left( r \partial_r U_* \right) + f'(U_*), \quad r \in (r_*, 1), \tag{4.34}$$

$$0 = \partial_r U_*(1), \tag{4.35}$$

$$0 = M_n(U_*(1)) \partial_r \mu(1), \tag{4.36}$$

We integrate (4.33) twice, using (4.36) to eliminate the first integration constant, then use the fact that $M_n(U_*)$ does not vanish inside $(r_*, 1)$ (because we expect infinite time touchdown only at $r_* = \lim_{t\to\infty} \overline{r}(t)$), and substitute (4.34) into (4.33) to obtain

$$\begin{aligned} -\frac{\varepsilon^2}{r}\frac{d}{dr}\left( r \frac{dU_*}{dr} \right) + f'(U_*) =& \sigma, \quad r \in (r_*, 1), \\ U_*'(1) =& 0, \end{aligned}$$

where $\sigma \in \mathbb{R}$ is an unknown integration constant. This system can be written as a system of first order non-degenerate ordinary differential equations that has no singularities for $r \in (r_*, 1)$. Therefore, solutions can be locally expanded in Taylor series.

In particular, as $r \to r_*$ we have

$$v_{annular} = 1 - U_* + o(1) = b_0 + b_1(r - r_*) + b_2(r - r_*)^2 + O((r - r_*)^3) + o(1),$$

for $\delta \ll 1$. Since the solution in the touchdown region is asymptotically small, compared to the annular region, we must have $b_0 = 0$. Due to the previous observation

in (4.31), we can also set $b_1 = 0$. Thus, the final annular problem is

$$-\frac{\varepsilon^2}{r}\frac{d}{dr}\left(r\frac{dU_*}{dr}\right) + f'(U_*) = \sigma, \quad r \in (r_*, 1), \tag{4.37}$$

$$U_*'(1) = 0, \tag{4.38}$$

$$U_*(r_*) = 1, \quad U_*'(r_*) = 0. \tag{4.39}$$

For $0 \leq r < r_*$ we set the solution to $U_* \equiv 1$. Note that this corresponds exactly to the stationary solution $U_*$ discussed in Chapters 2 and 4.1, which has been analysed in more detail by Lee et. al. [49]. Moreover, note that this problem does not depend on the degree of degeneracy of the mobility $n$. In [49], an approximation for $0 < \varepsilon \ll 1$ was found using matched asymptotics. Since we decided early on to only expand in time, we are keeping $\varepsilon$ fixed and we solve problem (4.37)-(4.39) numerically.

As in [49] one needs to add an extra condition to solve for unknown $r_*$, by either fixing the position of the interface, i.e. choosing $r_0 \in (r_*, 1)$ such that $U_*(r_0) = 0$, or adding the mass constraint that comes from the evolution equation. We will do the latter and define

$$S(r) := \int_{r_*}^{r} U_*(s) s \, ds.$$

The system (4.37)-(4.39) can be then written as the following system of first order ordinary differential equations:

$$S' = U_* r, \quad r \in (r_*, 1), \tag{4.40}$$

$$U_*' = W, \quad r \in (r_*, 1), \tag{4.41}$$

$$W' = \frac{2}{\varepsilon^2} U_*(U_*^2 - 1) - \frac{\sigma}{\varepsilon^2} - \frac{1}{r} W, \quad r \in (r_*, 1), \tag{4.42}$$

$$\sigma' = 0, \quad r \in (r_*, 1), \tag{4.43}$$

$$U_*(r_*) = 1, \quad W(r_*) = 0, \quad S(r_*) = 0 \tag{4.44}$$

$$W(1) = 0, \quad S(1) = m_1 \tag{4.45}$$

where $'$ denotes $\frac{d}{dr}$, $W := U_*''$ and we set

$$m_1 := \int_0^1 u_{init}(r) r dr - \frac{{r_*}^2}{2},$$

so that the mass is conserved in accordance with the initial condition of the evolution equation.

To solve this system numerically we use a bisection method. Specifically, for $r_*$ in a mesh of the interval $(0, 1)$ we solve equations (4.40)-(4.43) in the interval $(r_*, 1)$ with the boundary conditions

$$\begin{aligned} U_*(r_*) =& 1, \quad W(r_*) = 0, \quad S(r_*) = 0 \\ W(1) =& 0, \end{aligned}$$

until we identify a solution such that $S(1) = m_1$ up to a tolerance of $10^{-3}$. This gives us an estimate for $r_*$, $U_*$ and $\sigma$ that provides us with a solution which satisfies the stationary problem with the mass constraint. The existence and uniqueness of such a solution are not ensured by the theory. However, numerically, we found that there is a monotonic dependence between $r_*$ and $m_1$ which allows us to find a solution using the bisection method.

We note that, for each instance of $r_*$, we solve the system of ordinary differential equations (4.40)-(4.45) using bvp4c from Matlab, where we adopt the following guess to initialise the algorithm:

$$\begin{aligned} S(r) =& -\int_0^1 \tanh\left(\frac{r - 0.5}{\varepsilon}\right) r dr, \\ U_*(r) =& -\tanh\left(\frac{r - 0.5}{\varepsilon}\right), \\ W(r) =& -\frac{1}{\varepsilon}\left(\operatorname{sech}\left(\frac{r - 0.5}{\varepsilon}\right)\right)^2, \\ \sigma(r) =& 1. \end{aligned}$$

The initial guesses for $U_*$ and $W$ are near enough to the leading order expansion found in [49] so that the algorithm, which is very sensitive to the choice of initial guess, converges.

Before moving on to the matching, we state, for later use, the Taylor series of the annular approximation for $r$ close to $r_*$. For $r \to r_*$, we have

$$v_{annular}(r,\tau) = b_2(r-r_*)^2 + O((r-r_*)^4) + o(\delta), \tag{4.46}$$

where $0 < \delta \ll 1$, and

$$b_2 := \frac{\sigma}{2\varepsilon^2}, \tag{4.47}$$

which we have obtained from the asymptotic expansion $\check{v} := 1 - \check{u}$ defined in (A.15) in Appendix A.2, derived in Lee et. al. [49]. One could use a different approach to obtain an approximate value for $b_2$, namely using $b_2 = \frac{W'(r_*)}{2}$, which would remove the reliance on the Lee et. al. asymptotics. However, the error we are introducing by choosing to use the Lee et. al. approximation for $b_2$, instead of the numerical value, is comparable to other error contributions from the long-time expansion and would change the resulting plots only very slightly. In any case, the choice of $b_2 = \frac{W'(r_*)}{2}$ should be explored further in the future as a way to make the present approximations independent of [49].

### 4.2.4 Matching

*Central and touchdown regions.* To match the central and touchdown regions we need to match the leading orders of, first, the solutions, and then the fluxes. We already have an expansion for $\psi_0$ as $r \to r_*$, given by (4.24). Thus we only need to find the expansion for $\varphi_0$ as $\eta \to -\infty$.

We expand $\varphi_0$, solution to

$$\varphi_0^n \partial_{\eta\eta\eta}\varphi_0 = J, \quad \eta \in (-\infty, \infty),$$

as $\eta \to -\infty$, where $J > 0$ is unknown. Since we already know $\varphi_0$ has to match to a Taylor expansion from the central region, i.e. a polynomial in the variable $(r - r_*)$, we expect the expansion of the touchdown solution to be expressible in powers of $\eta$. If we let $x := -\eta$ and suppose that

$$\varphi_0(x) = Ax^p + o(x^p),$$

for some $p, A \in \mathbb{R}$, as $x \to \infty$, then

$$p(p-1)(p-2)A^{n+1}x^{(n+1)p-3} + o(x^{(n+1)p-3}) = -J. \tag{4.48}$$

Now there are two possibilities: either the leading order term on the left balances $-J$ or the higher order correction term does.

In the first case, we must have

$$p(p-1)(p-2)A^{n+1}x^{(n+1)p-3} = -J,$$

which implies that $p = \frac{3}{n+1}$ and

$$A^{n+1} = \frac{-J(n+1)^3}{3(n-1)(n-2)}.$$

If $n > 2$, then $A$ is negative and thus $\varphi_0 \to -\infty$ as $x \to \infty$. But we are looking for non-negative solutions, which eliminates this case.

The second case implies that the leading order term on the left-hand side of (4.48) must be zero. Because the solution is not identically zero this implies that $p$ takes one

of the values $0, 1, 2$. Moreover, since the central solution expansion (4.24) is linear to leading order, we focus on the case $p = 1$. Thus $\varphi_0$ must have the form

$$\varphi_0(x) = Ax + \phi(x) + o(\phi(x)),$$

where $\phi$ is a correction of order $o(x)$, which satisfies

$$(Ax + \phi + o(\phi))^n \phi''' = -J, \quad x \in (-\infty, \infty).$$

Again, we have two possibilities: either the leading term on the left balances $-J$ or $-J$ is of higher order. The first case implies that

$$A^n x^n \phi''' = -J.$$

If $2 < n < 3$ or $3 < n$, then by brute force integration we have

$$\phi = Bx^2 + Cx + \frac{Jx^{3-n}}{A^n(n-1)(n-2)(n-3)} + D,$$

where $B, C, D$ are unknown constants. Since $\phi$ should be of higher order as $x \to \infty$, we need only maintain the sublinear terms

$$\phi = \frac{Jx^{3-n}}{A^n(n-1)(n-2)(n-3)} + D,$$

where we have used that $x^{3-n} \ll x$ as $x \to \infty$ for $n > 2$. Note that $x^{3-n}$ is of higher order than $D$ if $n < 3$ and of lower order if $n > 3$.

On the other hand, if $n = 3$, integration gives us

$$\phi = Bx^2 + Cx + \frac{-J}{2A^3} \ln(x) + D,$$

where $B, C, D$ are unknown constants, and again we only keep

$$\phi = \frac{-J}{2A^3}\ln(x) + D.$$

If the next order term balances $-J$, then $\phi''' = 0$, and since $\phi$ must be sublinear, we obtain $\phi = D$ is constant.

We can summarise the expansion of $\varphi_0$ for $n > 2$ when $\eta \to -\infty$, in order of magnitude, as

$$\varphi_0(\eta) = \begin{cases} A_-\eta + \frac{J(-\eta)^{3-n}}{A_-^n(n-1)(n-2)(n-3)} + B_- + O(1) & \text{if } n < 3, \\ A_-\eta + \frac{J}{2A_-^3}\ln(-\eta) + B_- + O(1) & \text{if } n = 3, \\ A_-\eta + B_- + O(1) & \text{if } n > 3, \end{cases} \tag{4.49}$$

where $A_-, B_-$ are unknown constants.

We note that this analysis is inconsistent for $0 < n \leq 2$, since the correction one obtains is $\phi \sim x\ln(x)$ which is superlinear as $x \to \infty$. This implies that for $0 < n \leq 2$, the matching cannot be linear and thus the central problem must involve other terms and a different type of matching. Because this possibility constitutes an important part of the analysis, we must treat the case $0 < n \leq 2$ separately in Chapter 5.

We note that for $n = 3$, the second term in $v_{touchdown} = t^\alpha\varphi_0(\eta)$ after substituting $\varphi_0$ with (4.49), becomes

$$\frac{J}{2A_-^3}\delta^{-\beta}\tau^\beta \ln\left(-\frac{\delta^\gamma(r - r_*)}{\tau^\gamma}\right).$$

This term is actually $o(\delta^{-\beta})$, since $\delta^{-\beta}\ln\left(-\frac{\delta^\gamma(r-r_*)}{\tau^\gamma}\right) \to 0$ as $\delta \to 0$ (because $\beta, \gamma < 0$). Therefore, it is not involved in the leading order matching. For $n \neq 3$, the term

$\delta^{-\beta}\tau^{\beta}B_-$ is $O(\delta^{-\beta})$. In addition, the term

$$\delta^{-\beta+\gamma(3-n)}\tau^{\beta-\gamma(3-n)}\frac{J(r_*-r)^{3-n}}{A_-^n(n-1)(n-2)(n-3)}$$

is $O(\delta^{-\beta})$ if $n > 3$; however for $0 < n < 3$ it is $O(\delta^{-\beta+\gamma(3-n)})$ and we must keep it in the expansion.

Finally, we have that the central region expansion is

$$v_{central}(r,\tau) = a_1\delta^{-\alpha}\tau^{\alpha}(r-r_*) + O(\delta^{-\alpha}) = a_1\delta^{-\alpha-\gamma}\tau^{\alpha+\gamma}\eta + O(\delta^{-\alpha}),$$

as $r \to {r_*}^-$, where $a_1$ is given by (4.25), and the touchdown expansion is

$$v_{touchdown}(\tau,\eta) = A_-\delta^{-\beta}\tau^{\beta}\eta + O(\delta^{-\beta+\gamma(3-n)})$$

as $\eta \to -\infty$, with $A_- \in \mathbb{R}$ unknown. Thus, matching the two expansions at leading order requires

$$\alpha = \beta - \gamma, \quad A_- = -a_1. \tag{4.50}$$

Now that we have matched the solutions, we examine the flux (4.16). One can obtain a partial mass conservation condition in the interval $(0, r_*)$ by multiplying (4.10) by $r$, integrating over $(0, r_*)$ and using the boundary condition at $r = 0$ (4.15), which gives the following:

$$\int_0^{r_*} \partial_t v(r,t) r dr = -r_* M_n(v(r_*,t))\partial_r \mu(r_*,t).$$

This result means that the rate of change in the mass in the interval $(0, r_*)$ is equal to the flux at $r_*$. By using the asymptotic approximations (4.17) and (4.27), this

implies, up to leading order, that

$$\alpha\delta^{-\alpha+1}\tau^{\alpha-1}\int_0^{r_*}\psi_0(r)rdr = -r_*\delta^{-\beta(n+1)+3\gamma}\tau^{\beta(n+1)-3\gamma}2^n\varepsilon^2\varphi_0^n(\eta)\partial_{\eta\eta\eta}\varphi_0(\eta). \quad (4.51)$$

We substitute the function $\psi_0$ obtained in (4.23) into the left-hand side of (4.51) and use that $\varphi_0$ satisfies equation (4.30) to obtain the following:

$$-\alpha\delta^{-\alpha+1}\tau^{\alpha-1}\frac{c_2{r_*}^2}{2}I_2\left(\frac{2r_*}{\varepsilon}\right) = -r_*\delta^{-\beta(n+1)+3\gamma}\tau^{\beta(n+1)-3\gamma}2^n\varepsilon^2 J,$$

To match the two sides we require

$$\alpha - 1 = \beta(n+1) - 3\gamma \quad (4.52)$$

and

$$\alpha\frac{c_2 r_*}{2^{n+1}\varepsilon^2}I_2\left(\frac{2r_*}{\varepsilon}\right) = J. \quad (4.53)$$

*Annular and touchdown regions.* We wish to match $\varphi_0$ with $1-U_*$. As before, we already have an expansion for $1-U_*$ as $r \to r_*$, given by (4.46). Thus we only need to find an appropriate expansion for $\varphi_0$ as $\eta \to \infty$.

We expand $\varphi_0$, solution to

$$\varphi_0^n\partial_{\eta\eta\eta}\varphi_0 = J,$$

as $\eta \to \infty$, where $J > 0$ is an unknown constant. Again we expect the expansion of the touchdown solution to be in powers of $\eta$, i.e. we suppose

$$\varphi_0(\eta) = A\eta^p + o(\eta^p),$$

for some $p, A \in \mathbb{R}$. Then

$$p(p-1)(p-2)A^{n+1}\eta^{(n+1)p-3} + o(\eta^{(n+1)p-3}) = J. \quad (4.54)$$

Again there are two possibilities: either the leading order term on the left-hand side balances $J$ or $J$ is of higher order.

In the first case, we have

$$p(p-1)(p-2)A^{n+1}\eta^{(n+1)p-3} = J,$$

which implies $p = \frac{3}{n+1}$ and

$$A = \left(\frac{J(n+1)^3}{3(n-1)(n-2)}\right)^{\frac{1}{n+1}}.$$

We must discard this case since we wish to match to the leading order of the annular region, which is quadratic in $(r - r_*)$. Therefore, we need at least $p = 2$, which eliminates this case.

The second case implies that the leading order term on the left-hand side of (4.54) must be zero, which implies that $p = 0, 1, 2$, and since the leading order of expansion (4.46) is quadratic we focus on the case $p = 2$. It then follows that $\varphi_0$ must have the form

$$\varphi_0(\eta) = A\eta^2 + \phi(\eta) + o(\phi(\eta)),$$

where $\phi$ is of order $o(\eta^2)$ and satisfies

$$(A\eta^2 + \phi + o(\phi))^n \phi''' = J.$$

Again, we have two possibilities. If the leading term on the left balances $J$, then, by integrating we obtain

$$\phi = B\eta^3 + C\eta^2 + D\eta + \frac{-J\eta^{3-2n}}{A^n(2n-1)(2n-2)(2n-3)} + E,$$

where $B, C, D, E$ are constants. Note that $\eta^{3-2n}$ is sub-quadratic if and only if $n > \frac{1}{2}$.

Since $n > 2$ then

$$\phi = D\eta + \frac{-J\eta^{3-2n}}{A^n(2n-1)(2n-2)(2n-3)} + E,$$

Note that $\eta^{3-2n}$ is sublinear for all $n > 1$ and, moreover, is $O(1)$ for $n > 3/2$.

If, on the other hand, the next order term balances $J$, then $\phi''' = 0$ and $\phi = D\eta + E$, where $D$ and $E$ are constants.

Summarising, this means that, as $\eta \to \infty$, for all possible consistent balances we have

$$\varphi_0 = A_+\eta^2 + B_+\eta + C_+ + O(1), \tag{4.55}$$

with $A_+, B_+, C_+$ unknown integration constants.

Finally, we recall the expansion in the annular region

$$v_{annular}(r,\tau) = b_2(r - r_*)^2 + O(\delta^{-2\gamma}) = b_2\delta^{-2\gamma}\tau^{2\gamma}\eta^2 + O(\delta^{-2\gamma}),$$

as $r \to {r_*}^+$, where $b_2$ is given by (4.47), and in the touchdown region we have

$$v_{touchdown}(\tau, r) = A_+\delta^{-\beta+2\gamma}\tau^{\beta-2\gamma}\eta^2 + O(\delta^{-\beta}),$$

as $\eta \to \infty$, for $A_+ \in \mathbb{R}$ unknown. To match both leading terms we need

$$\beta = 2\gamma, \quad A_+ = b_2. \tag{4.56}$$

Using (4.50), (4.52) and (4.56), we obtain that

$$\alpha = \gamma = -\frac{1}{2(n-1)}, \quad \beta = -\frac{1}{(n-1)},$$

which correspond exactly to the values that we observed in the numerical results in

the previous section.

**Remark 4.3.** *Consistency of the touchdown region expansions does not automatically guarantee that there exists a solution to (4.30) with the prescribed behaviour at $\eta \to \pm\infty$. However, by transforming the third-order problem into a second order one, Boatto et al. [16] could systematically investigate the solutions to this equation under different boundary conditions at the limit points $\eta = \pm\infty$. In particular, they found that solutions with linear behaviour as $\eta \to -\infty$ and quadratic behaviour as $\eta \to +\infty$ arise in the case $n > 2$. In what follows, we will compute these solutions numerically, for the purpose of incorporating them into a composite expansion of the full problem.*

## 4.3 Solution in the touchdown region

Finally, the leading order problem in the touchdown region is

$$\varphi_0^n(\eta)\partial_{\eta\eta\eta}\varphi_0(\eta) = J, \quad \eta \in (-\infty, \infty), \tag{4.57}$$

$$\varphi_0(\eta) = \begin{cases} A_-\eta + \frac{JA_-^{-n}(-\eta)^{3-n}}{(n-1)(n-2)(n-3)} + B_- + O(1) & \text{if } 2 < n < 3, \\ A_-\eta + \frac{J}{2A_-^3}\ln(-\eta) + B_- + O(1) & \text{if } n = 3, \\ A_-\eta + B_- + O(1) & \text{if } n > 3, \end{cases} \quad \text{as } \eta \to -\infty, \tag{4.58}$$

$$\varphi_0(\eta) = A_+\eta^2 + B_+\eta + C_+ + O(1) \text{ as } \eta \to \infty \tag{4.59}$$

where $A_\pm$, $B_\pm$, $C_+$, $J$ are unknown constants.

Problem (4.57)-(4.59) has 6 degrees of freedom reflecting the unknown constants, $A_\pm$, $B_\pm$, $C_+$ and $J$. Two of these constants ($A_+$ and $A_-$) have been fixed by matching to the appropriate outer problems. The third-order differential equation and its boundary conditions take care of another three degrees of freedom, so that only one degree of freedom remains. This degree of freedom, however, is the result of the ordinary differential equation being invariant under translations of $\eta$, i.e. being au-

tonomous. Thus, this degree of freedom corresponds to a shift in the solution and is fixed by the requirement that $\eta$ is defined in (4.26) through the position $r_*$ where $v$ touches down for $t \to \infty$. Hence, one can fix this degree by translating $\eta$ so that $\varphi_0$ has its minimum at $\eta = 0$. Thus, we have enough information to determine the touchdown region.

Let us recall that we still have one unknown constant, $c_2$, left in the central region, which we can now determine. We will solve the touchdown problem numerically and use it to obtain $c_2$ through the matching conditions.

To work only with one expansion of $\varphi_0$ as $\eta \to -\infty$ we focus on the case $n > 3$. We solve problem (4.57)-(4.59) only with boundary conditions at $\eta \to -\infty$, i.e.

$$\begin{aligned} \varphi_0^n(\eta)\partial_{\eta\eta\eta}\varphi_0(\eta) = J, \quad \eta \in (-\infty, \infty), \\ \varphi_0(\eta) = A_-\eta + B_- \text{ as } \eta \to -\infty, \end{aligned}$$

where we can choose $B_- = 0$ as it only represents a translation in $\eta$, to which the equation is invariant. We can also simplify the problem by introducing a scaling and new variables

$$\varphi_0(\eta) = c\phi(y), \quad \eta = dy,$$

and by defining

$$c := \left(\frac{J}{(-A_-)^3}\right)^{\frac{1}{n-2}}, \quad d := \left(\frac{J}{(-A_-)^{n+1}}\right)^{\frac{1}{n-2}}, \tag{4.60}$$

where $c$, $d > 0$; we obtain that $\phi$ solves the following parameter free problem

$$\begin{aligned} \phi^n(y)\partial_{yyy}\phi(y) = 1, \quad y \in (-\infty, \infty), \\ \phi(y) = -y \text{ as } y \to -\infty. \end{aligned}$$

For $y_0 \in \mathbb{R}_+$, we solve numerically

$$\begin{aligned}
\phi^n \partial_{yyy}\phi =& 1, \quad y \in (-y_0, y_0),\\
\phi(-y_0) =& -y_0,\\
\partial_y \phi(-y_0) =& -1,\\
\partial_{yy}\phi(-y_0) =& 0,
\end{aligned}$$

and read off $\kappa := \partial_{yy}\phi(y_0)$ from the solution $\phi$. We know that $\kappa \sim \lim_{y\to+\infty} \phi''(y)$. By reverting to the earlier scaling, we get that $\lim_{y\to+\infty} \varphi''(y) \sim \kappa \frac{c}{d^2}$ and also that $\lim_{y\to+\infty} \varphi''(y) \sim 2A_+$. Using this and the fact that $A_+ = \frac{\sigma}{2\varepsilon^2}$, we get

$$\frac{\sigma}{\varepsilon^2} = \kappa \frac{c}{d^2}. \tag{4.61}$$

Substituting $c$, $d$ from (4.60) into (4.61) we obtain:

$$\frac{\sigma}{\varepsilon^2} = \kappa \frac{\left(\frac{J}{(-A_-)^3}\right)^{\frac{1}{n-2}}}{\left(\frac{J}{(-A_-)^{n+1}}\right)^{\frac{2}{n-2}}}, \tag{4.62}$$

We can express $A_-$ and $J$ in terms $c_2$ by using (4.50) and (4.53), respectively. Thus, equation (4.62) becomes

$$\frac{\sigma}{\varepsilon^2} = \kappa \left(\frac{\alpha \frac{c_2 r_*}{2^{n+1}\varepsilon^2} I_2\left(\frac{2r_*}{\varepsilon}\right)}{\left(\frac{2c_2}{\varepsilon} I_0'\left(\frac{2}{\varepsilon} r_*\right)\right)^3}\right)^{\frac{1}{n-2}} \left(\frac{\alpha \frac{c_2 r_*}{2^{n+1}\varepsilon^2} I_2\left(\frac{2r_*}{\varepsilon}\right)}{\left(\frac{2c_2}{\varepsilon} I_0'\left(\frac{2}{\varepsilon} r_*\right)\right)^{n+1}}\right)^{-\frac{2}{n-2}}.$$

Thus, simplifying we can obtain $c_2$ in terms of known parameters and functions,

$$c_2 = \left| \frac{\sigma_0^{n-2} \varepsilon I_2\left(\frac{2r_*}{\varepsilon}\right)}{2^{3n+1}(n-1)\kappa^{n-2} I_1\left(\frac{2r_*}{\varepsilon}\right)^{2n-1}} \right|^{\frac{1}{2(n-1)}},$$

from which we can get $A_-$ and $J$ explicitly. Thus, the solutions to the leading order

problems in each region are completely determined and solved.

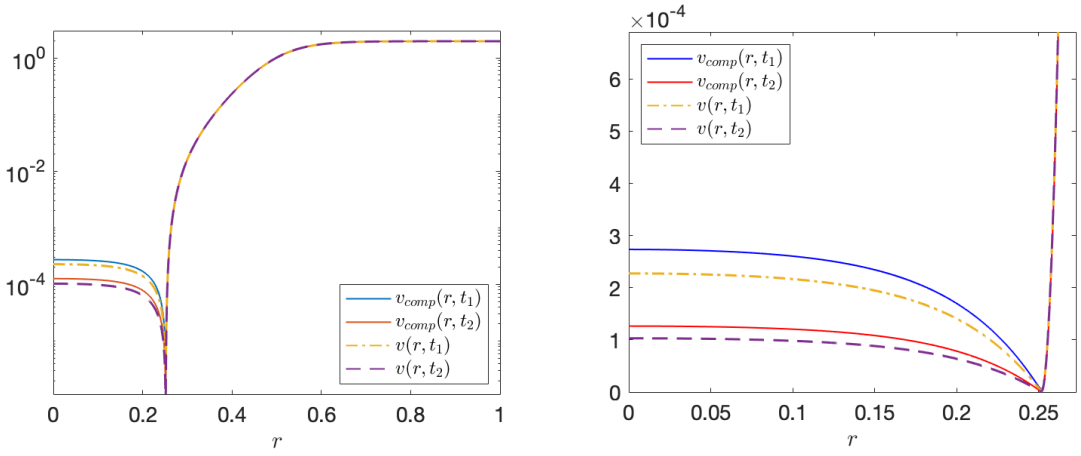
## 4.4 Composite expansion and comparison with numerical results

We will now construct a composite approximation from the asymptotic solutions found in the previous sub-sections. Formally, the composite expansion corresponds to each of the approximations - central, touchdown and annular - minus the terms that they have in common in the intermediate regions between them, in other words

$$\begin{aligned} v_{comp}(r,t) :=& v_{central}(r,t) + v_{touchdown}(r,t) + v_{annular}(r,t) \\ & - A_{-}t^{\alpha}(r-r_*)_{-} - A_{+}(r-r_*)_{+}^{2}, \end{aligned}$$

where $(x)_{-} = x$ if $x \leq 0$ and $(x)_{-} = 0$ if $x > 0$. In Figure 4.11 we present the leading order of the composite expansion at two times, $t_1 = 10^{13}$ and $t_2 = 10^{15}$, and compare them with the numerical partial differential equation solution for $r \in [0,1]$ at both times. We use a semi-log plot in 4.11(b) so that all relevant parts of the solution, which differ by several orders of magnitude, can be shown in a single plot. Note that we only use the partial differential equation solution for comparison and the only external data that is fed into the computation of composite expansion is the mass of the initial condition $m_0$. The composite solution closely follows the numerical solution of the full problem for $v$ in the whole interval $[0,1]$. In particular, around the minimum of the solution and in the annular region the agreement is excellent, as shown in Fig. 4.11(a) and (b), at times $t = t_1$ and $t_2$.

Moreover, the overall agreement between the composite approximation and the numerical solution of the partial differential equation becomes better at $t_2$. To quan-




(a) (b)

Figure 4.11: (a) Plot of composite and numerical solutions on a log scale, for $n = 4$, $t_1 = 10^{13}$, $t_2 = 10^{15}$. (b) Zoom of (a) using the original scale in the central and touchdown regions.

tify this, we define their absolute error as

$$error(t) = \max_{r\in(0,1)} |v(t_2, r) - v_{comp}(t, r)|.$$

For the simulation portrayed in Figure 4.11, we have

$$error(t_1) = 0.000171, \quad error(t_2) = 0.000023,$$

which indicates that the error decreases by a factor of 7.4 between $t_1$ and $t_2$. Note that in the central region we expect an error of order $o(\delta^{-\alpha}) \sim o(10^{-3})$, in the touchdown of order $o(\delta^{-\beta}) \sim o(10^{-4})$, for $\delta = 10^{-15}$, and in the annular region of order $\sim O(\delta) \sim O(10^{-15})$. Therefore, the overall error of order $O(10^{-4})$ is better than expected. Moreover, we can see in Fig. 4.12 (b) that, once the radius at which the error is achieved stabilises (from $t = 10^{12}$ onward), the error decreases as a power law in time.

We can also plot the dependence of the error on $r$ by defining

$$error_t(r) := |v(t,r) - v_{comp}(t,r)|.$$

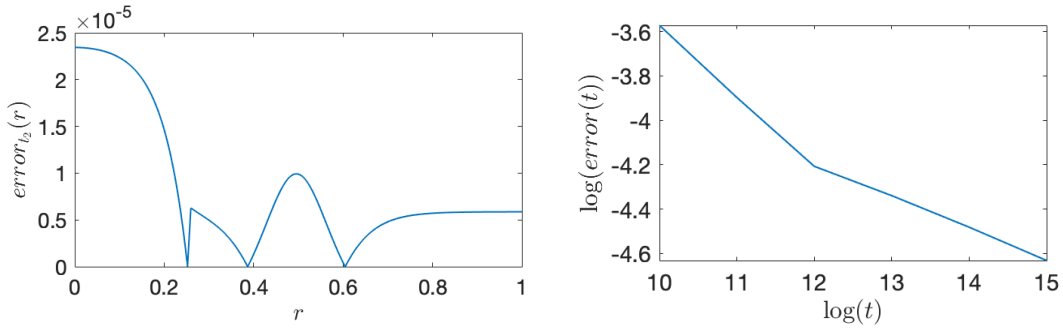
In Figure 4.12 we can see that $error_{t_2} \sim O(10^{-5})$ for $t_2 = 10^{15}$ across the entire domain, which confirms that the agreement between the leading order of the composite expansion and the numerical solution is excellent. It is clear from the figure that the maximum error is given by the approximation in the central and touchdown regions, as expected from the previous discussion.

We note that the jumps that appear in Figure 4.12 (a) are due to extending numerically the functions that are only defined in a subdomain. For example, the touchdown solution is a priori only computed for $y \in (-y_0, y_0)$ instead of all of $y \in (-\infty, \infty)$. Substituting $y = d\eta = \frac{r-r_*}{\delta^{-\gamma}\tau^{\gamma}}$ in the boundary of the interval implies that the touchdown solution is only defined in an interval centered at $r_*$ that is strictly inside $(0,1)$. Therefore, to use the touchdown region solution in the composite expansion we must extend it to the entire domain. We extend it by the leading order term in the expansions of $\varphi_0$ as $\eta \to \pm\infty$ shown in (4.49) and (4.55). This requires adjusting the height of the functions we are glueing, which we can do up to $10^{-5}$ of accuracy, which is where the jumps come from.

Summarising, in this section, we have shown that for $n > 2$ there is a numerical solution to (2.6)-(2.11) that converges to an asymptotic approximation which presents an infinite time touchdown. Up to leading order, this approximation is divided into three main regions - central, touchdown and annular - where the first two have the following self-similar profiles (to leading order)

$$v_{central} \sim t^{-\frac{1}{2(n-1)}}\psi_0(r), \quad v_{touchdown} \sim t^{-\frac{1}{n-1}}\varphi_0(\eta), \quad \eta := \frac{r-r_*}{t^{-\frac{1}{2(n-1)}}}$$

respectively, and the third one is almost stationary and coincides, to leading order,




(a) (b)

Figure 4.12: (a) $error_{t_2}(r)$ versus $r$ for $n = 4$ and $t_2 = 10^{15}$. (b) Plot of $error(t)$ (defined in main text) versus $\log(t)$ for times $t = 10^{10}, 10^{11}, 10^{12}, 10^{13}, 10^{14}, 10^{15}$. For $n = 4$ and $\varepsilon = 0.1$.

with the stationary solution obtained in Lee et al. [49].

Note that from the above expressions, the self-similar exponents are valid for all $n \neq 1$. However, the matching between the leading order of $v_{central}$ and $v_{touchdown}$, which is linear in space, can only occur for $n > 2$ because the touchdown region expansion as $\eta \to -\infty$ breaks down for lower values of $n$. Meanwhile, the matching between the leading order of $v_{touchdown}$ and $v_{annular}$, which is quadratic in space, can occur for all $n > 1/2$. Thus, in combination, to match all three regions we require $n > 2$.

# Chapter 5

# Case $n < 2$

In this section we study the problem formulated on Section 2 for the case $n < 2$. The overall asymptotic structure is the same as in the case $n > 2$, as described in Chapter 4; namely, we have again central, touchdown and annular regions, with the solutions in the first two being self-similar to leading order, and stationary to leading order in the third region.

The main difference between the two cases arises in regard to the asymptotic matching of the leading order expansions in the central and touchdown regions. In the case $n > 2$, the common term in both regions was linear in space. This was only possible for $n > 2$, since the expansion in the touchdown region as $\eta \to -\infty$ broke down for values $n \leq 2$. This implies that we must employ one of the other possible asymptotic expansions in the touchdown region; namely: fractional, constant or quadratic behaviour. We will see in this chapter that, actually, it must be fractional in space. This change directly affects the central region, since it cannot have the same behaviour as in the case $n > 2$ anymore. Therefore, we reintroduce the time derivative in that region. This leads to a change from constant flux in the case $n > 2$ to non-constant flux in the case $n < 2$, in the central region. As a consequence, now the central region leading order equation cannot be solved analytically. Thus, we must

devise a method for solving it numerically.

## 5.1 Numerical Results

In the present section we study numerical solutions of the problem (2.1)-(2.5) for different degrees of degeneracy in the range $\frac{1}{2} < n < 2$. More specifically, we study the cases $n = 1, \frac{3}{2}, 2$. Here we include $n = 2$ only for comparison. We note that for $n$'s closer to $\frac{1}{2}$ the solution becomes increasingly unstable numerically and requires a different approach, so we will not treat them in the present work. We use the same values of $\varepsilon$ and $u_{init}$ as in the simulations in Section 3.

### 5.1.1 Central region

We proceed as in Section 4.1.1. Thus, we make the following general ansatz:

$$v(r,t) \sim \xi(t)\psi(r), \tag{5.1}$$

where $\psi$, $\xi$ are unknown functions at the moment.

In Figure 5.1 we can see that the location $\bar{r}(t)$ of the minimum of $v$ appears to converge to a limit $r_*$ early on in the evolution of the solution. In the case $n = 3/2$, this limit is approximately $r_* = 0.25$, the same as in the case $n = 4$. This is in line with what we saw in Section 4.2.3, i.e. that $r_*$ is fixed only by the initial mass and $\varepsilon$, and hence is independent of $n$.

We can check that (5.1) holds for the numerical solution by plotting $\frac{v(r,t)}{v(0,t)}$, since

$$\frac{v(r,t)}{v(0,t)} \sim \frac{\psi(r)}{\psi(0)},$$

which is independent of time if (5.1) holds.

We note that $t = 10^5$ is the maximum interval for which it was practical to

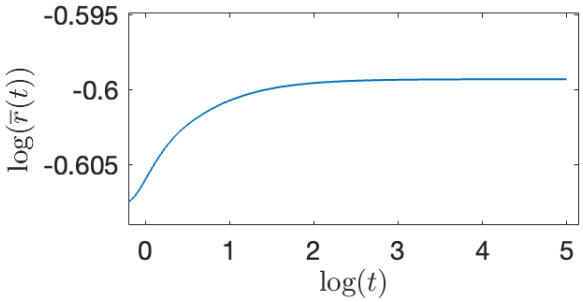



Figure 5.1: $\log(\overline{r}(t))$ versus $\log(t)$ over a long-time interval, with $n = 3/2$ and $\varepsilon = 0.1$.

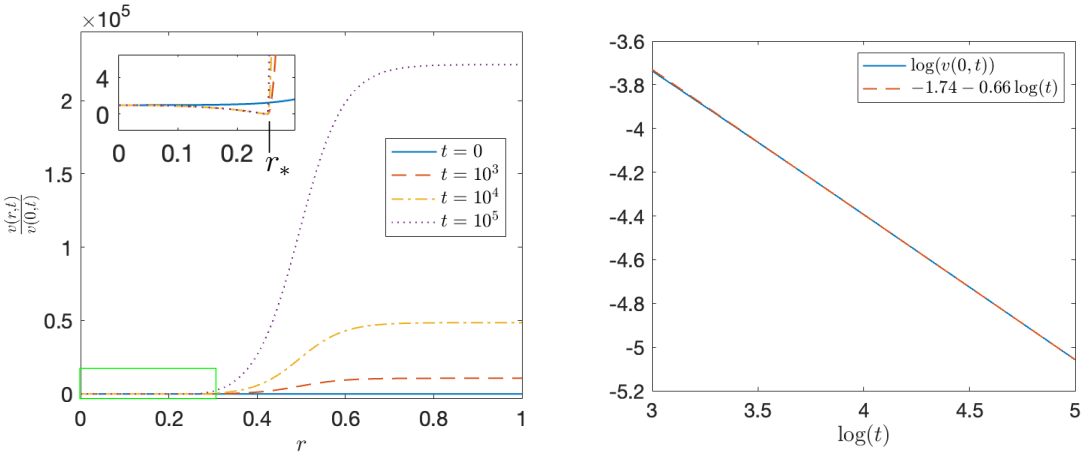



Figure 5.2: (a) $v(r,t)/v(0,t)$ versus $r$ at different times. (b) Log-log plot of $v(0,t)$. For $n = 3/2$.

compute the numerical solution, as we already needed a million grid points to get a solution with accuracy $10^{-6}$. This phenomenon gets worse as $n$ approaches $1/2$.

We can observe in Figure 5.2 (a) and its inset that all curves collapse onto each other in the central region. This implies that $\frac{v(r,t)}{v(0,t)}$ is, in fact, roughly independent of time on the interval $(0, r_*)$.

In Figure 5.2 (b) we observe that the data can be fitted to a line, suggesting power law behaviour for $\xi(t)$. Hence, there should exist $\alpha \in \mathbb{R}$ such that

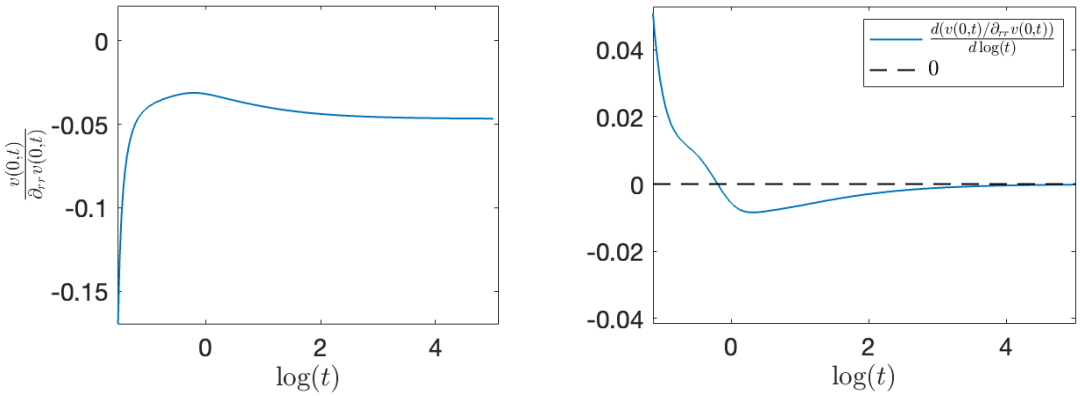
$$\log(v(0,t)) \sim \log(\psi(0)) + \alpha \log(t).$$

Figure 5.2 (b) confirms this prediction with $\alpha$ negative, which can be obtained numerically from the slope of the linear fitting. Hence $v(r,t) \sim t^\alpha \psi(r)$ as $t \to \infty$ for some $\alpha < 0$. We can corroborate this by showing that there cannot be a scaling of the independent variable $r$. Thus, we check that $v(0,t)$ and $\partial_{rr} v(0,t)$ have the same scaling. Using $v(r,t) \sim t^\alpha \psi(r)$, we have that

$$v(0,t) \sim t^\alpha \psi(0),$$
$$\partial_{rr} v(0,t) \sim t^\alpha \partial_{rr} \psi(0).$$

We plot $\frac{v(0,t)}{\partial_{rr} v(0,t)}$ in Figure 5.3 (a). The curve seems to converge to a constant at long times, which means that they must have the same scaling, at least at longer times. In fact, in Figure 5.3 (b) we confirm that the slope of $\frac{v(0,t)}{\partial_{rr} v(0,t)}$ converges to zero as $t \to 10^5$.

At this point, there is vast evidence for self-similar behaviour in the central region following (5.1) and we can obtain $\alpha$ from the slope of a linear approximation of $\log(v(0,t))$ at long times. The resulting approximate exponent of the power-law behaviour, is shown in Figure 5.4 for $n = 1, 3/2, 2$. Note that in Figure 5.4, the function $\frac{d\log(v(0,t))}{d\log(t)}$ exhibits a transitional minimum between early and late time stages.




(a) (b)

Figure 5.3: (a) $\frac{v(0,t)}{\partial_{rr}v(0,t)}$ versus $\log(t)$. (b) $\frac{d(v(0,t)/\partial_{rr}v(0,t))}{d\log(t)}$. For $n = 3/2$.

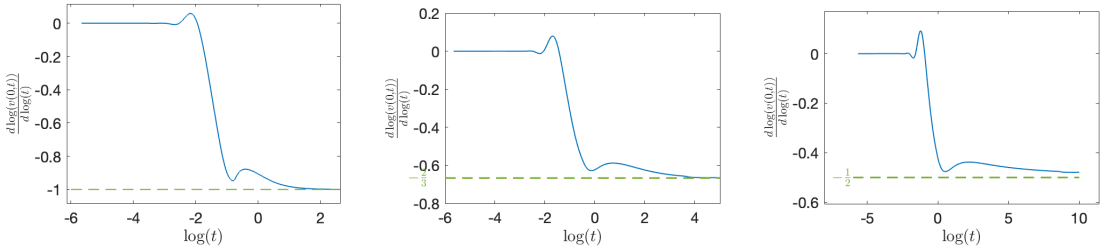



Figure 5.4: Numerical approximation for the power law exponent $\alpha$ for final times $t_{final} = 2 \times 10^2, 10^5, 10^{10}$ where we stopped each simulation, and $\varepsilon = 0.1$, for (a), left: $n = 1$, (b), middle: $n = 3/2$ and (c), right: $n = 2$.

We saw the same behaviour for the case $n > 2$. However, in this case, the minimum value attained in this transitional stage is not as easy to identify. We note that after this transitional minimum the function seems to converge to a more stable minimum. In fact, it tends to $-1$, $-2/3$, $-1/2$, respectively, as $t \to \infty$. This suggests that for very long times, we have that

$$\alpha = -\frac{1}{n}. \tag{5.2}$$

### 5.1.2 Touchdown region

Proceeding as in Section 4.1.2, we assume the following ansatz for the solution near $r = r_*$:

$$v(r,t) \sim \xi_1(t)\varphi(\eta), \quad \eta(r) := \frac{(r - r_*)}{\xi_2(t)}, \tag{5.3}$$

where $\varphi, \xi_1, \xi_2$ are unknown functions. (5.3) holds if and only if

$$\frac{v(r,t)}{v(r_*,t)} \sim \frac{\varphi(\eta)}{\varphi(0)},$$

where, for fixed $\eta$, the right-hand side does not depend on time. Let

$$w(r,t) := \frac{v(r,t)}{v(\overline{r}(t),t)},$$

where again we set $\overline{r}(t) = \text{argmin}_{r\in(0,1)} v(r,t)$. Since we cannot plot $w$ as a function of $\eta$ directly, we define

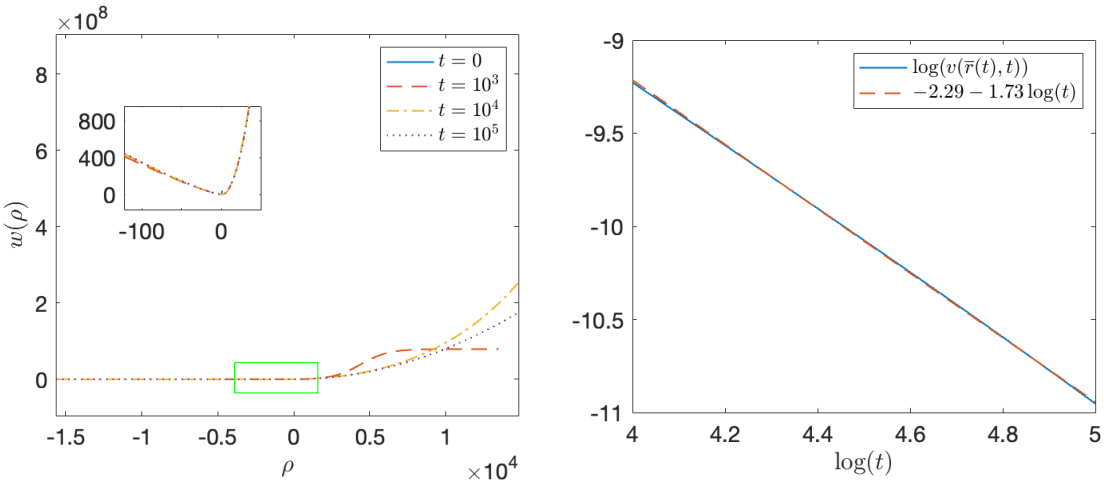
$$\rho := \left(\frac{\partial_{rr} v(r_*,t)}{v(r_*,t)}\right)^{1/2} (r - \overline{r}(t)).$$

If (4.5) holds at longer times, then to leading order

$$\left(\frac{\partial_{rr} v(r_*,t)}{v(r_*,t)}\right)^{-1/2} \sim \xi_2(t).$$

Plotting $w$ versus $\rho$ in Figure 4.6 (a) allows us to see that the curves collapse together onto one curve nicely around $\rho = 0$, i.e. $r = r_*$, at several long times.

Figure 5.5 (b) confirms that $\xi_1$ is a power law $v(r,t) \sim t^\beta \varphi(\eta)$ with exponent $\beta < 0$. We obtain $\beta$ in Figure 5.6. As in the central region, the curves in Figure 5.6 have an initial dip, which does not approach a simple constant. However, as $t \to \infty$ the curves converge to the values $-4$, $-5/3$, $-1$ for $n = 1, 3/2, 2$ respectively. This




(a) (b)

Figure 5.5: (a) $w(\rho, t)$ versus $\rho$. (b) Log-log plot of $v(\overline{r}(t), t)$. For $n = 3/2$.

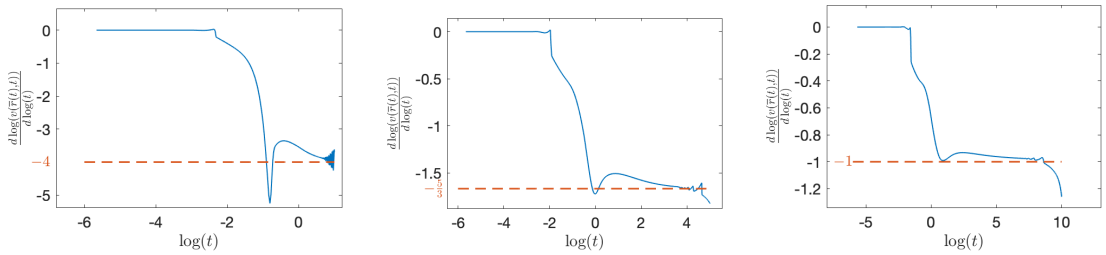



Figure 5.6: Numerical approximation for the power law exponent $\beta$ for final times $t_{final} = 10, 10^5, 10^{10}$ where the simulations were stopped, respectively, and $\varepsilon = 0.1$, for (a), left: $n = 1$, (b), middle: $n = 3/2$ and (c), right: $n = 2$.

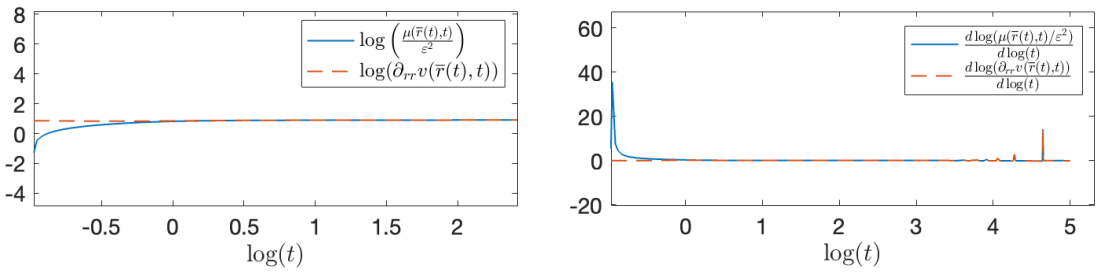
suggests that a good approximation for the power-law exponent is

$$\beta(n) = -\frac{2(n+1)}{n(2n-1)}. \tag{5.4}$$

This exact formula was originally obtained from the results for thin-film models by Bertozzi et. al. [13]. We were able to confirm with our numerical results that (5.4) is also a good approximation in our case.

The only feature left to characterise is $\xi_2$. If $\xi_2(t) = t^\gamma$ for some $\gamma \in \mathbb{R}$, then

$$\partial_{rr} v(r_*, t) \sim t^{\beta - 2\gamma} \partial_{\eta\eta} \varphi(\eta).$$




(a) (b)

Figure 5.7: (a) Log-log plots for $\mu(\overline{r},t)/\varepsilon^2$ and $\partial_{rr}v(\overline{r},t)$, (b) Slope of curve in (a) for $n = 3/2$ and $\varepsilon = 0.1$. The spikes in (b) for $t \sim 10^5$ are due to the numerical solution becoming unstable, which happens for increasingly shorter times as we approach $n = 1/2$.

Moreover, when $t$ is large we can approximate the leading order of the chemical potential by $\mu(r,t) \sim \varepsilon^2 \partial_{rr} v(r,t)$. As a consequence, both functions, $\mu(r,t)$ and $\partial_{rr}v(r,t)$, should behave linearly when we plot their logarithms. We can see in Figure 5.7 (a) that at long times both plots are linear and coincide. Moreover, in Figure 5.7 (b) the slope of both curves converges to 0 at long times, which indicates that $\beta - 2\gamma = 0$, and hence $\gamma = \frac{\beta}{2}$.

In summary, for $n \leq 2$, the analysis of the numerical solution suggests that at very long times, the exponents of the self-similar solutions are given by

$$\alpha(n) = -\frac{1}{n}, \quad \beta(n) = -\frac{2(n+1)}{n(2n-1)}, \quad \gamma(n) = -\frac{(n+1)}{n(2n-1)}.$$

We remark that $\beta$ and $\gamma$ become singular at $n = 1/2$ and, hence, these approximations are only valid for $1/2 < n < 2$. We also note that the formula for $\beta$ was originally obtained from Bertozzi et. al. [13] in a different context.

## 5.2 Long-time asymptotic expansion

In this section, we carry out a long-time asymptotic analysis of the solution to the radially symmetric system in two dimensions via singular perturbation theory for

$1/2 < n < 2$. As in Section 4.2 we use $t = \frac{\tau}{\delta}$, where $0 < \delta \ll 1$ is a small parameter on which the asymptotic analysis is based.

The asymptotic analysis in the annular region carries over directly from the case $n > 2$, so we will focus solely on the central and touchdown regions, where there are major changes.

Recall that we are analysing problem (4.10)-(4.15), which is in terms of $v = 1 - u$ and $\tau$.

### 5.2.1 Central region

We assume, using the insight gained from the numerical results, that $v$ can be expanded as

$$v_{central}(r, \tau) = \delta^{-\alpha}\tau^{\alpha}\psi_0(r, \tau) + o(\delta^{-\alpha}), \tag{5.5}$$

for some $\alpha \in \mathbb{R}$ and some non-negative function $\psi_0$. We focus on the case $\alpha < 0$, assuming that $v_{\text{central}}$ strictly decreases for large times.

Substituting (5.5) in (4.10)-(4.11) and expanding in powers of $\delta$ we get at lowest order the equation

$$\delta^{-\alpha+1}(\alpha\tau^{\alpha-1}\psi_0 + \tau^{\alpha}\partial_\tau\psi_0) = -\delta^{-(n+1)\alpha}\tau^{(n+1)\alpha}\frac{2^n}{r}\partial_r\left[r\psi_0^n\partial_r\left(\varepsilon^2\left(\partial_{rr}\psi_0 + \frac{1}{r}\partial_r\psi_0\right) - 4\psi_0\right)\right].$$

As in the case $n > 2$, we expect $\psi_0$ to depend only on $r$. If we thus assume that $\partial_\tau\psi_0 = 0$, then

$$\delta^{-\alpha+1}\alpha\tau^{\alpha-1}\psi_0 = -\delta^{-(n+1)\alpha}\tau^{(n+1)\alpha}\frac{2^n}{r}\partial_r\left[r\psi_0^n\partial_r\left(\varepsilon^2\left(\partial_{rr}\psi_0 + \frac{1}{r}\partial_r\psi_0\right) - 4\psi_0\right)\right].$$

Balancing the two sides implies that

$$\alpha = -\frac{1}{n},$$

which is consistent with our numerical results, and yields the following ordinary differential equation

$$-\frac{1}{n}\psi_0 = -\frac{2^n}{r}\partial_r\left[r\psi_0^n\partial_r\left(\varepsilon^2\left(\partial_{rr}\psi_0+\frac{1}{r}\partial_r\psi_0\right)-4\psi_0\right)\right] \text{ in } (0,r_*), \tag{5.6}$$

$$\psi_0(r_*) = 0, \tag{5.7}$$

$$\partial_r\psi_0(0) = 0, \quad \partial_r\mu_0(0) = 0, \tag{5.8}$$

where

$$\mu_0(r) := \varepsilon^2\left(\partial_{rr}\psi_0+\frac{1}{r}\partial_r\psi_0\right)-4\psi_0.$$

The main difference between this equation and its analogue for the case $n > 2$ is that the left-hand side of (5.6) does not vanish a priori. This implies that the flux in the central region does not have to be constant for this case and it can depend on $r$.

We can summarise the asymptotic expansions that we have obtained for $\psi_0$ as follows:

**Summary 5.1.** *As $r \to 0^+$ we have that*

$$\psi_0(r) = a_0^- + a_2^- r^2 + h.o.t.,$$

*where $a_0^-$ and $a_2^-$ are unknown constants.*

*And as $r \to r_*^-$ we have that*

$$\psi_0(r) = a_0^+(r_*-r)^{\frac{3}{n+1}} + a_1^+(r_*-r)^{\frac{4n+1+\sqrt{-8n^2+20n+1}}{2(n+1)}} + h.o.t.,$$

*where $a_0^+$, $a_1^+ \in \mathbb{R}$ are unknown constants. We note that these expansions contain four degrees of freedom for the fourth-order ordinary differential equation (5.6).*

In the remainder of this subsection, we will explain how we obtained these expansions.

**Expansion as $r \to 0^+$:** We wish to expand the solution to (5.6) with boundary conditions (5.8) in powers of $r$ as $r \to 0$. We rewrite equation (5.6) as

$$\frac{r}{n2^n}\psi_0 = \left[ r\psi_0^n \left( \varepsilon^2 \left( \psi_0''' - \frac{1}{r^2}\psi_0' + \frac{1}{r}\psi_0'' \right) - 4\psi_0' \right) \right]',$$

where $' = \partial_r$. Expanding out the expression above, we obtain that

$$\begin{aligned}
\frac{r}{n2^n}\psi_0 =& \varepsilon^2 \psi_0^n \left( \psi_0''' - \frac{1}{r^2}\psi_0' + \frac{1}{r}\psi_0'' \right) \\
&+ r\varepsilon^2 n \psi_0^{n-1}\psi_0' \left( \psi_0''' - \frac{1}{r^2}\psi_0' + \frac{1}{r}\psi_0'' \right) \\
&+ r\varepsilon^2 \psi_0^n \left( \psi_0'''' + \frac{2}{r^3}\psi_0' - \frac{2}{r^2}\psi_0'' + \frac{1}{r}\psi_0''' \right) \\
&- 4\psi_0^n\psi_0' - 4rn\psi_0^{n-1}{\psi_0'}^2 - 4r\psi_0^n\psi_0''.
\end{aligned}$$

From the numerical simulations, we expect that $0 < \psi_0(0) < +\infty$. Accordingly, we assume the following ansatz:

$$\psi_0(r) = \tilde{a}_0 + \phi(r),$$

where $\tilde{a}_0 \in \mathbb{R}$, $\tilde{a}_0 > 0$ and $|\phi(r)| \ll \tilde{a}_0$ as $r \to 0^+$. Substitution of the ansatz yields

$$\begin{aligned}
\frac{r}{n2^n}(\tilde{a}_0 + \phi) =& \varepsilon^2 (\tilde{a}_0 + \phi)^n \left( (\tilde{a}_0 + \phi)''' - \frac{1}{r^2}(\tilde{a}_0 + \phi)' + \frac{1}{r}(\tilde{a}_0 + \phi)'' \right) \\
&+ r\varepsilon^2 n (\tilde{a}_0 + \phi)^{n-1}(\tilde{a}_0 + \phi)' \left( (\tilde{a}_0 + \phi)'' - \frac{1}{r^2}(\tilde{a}_0 + \phi)' + \frac{1}{r}(\tilde{a}_0 + \phi)'' \right) \\
&+ r\varepsilon^2 (\tilde{a}_0 + \phi)^n \left( (\tilde{a}_0 + \phi)'''' + \frac{2}{r^3}(\tilde{a}_0 + \phi)' - \frac{2}{r^2}(\tilde{a}_0 + \phi)'' + \frac{1}{r}(\tilde{a}_0 + \phi)''' \right) \\
&- 4(\tilde{a}_0 + \phi)^n (\tilde{a}_0 + \phi)' - 4rn(\tilde{a}_0 + \phi)^{n-1}(\tilde{a}_0 + \phi)'^2 \\
&- 4r(\tilde{a}_0 + \phi)^n (\tilde{a}_0 + \phi)'', \qquad (5.9)
\end{aligned}$$

and note that

$$(\tilde{a}_0 + \phi)^n = \tilde{a}_0^n + \sum_{i=1}^{n} \binom{n}{i} \phi^i \tilde{a}_0^{n-i}.$$

Now, in the first factor in each term on the right-hand side of (5.9), we only keep the lowest order contribution, i.e. $\tilde{a}_0^n$, and eliminate nonlinear terms in $\phi$ or its derivatives. Following this procedure yields

$$\begin{aligned}\frac{r}{n2^n}(\tilde{a}_0+\phi) =&\varepsilon^2\tilde{a}_0^n\left(\phi'''-\frac{1}{r^2}\phi'+\frac{1}{r}\phi''\right)+r\varepsilon^2\tilde{a}_0^n\left(\phi''''+\frac{2}{r^3}\phi'-\frac{2}{r^2}\phi''+\frac{1}{r}\phi'''\right)\\&-4\tilde{a}_0^n\phi'-4r\tilde{a}_0^n\phi''+h.o.t.\end{aligned}$$

If we assume that $\phi \sim r^\lambda$ for some $\lambda > 1$, then there are two types of terms on the right-hand side of the expression above; namely, the top line is $O(r^{\lambda-3})$ and the bottom line in $O(r^{\lambda-1})$. Thus the dominant terms are

$$\frac{r}{n2^n}\tilde{a}_0 =\varepsilon^2\tilde{a}_0^n\left(\phi'''-\frac{1}{r^2}\phi'+\frac{1}{r}\phi''\right)+r\varepsilon^2\tilde{a}_0^n\left(\phi''''+\frac{2}{r^3}\phi'-\frac{2}{r^2}\phi''+\frac{1}{r}\phi'''\right)+h.o.t.,$$

which we can regroup as

$$\frac{r}{n2^n}\tilde{a}_0 =\varepsilon^2\tilde{a}_0^n\left(r\phi''''+2\phi'''-\frac{1}{r}\phi''+\frac{1}{r^2}\phi'\right)+h.o.t.$$

If the right-hand side balances the left-hand side then $r \sim r^{\lambda-3}$, i.e. $\lambda = 4$, and thus $\phi = \frac{1}{n2^{n+6}\varepsilon^2}r^4$, which does not add a degree of freedom to the problem. If the right-hand side does not enter the dominant balance at this stage, then $\lambda > 4$, and no other higher order corrections will be able to match the left-hand side. This will not lead to a solution and thus this case can be ruled out. If, however, the left-hand side is the one that does not enter the dominant balance, then there will be corrections with $\lambda < 4$ that constitute higher order terms at this stage, yielding

$$\mathcal{L}(\phi) :=\phi''''+\frac{2}{r}\phi'''-\frac{1}{r^2}\phi''+\frac{1}{r^3}\phi'=0,$$

to leading order. This is a linear ordinary differential equation for $\phi$ with a regu-

lar singular point at $r = 0$, which can be solved using the Frobenius method. In Appendix C we explain this method for general fourth-order ordinary differential equations. Accordingly, we assume that the solution has the following form

$$\phi(r) = r^{\lambda} \sum_{k=0}^{\infty} a_k r^k, \tag{5.10}$$

and then the operator $\mathcal{L}$ is given by

$$\begin{aligned}\mathcal{L}(\phi) =& r^{\lambda-4} \sum_{k=0}^{\infty} [(\lambda+k)(\lambda+k-1)(\lambda+k-2)(\lambda+k-3) \\ &+2(\lambda+k)(\lambda+k-1)(\lambda+k-2) - (\lambda+k)(\lambda+k-1) + (\lambda+k)]\, a_k r^k,\end{aligned}$$

which can be rewritten as

$$\mathcal{L}(\phi) = \sum_{k=0}^{\infty} F(\lambda+k) a_k r^{k+\lambda-4}, \tag{5.11}$$

where

$$F(x) := x^2(x-2)^2.$$

For the equation

$$\mathcal{L}(\phi) = 0$$

to be satisfied, we need $F(\lambda+k)a_k = 0 \ \forall k \in \mathbb{N}_0$. The first term, with $k = 0$, gives us

$$0 = \lambda^2(\lambda-2)^2 a_0.$$

Assuming $a_0 \neq 0$, this corresponds to the indicial equation

$$F(\lambda) = \lambda^2(\lambda-2)^2 = 0,$$

which has two double roots:

$$\lambda_1 = 2, \quad \lambda_2 = 0.$$

Thus we have two double roots whose difference $\lambda_1 - \lambda_2$ is a positive integer. By the Frobenius method, the resulting solution is given by

$$\phi(r) = \sum_{k=0}^{\infty}(b_k + c_k \ln(r))r^k + \sum_{k=0}^{\infty}(d_k + e_k \ln(r))r^{k+2},$$

where $c_k$ and $e_k$ can be obtained from $b_k$ and $d_k$, respectively, following the method outlined in Appendix C.

Therefore, we can expand $\phi$ as

$$\phi(r) = g_0 + g_1 \ln(r) + g_2 r^2 + g_3 \ln(r) r^2 + h.o.t.,$$

where $g_0 := b_0 + c_0$, $g_1 := b_0$, $g_2 := d_0 + e_0$ and $g_3 := d_0$. We note that this expansion is consistent with the assumption that there are corrections with exponents $\lambda < 4$.

Because $|\phi| \ll \tilde{a}_0$ as $r \to 0^+$ we require $g_0 = g_1 = 0$. Recalling our earlier ansatz,

$$\psi_0(r) = \tilde{a}_0 + g_2 r^2 + g_3 r^2 \ln(r) + h.o.t.,$$

which implies that

$$\psi_0' = 2g_2 r + g_3 r(2\ln(r) + 1) + h.o.t..$$

This satisfies $\psi_0'(0) = 0$, in accordance with (5.8). If we differentiate twice more

$$\psi_0'' = 2(g_2 + g_3) + g_3(2\ln(r) + 1) + h.o.t.,$$

then

$$\begin{aligned}\mu_0(r) =&4\varepsilon^2(g_2+g_3)-4(\tilde{a}_0+a_3)-4g_2r^2+4\varepsilon^2 g_3\ln(r)-4g_3r^2\ln(r),\\ \mu_0'(r) =&(-8g_2-4g_3)r+\frac{4\varepsilon^2 g_3}{r}-8g_3r\ln(r).\end{aligned}$$

In order to satisfy (5.8), namely $\mu_0'''(0)=0$, we need $g_3=0$. This leaves us with

$$\psi_0(r)=a_0^-+a_2^-r^2+h.o.t.,$$

where $a_0^-$ and $a_2^-$ are free constants that we have renamed to make our later analysis clearer.

**Expansion as $r\to r_*^-$:** Recalling (5.6)-(5.7),

$$\begin{aligned}-\frac{1}{n}\psi_0 =&-\frac{2^n}{r}\partial_r\left[r\psi_0^n\partial_r\left(\varepsilon^2\left(\partial_{rr}\psi_0+\frac{1}{r}\partial_r\psi_0\right)-4\psi_0\right)\right],\quad r\in(0,r_*),\\ \psi_0(r_*) =&0.\end{aligned}$$

We wish to expand the solution in powers of $\rho:=(r_*-r)$ as $\rho\to 0^+$. After changing variables, the equation becomes

$$\frac{1}{n}\psi_0=\frac{2^n}{r_*-\rho}\partial_\rho\left[(r_*-\rho)\psi_0^n\partial_\rho\left(\varepsilon^2\left(\partial_{\rho\rho}\psi_0-\frac{1}{r_*-\rho}\partial_\rho\psi_0\right)-4\psi_0\right)\right].$$

Expanding out the derivatives, we obtain

$$\begin{aligned}\frac{1}{n2^n}\psi_0 =&n\psi_0^{n-1}\partial_\rho\psi_0\left(\varepsilon^2\left(\partial_{\rho\rho\rho}\psi_0-\frac{1}{r_*-\rho}\partial_{\rho\rho}\psi_0-\frac{1}{(r_*-\rho)^2}\partial_\rho\psi_0\right)-4\partial_\rho\psi_0\right)\\ &+\psi_0^n\left(\varepsilon^2\left(\partial_{\rho\rho\rho\rho}\psi_0-\frac{1}{r_*-\rho}\partial_{\rho\rho\rho}\psi_0-\frac{2}{(r_*-\rho)^2}\partial_{\rho\rho}\psi_0-\frac{2}{(r_*-\rho)^3}\partial_\rho\psi_0\right)\right.\\ &\left.-4\partial_{\rho\rho}\psi_0\right)\\ &-\frac{\psi_0^n}{(r_*-\rho)}\left(\varepsilon^2\left(\partial_{\rho\rho\rho}\psi_0-\frac{1}{r_*-\rho}\partial_{\rho\rho}\psi_0-\frac{1}{(r_*-\rho)^2}\partial_\rho\psi_0\right)-4\partial_\rho\psi_0\right).\end{aligned}$$

Note that for $\rho \to 0^+$ we have

$$\frac{1}{(r_* - \rho)^m} = \frac{1}{{r_*}^m} + \frac{m}{{r_*}^{m+1}}\rho + O(\rho^2), \qquad m \in \mathbb{N},$$

therefore

$$\begin{aligned}
\frac{1}{n2^n}\psi_0 =& n\psi_0^{n-1}\partial_\rho\psi_0\left(\varepsilon^2\left(\partial_{\rho\rho\rho}\psi_0 - \frac{1}{r_*}\partial_{\rho\rho}\psi_0 - \frac{1}{{r_*}^2}\partial_\rho\psi_0\right) - 4\partial_\rho\psi_0\right) \\
&+ \psi_0^n\left(\varepsilon^2\left(\partial_{\rho\rho\rho\rho}\psi_0 - \frac{1}{r_*}\partial_{\rho\rho\rho}\psi_0 - \frac{2}{{r_*}^2}\partial_{\rho\rho}\psi_0 - \frac{2}{{r_*}^3}\partial_\rho\psi_0\right) - 4\partial_{\rho\rho}\psi_0\right) \\
&- \psi_0^n\left(\varepsilon^2\left(\frac{1}{r_*}\partial_{\rho\rho\rho}\psi_0 - \frac{1}{{r_*}^2}\partial_{\rho\rho}\psi_0 - \frac{1}{{r_*}^3}\partial_\rho\psi_0\right) - \frac{4}{r_*}\partial_\rho\psi_0\right) + h.o.t. \\
=& n\psi_0^{n-1}\partial_\rho\psi_0\left(\varepsilon^2\left(\partial_{\rho\rho\rho}\psi_0 - \frac{1}{r_*}\partial_{\rho\rho}\psi_0 - \frac{1}{{r_*}^2}\partial_\rho\psi_0\right) - 4\partial_\rho\psi_0\right) \\
&+ \psi_0^n\left(\varepsilon^2\left(\partial_{\rho\rho\rho\rho}\psi_0 - \frac{2}{r_*}\partial_{\rho\rho\rho}\psi_0 - \frac{1}{{r_*}^2}\partial_{\rho\rho}\psi_0 - \frac{1}{{r_*}^3}\partial_\rho\psi_0\right) - 4\partial_{\rho\rho}\psi_0 - \frac{4}{r_*}\partial_\rho\psi_0\right) \\
&+ h.o.t.
\end{aligned}$$

Suppose that $\psi_0 \sim \rho^s$ with $s > 0$, then

$$\begin{aligned}
\psi_0^{n-1}\partial_\rho\psi_0 \sim& \rho^{sn-1}, \\
\partial_\rho\psi_0 \sim& \rho^{s-1}, \\
\partial_{\rho\rho}\psi_0 \sim& \rho^{s-2}, \\
\partial_{\rho\rho\rho}\psi_0 \sim& \rho^{s-3}, \\
\partial_{\rho\rho\rho\rho}\psi_0 \sim& \rho^{s-4}, \\
\psi_0^n \sim& \rho^{sn}.
\end{aligned}$$

Therefore, the leading order terms on the right-hand side are the first terms on each line, i.e. the ones of order $O(\rho^{s(n+1)-4})$. Hence

$$\frac{1}{n2^n}\psi_0 = n\psi_0^{n-1}\partial_\rho\psi_0\varepsilon^2\partial_{\rho\rho\rho}\psi_0 + \psi_0^n\varepsilon^2\partial_{\rho\rho\rho\rho}\psi_0 + h.o.t.,$$

$$=\varepsilon^2\partial_\rho[\psi_0^n\partial_{\rho\rho\rho}\psi_0]+h.o.t. \tag{5.12}$$

which is the dominant balance for the equation.

Let

$$\psi_0(\rho)=\phi_0(\rho)+\phi_1(\rho),$$

where $|\phi_1(\rho)|\ll|\phi_0(\rho)|$ as $\rho\to 0$. Substituting this expression into (5.12) yields

$$\begin{aligned}\frac{1}{n2^n\varepsilon^2}(\phi_0+\phi_1)=&\partial_\rho\left[(\phi_0+\phi_1)^n\partial_{\rho\rho\rho}(\phi_0+\phi_1)\right],\\ =&\partial_\rho\left[\left(\phi_0^n+n\phi_0^{n-1}\phi_1+\sum_{i=2}^{n}\binom{n}{i}\phi_0^{n-i}\phi_1^i\right)(\partial_{\rho\rho\rho}\phi_0+\partial_{\rho\rho\rho}\phi_1)\right].\end{aligned}$$

We eliminate lower order terms, namely powers of the correction $\phi_1$, but keep terms with $\phi_0^{n-1}\phi_1$ as they may enter into the dominant balance.

$$\begin{aligned}\frac{1}{n2^n\varepsilon^2}(\phi_0+\phi_1)=&\partial_\rho\left[\left(\phi_0^n+n\phi_0^{n-1}\phi_1\right)(\partial_{\rho\rho\rho}\phi_0+\partial_{\rho\rho\rho}\phi_1)\right],\\ =&\partial_\rho\left[\phi_0^n\partial_{\rho\rho\rho}\phi_0+n\phi_0^{n-1}\phi_1\partial_{\rho\rho\rho}\phi_0+\phi_0^n\partial_{\rho\rho\rho}\phi_1+n\phi_0^{n-1}\phi_1\partial_{\rho\rho\rho}\phi_1\right].\end{aligned}$$

Let $\phi_0(\rho)=a_0\rho^s$, $s>0$. Then, recalling that $|\phi_1|\ll|\phi_0|=a_0\rho^s$,

$$\begin{aligned}\frac{1}{n2^n\varepsilon^2}(a_0\rho^s+\phi_1)=&\partial_\rho\left[a_0^{n+1}s(s-1)(s-2)\rho^{s(n+1)-3}+na_0^n\phi_1 s(s-1)(s-2)\rho^{sn-3}\right.\\ &\left.+a_0^n\rho^{sn}\partial_{\rho\rho\rho}\phi_1+n\rho^{s(n-1)}a_0^{n-1}\phi_1\partial_{\rho\rho\rho}\phi_1\right],\\ =&a_0^{n+1}s(s-1)(s-2)(s(n+1)-3)\rho^{s(n+1)-4}\\ &+na_0^n\phi_1 s(s-1)(s-2)(sn-3)\rho^{sn-4}\\ &+na_0^n s(s-1)(s-2)\rho^{sn-3}\partial_\rho\phi_1+a_0^n sn\rho^{sn-1}\partial_{\rho\rho\rho}\phi_1\\ &+a_0^n\rho^{sn}\partial_{\rho\rho\rho\rho}\phi_1+ns(n-1)\rho^{s(n-1)-1}a_0^{n-1}\phi_1\partial_{\rho\rho\rho}\phi_1\\ &+n\rho^{s(n-1)}a_0^{n-1}\partial_\rho\phi_1\partial_{\rho\rho\rho}\phi_1+n\rho^{s(n-1)}a_0^{n-1}\phi_1\partial_{\rho\rho\rho\rho}\phi_1.\end{aligned}$$

Hence, the leading order terms are

$$\frac{1}{n2^n\varepsilon^2}a_0\rho^s = a_0^{n+1}s(s-1)(s-2)(s(n+1)-3)\rho^{s(n+1)-4}. \tag{5.13}$$

We have three options:

- $s = (n+1)s-4$, i.e. $s = \frac{4}{n}$. It will turn out that this cannot match the leading order in the touchdown region.

- $s < (n+1)s-4$, i.e. $s > \frac{4}{n}$. This case can be eliminated as it would mean that neither the leading order nor higher order corrections would be able to balance the left-hand side of equation (5.13).

- $s > (n+1)s-4$, i.e. $s < \frac{4}{n}$. In this case $\rho^{s(n+1)-4} \gg \rho^s$ for $\rho \to 0$ and hence the constant coefficients on the right-hand side of equation (5.13) must drop out. Hence

  $$s(s-1)(s-2)(s(n+1)-3) = 0.$$

  This polynomial has four single roots $s = 0,\ 1,\ 2,\ \frac{3}{n+1}$ for $n < 2$, and it has two single roots $s = 0,\ 2$ and one double root $s = 1$ for $n = 2$. We can rule out $s = 0$ as $\psi_0(\rho) \to 0$ as $\rho \to 0$. Moreover, we can also directly rule out $s = 1$ since this would lead to a linear matching, which we know does not work for $n < 2$. Because $\frac{3}{n+1} < 2$ for $1/2 < n < 2$, we assume the leading order is given by the exponent

  $$s = \frac{3}{n+1}, \tag{5.14}$$

  which is a single root for $\frac{1}{2} < n < 2$ and a double root for $n = 2$. This implies that we could have a quadratic term in the next order of the expansion by making use of the $s = 2$ exponent.

The above analysis leaves $a_0 \in \mathbb{R}$ free, and $\phi_1$ must satisfy

$$\begin{aligned}\frac{1}{n2^n\varepsilon^2}a_0\rho^s =& na_0^n\phi_1 s(s-1)(s-2)(sn-3)\rho^{sn-4}\\ &+ na_0^n s(s-1)(s-2)\rho^{sn-3}\partial_\rho\phi_1 + a_0^n sn\rho^{sn-1}\partial_{\rho\rho\rho}\phi_1\\ &+ a_0^n\rho^{sn}\partial_{\rho\rho\rho\rho}\phi_1 + ns(n-1)\rho^{s(n-1)-1}a_0^{n-1}\phi_1\partial_{\rho\rho\rho}\phi_1\\ &+ n\rho^{s(n-1)}a_0^{n-1}\partial_\rho\phi_1\partial_{\rho\rho\rho}\phi_1 + n\rho^{s(n-1)}a_0^{n-1}\phi_1\partial_{\rho\rho\rho\rho}\phi_1.\end{aligned}$$

Note that the expression eliminates the possibility of $\phi_1(\rho) = a_1\rho^2$ since, in that case, the right-hand side would become

$$\begin{aligned}\frac{1}{n2^n\varepsilon^2}a_0\rho^s =& na_0^n a_1 s(s-1)(s-2)(sn-3)\rho^{sn-2}\\ &+ 2na_0^n a_1 s(s-1)(s-2)\rho^{sn-3}.\end{aligned} \tag{5.15}$$

If the second term on the right-hand side of (5.15) is not balanced, then it will also not be balanced by higher order corrections as these will correspond to higher powers in $\rho$.

Accordingly, we set $\phi_1(\rho) = a_1\rho^\ell$, where $\ell > s$, and hence

$$\begin{aligned}\frac{1}{n2^n\varepsilon^2}a_0\rho^s =& na_0^n a_1 s(s-1)(s-2)(sn-3)\rho^{sn+\ell-4}\\ &+ na_0^n s(s-1)(s-2)a_1\ell\rho^{sn+\ell-4}\\ &+ a_0^n sna_1\ell(\ell-1)(\ell-2)\rho^{sn+\ell-4}\\ &+ a_0^n a_1\ell(\ell-1)(\ell-2)(\ell-3)\rho^{sn+\ell-4}\\ &+ ns(n-1)a_0^{n-1}a_1^2\ell(\ell-1)(\ell-2)\rho^{s(n+1)+2\ell-4}\\ &+ na_0^{n-1}a_1^2\ell^2(\ell-1)(\ell-2)\rho^{s(n-1)+2\ell-4}\\ &+ na_0^{n-1}a_1^2\ell(\ell-1)(\ell-2)(\ell-3)\rho^{s(n-1)+2\ell-4}.\end{aligned}$$

Note that the highest order terms on the right-hand side are the $\rho^{sn+\ell-4}$ terms, thus

$$\frac{1}{n2^n\varepsilon^2}a_0\rho^s = a_0^n a_1 P(\ell)\rho^{sn+\ell-4}, \tag{5.16}$$

where

$$\begin{aligned} P(\ell) :=& (sn+\ell-3)\left[ns(s-1)(s-2)+\ell(\ell-1)(\ell-2)\right], \\ =& \left(\ell - \frac{3}{n+1}\right)\left[\frac{3n(2-n)(1-2n)}{(n+1)^3} + \ell(\ell-1)(\ell-2)\right]. \end{aligned}$$

We have three possibilities,

- $s < ns - 4 + \ell$, i.e. $\ell > \frac{n+7}{n+1}$. Then $\phi_1$ is too small to balance the left-hand side, which cannot be balanced by higher order corrections. Thus, we eliminate this case.

- $s = ns - 4 + \ell$, i.e. $\ell = \tilde{\ell} := \frac{n+7}{n+1}$, then the second order term balances the left-hand side and $a_1 = \frac{1}{n2^n\varepsilon^2 a_0^{n-1}P(\tilde{\ell})}$. In this case, no new degree of freedom is introduced. Note that this power can still appear later in the expansion (for example, after the terms associated with the case $s > ns - 4 + \ell$) but it will still introduce no degree of freedom.

- $s > ns - 4 + \ell$, i.e. $\ell < \frac{n+7}{n+1}$. Then the dominant balance includes the term on the right-hand side of $O(\rho^{sn+\ell-4})$ but not the term on the left-hand side. This means that $a_0^n a_1 P(\ell) = 0$. Given that $a_0$, $a_1 \neq 0$, then either $\ell = \frac{3}{n+1} = s$, which implies that $\phi_1$ is either not consistent with the leading order, or else

$$\frac{3n(2-n)(1-2n)}{(n+1)^3} + \ell(\ell-1)(\ell-2) = 0,$$

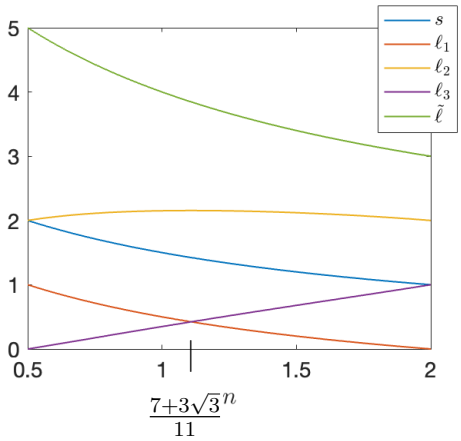



Figure 5.8: Exponents of terms in central region expansion as $r \to r_*$. We remark that wherever the lines for $\ell_1$, $\ell_2$, $\ell_3$ cross logarithmic terms will appear, as we will see in the expansions for the touchdown region.

which has the following solutions

$$\ell_1 := \frac{2-n}{n+1}, \tag{5.17}$$

$$\ell_2 := \frac{4n+1+\sqrt{-8n^2+20n+1}}{2(n+1)}, \tag{5.18}$$

$$\ell_3 := \frac{4n+1-\sqrt{-8n^2+20n+1}}{2(n+1)}. \tag{5.19}$$

These exponents are ordered for $1/2 < n < 2$ as shown in Figure 5.8. The only one larger than $s$ in this range of degrees of degeneracy is $\ell_2$. This introduces one degree of freedom, i.e. $a_1$.

Therefore the leading order expansion for $\psi_0$ as $r \to r_*^-$ is

$$\psi_0(r) = a_0^+(r_* - r)^s + a_1^+(r_* - r)^{\ell_2} + h.o.t.,$$

where $a_0^+$, $a_1^+ \in \mathbb{R}$ are to be determined.

Summarising, the leading order problem in the central region can be written as

$$-\frac{1}{n}\psi_0 = -\frac{2^n}{r}\partial_r\left[r\psi_0^n\partial_r\left(\varepsilon^2\left(\partial_{rr}\psi_0 + \frac{1}{r}\partial_r\psi_0\right) - 4\psi_0\right)\right] \text{ in } (0, r_*), \tag{5.20}$$

$$\psi_0(r) = a_0^- + a_2^- r^2 + h.o.t. \quad \text{as } r \to 0, \tag{5.21}$$

$$\psi_0(r) = a_0^+ (r_* - r)^{\frac{3}{n+1}} + a_1^+ (r_* - r)^{\frac{4n+1+\sqrt{-8n^2+20n+1}}{2(n+1)}} + h.o.t. \quad \text{as } r \to r_*. \tag{5.22}$$

Note that we have two singular points, at $r = 0$ and at $r = r_*$. The first because of the equation's coefficients and the second because of the boundary conditions, since for $n \in (1/2, 2)$ we have $\frac{3}{n+1} \in (1, 2)$.

### 5.2.2 Central region: Another method

The method that we have used for obtaining approximations in each of the regions is based on expanding a nonlinear equation, obtaining the leading order terms, balancing the two sides and obtaining a leading order equation, substituting this together with an unknown correction back into the nonlinear equation and then repeating the process. This method requires careful consideration at each stage at which we discard terms that we consider as higher order and the examination of the various cases arising in balancing the leading order terms. This ensures that we maintain all terms in the expansion, including terms with degrees of freedom and intermediate terms that do not introduce new degrees of freedom.

Another method for expanding is to linearise the equation around a known solution, for which we have a leading order approximation, and to obtain a correction by solving the resultant linearised equation. This method gives us the terms corresponding to the degrees of freedom as the correction can be expected to be much smaller than the leading order solution. Thus, the linearised equation should be a good approximation. This makes counting degrees of freedom easier, but it will not necessarily give us all the intermediate terms in the expansion.

In what follows, we apply the linearisation method to the expansion in the central region as $r \to r_*^-$ in order to check that we obtain the same degrees of freedom as we did with the other method.

**Expansion as $r \to r_*^-$:** Recall that we want to find an expansion for the solution of

$$\begin{aligned}
-\frac{1}{n}\psi_0 =& -\frac{2^n}{r}\partial_r\left[r\psi_0^n\partial_r\left(\varepsilon^2\left(\partial_{rr}\psi_0+\frac{1}{r}\partial_r\psi_0\right)-4\psi_0\right)\right], \quad r\in(0,r_*),\\
\psi_0(r_*) =& 0.
\end{aligned}$$

We expand the solution in powers of $\rho := (r_* - r)$ as $\rho \to 0^+$, changing variables and using the notation $\partial_\rho = '$. Then the equation above becomes

$$\frac{1}{n}\psi_0 = \frac{2^n}{r_*-\rho}\left[(r_*-\rho)\psi_0^n\left(\varepsilon^2\left(\psi_0''-\frac{1}{r_*-\rho}\psi_0'\right)'-4\psi_0\right)\right]'.$$

We define

$$\mathcal{L}(\psi_0,\psi_0',\psi_0'',\psi_0''',\psi_0'''') := \frac{2^n}{r_*-\rho}\left[(r_*-\rho)\psi_0^n\left(\varepsilon^2\left(\psi_0''-\frac{1}{r_*-\rho}\psi_0'\right)'-4\psi_0\right)\right]'-\frac{1}{n}\psi_0.$$

Let $\psi_0 = \phi_0 + \phi_1$, $|\phi_1| \ll |\phi_0|$, and let us use the notation $\vec{\psi_0} := (\psi_0, \psi_0', \psi_0'', \psi_0''', \psi_0'''')$. If we suppose that $\mathcal{L}(\vec{\psi_0}) = 0$, then

$$\begin{aligned}
\mathcal{L}(\vec{\psi_0}) =& \mathcal{L}(\vec{\phi_0}+\vec{\phi_1}),\\
=& \mathcal{L}(\vec{\phi_0}) + D\mathcal{L}(\vec{\phi_0})(\vec{\phi_1}) + O(\|\vec{\phi_1}\|^2),\\
=& \frac{2^n}{r_*-\rho}\left[(r_*-\rho)n\phi_0^{n-1}\phi_1\left(\varepsilon^2\left(\phi_0''-\frac{1}{r_*-\rho}\phi_0'\right)'-4\phi_0\right)\right]'\\
&+\frac{2^n}{r_*-\rho}\left[(r_*-\rho)\phi_0^n\left(\varepsilon^2\left(\phi_1''-\frac{1}{r_*-\rho}\phi_1'\right)'-4\phi_1\right)\right]'-\frac{1}{n}\phi_1\\
&+O(\|\vec{\psi_1}\|^2),\\
=& \frac{2^n}{r_*-\rho}\left[(r_*-\rho)n\phi_0^{n-1}\phi_1\left(\varepsilon^2\left(\phi_0'''-\frac{1}{r_*-\rho}\phi_0''-\frac{1}{(r_*-\rho)^2}\phi_0'\right)-4\phi_0\right)\right]'\\
&+\frac{2^n}{r_*-\rho}\left[(r_*-\rho)\phi_0^n\left(\varepsilon^2\left(\phi_1'''-\frac{1}{r_*-\rho}\phi_1''-\frac{1}{(r_*-\rho)^2}\phi_1'\right)-4\phi_1\right)\right]'\\
&-\frac{1}{n}\phi_1+O(\|\vec{\psi_1}\|^2)
\end{aligned}$$

$$
\begin{aligned}
=&\frac{2^n}{r_*-\rho}\left[-n\phi_0^{n-1}\phi_1\left(\varepsilon^2\left(\phi_0'''-\frac{1}{r_*-\rho}\phi_0''+\frac{1}{(r_*-\rho)^2}\phi_0'\right)-4\phi_0\right)\right.\\
&+(r_*-\rho)n(n-1)\phi_0^{n-2}\phi_0'\phi_1\left(\varepsilon^2\left(\phi_0'''-\frac{1}{r_*-\rho}\phi_0''+\frac{1}{(r_*-\rho)^2}\phi_0'\right)-4\phi_0\right)\\
&+(r_*-\rho)n\phi_0^{n-1}\phi_1'\left(\varepsilon^2\left(\phi_0'''-\frac{1}{r_*-\rho}\phi_0''+\frac{1}{(r_*-\rho)^2}\phi_0'\right)-4\phi_0\right)\\
&+(r_*-\rho)n\phi_0^{n-1}\phi_1\left(\varepsilon^2\left(\phi_0''''-\frac{1}{r_*-\rho}\phi_0'''+\frac{2}{(r_*-\rho)^2}\phi_0''-\frac{1}{(r_*-\rho)^3}\phi_0'\right)-4\phi_0'\right)\\
&-\phi_0^n\left(\varepsilon^2\left(\phi_1'''-\frac{1}{r_*-\rho}\phi_1''+\frac{1}{(r_*-\rho)^2}\phi_1'\right)-4\phi_1\right)\\
&+(r_*-\rho)n\phi_0^{n-1}\phi_0'\left(\varepsilon^2\left(\phi_1'''-\frac{1}{r_*-\rho}\phi_1''+\frac{1}{(r_*-\rho)^2}\phi_1'\right)-4\phi_1\right)\\
&\left.+(r_*-\rho)\phi_0^n\left(\varepsilon^2\left(\phi_1''''-\frac{1}{r_*-\rho}\phi_1'''+\frac{2}{(r_*-\rho)^2}\phi_1''-\frac{1}{(r_*-\rho)^3}\phi_1'\right)-4\phi_1'\right)\right]\\
&-\frac{1}{n}\phi_1+O(\|\vec{\psi}_1\|^2).
\end{aligned}
$$

We now reorganise the equation above into the form

$$
A(\rho,\phi_0)\phi_1+B(\rho,\phi_0)\phi_1'+C(\rho,\phi_0)\phi_1''+D(\rho,\phi_0)\phi_1'''+E(\rho,\phi_0)\phi_1'''',
$$

which leads to

$$
\begin{aligned}
\mathcal{L}(\vec{\psi}_0)=&\phi_1\left[-\frac{n2^n}{r_*-\rho}\phi_0^{n-1}\left(\varepsilon^2\left(\phi_0'''-\frac{1}{r_*-\rho}\phi_0''+\frac{1}{(r_*-\rho)^2}\phi_0'\right)-4\phi_0\right)\right.\\
&+n2^n(n-1)\phi_0^{n-2}\phi_0'\left(\varepsilon^2\left(\phi_0'''-\frac{1}{r_*-\rho}\phi_0''+\frac{1}{(r_*-\rho)^2}\phi_0'\right)-4\phi_0\right)\\
&+n2^n\phi_0^{n-1}\left(\varepsilon^2\left(\phi_0''''-\frac{1}{r_*-\rho}\phi_0'''+\frac{2}{(r_*-\rho)^2}\phi_0''-\frac{1}{(r_*-\rho)^3}\phi_0'\right)-4\phi_0'\right)\\
&\left.+4\frac{2^n}{r_*-\rho}\phi_0^n-4n2^n\phi_0^{n-1}\phi_0'-\frac{1}{n}\right]\\
&+\phi_1'\left[n2^n\phi_0^{n-1}\left(\varepsilon^2\left(\phi_0'''-\frac{1}{r_*-\rho}\phi_0''+\frac{1}{(r_*-\rho)^2}\phi_0'\right)-4\phi_0\right)\right.\\
&\left.-\phi_0^n2^n\varepsilon^2\frac{1}{(r_*-\rho)}+n2^n\phi_0^{n-1}\phi_0'\varepsilon^2\frac{1}{(r_*-\rho)^2}+2^n\phi_0^n\left(-\frac{\varepsilon^2}{(r_*-\rho)^3}-4\right)\right]\\
&+\phi_1''\left[\frac{\varepsilon^2 2^n}{(r_*-\rho)^2}\phi_0^n+\frac{n2^n\varepsilon^2}{(r_*-\rho)}\phi_0^{n-1}\phi_0'+2\frac{2^n\varepsilon^2}{(r_*-\rho)^2}\phi_0^n\right]
\end{aligned}
$$

$$
\begin{aligned}
&+\phi_1'''\left[-\frac{2^n\varepsilon^2}{r_*-\rho}\phi_0^n+n2^n\varepsilon^2\phi_0^{n-1}\phi_0'-\frac{2^n\varepsilon^2}{r_*-\rho}\phi_0^n\right]\\
&+\phi_1''''2^n\varepsilon^2\phi_0^n.
\end{aligned}
$$

Note that for $\rho\to 0^+$,

$$
\frac{1}{(r_*-\rho)^m}=\frac{1}{{r_*}^m}+\frac{m}{{r_*}^{m+1}}\rho+O(\rho^2),\qquad m\in\mathbb{N}.
$$

Thus

$$
\begin{aligned}
\mathcal{L}(\vec{\psi}_0)=&\phi_1\left[-\frac{n2^n}{r_*}\phi_0^{n-1}\left(\varepsilon^2\left(\phi_0'''-\frac{1}{r_*}\phi_0''+\frac{1}{{r_*}^2}\phi_0'\right)-4\phi_0\right)\right.\\
&+n2^n(n-1)\phi_0^{n-2}\phi_0'\left(\varepsilon^2\left(\phi_0'''-\frac{1}{r_*}\phi_0''+\frac{1}{{r_*}^2}\phi_0'\right)-4\phi_0\right)\\
&+n2^n\phi_0^{n-1}\left(\varepsilon^2\left(\phi_0''''-\frac{1}{r_*}\phi_0'''+\frac{2}{{r_*}^2}\phi_0''-\frac{1}{{r_*}^3}\phi_0'\right)-4\phi_0'\right)\\
&\left.+4\frac{2^n}{r_*}\phi_0^n-4n2^n\phi_0^{n-1}\phi_0'-\frac{1}{n}\right]\\
&+\phi_1'\left[n2^n\phi_0^{n-1}\left(\varepsilon^2\left(\phi_0'''-\frac{1}{r_*}\phi_0''+\frac{1}{{r_*}^2}\phi_0'\right)-4\phi_0\right)\right.\\
&\left.-\phi_0^n2^n\varepsilon^2\frac{1}{r_*}+n2^n\phi_0^{n-1}\phi_0'\varepsilon^2\frac{1}{{r_*}^2}+2^n\phi_0^n\left(-\frac{\varepsilon^2}{{r_*}^3}-4\right)\right]\\
&+\phi_1''\left[\frac{\varepsilon^2 2^n}{{r_*}^2}\phi_0^n+\frac{n2^n\varepsilon^2}{r_*}\phi_0^{n-1}\phi_0'+2\frac{2^n\varepsilon^2}{{r_*}^2}\phi_0^n\right]\\
&+\phi_1'''\left[-\frac{2^n\varepsilon^2}{r_*}\phi_0^n+n2^n\varepsilon^2\phi_0^{n-1}\phi_0'-\frac{2^n\varepsilon^2}{r_*}\phi_0^n\right]\\
&+\phi_1''''2^n\varepsilon^2\phi_0^n,\\
=&A(\rho)\phi_1+B(\rho)\phi_1'+C(\rho)\phi_1''+D(\rho)\phi_1'''+E(\rho)\phi_1'''',
\end{aligned}
$$

where

$$
\begin{aligned}
A(\rho,\phi_0):=&-\frac{n2^n}{r_*}\phi_0^{n-1}\left(\varepsilon^2\left(\phi_0'''-\frac{1}{r_*}\phi_0''+\frac{1}{{r_*}^2}\phi_0'\right)-4\phi_0\right)\\
&+n2^n(n-1)\phi_0^{n-2}\phi_0'\left(\varepsilon^2\left(\phi_0'''-\frac{1}{r_*}\phi_0''+\frac{1}{{r_*}^2}\phi_0'\right)-4\phi_0\right)
\end{aligned}
$$

$$
\begin{aligned}
&+ n2^n\phi_0^{n-1}\left(\varepsilon^2\left(\phi_0'''' - \frac{1}{r_*}\phi_0''' + \frac{2}{{r_*}^2}\phi_0'' - \frac{1}{{r_*}^3}\phi_0'\right) - 4\phi_0'\right)\\
&+ 4\frac{2^n}{r_*}\phi_0^n - 4n2^n\phi_0^{n-1}\phi_0' - \frac{1}{n},\\
B(\rho,\phi_0) :=& n2^n\phi_0^{n-1}\left(\varepsilon^2\left(\phi_0''' - \frac{1}{r_*}\phi_0'' + \frac{1}{{r_*}^2}\phi_0'\right) - 4\phi_0\right)\\
&+ n2^n\phi_0^{n-1}\phi_0'\varepsilon^2\frac{1}{{r_*}^2} + 2^n\phi_0^n\left(-\frac{\varepsilon^2}{r_*} - \frac{\varepsilon^2}{{r_*}^3} - 4\right),\\
C(\rho,\phi_0) :=& \frac{3\varepsilon^2 2^n}{{r_*}^2}\phi_0^n + \frac{n2^n\varepsilon^2}{r_*}\phi_0^{n-1}\phi_0',\\
D(\rho,\phi_0) :=& -2\frac{2^n\varepsilon^2}{r_*}\phi_0^n + n2^n\varepsilon^2\phi_0^{n-1}\phi_0',\\
E(\rho,\phi_0) :=& 2^n\varepsilon^2\phi_0^n.
\end{aligned}
$$

Now we substitute the expansion $\psi_0(\rho) = a_0\rho^s + h.o.t.$ with $s = \frac{3}{n+1}$, which corresponds to the leading order expression that matches to the solution in the touchdown region. Here we have used $a_0$ instead of $a_0^+$ for convenience. This yields

$$
\begin{aligned}
A(\rho) =& \varepsilon^2 n2^n a_0^n s(s-1)(s-2)(sn-3)\rho^{sn-4} - \frac{\varepsilon^2 n2^n a_0^n}{r_*}s(s-1)(s(n+1)-4)\rho^{sn-3}\\
&+ \frac{\varepsilon^2 n2^n a_0^n}{{r_*}^2}s(s(n+2)-3)\rho^{sn-2} - n2^n a_0^n s\left(\frac{2}{{r_*}^3} + 4(n+1)\right)\rho^{sn-1}\\
&+ 4\frac{2^n a_0^n(n+1)}{r_*}\rho^{sn} - \frac{1}{n},\\
B(\rho) =& \varepsilon^2 n2^n a_0^n s(s-1)(s-2)\rho^{sn-3} + \frac{\varepsilon^2 n2^n a_0^n}{{r_*}^2}s(s-1)\rho^{sn-2}\\
&- n2^n a_0^n s\left(\frac{1}{{r_*}^3} - \frac{1}{{r_*}^2}\right)\rho^{sn-1} + 2^n a_0^n\left(\frac{4n-\varepsilon^2}{r_*} - \frac{\varepsilon^2}{{r_*}^3} - 4\right)\rho^{sn},\\
C(\rho) =& \frac{n\varepsilon^2 2^n a_0^n}{r_*}s\rho^{sn-1} + 3\frac{\varepsilon^2 2^n a_0^n}{{r_*}^2}\rho^{sn},\\
D(\rho) =& n2^n\varepsilon^2 a_0^n s\rho^{sn-1} - 2\frac{2^n\varepsilon^2 a_0^n}{r_*}\rho^{sn},\\
E(\rho) =& 2^n\varepsilon^2 a_0^n\rho^{sn}.
\end{aligned}
$$

As $\rho \to 0$, the leading order terms are powers of $\delta$ with the lowest exponents. Thus,

to leading order,

$$\begin{aligned}\mathcal{L}(\vec{\psi}_0) =&\varepsilon^2 2^n a_0^n \left[ns(s-1)(s-2)(sn-3)\rho^{sn-4}\phi_1 + ns(s-1)(s-2)\rho^{sn-3}\phi_1'\right.\\ &\left.+\frac{n}{r_*}s\rho^{sn-1}\phi_1'' + ns\rho^{sn-1}\phi_1''' + \rho^{sn}\phi_1''''\right].\end{aligned}$$

Hence, to solve $\mathcal{L}(\vec{\psi}_0)$, we can apply the Frobenius method, see Appendix C. Accordingly, we assume that

$$\phi_1(r) = \sum_{k=0}^{\infty} b_k \rho^{\lambda+k},$$

with $b_0 = 1$. Then

$$\begin{aligned}\mathcal{L}(\vec{\psi}_0) =&\varepsilon^2 2^n a_0^n \left[ns(s-1)(s-2)(sn-3)\rho^{sn-4}\sum_{k=0}^{\infty} b_k\rho^{\lambda+k}\right.\\ &+ ns(s-1)(s-2)\rho^{sn-3}\sum_{k=0}^{\infty} b_k(\lambda+k)\rho^{\lambda+k-1}\\ &+ \frac{n}{r_*}s\rho^{sn-1}\sum_{k=0}^{\infty} b_k(\lambda+k)(\lambda+k-1)\rho^{\lambda+k-2}\\ &+ ns\rho^{sn-1}\sum_{k=0}^{\infty} b_k(\lambda+k)(\lambda+k-1)(\lambda+k-2)\rho^{\lambda+k-3}\\ &\left.+\rho^{sn}\sum_{k=0}^{\infty} b_k(\lambda+k)(\lambda+k-1)(\lambda+k-2)(\lambda+k-3)\rho^{\lambda+k-4}\right].\end{aligned}$$

Thus

$$\begin{aligned}\frac{\mathcal{L}(\vec{\psi}_0)}{\varepsilon^2 2^n a_0^n \rho^{\lambda+sn-4}} =&\sum_{k=0}^{\infty}\left[ns(s-1)(s-2)(sn-3) + ns(s-1)(s-2)(\lambda+k)\right.\\ &+ ns(\lambda+k)(\lambda+k-1)(\lambda+k-2)\\ &\left.+(\lambda+k)(\lambda+k-1)(\lambda+k-2)(\lambda+k-3)\right] b_k\rho^k\\ &+ \frac{n}{r_*}s\sum_{k=0}^{\infty} b_k(\lambda+k)(\lambda+k-1)\rho^{k+1}.\end{aligned}$$

Let

$$F(\lambda) := \left(\lambda - \frac{3}{(n+1)}\right)\left[\frac{3n(2-n)(1-2n)}{(n+1)^3} + \lambda(\lambda-1)(\lambda-2)\right].$$

Assuming that $\mathcal{L}(\vec{\psi}_0) = 0$ and reorganising all terms into one sum, we obtain that

$$0 = F(\lambda)b_0 + \sum_{k=1}^{\infty}\left[F(\lambda+k)b_k + \frac{n}{r_*}s(\lambda+k-1)(\lambda+k-2)b_{k-1}\right]\rho^k.$$

To satisfy the above equation, we set

$$F(\lambda) = 0, \qquad F(\lambda+k)b_k = -\frac{n}{r_*}s(\lambda+k-1)(\lambda+k-2)b_{k-1}, \quad \forall k \geq 1. \tag{5.23}$$

Here $F(\lambda) = 0$ is the indicial equation and it has the roots $s$, $\ell_1$, $\ell_2$ and $\ell_3$ as defined in (5.14), (5.17), (5.18), (5.19), respectively. Note that all the roots are different if $n \neq \frac{7+3\sqrt{3}}{11}$ and $s - \ell_1 = 1 \in \mathbb{Z}$.

The general solution should, a priori, be given by a linear combination of the four linearly independent solutions given by each of these indices. However, we note that $s$, $\ell_1$ and $\ell_3$ are larger or equal to the leading order of the expansion of $\phi_0$. This implies that the leading order of the linearly independent solutions given by $s$, $\ell_1$ and $\ell_3$ are not consistent with a correction to the leading order of the expansion (since $\phi_0(\rho) \sim \rho^s$). Hence, the expansion of the solution is given by

$$\phi_1(\rho) = a_0^+\rho^{\ell_2} + h.o.t.,$$

where $a_0^+ \in \mathbb{R}$ is unknown. This coincides with the result that we obtained in the previous section.

### 5.2.3 Central region comparison with case $n > 2$

To understand how the problem in the central region changes as we vary $n$ from $n > 2$ to $n < 2$, we focus now on the asymptotics for the case $n > 2$. If we did not have an analytical solution, then we would have needed to undertake similar expansions as for the case $n < 2$. So, let us recall the leading order problem in the central region after balancing:

$$0 = \partial_r \left[ r\psi_0^n \partial_r \left( \varepsilon^2 \left( \partial_{rr}\psi_0 + \frac{1}{r}\partial_r\psi_0 \right) - 4\psi_0 \right) \right] \text{ in } (0, r_*), \tag{5.24}$$

$$\psi_0(r_*) = 0, \tag{5.25}$$

$$\partial_r\psi_0(0) = 0, \quad \partial_r\mu_0(0) = 0. \tag{5.26}$$

**Expansion as $r \to 0^+$:** We use again the notation $' = \partial_r$, expand all derivatives, and employ the following ansatz

$$\psi_0(r) = \tilde{a}_0 + \phi(r),$$

where $\tilde{a}_0 \in \mathbb{R}$, $\tilde{a}_0 > 0$ and $|\phi(r)| \ll \tilde{a}_0$ as $r \to 0^+$. This yields

$$\begin{aligned}
0 =& \varepsilon^2(\tilde{a}_0+\phi)^n \left( (\tilde{a}_0+\phi)''' - \frac{1}{r^2}(\tilde{a}_0+\phi)' + \frac{1}{r}(\tilde{a}_0+\phi)'' \right) \\
&+ r\varepsilon^2 n(\tilde{a}_0+\phi)^{n-1}(\tilde{a}_0+\phi)' \left( (\tilde{a}_0+\phi)'' - \frac{1}{r^2}(\tilde{a}_0+\phi)' + \frac{1}{r}(\tilde{a}_0+\phi)'' \right) \\
&+ r\varepsilon^2(\tilde{a}_0+\phi)^n \left( (\tilde{a}_0+\phi)'''' + \frac{2}{r^3}(\tilde{a}_0+\phi)' - \frac{2}{r^2}(\tilde{a}_0+\phi)'' + \frac{1}{r}(\tilde{a}_0+\phi)''' \right) \\
&- 4(\tilde{a}_0+\phi)^n(\tilde{a}_0+\phi)' - 4rn(\tilde{a}_0+\phi)^{n-1}(\tilde{a}_0+\phi)'^2 - 4r(\tilde{a}_0+\phi)^n(\tilde{a}_0+\phi)''.
\end{aligned}$$

We only keep the lowest order contributions, i.e. the terms associated with $\tilde{a}_0^n$, and we eliminate nonlinear terms in $\phi$ or its derivatives. This procedure leaves us with

the following

$$0 = \varepsilon^2 \tilde{a}_0^n \left( \phi''' - \frac{1}{r^2}\phi' + \frac{1}{r}\phi'' \right) + r\varepsilon^2 \tilde{a}_0^n \left( \phi'''' + \frac{2}{r^3}\phi' - \frac{2}{r^2}\phi'' + \frac{1}{r}\phi''' \right) - 4\tilde{a}_0^n \phi' - 4r\tilde{a}_0^n \phi'' + h.o.t.$$

Assuming that $\phi \sim r^\lambda$ for some $\lambda > 1$, then there are two types of terms on the right-hand side, the top line is $O(r^{\lambda-3})$ and the bottom line in $O(r^{\lambda-1})$. Thus the dominant terms are

$$0 = \varepsilon^2 \tilde{a}_0^n \left( \phi''' - \frac{1}{r^2}\phi' + \frac{1}{r}\phi'' \right) + r\varepsilon^2 \tilde{a}_0^n \left( \phi'''' + \frac{2}{r^3}\phi' - \frac{2}{r^2}\phi'' + \frac{1}{r}\phi''' \right) + h.o.t.,$$

which we can regroup and simplify since $\varepsilon^2 \tilde{a}_0^n > 0$. Accordingly, we obtain

$$0 = r\phi'''' + 2\phi''' - \frac{1}{r}\phi'' + \frac{1}{r^2}\phi' + h.o.t.$$

If the right-hand side balances the left-hand side, then $\lambda = 3$. Therefore $\phi = \tilde{a}_1 r^4$, but then $\tilde{a}_1 = 0$. If the left-hand side does not enter the dominant balance, then

$$\mathcal{L}(\phi) := \phi'''' + \frac{2}{r}\phi''' - \frac{1}{r^2}\phi'' + \frac{1}{r^3}\phi' = 0.$$

This is the same equation that we solved for $n < 2$, where we obtained $\phi = a_2^- r^2 + h.o.t.$ Thus we may conclude that

$$\psi_0(r) = a_0^- + a_2^- r^2 + h.o.t.$$

with $a_0^-$ and $a_2^-$ as free constants. This expansion satisfies the boundary conditions (5.26).

One can also derive the same expansion by integrating at the outset, imposing the

boundary condition $\mu_0' = 0$, and then solving the remaining equation.

Thus, at this stage, the behaviour in the central region is the same as for the case $n < 2$.

**Expansion as $r \to r_*^-$:** Recall that

$$\begin{aligned} 0 =& -\frac{2^n}{r}\partial_r\left[r\psi_0^n\partial_r\left(\varepsilon^2\left(\partial_{rr}\psi_0 + \frac{1}{r}\partial_r\psi_0\right) - 4\psi_0\right)\right], \quad r \in (0, r_*), \\ \psi_0(r_*) =& 0, \end{aligned}$$

We expand the solution in powers of $\rho := (r_* - r)$ as $\rho \to 0^+$, changing variables from $r$ to $\rho$, expanding all the $(r_* - \rho)$ terms and maintaining only the leading order terms. This yields

$$\begin{aligned} 0 =& n\psi_0^{n-1}\partial_\rho\psi_0\left(\varepsilon^2\left(r_*\partial_{\rho\rho\rho}\psi_0 - \partial_{\rho\rho}\psi_0 - \frac{1}{r_*}\partial_\rho\psi_0\right) - 4r_*\partial_\rho\psi_0\right) \\ &+ \psi_0^n\left(\varepsilon^2\left(r_*\partial_{\rho\rho\rho\rho}\psi_0 - \partial_{\rho\rho\rho}\psi_0 - \frac{2}{r_*}\partial_{\rho\rho}\psi_0 - \frac{2}{{r_*}^2}\partial_\rho\psi_0\right)\right. \\ &\left. - 4r_*\partial_{\rho\rho}\psi_0\right) \\ &- \psi_0^n\left(\varepsilon^2\left(\partial_{\rho\rho\rho}\psi_0 - \frac{1}{r_*}\partial_{\rho\rho}\psi_0 - \frac{1}{{r_*}^2}\partial_\rho\psi_0\right) - 4\partial_\rho\psi_0\right). \end{aligned}$$

Suppose that $\psi_0 \sim \rho^s$ with $s > 0$. Then the leading order terms on the right-hand side of the above equation correspond to the first terms on each line, i.e. those terms of order $O(\rho^{s(n+1)-4})$. Hence

$$0 = \varepsilon^2\partial_\rho[\psi_0^n\partial_{\rho\rho\rho}\psi_0] + h.o.t.$$

Following the same steps as in the corresponding expansion for $n < 2$, we obtain that for $\psi_0 = a_0\rho^s + \phi_1(\rho)$, with $|\phi_1| \ll \rho^s$ as $\rho \to 0$, the leading order equation is

$$0 = a_0^{n+1}s(s-1)(s-2)(s(n+1)-3)\rho^{s(n+1)-4},$$

where we must now consider the case $s = 1$ instead of $s = \frac{3}{n+1}$.

For the next order correction $\phi_1(\rho) = a_1\rho^\ell$, we would again have (5.16), but with no left-hand side i.e.

$$0 = a_0^n a_1 P(\ell)\rho^{n+\ell-4},$$

where $P(\ell) := (\ell - 3 + n)\,\ell(\ell-1)(\ell-2)$. To obtain $\ell$ we require $P(\ell) = 0$, which has the solutions $\tilde{\ell}_0 = 3 - n$, $\tilde{\ell}_1 = 0$, $\tilde{\ell}_2 = 1$, $\tilde{\ell}_3 = 2$. Because $n > 2$ and $|\phi_1| \ll |\phi_0|$ as $\rho \to 0$, the only viable correction has exponent $\tilde{\ell}_3 = 2$.

Therefore, for $n > 2$, the leading order expansion for $\psi_0$ as $r \to r_*^-$ is

$$\psi_0(r) = a_0^+(r_* - r) + a_1^+(r_* - r)^2 + h.o.t.$$

where $a_0^+$, $a_1^+ \in \mathbb{R}$ are free. We note that this expansion satisfies the boundary condition (5.25), and it coincides with the Taylor expansion we obtained from the analytical solution of the central region in the case $n > 2$, see (4.24).

Up to this point, the amount of degrees of freedom seems to be the same as in the case $n < 2$. However, we know from Section 5.2.1 that there is an extra degree of freedom in the case $n > 2$, which we called $c_2$.

To understand how this can be possible, we first note that, in summary, we have

$$0 = -\frac{2^n}{r}\partial_r\left[r\psi_0^n\partial_r\left(\varepsilon^2\left(\partial_{rr}\psi_0 + \frac{1}{r}\partial_r\psi_0\right) - 4\psi_0\right)\right] \text{ in } (0, r_*), \tag{5.27}$$

$$\psi_0(r) = a_0^- + a_2^- r^2 + h.o.t. \quad \text{as } r \to 0, \tag{5.28}$$

$$\psi_0(r) = a_0^+(r_* - r) + a_1^+(r_* - r)^2 + h.o.t., \quad \text{as } r \to r_*. \tag{5.29}$$

If we integrate (5.27), then we obtain a third-order ordinary differential equation with an unknown integration constant $j$ representing the flux. Using the expansion (5.28) yields $j = 0$. Thus, the problem becomes a third-order ordinary differential equation

with four degrees of freedom $a_0^-$, $a_2^-$, $a_0^+$ and $a_1^+$.

As a consequence, the central region problem has one more degree of freedom in the case $n > 2$ than for $n < 2$. From Chapter 4 we know that this extra degree of freedom is balanced by the information coming from the touchdown region, namely we use the solution in the touchdown region to obtain the unknown integration variable $c_2$ from (4.23). We will see later that for $n < 2$, this extra degree of freedom from the central region will appear, instead, in the touchdown region. Thus, the new balance of information between the constants is reversed, i.e. for $n > 2$ we use the touchdown region to inform the central region, and for $n < 2$ we use the central region to inform the touchdown region.

### 5.2.4 Touchdown region

In this region, we use the independent variable $\eta := \frac{r-r_*}{\delta^{-\gamma}\tau^\gamma}$, with $\gamma < 0$. We expand the solution as

$$v_{touchdown}(\eta, \tau) = \delta^{-\beta}\tau^\beta \varphi_0(\eta) + o(\delta^{-\beta}), \tag{5.30}$$

where $\beta < 0$. The analysis undertaken to obtain the leading order equation in section 4.2.2 is still valid for $n < 2$. The numerical simulations also suggest that $\beta = 2\gamma$ in this case. Thus the leading order equation is given by (4.30), namely

$$\varphi_0^n(\eta)\partial_{\eta\eta\eta}\varphi_0(\eta) = J,$$

where the flux $J$ is unknown.

The following is a summary of the expansions we will obtain in this section, so that the reader has an overview of the resulting leading order behaviour of the solution in the touchdown region before going into the details of each asymptotic expansion.

**Summary 5.2.** *In the touchdown region when* $1/2 < n < 2$ *as* $\eta \to -\infty$, *we have*

*the following asymptotic expansions*

$$\varphi_0(\eta)=\begin{cases} A_-(-\eta)^{\frac{3}{(n+1)}}+B_-(-\eta)^{\frac{2-n}{n+1}}+C_-(-\eta)^{\frac{4n+1-\sqrt{-8n^2+20n+1}}{2(n+1)}}+h.o.t., & \frac{1}{2}<n<\frac{7+3\sqrt{3}}{11}, \\ A_-(-\eta)^{2-\frac{\sqrt{3}}{3}}+B_-(-\eta)^{1-\frac{\sqrt{3}}{3}}\ln\left(-\frac{1}{\eta}\right)+C_-(-\eta)^{1-\frac{\sqrt{3}}{3}}+h.o.t., & n=\frac{7+3\sqrt{3}}{11}, \\ A_-(-\eta)^{\frac{3}{(n+1)}}+B_-(-\eta)^{\frac{4n+1-\sqrt{-8n^2+20n+1}}{2(n+1)}}+C_-(-\eta)^{\frac{2-n}{n+1}}+h.o.t., & \frac{7+3\sqrt{3}}{11}<n<2, \end{cases}$$

*where*

$$A_-=\left|\frac{-J(n+1)^3}{3(1-2n)(2-n)}\right|^{\frac{1}{n+1}} \tag{5.31}$$

*and $J$, $B_-$ and $C_-$ are unknown.*

*On the other hand, as $\eta\to+\infty$, we have*

$$\varphi_0=\begin{cases} A_+\eta^2+\frac{-J\eta^{3-2n}}{A_+^n(2n-1)(2n-2)(2n-3)}+B_+\eta+C_+, & \frac{1}{2}<n<1, \\ A_+\eta^2+\frac{-J}{A_+}\eta(\ln(\eta)+1)+B_+\eta+C_+, & n=1, \\ A_+\eta^2+B_+\eta+\frac{-J\eta^{3-2n}}{A_+^n(2n-1)(2n-2)(2n-3)}+C_+, & 1<n<\frac{3}{2}, \\ A_+\eta^2+B_+\eta+\frac{J}{2A_+^{3/2}}\ln(\eta)+C_+, & n=\frac{3}{2}, \\ A_+\eta^2+B_+\eta+C_++\frac{-J\eta^{3-2n}}{A_+^n(2n-1)(2n-2)(2n-3)}, & \frac{3}{2}<n<2, \end{cases}$$

*where $A_+, B_+, C_+$ are unknown integration constants.*

**Expansion as $\eta\to-\infty$:** We expand $\varphi_0$, solution to (4.30), as $\eta\to-\infty$. We suppose the expansion of the touchdown solution can be expressed in powers of $\eta$. Accordingly, if we let $x:=-\eta$, then

$$\varphi_0^n(x)\varphi_0'''(x)=-J, \tag{5.32}$$

where $'=\partial_x$, and

$$\varphi_0(x)=\phi_0(x)+o(x^p), \qquad \phi_0(x):=Ax^p,$$

for some $p, A \in \mathbb{R}$, as $x \to \infty$. Thus

$$p(p-1)(p-2)A^{n+1}x^{(n+1)p-3} + o(x^{(n+1)p-3}) = -J. \tag{5.33}$$

If the leading order term on the left balances $-J$, then

$$p(p-1)(p-2)A^{n+1}x^{(n+1)p-3} = -J, \tag{5.34}$$

which implies that

$$p = \frac{3}{n+1}, \quad A^{n+1} = \frac{-J(n+1)^3}{3(1-2n)(2-n)} > 0,$$

for $n \in \left(\frac{1}{2}, 2\right)$. Note that for $n \in (1/2, 2)$ we have that $p \in (1, 2)$.

Substituting $\varphi_0 = \phi_0 + \phi_1$, where $0 \neq |\phi_1| \ll |\phi_0|$ as $x \to \infty$, into equation (5.32) gives us

$$\begin{gathered}
\left(\phi_0^n + \sum_{i=1}^{n} \binom{n}{i} \phi_0^{n-i}\phi_1^i\right)(\phi_0''' + \phi_1''') = -J, \\
\sum_{i=1}^{n} \binom{n}{i} \phi_0^{n-i}\phi_1^i\phi_0''' + \sum_{i=0}^{n} \binom{n}{i} \phi_0^{n-i}\phi_1^i\phi_1''' = -J - \phi_0^n\phi_0''', \\
\sum_{i=1}^{n} \binom{n}{i} \phi_0^{n-i}\phi_1^i\phi_0''' + \sum_{i=0}^{n} \binom{n}{i} \phi_0^{n-i}\phi_1^i\phi_1''' = 0,
\end{gathered}$$

where the terms on the right-hand side cancel out by assumption (5.34). Since $|\phi_1| \ll |\phi_0|$, the leading order terms are those which correspond to $i = 1$ and $i = 0$, respectively. Then, assuming that $\phi_0 \neq 0$, we obtain

$$0 = \phi_0^n \left(n\frac{\phi_0'''}{\phi_0}\phi_1 + \phi_1'''\right) + h.o.t.,$$

and hence

$$0 = n\frac{\phi_0'''}{\phi_0}\phi_1 + \phi_1''' + h.o.t.$$

Since

$$\phi_0''' = Ap(p-1)(p-2)x^{p-3} = p(p-1)(p-2)x^{-3}\phi_0,$$

it follows that

$$0 = np(p-1)(p-2)x^{-3}\phi_1 + \phi_1''' + h.o.t.$$

Namely,

$$0 = \phi_1''' - \frac{3n(2-n)(2n-1)}{(n+1)^3}\frac{\phi_1}{x^3} + h.o.t. \tag{5.35}$$

If the second term on the right-hand side of the equation above is subdominant, then $\phi_1''' = 0$. This implies that $\phi_1(x) = c_0 + c_1 x + c_2 x^2$, and therefore the term $\frac{\phi_1}{x^3}$ has to be balanced by a higher order term $\phi_2$ such that $|\phi_2| \ll |\phi_1|$ as $x \to \infty$ and $\phi_2''' \sim \frac{\phi_1}{x^3} = \frac{c_0}{x^3} + \frac{c_1}{x^2} + \frac{c_2}{x}$. Integrating three times, we obtain that $\phi_2 = O(x^2 \ln(x)) \gg O(x^p) = \phi_1$, which is a contradiction.

If, on the other hand, both terms in (5.35) balance each other, then $\phi_1$ must satisfy

$$\phi_1''' - \frac{3n(2-n)(2n-1)}{(n+1)^3}\frac{\phi_1}{x^3} = 0,$$

which has a singular point at $x = +\infty$. We change variables $x = 1/z$ so that the new singular point is at $z = 0$, then

$$\begin{aligned}\frac{d\phi_1}{dx} &= -z^2\frac{d\phi_1}{dz},\\ \frac{d^2\phi_1}{dx^2} &= 2z^3\frac{d\phi_1}{dz} + z^4\frac{d^2\phi_1}{dz^2},\end{aligned}$$

$$\frac{d^3\phi_1}{dx^3} = -6z^4\frac{d\phi_1}{dz} - 6z^5\frac{d^2\phi_1}{dz^2} - z^6\frac{d^3\phi_1}{dz^3},$$

and hence

$$0 = \phi_1''' + \frac{6}{z}\phi_1'' + \frac{6}{z^2}\phi_1' + \frac{3n(2-n)(2n-1)}{(n+1)^3}\frac{\phi_1}{z^3}. \tag{5.36}$$

Therefore $z = 0$ is a regular singular point of this linear ordinary differential equation, and we can apply the Frobenius method. Accordingly, we let

$$\phi_1(x) = \sum_{k=0}^{\infty} a_k z^{k+\lambda},$$

where $\lambda \in \mathbb{R}$ is unknown. We substitute this expression for $\phi_1(x)$ into (5.36) and obtain

$$\begin{aligned} 0 = \sum_{k=0}^{\infty} &[(\lambda+k)(\lambda+k-1)(\lambda+k-2) + 6(\lambda+k)(\lambda+k-1) + 6(\lambda+k) \\ &+ \frac{3n(2-n)(2n-1)}{(n+1)^3}\Bigg] a_k z^{k+\lambda-3}. \end{aligned}$$

Assuming that $a_0 \neq 0$, we obtain the indicial equation by setting $k = 0$

$$\left[\lambda(\lambda-1)(\lambda-2) + 6\lambda(\lambda-1) + 6\lambda + \frac{3n(2-n)(2n-1)}{(n+1)^3}\right] = 0.$$

This equation has three roots at

$$\begin{aligned} \lambda_1 &:= -\ell_1 > -p, \\ \lambda_2 &:= -\ell_2 < -p, \\ \lambda_3 &:= -\ell_3 > -p, \end{aligned}$$

for $n \in (1/2, 2)$, where $\ell_1$, $\ell_2$ and $\ell_3$ are given by (5.17), (5.18) and (5.19), respectively.

We note that these are all single roots for $n \in \left(\frac{1}{2}, \frac{7+3\sqrt{3}}{11}\right) \cup \left(\frac{7+3\sqrt{3}}{11}, 2\right)$ and $\lambda_1 = \lambda_3$ is a double root for $n = \frac{7+3\sqrt{3}}{11}$.

- For $n \in (1/2, \frac{7+3\sqrt{3}}{11}) \cup (\frac{7+3\sqrt{3}}{11}, 2)$ we have

$$\phi_1(x) = B_- x^{\ell_1} + C_- x^{\ell_3},$$

  where $B_-, C_- \in \mathbb{R}$ are free. Here we have dropped $\ell_2$ as $\ell_2 > p$ is inconsistent with the leading order.

- For $n = \frac{7+3\sqrt{3}}{11}$ we have $\ell_1 = \ell_3 = 1 - \frac{\sqrt{3}}{3}$. Applying the Frobenius method for double roots we get

$$\phi_1(z) = B_- x^{1-\frac{\sqrt{3}}{3}} \ln\left(\frac{1}{x}\right) + C_- x^{1-\frac{\sqrt{3}}{3}},$$

  where $B_-, C_- \in \mathbb{R}$ are free. Recall that the leading order term in the expansion is

$$\phi_0(z) = A x^{2-\frac{\sqrt{3}}{3}},$$

  and since $\ln\left(\frac{1}{x}\right) = -\ln(x)$ goes to infinity slower than $x$ as $x \to \infty$, this means that all terms in $\phi_1$ are consistent corrections.

Now, we can go to next order corrections. To make this easier to work with we define $\bar{\phi}_0 := \phi_0 + \phi_1$ and add the correction term as $\phi_2$, i.e.

$$\varphi_0 = \bar{\phi}_0 + \phi_2,$$

where $0 < |\phi_2| \ll |\phi_1|$ as $x \to \infty$. Then equation (5.32) becomes

$$\left(\bar{\phi}_0^n + \sum_{i=1}^{n} \binom{n}{i} \bar{\phi}_0^{n-i} \phi_2^i\right) \left(\bar{\phi}_0''' + \phi_2'''\right) = -J,$$

$$\sum_{i=1}^{n}\binom{n}{i}\bar{\phi}_0^{n-i}\phi_2^i\bar{\phi}_0''' + \sum_{i=0}^{n}\binom{n}{i}\bar{\phi}_0^{n-i}\phi_2^i\phi_2''' = -J - \bar{\phi}_0^n\bar{\phi}_0''' =: G(\bar{\phi}_0).$$

We note that $G(\bar{\phi}_0) \neq 0$, since $\bar{\phi}_0$ is not an exact solution. Then, to leading order, the equation is given by

$$\phi_2''' + n\frac{\bar{\phi}_0'''}{\bar{\phi}_0}\phi_2 = \frac{G(\bar{\phi}_0)}{\bar{\phi}_0^n}.$$

If the left-hand side of the equation above balances the right-hand side, then we obtain the same type of solution as before and no degree of freedom is added, so the amount of degrees of freedom stays the same. If there is no balance and the right-hand side remains to be absorbed by a higher order term, then we may introduce new degrees of freedom. Thus

$$\phi_2''' + n\frac{\bar{\phi}_0'''}{\bar{\phi}_0}\phi_2 = 0.$$

Since $\bar{\phi}_0 = \phi_0 + \phi_1$ where $|\phi_1| \ll |\phi_0|$ as $x \to \infty$, we can approximate this equation by

$$\phi_2''' - \frac{3n(2-n)(2n-1)}{(n+1)^3}\frac{\phi_2}{x^3} = 0.$$

This equation is the same as (5.35) so it will lead to the same exponents $\ell_1$, $\ell_2$ and $\ell_3$. Hence, $\phi_2$ can be absorbed by $\phi_1$, introducing no new degrees of freedom.

**Expansion as $\eta \to +\infty$:** We expand $\varphi_0$, solution to (4.30), as $\eta \to \infty$ where $J > 0$ is unknown. Again we expect the expansion of the touchdown solution to be in powers of $\eta$, i.e. we suppose

$$\varphi_0(\eta) = A\eta^p + o(\eta^p),$$

for some $p, A \in \mathbb{R}$. Then

$$p(p-1)(p-2)A^{n+1}\eta^{(n+1)p-3} + o(\eta^{(n+1)p-3}) = J. \tag{5.37}$$

Since we need $\varphi_0$ to match to the leading order term in the annular region expansion, which is quadratic in $\eta$, we focus on the case $p = 2$. It follows that $\varphi_0$ must have the form

$$\varphi_0(\eta) = A\eta^2 + \phi(\eta) + o(\phi(\eta)),$$

where $\phi$ is of order $o(\eta^2)$ and satisfies

$$(A\eta^2 + \phi + o(\phi))^n \phi''' = J.$$

Again, we have two possibilities. If the leading order on the left-hand side, $(A\eta^2)^n$, balances $J$, then the correction must satisfy

$$\phi''' = \frac{J}{A^n \eta^{2n}}.$$

If, on the other hand, the next order term balances $J$, then $\phi''' = 0$. Thus $\phi = B\eta + C$, where $B$ and $C$ are unknown constants and we have discarded the quadratic term as $\phi = o(\eta^2)$. This is also a solution to the homogeneous problem in the previous case.

Collecting the results for all the cases gives us

$$\phi = \begin{cases} \frac{-J\eta^{3-2n}}{A^n(2n-1)(2n-2)(2n-3)} + B\eta + C, & \frac{1}{2} < n < 1, \\ \frac{-J}{A}\eta(\ln(\eta) + 1) + B\eta + C, & n = 1, \\ B\eta + \frac{-J\eta^{3-2n}}{A^n(2n-1)(2n-2)(2n-3)} + C, & 1 < n < \frac{3}{2}, \\ B\eta + \frac{J}{2A^{3/2}}\ln(\eta) + C, & n = \frac{3}{2}, \\ B\eta + C + \frac{-J\eta^{3-2n}}{A^n(2n-1)(2n-2)(2n-3)}, & \frac{3}{2} < n < 2, \end{cases}$$

where $B, C$ are unknown constants. We do not include the calculations here as they are analogous to the case $n > 2$.

### 5.2.5 Matching

In the case $n > 2$ we expanded the solution in the touchdown region at the same time as we matched its leading order to the solution in the central region. In that case, we were required to know what type of matching was needed before obtaining the appropriate expansions. On the other hand, for $n < 2$, we separate the expansions from the final matching to make the conclusions of each step easier to follow. However, the expansions that we have obtained for the solution in the central and touchdown regions as $r \to r_*$ are still informed by the matching. In particular, they are being influenced by the fact that the leading order must not be linear in space, and instead, it should be a fractional power, namely $s = 3/(n+1)$.

In what follows we summarise the expansions for the solutions in each region. Then we match adjacent regions and, finally, we obtain conditions on the exponents and unknown constants.

*Matching between the central and the touchdown region:* Recall that for $n < 2$ and $r \to r_*^-$ we have

$$\psi_0(r) = a_0^+ (r_* - r)^{\frac{3}{n+1}} + h.o.t.,$$

and for $1/2 < n < 2$ and $\eta \to -\infty$ we have

$$\varphi_0(\eta) = A_- (-\eta)^{\frac{3}{(n+1)}} + h.o.t.$$

Recalling that $v_{\text{central}} = \tau^\alpha \delta^{-\alpha} \psi_0(r)$ and $v_{\text{touchdown}} = \tau^\beta \delta^{-\beta} \varphi_0(\eta)$, we have

$$v_{\text{central}} = a_0^+ \tau^\alpha \delta^{-\alpha} (r_* - r)^{\frac{3}{n+1}} + h.o.t.$$

and, setting $-\eta = \frac{r_*-r}{\tau^\gamma \delta^{-\gamma}}$ in $\varphi_0(\eta)$, we have that

$$\begin{aligned} v_{touchdown} =& \tau^\beta \delta^{-\beta} \varphi_0(\eta), \\ =& A_- \tau^{\beta-\gamma\frac{3}{(n+1)}} \delta^{-\beta+\gamma\frac{3}{(n+1)}} (r_*-r)^{\frac{3}{(n+1)}} + h.o.t. \end{aligned}$$

Thus, for all $n \in \left(\frac{1}{2}, 2\right]$, matching at leading order requires

$$a_0^+ \tau^\alpha \delta^{-\alpha} (r_*-r)^{\frac{3}{n+1}} = A_- \tau^{\beta-\gamma\frac{3}{(n+1)}} \delta^{-\beta+\gamma\frac{3}{(n+1)}} (r_*-r)^{\frac{3}{(n+1)}},$$

which implies

$$a_0^+ = A_-, \tag{5.38}$$

$$\alpha = \beta - \gamma \frac{3}{n+1}, \tag{5.39}$$

where $A_-$ satisfies (5.31).

*Matching between the touchdown and the annular region:* Recall that for $\eta \to \infty$,

$$\varphi_0 = \begin{cases} A_+\eta^2 + \frac{-J\eta^{3-2n}}{A_+^n(2n-1)(2n-2)(2n-3)} + B_+\eta + C_+, & \frac{1}{2} < n < 1, \\ A_+\eta^2 + \frac{-J}{A_+}\eta(\ln(\eta)+1) + B_+\eta + C_+, & n = 1, \\ A_+\eta^2 + B_+\eta + \frac{-J\eta^{3-2n}}{A_+^n(2n-1)(2n-2)(2n-3)} + C_+, & 1 < n < \frac{3}{2}, \\ A_+\eta^2 + B_+\eta + \frac{J}{2A_+^{3/2}}\ln(\eta) + C_+, & n = \frac{3}{2}, \\ A_+\eta^2 + B_+\eta + C_+ + \frac{-J\eta^{3-2n}}{A_+^n(2n-1)(2n-2)(2n-3)}, & \frac{3}{2} < n < 2, \end{cases}$$

and for $r \to r_*^+$,

$$v_{annular} = b_2(r_*-r)^2 + h.o.t. \quad n < 2.$$

Hence to leading order in terms of $r$,

$$v_{touchdown} = \tau^{\beta-2\gamma}\delta^{-\beta+2\gamma}A_+(r_* - r)^2 + h.o.t.,$$

and

$$v_{annular} = b_2(r_* - r)^2 + h.o.t.$$

Matching now requires that

$$\begin{aligned}\beta =& 2\gamma,\\ A_+ =& b_2,\end{aligned}$$

where $b_2$ is given by (4.47).

Since in the central region equation we required the two sides to balance each other, we obtain a third equation, namely $\alpha = -\frac{1}{n}$. Thus we conclude that

$$\alpha = -\frac{1}{n}, \quad \beta = -\frac{2(n+1)}{n(2n-1)}, \quad \gamma = -\frac{(n+1)}{n(2n-1)},$$

which agrees with our numerical results.

**Remark 5.3.** *An interesting feature of the case $n < 2$ is that the role of the degrees of freedom in the touchdown and central regions gets exchanged. Recall that for the case $n > 2$, we had an extra degree of freedom in the central region, $c_2$, but the matching and the numerical solution in the touchdown region allowed us to obtain an expression for this constant. In a sense, the information that allows us to set the unknown constants of the problem travels from the annular to the central region. Now, for the case $n < 2$, the central region has no extra degrees of freedom, but the touchdown region does have one extra degree, so we expect the opposite to happen, i.e. that some information from the central region can be used to solve the touchdown*

*region.*

## 5.3 Solution in the central region

We wish to find a numerical solution to the leading order problem in the central region, i.e.

$$\begin{aligned}
-\frac{1}{n}\psi_0 =& -\frac{2^n}{r}\partial_r\left[r\psi_0^n\partial_r\left(\varepsilon^2\left(\partial_{rr}\psi_0+\frac{1}{r}\partial_r\psi_0\right)-4\psi_0\right)\right] \text{ in } (0,r_*),\\
\psi_0(r) =& a_0^- + a_2^- r^2 + h.o.t. \quad \text{as } r\to 0,\\
\psi_0(r) =& a_0^+(r_*-r)^{\frac{3}{n+1}} + a_1^+(r_*-r)^{\frac{4n+1+\sqrt{-8n^2+20n+1}}{2(n+1)}} + h.o.t., \quad \text{as } r\to r_*,
\end{aligned}$$

where $a_0^-$, $a_2^-$, $a_0^+$, $a_1^+$ are unknown constants. This corresponds to the number of free parameters that we need to solve this fourth-order ordinary differential equation.

We can rewrite the equation as the following system, for $r\in(0,r_*)$,

$$\Psi_0' = \Psi_1, \tag{5.40}$$

$$\Psi_1' = \Psi_2, \tag{5.41}$$

$$\Psi_2' = \Psi_3, \tag{5.42}$$

$$\Psi_3' = \frac{1}{n2^n\varepsilon^2}\Psi_0^{1-n} - \Psi_1\left(\frac{1}{r^3}-\frac{4}{r\varepsilon^2}-\frac{n}{r^2\Psi_0}\Psi_1-\frac{4n}{\varepsilon^2\Psi_0}\Psi_1\right) \tag{5.43}$$

$$-\Psi_2\left(-\frac{1}{r^2}+\frac{n}{r\Psi_0}\Psi_1-\frac{4}{\varepsilon^2}\right)-\Psi_3\left(\frac{2}{r}+\frac{n}{\Psi_0}\Psi_1\right). \tag{5.44}$$

We focus on shooting from the left of the interval. Since the equation is singular at $r=0$, we set $\nu=10^{-10}$ and solve in an interval $r\in(\nu,r_*)$. We use the following initial conditions

$$\Psi_0(\nu) = a_0^- + a_2^-\nu^2, \tag{5.45}$$

$$\Psi_1(\nu) = 2a_2^-\nu, \tag{5.46}$$

$$\Psi_2(\nu) = 2a_2^-, \tag{5.47}$$

$$\Psi_3(\nu) = 0. \tag{5.48}$$

We solve problem (5.40)-(5.44) with initial conditions (5.45)-(5.48) using ode45 from Matlab. The algorithm performs a binary search to find $a_0^-$ and $a_2^-$ as follows:

1. Initialise the interval for the binary search as $I := (a0_{init}, a0_{final})$ and set $a0_{mid} := \frac{a0_{final}+a0_{init}}{2}$. Let $I_R := (\nu, \tilde{r})$ where $\tilde{r}$ is chosen to be larger than $r_*$.

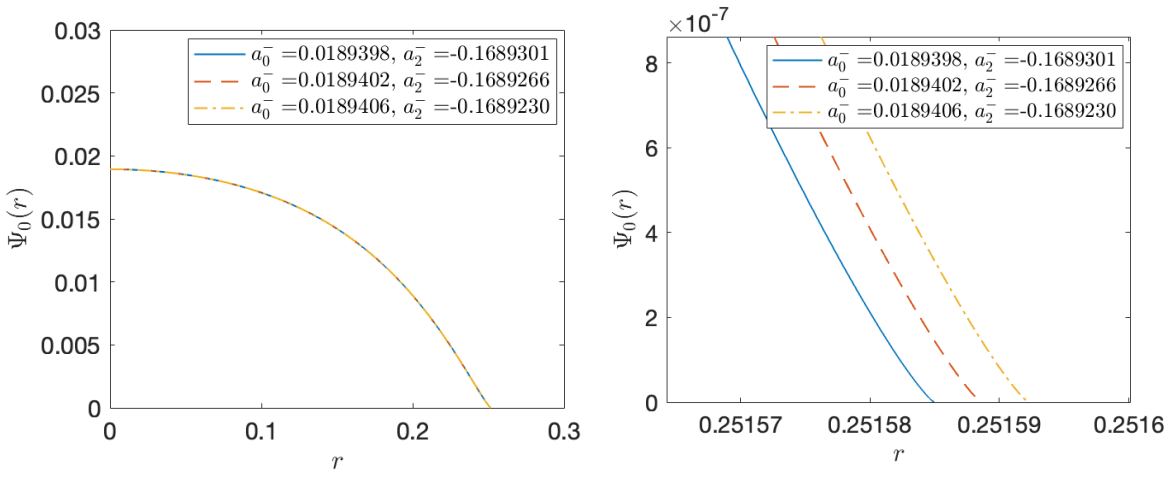
2. For each $a0 \in \{a0_{init}, a0_{mid}, a0_{final}\}$ find, using a binary search in an interval $H := (a2_{init}, a2_{final})$, the largest $a2$ such that the solution to problem (5.40)-(5.44) in $I_R$, denoted $\Psi(r, a0, a2)$, is computed by ode45 up to a radius $r < \tilde{r}$. This implies that ode45 stopped solving because $\Psi(r, a0, a2)$ reached 0 (up to machine precision) before $\tilde{r}$.

3. Update $I = (a0_{init}, a0_{final})$ so that the updated $a0_{init}$ and $a0_{final}$ generate the solution such that its minimum is achieved closest to $r_*$.

4. Repeat until the difference between $r_*$ and $\hat{r} := \text{argmin}_{r\in(0,1)}\Psi(r, a0_{init}, a2_{init})(r)$ is less than $tol_1$.

For the simulations shown here, we started with $I = (-0.18, -0.16)$ and $H = (-0.18, -0.16)$. We note that solutions for large $a_2^-$ reached a positive minimum, as shown in Figure 5.10. The three solutions obtained at the last step of the binary search for $a_0^-$ can be seen in Figure 5.9, where we can observe how each $\Psi_0(r, a_0^-, a_2^-)$ touches 0 at different radii.

We can check that the resulting numerical solution has the expected behaviour $(r_* - r)^{3/(n+1)}$ near $r_*$ by plotting $\log(\Psi_0(r))$ against $\log(\hat{r} - r)$, see Figure 5.11. Note that we plot $\log(\hat{r} - r)$, where $\hat{r}$ is the radius at which each solution $\Psi_0$ reaches its




(a) (b)

Figure 5.9: (a) $\Psi_0(r)$ versus $r$ for different $a_0^-$ and $a_2^-$, for $n = 3/2$, $\varepsilon = 0.1$, $tol_1 = 10^{-6}$ and $tol_2 = 10^{-9}$. (b) Zoom of (a) near the minimum of the curves.

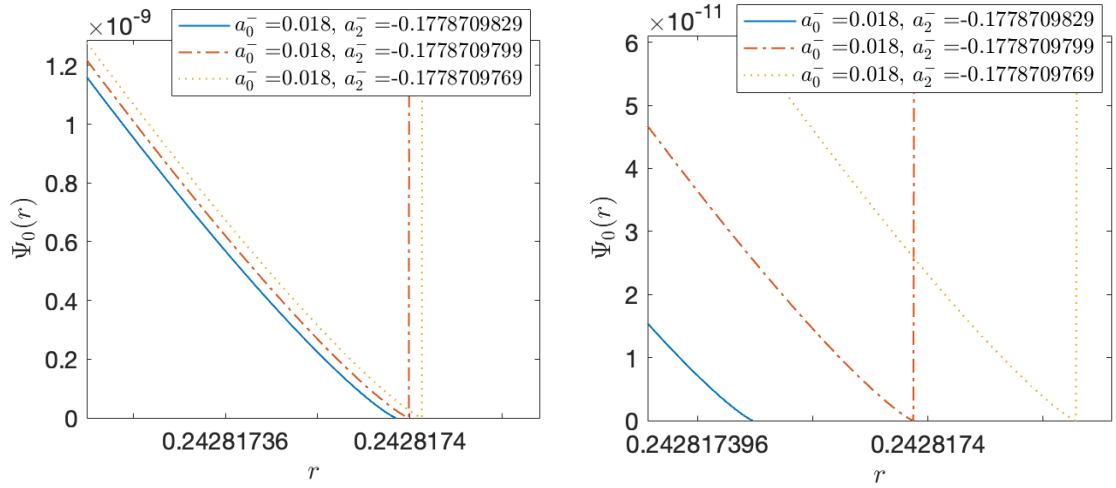
minimum 0, instead of $\log(r_* - r)$, because for some initial conditions $\hat{r} > r_*$ and this causes problems with the logarithmic plots.

In Figure 5.11 we see that the solution is well fitted by a line with slope 1.1977, which is very close to the expected value $\frac{3}{n+1} = 1.2$ for the case $n = 3/2$. We also note that when $r \to r_*$, i.e. $\log(\hat{r} - r) \sim -16$, the curve seems to turn upwards. This is a result of the finite accuracy of the computation. Moreover, this behaviour can be pushed to the right by increasing $tol_2$. In particular, for $tol_2 = 10^{-9}$ we obtain the expected slope for $(\hat{r} - r) \in (10^{-15}, 10^{-3})$.

## 5.4 Solution in the touchdown region

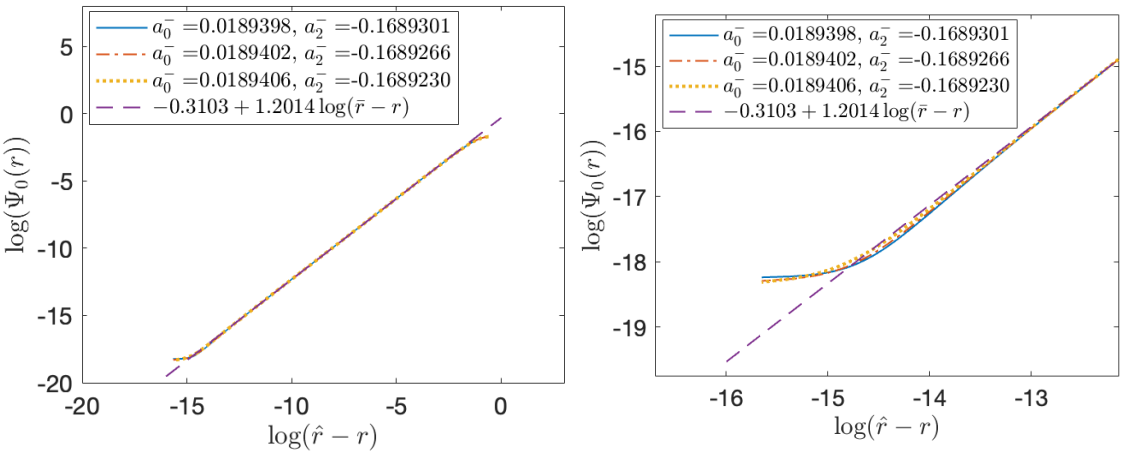
Recall the leading order problem in the touchdown region:

$$\varphi_0^n(\eta)\partial_{\eta\eta\eta}\varphi_0(\eta) = J, \quad \eta \in (-\infty, \infty). \tag{5.49}$$




(a) (b)

Figure 5.10: (a) $\Psi_0(r)$ versus $r$ for fixed $a_0^- = 0.018$ and different $a_2^-$. (b) Zoom of (a) near the minimum of the curves. For $n = 3/2$, $\varepsilon = 0.1$ and $tol_2 = 10^{-9}$.




(a) (b)

Figure 5.11: (a) $\log(\Psi_0(r))$ versus $\log(\hat{r} - r)$ for $tol_1 = 10^{-6}$, $tol_2 = 10^{-9}$, $n = 3/2$ and $\varepsilon = 0.1$. (b) Zoom of (a) for $\log(\hat{r} - r) \in (-16, -13)$.

As $\eta \to +\infty$, we have

$$\varphi_0(\eta) = \begin{cases} A_-(-\eta)^{\frac{3}{(n+1)}} + B_-(-\eta)^{\frac{2-n}{n+1}} + C_-(-\eta)^{\frac{4n+1-\sqrt{-8n^2+20n+1}}{2(n+1)}} + h.o.t., & \frac{1}{2} < n < \frac{7+3\sqrt{3}}{11}, \\ A_-(-\eta)^{2-\frac{\sqrt{3}}{3}} + B_- x^{1-\frac{\sqrt{3}}{3}} \ln\left(\frac{1}{x}\right) + C_- x^{1-\frac{\sqrt{3}}{3}} + h.o.t., & n = \frac{7+3\sqrt{3}}{11}, \\ A_-(-\eta)^{\frac{3}{(n+1)}} + B_-(-\eta)^{\frac{4n+1-\sqrt{-8n^2+20n+1}}{2(n+1)}} + C_-(-\eta)^{\frac{2-n}{n+1}} + h.o.t., & \frac{7+3\sqrt{3}}{11} < n < 2, \end{cases} \tag{5.50}$$

where

$$A_- = \left| \frac{-J(n+1)^3}{3(1-2n)(2-n)} \right|^{\frac{1}{n+1}}. \tag{5.51}$$

On the other hand, as $\eta \to +\infty$,

$$\varphi_0 = \begin{cases} A_+\eta^2 + \frac{-J\eta^{3-2n}}{A_+^n(2n-1)(2n-2)(2n-3)} + B_+\eta + C_+, & \frac{1}{2} < n < 1, \\ A_+\eta^2 + \frac{-J}{A_+}\eta(\ln(\eta)+1) + B_+\eta + C_+, & n = 1, \\ A_+\eta^2 + B_+\eta + \frac{-J\eta^{3-2n}}{A_+^n(2n-1)(2n-2)(2n-3)} + C_+, & 1 < n < \frac{3}{2}, \\ A_+\eta^2 + B_+\eta + \frac{J}{2A_+^{3/2}}\ln(\eta) + C_+, & n = \frac{3}{2}, \\ A_+\eta^2 + B_+\eta + C_+ + \frac{-J\eta^{3-2n}}{A_+^n(2n-1)(2n-2)(2n-3)}, & \frac{3}{2} < n < 2, \end{cases} \tag{5.52}$$

where $B_\pm$, $C_\pm$, $J$ are the only unknown constants, since $A_-(J)$ and $A_+$ are known from the expansions and by matching. By solving in the central region, we obtain $J$, leaving only $B_\pm$, $C_\pm$ to be determined. One of these can be fixed arbitrarily because the equation is translation invariant, as it was in the case $n > 2$. This then leaves 3 degrees of freedom for a third-order ordinary differential equation. Thus, we can reasonably expect that the boundary value problem is well determined.

In what follows of this chapter we will study the case $n = 3/2$ to simplify our analysis (as there are many cases in each expansion of the solution in the touchdown region).

Now, we can show that the expansion of $\varphi_0(\eta)$ as $\eta \to -\infty$ given in (5.50) is also

translation invariant. If we substitute $\eta$ by $\eta+\nu$ in the expansion for $\frac{7+3\sqrt{3}}{11} < n < 2$, then

$$\begin{aligned}
\varphi_0(\eta+\nu) =& A_-(-\eta-\nu)^{\frac{3}{(n+1)}} + B_-(-\eta-\nu)^{\frac{4n+1-\sqrt{-8n^2+20n+1}}{2(n+1)}} + C_-(-\eta-\nu)^{\frac{2-n}{n+1}} + h.o.t.,\\
=& A_-\left[(-\eta)^{\frac{3}{(n+1)}} + (-\eta)^{\frac{3}{(n+1)}-1}\nu + h.o.t.\right]\\
&+ B_-\left[(-\eta)^{\frac{4n+1-\sqrt{-8n^2+20n+1}}{2(n+1)}} + (-\eta)^{\frac{4n+1-\sqrt{-8n^2+20n+1}}{2(n+1)}-1}\nu + h.o.t.\right]\\
&+ C_-\left[(-\eta)^{\frac{2-n}{n+1}} + (-\eta)^{\frac{2-n}{n+1}-1}\nu + h.o.t.\right] + h.o.t.,\\
=& A_-(-\eta)^{\frac{3}{(n+1)}} + A_-(-\eta)^{\frac{2-n}{(n+1)}}\nu\\
&+ B_-(-\eta)^{\frac{4n+1-\sqrt{-8n^2+20n+1}}{2(n+1)}} + B_-(-\eta)^{\frac{4n+1-\sqrt{-8n^2+20n+1}}{2(n+1)}-1}\nu\\
&+ C_-(-\eta)^{\frac{2-n}{n+1}} + C_-(-\eta)^{\frac{1-2n}{n+1}}\nu + h.o.t.
\end{aligned}$$

Noting that for $\frac{7+3\sqrt{3}}{11} < n < 2$ we have that

$$\frac{1-2n}{n+1} < \frac{4n+1-\sqrt{-8n^2+20n+1}}{2(n+1)} - 1 < \frac{2-n}{n+1} < \frac{4n+1-\sqrt{-8n^2+20n+1}}{2(n+1)},$$

it follows that

$$\begin{aligned}
\varphi_0(\eta+\nu) =& A_-(-\eta)^{\frac{3}{(n+1)}} + B_-(-\eta)^{\frac{4n+1-\sqrt{-8n^2+20n+1}}{2(n+1)}}\\
&+ (C_- + A_-\nu)(-\eta)^{\frac{2-n}{n+1}} + h.o.t.
\end{aligned}$$

Hence, the spatial translation $\nu$ can be absorbed into the constant accompanying the term $(-\eta)^{\frac{2-n}{n+1}}$ by setting $\tilde{C}_- := C_- + A_-\nu$. Thus, without loss of generality, we set $C_- = 0$ in the expansion (5.50).

Let us now focus on solving problem (5.49)-(5.52) with only the boundary conditions at $\eta \to -\infty$, i.e.

$$\varphi_0^n(\eta)\partial_{\eta\eta\eta}\varphi_0(\eta) = J, \quad \eta \in (-\infty, \infty),$$

$$\varphi_0(\eta) = A_-(-\eta)^{\frac{3}{(n+1)}} + B_-(-\eta)^{\frac{4n+1-\sqrt{-8n^2+20n+1}}{2(n+1)}} \text{ as } \eta \to -\infty,$$

where $B_-$ is an unknown constant. Although we already know $J$ and $A_-$, we can simplify the above problem further by introducing a new scaling and a new variable

$$\varphi_0(\eta) = c\phi(y), \quad \eta = dy.$$

Then, we define

$$c := A_-^{\frac{2}{3}} J^{\frac{1}{3(n+1)}}, \quad d := \left(\frac{J}{A_-^{n+1}}\right)^{\frac{1}{6}}, \tag{5.53}$$

where $c$, $d > 0$. Accordingly, we obtain that $\phi$ should solve the following problem

$$\begin{aligned}
&\phi^n(y)\partial_{yyy}\phi(y) = 1, \quad y \in (-\infty, \infty),\\
&\qquad \phi(y) = (-y)^{\frac{3}{(n+1)}} + \tilde{B}_-(-y)^{\frac{4n+1-\sqrt{-8n^2+20n+1}}{2(n+1)}} \text{ as } y \to -\infty,
\end{aligned}$$

where $\tilde{B}_- := \frac{d^{\frac{4n+1-\sqrt{-8n^2+20n+1}}{2(n+1)}}}{c} B_-$.

For $y_0 \in \mathbb{R}_+$, we solve numerically

$$\phi^n \partial_{yyy}\phi = 1, \quad y \in (-y_0, y_0), \tag{5.54}$$

$$\phi(-y_0) = y_0^{\frac{3}{(n+1)}} + \tilde{B}_- y_0^{\frac{4n+1-\sqrt{-8n^2+20n+1}}{2(n+1)}}, \tag{5.55}$$

$$\partial_y\phi(-y_0) = -\frac{3}{(n+1)} y_0^{\frac{2-n}{(n+1)}} - \frac{4n+1-\sqrt{-8n^2+20n+1}}{2(n+1)} \tilde{B}_- y_0^{\frac{4n+1-\sqrt{-8n^2+20n+1}}{2(n+1)}-1}, \tag{5.56}$$

$$\begin{aligned}
\partial_{yy}\phi(-y_0) = &\left(\frac{3}{(n+1)}\right)\left(\frac{2-n}{(n+1)}\right) y_0^{\frac{1-2n}{(n+1)}} + \left(\frac{4n+1-\sqrt{-8n^2+20n+1}}{2(n+1)}\right)\\
&\cdot \left(\frac{4n+1-\sqrt{-8n^2+20n+1}}{2(n+1)} - 1\right) \tilde{B}_- y_0^{\frac{4n+1-\sqrt{-8n^2+20n+1}}{2(n+1)}-2},
\end{aligned} \tag{5.57}$$

and read off $\kappa := \partial_{yy}\phi(y_0)$ from the numerical solution. Afterwards, by reverting to

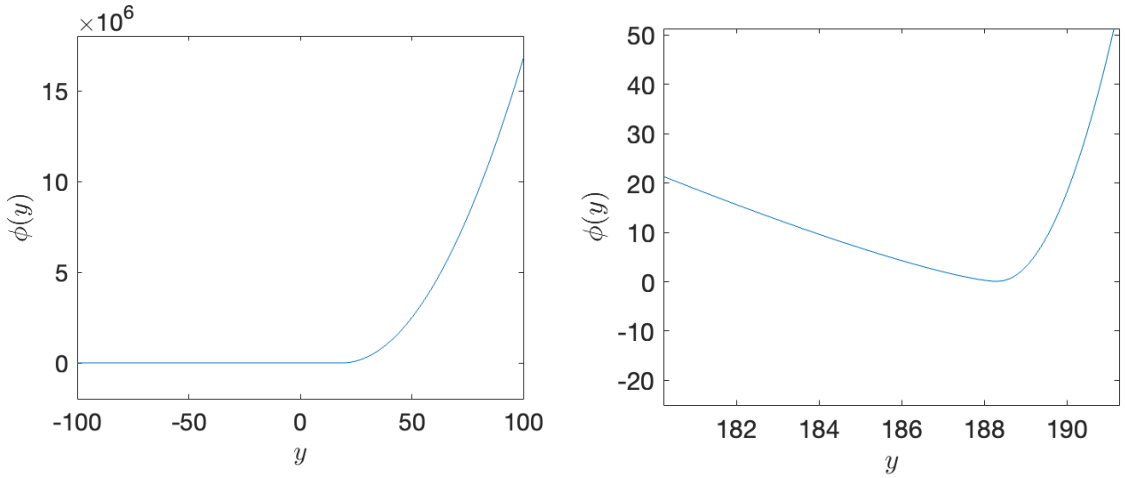



Figure 5.12: (a) Plot of the numerical solution $\phi(y)$ for $\tilde{B}_- = 41.07491605$ and $n = 3/2$. (b) Zoom of (a) for $y \in (181, 191)$.

the earlier scaling, we obtain that $\lim_{\eta\to+\infty} \varphi''(\eta) \sim \kappa\frac{c}{d^2}$ and also that $\lim_{\eta\to+\infty} \varphi''(\eta) \sim 2A_+$, where $A_+ = b_2$ is known from the annular region by (4.47). We use a binary search to find $\tilde{B}_- \in (0, 20)$, such that its associated solution of problem (5.54)-(5.57) satisfies $\kappa\frac{c}{d^2} = 2A_+$ up to a tolerance of $10^{-5}$.

In Figure 5.12 (a), we plot the solution obtained for $n = 3/2$ on the interval $(-100, 100)$. If we zoom in to look at the minimum of the curve, we obtain Figure 5.12 (b), where we can see that the minimum is achieved at $y \sim 188$. The fact that the minimum is not achieved at $y = 0$ (i.e. $\eta = 0$) is due to the translation invariance of the problem, which we used when setting $C_- = 0$. The constant $C_-$ can be altered arbitrarily by shifting the solution until the minimum is achieved at 0.

## 5.5 Composite expansion and comparison with numerical results

We now construct a composite approximation based on the asymptotic solutions found in the previous sections. The resultant composite approximation can be expressed as

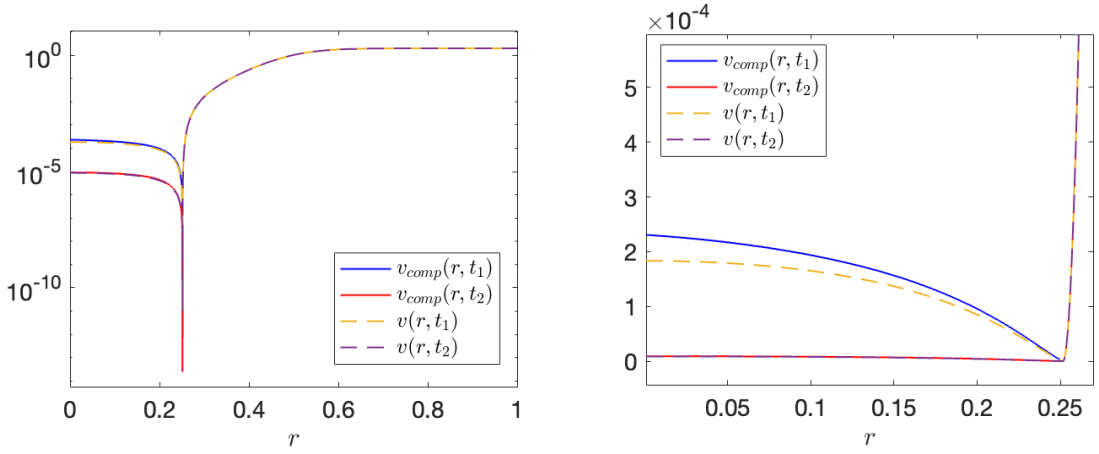
$$\begin{aligned} v_{comp}(r,t) :=& v_{central}(r,t) + v_{touchdown}(r,t) + v_{annular}(r,t) \\ & - A_{-}t^{\alpha}[(r-r_*)_{-}]^{\frac{3}{(n+1)}} - A_{+}[(r-r_*)_{+}]^2. \end{aligned}$$

In Figure 5.13 we can see the leading order of the composite expansion at two times, $t_1 = 10^3$ and $t_2 = 10^5$, and the numerical partial differential equation solution $v$ at both times. The composite solution closely matches the numerical solution in the interval $[0, 1]$. In particular, around the minimum of the solution and in the annular region the agreement is excellent, as shown in Figure 5.13(a) and (b), at times $t = t_1$ and $t_2$. Moreover, the overall agreement between the composite approximation and the numerical solution of the partial differential equation becomes better at $t_2$. For the simulation portrayed in Figure 5.13, we have

$$error(t_1) = 0.001114, \quad error(t_2) = 0.000003,$$

which indicates that the error decreased by a factor of 371 in going from $t_1$ to $t_2$. This is expected since $t_1 = 10^3$ is an early time for the evolution of $v$ and, thus, the composite expansion is not expected to fit $v$ well at this stage. In contrast, at $t_2 = 10^5$ the solution has already entered the long-time behaviour regime, where the self-similar profiles have stabilised, and thus the agreement between $v_{comp}$ and $v$ is expected to be excellent.

We also plot the dependence of the error on $r$ in Figure 5.14 (a), where we can observe that $error_{t_2} \sim O(10^{-6})$ for $t_2 = 10^5$ over the entire domain, thus confirming




(a) (b)

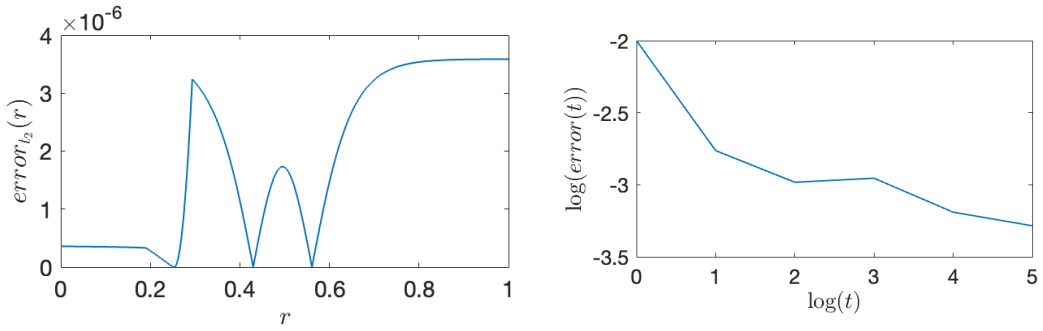
Figure 5.13: (a) Plot of the composite and numerical solutions on a log scale, for $n = 3/2$, $t_1 = 10^3$, $t_2 = 10^5$. (b) Zoom of (a) using the original scale in the central and touchdown regions.

that the agreement between the leading order of the composite expansion and the numerical solution is excellent. It is clear from the figure that the maximum error occurs in the touchdown and annular regions, which implies that we have more accuracy in the central region than for the case $n > 2$. In addition, Figure 5.14 (b) shows $error(t)$ for $t = 10^0, 10^1, 10^2, 10^3, 10^4, 10^5$. We can see that the error decreases as time increases.

Summarising, in this section, we have shown that for $\frac{1}{2} < n < 2$ there is a numerical solution to (2.6)-(2.11) that converges to an asymptotic approximation which exhibits infinite time touchdown. Up to leading order, this approximation is divided into three main regions - central, touchdown and annular - where the first two have the following self-similar profiles

$$v_{central} \sim t^{-\frac{1}{n}}\psi_0(r), \quad v_{touchdown} \sim t^{-\frac{2(n+1)}{n(2n-1)}}\varphi_0(\eta), \quad \eta := \frac{r - r_*}{t^{-\frac{(n+1)}{n(2n-1)}}}$$

respectively, and the third one is almost stationary and coincides, up to leading order, with the stationary solution obtained in Lee et al. [49].




(a) (b)

Figure 5.14: (a) $error_{t_2}(r)$ versus $r$ for $n = 3/2$ and $t_2 = 10^5$. (b) Plot of $error(t)$ (defined in main text) versus $\log(t)$ at times $t = 10^0, 10^1, 10^2, 10^3, 10^4, 10^5$. For $n = 3/2$ and $\varepsilon = 0.1$.

# Chapter 6

# Existence and regularity of solutions

In this chapter, we study the existence and regularity of solutions of the 2-dimensional radially symmetric degenerate Cahn-Hilliard equation, i.e. for $u = u(r,t)$ satisfying

$$\partial_t u = \frac{1}{r}\partial_r \left( r M_n(u) \partial_r \mu \right), \qquad \text{in } (0,1)\times(0,T) \tag{6.1}$$

$$\mu = -\varepsilon^2 \frac{1}{r}\partial_r \left( r \partial_r u \right) + f'(u), \qquad \text{in } (0,1)\times(0,T), \tag{6.2}$$

$$\partial_r u = M_n(u)\partial_r \mu = 0, \qquad \text{on } \{0,1\}\times(0,T), \tag{6.3}$$

$$u(\cdot,0) = u_0(r), \qquad \text{in } (0,1), \tag{6.4}$$

where the mobility and homogeneous free energy are given respectively by

$$M_n(u) := [(1-u^2)_+]^n, \quad n \in \mathbb{R}^+, \quad f(u) := \frac{(1-u^2)^2}{2}. \tag{6.5}$$

We note that we have changed the notation for the initial condition from $u_{init}$ to $u_0$ as in this chapter there is no confusion with other functions by the same name (as in the leading order approximations of Chapters 4 and 5) and this allows for shorter

mathematical expressions.

As we mentioned in the introduction, Elliott and Garcke [32] proved weak existence and regularity for a fairly general version of the problem. We state their result here as it can be applied to a degenerate Cahn-Hilliard problem in a general 2-dimensional domain. Let

$$\partial_t u = -\nabla \cdot \mathbf{j}, \qquad \text{in } \Omega \times (0,\infty), \tag{6.6}$$

$$\mathbf{j} = -M(u)\nabla\mu, \tag{6.7}$$

$$\mu = -\gamma\Delta u + \Psi'(u), \tag{6.8}$$

for $\gamma > 0$, with Neumann and no-flux boundary conditions as given in (2.4), (2.5), respectively. Here, the homogeneous free energy $\Psi$ takes the form

$$\Psi(u) := \Psi_1(u) + \Psi_2(u),$$

with $\Psi_2$ such that $\|\Psi_2\|_{C^2[-1,1]} \leq C$ and $\Psi_1 : (-1,1) \to \mathbb{R}$ is convex and of the form

$$\Psi_1''(u) = (1-u^2)^{-m} F(u),$$

where $m \geq 1$ is a constant and $F : [-1,1] \to \mathbb{R}_0^+$ is a $C^1$-function. The authors also assume a mobility of the form

$$M(u) = (1-u^2)^m \overline{M}(u),$$

where $\overline{M} : [-1,1] \to \mathbb{R}$ is a $C^1$-function which is bounded above and below by positive constants when $u \in [-1,1]$. This mobility is extended outside of $[-1,1]$ by 0. They define an auxiliary function $\Phi : (-1,1) \to \mathbb{R}_0^+$ (which is called entropy in most of the

literature) such that

$$\Phi''(u) = \frac{1}{M(u)}, \quad \Phi'(0) = 0, \quad \Phi(0) = 0.$$

Then, Elliott and Garcke's result, as stated in [32], is:

**Theorem 6.1.** *(Theorem 1 from [32]) Let either $\partial\Omega \in C^{1,1}$ or $\Omega$ be convex. Suppose $u_0 \in H^1(\Omega)$ satisfies $|u_0| \leq 1$ a.e. in $\Omega$ and*

$$\int_\Omega (\Psi(u_0) + \Phi(u_0)) \leq C, \quad C \in \mathbb{R}^+.$$

*Then there exists a pair $(u, \boldsymbol{j})$ such that*

*(a)* $u \in L^2(0,T;H^2(\Omega)) \cap L^\infty(0,T;H^1(\Omega)) \cap C([0,T];L^2(\Omega))$,

*(b)* $\partial_t u \in L^2(0,T;H^{-1}(\Omega))$,

*(c)* $u(0) = u_0$ *and* $\nabla u \cdot \boldsymbol{n} = 0$ *on* $(0,T) \times \partial\Omega$,

*(d)* $|u| \leq 1$ *a.e. in* $\Omega_T := \Omega \times (0,T)$,

*(e)* $\boldsymbol{j} \in L^2(\Omega_T, \mathbb{R}^N)$,

*which satisfies*

$$\int_0^T \langle \zeta(t), \partial_t u(t) \rangle_{H^1, H^{-1}} = \int_{\Omega_T} \boldsymbol{j} \cdot \nabla\zeta, \qquad \forall \zeta \in L^2(0,T;H^1(\Omega)),$$

*and*

$$\int_{\Omega_T} \boldsymbol{j} \cdot \eta = -\int_{\Omega_T} [\gamma \Delta u \nabla \cdot (M(u)\eta) + (M\Psi'')(u)\nabla u \cdot \eta],$$

*for all $\eta \in L^2(0,T;H^1(\Omega,\mathbb{R}^N)) \cap L^\infty(\Omega_T,\mathbb{R}^N)$ such that $\eta \cdot \boldsymbol{n} = 0$ on $\partial\Omega \times (0,T)$.*

Their proof is divided into two parts. First, they use Galerkin approximations to prove that there exists a weak solution for strictly positive mobilities and then they approximate the degenerate problem using positive mobilities and pass to the limit.

To try to apply Theorem 6.1 to the radially symmetric problem (6.1)-(6.4) we could set

$$\gamma = 1, \quad F \equiv 0, \quad \Psi_2(u) = \frac{(1-u^2)^2}{2}, \quad \overline{M}(u) \equiv 1.$$

By Theorem 6.1 we would, then, obtain a solution to the 2-dimensional equation (6.6)-(6.8) for arbitrary initial data $u_0 \in H^1(\Omega)$, which we may choose to be radial. This does not ensure that the resultant solution is actually radially symmetric. To demonstrate this fundamental property, we adapt Elliott and Garcke's proof [32] step by step to the radial setting (6.1)-(6.4) with degenerate the mobility and double-well homogeneous free energy given by (6.5). As a consequence, we will review some known embeddings for Sobolev spaces of radial functions and adapt them to our specific setting.

## 6.1 Sobolev spaces of radial functions

Let $B_T := B \times (0,T)$ for $T > 0$, where $B := \{x \in \mathbb{R}^2 : |x| < 1\}$ is the unit open ball in two dimensions. We will use the following spaces

$$L^2_{\text{rad}}(B) := \{u \in L^2(B) : \, u(x) = u(|x|)\},$$

$$W^{m,p}_{\text{rad}}(B) := \{u \in W^{m,p}(B) : \, u(x) = u(|x|)\},$$

and $H^{-1}_{\text{rad}}(B) = (H^1_{\text{rad}}(B))^*$ is the dual space of $H^1_{\text{rad}}(B) = W^{1,2}_{\text{rad}}(B)$.

We note that Sobolev spaces of radial functions are closely related to weighted Sobolev spaces, i.e.

$$H^1((0,1),r) := \left\{ u \in H^1(0,1) : \int_0^1 \left(|u(r)|^2 + |u'(r)|^2\right) \, r dr < \infty \right\}.$$

It has been shown (see Theorem 2.3 in [37]) that

$$H^1_{\text{rad}}(B) \equiv H^1((0,1), r).$$

This allows us to associate the radial spaces with the following inner products:

$$(u,v)_{L^2_{\text{rad}}(B)} = \int_0^1 u(r)v(r)\ r dr,$$

$$(u,v)_{H^1_{\text{rad}}(B)} = \int_0^1 u(r)v(r)\ r dr + \int_0^1 \partial_r u(r)\partial_r v(r)\ r dr,$$

which define the norms $\|\cdot\|_{L^2_{\text{rad}}(B)}$ and $\|\cdot\|_{H^1_{\text{rad}}(B)}$, respectively.

We will also make use of continuous and compact Sobolev embeddings which we state below.

**Theorem 6.2** (Rellich-Kondrachov Compactness Theorem)**.** *Assume $U$ is a bounded open subset in $\mathbb{R}^N$, $\partial U$ is $C^1$ and let $N > mp \geq 1$. If $1 \leq q < \frac{pN}{N-mp}$, then the embedding*

$$W^{m,p}(U) \hookrightarrow L^q(U)$$

*is compact.*

**Theorem 6.3** (Corollary 1.2 from [37])**.** *Let $N > mp$ and $\beta > 0$. If $1 \leq q < \frac{p(N+\beta)}{N-mp}$, then the embedding*

$$W^{m,p}_{rad}(B) \hookrightarrow L^q(B, |x|^\beta)$$

*is compact.*

We note that this result means that radial symmetry allows an increase in the range of values that $q$ can assume, by the amount $\frac{p\beta}{N-mp}$.

Unfortunately, when applying this to obtain embeddings in the case $N = mp$ one does not gain more regularity compared to usual Sobolev embeddings.

**Proposition 6.4.** *Let $N = mp$ and $\beta \geq 0$. Then the embedding*

$$W^{m,p}_{rad}(B) \hookrightarrow L^q(B, |x|^\beta)$$

*is compact for all $1 \leq q < \infty$.*

To our knowledge Proposition 6.4 has not been demonstrated in the literature, so we do it here. The following proof is based on the one for the same fact for non-symmetric Sobolev spaces.

*Proof.* Let $\theta > 0$ be a sufficiently small parameter, then the embedding

$$W^{m,p}_{\text{rad}}(B) \hookrightarrow W^{m,p-\theta}_{\text{rad}}(B)$$

is continuous, because

$$\begin{aligned}\int_B |f|^{p-\theta} dx &\leq \left(\int_B |f|^p dx\right)^{\frac{p-\theta}{p}} |B|^{\frac{\theta}{p}} \\ &\leq \left(\int_B |f|^p dx\right)^{\frac{p-\theta}{p}},\end{aligned}$$

where $|B|$ is the volume of $B$.

Since, $N = mp > m(p-\theta)$, we can apply Corollary 1.2 from [37] to $p-\theta$ for any $\beta \geq 0$ to obtain that the embedding

$$W^{m,p-\theta}_{\text{rad}}(B) \hookrightarrow L^q(B, |x|^\beta)$$

is compact for all $1 \leq q < \frac{(p-\theta)(N+\beta)}{N-m(p-\theta)} = \frac{(p-\theta)(mp+\beta)}{m\theta}$. For $q \in [1, \infty)$ we can choose $\theta$ such that

$$0 < \theta < \frac{p(mp+\beta)}{mp+\beta+mq}.$$

Composing a compact embedding with a continuous embedding preserves compact-

ness, which concludes the proof. □

**Remark 6.5.** *Taking $\beta = 1$, $m = 1$ and $p = 2$ in Proposition 6.4, we obtain*

$$H^1_{rad}(B) \hookrightarrow L^q_{rad}(B)$$

*is compact for all $1 \leq q < \infty$. In particular, this implies the compact embedding $H^1_{rad}(B) \hookrightarrow L^2_{rad}(B)$.*

Since we are working with an evolution equation, we would like a way to adapt these embeddings to time-dependent spaces. Accordingly, we recall the following theorem from Simon [66]:

**Lemma 6.6.** *(Simon, 1987, [66]) Let $X, Y$ and $Z$ be Banach spaces with $X \hookrightarrow Y$ compactly and $Y \hookrightarrow Z$ continuously, then the embeddings*

$$\{u \in L^2(0,T); X) | \partial_t u \in L^2(0,T;Z)\} \hookrightarrow L^2(0,T;Y)$$

*and*

$$\{u \in L^\infty(0,T;X) | \partial_t u \in L^2(0,T;Z)\} \hookrightarrow C([0,T];Y)$$

*are compact.*

The following is a generalised version of Lebesgue's Dominated Convergence Theorem given in Robinson [64].

**Lemma 6.7.** *(Lemma 8.3 from [64]) Let $U$ be a bounded open set in $\mathbb{R}^m$, $p \in [1, \infty)$, and let $g_j$ be a sequence of functions in $L^p(U)$ with*

$$\|g_j\|_{L^p(U)} \leq C \quad \text{for all} \quad j \in \mathbb{N}.$$

*If $g \in L^p(U)$ and $g_j \to g$ almost everywhere, then $g_j \rightharpoonup g$ in $L^p(U)$.*

In particular, this Lemma can be stated for radially symmetric Lebesgue spaces $L^p_{\text{rad}}(U)$ by noting that for $g \in L^p_{\text{rad}}(B)$ we have that

$$\|g\|_{L^p_{\text{rad}}(B)} = \|g\|_{L^p((0,1),r)} = \|g\|_{L^p(B)}.$$

Moreover, if we apply Lemma 6.7 in space and time we obtain the following statement:

**Lemma 6.8.** *Let $p \in [1, \infty)$, and let $\varphi_j$ be a sequence of functions in $L^2(0,T; L^p_{rad}(B))$ with*

$$\|\varphi_j\|_{L^2(0,T;L^p_{rad}(B))} \leq C \quad \text{for all} \quad j \in \mathbb{N}.$$

*If $\varphi \in L^2(0,T; L^p_{rad}(B))$ and $\varphi_j \to \varphi$ almost everywhere, then*

$$\varphi_j \rightharpoonup \varphi \quad \text{in } L^2(0,T; L^p_{rad}(B)).$$

In what follows, we will use all these results to obtain the existence of radially symmetric solutions to our degenerate Cahn-Hilliard equation.

## 6.2 Existence and regularity for positive mobilities

Recall that we are considering problem (2.6)-(2.10) with

$$f(u) = \frac{(1-u^2)^2}{2}.$$

We note that this free energy satisfies $f \in C^1(\mathbb{R}, \mathbb{R})$ and

$$|f'(u)| \leq 2\left(|u|^3 + |u|\right) \quad \text{and} \quad 0 \leq f(u).$$

**Remark 6.9.** *A priori, one could take a more general form for $f$, see the conditions on the homogeneous free energy $\Psi$ in Theorem 6.1 from [32], but we do not do this*

*here as we are focusing on a specific instance of the problem.*

We also recall that we originally set $M_n(u) = [(1-u^2)_+]^n$, but because this mobility degenerates at $|u| = 1$, we will first work with a cut-off version. Let $\delta > 0$, we define

$$M_\delta(u) := \begin{cases} M_n(-1+\delta) & \text{for } u \le -1+\delta, \\ M_n(u) & \text{for } |u| \le 1-\delta, \\ M_n(1-\delta) & \text{for } u \ge 1-\delta, \end{cases}$$

We note that $M_\delta \in C(\mathbb{R}, \mathbb{R})$ and there exists $m_1$, $m_2 > 0$ such that

$$m_1 \le M_\delta(u) \le m_2.$$

For the remainder of this chapter we use $C \in \mathbb{R}^+$ as a generic constant in estimates, unless it is stated otherwise.

**Theorem 6.10.** *Suppose $u_0 \in H^1_{rad}(B)$. Then there exists a pair of functions $(u, \mu)$ such that*

*(a) $u \in L^\infty(0,T; H^1_{rad}(B)) \cap C([0,T]; L^2_{rad}(B))$,*

*(b) $u_t \in L^2(0,T; H^{-1}_{rad}(B))$,*

*(c) $u(0) = u_0$ a.e. on $B$ and $\partial_r u = 0$ on $\{0,1\} \times (0,T)$,*

*(d) $\mu \in L^2(0,T; H^1_{rad}(B))$,*

*which satisfy the equations with the non-degenerate mobility $M_\delta$ in the following weak sense:*

$$\int_0^T \langle \zeta(t), u_t(t) \rangle_{H^1_{rad}, H^{-1}_{rad}} \, dt = -\int_0^T \int_0^1 M_\delta(u) \partial_r \mu \partial_r \zeta \; r dr dt, \tag{6.9}$$

$\forall \zeta \in L^2(0,T; H^1_{rad}(B))$, *and*

$$\int_0^1 \mu \phi \; r dr = \varepsilon^2 \int_0^1 \partial_r u \partial_r \phi \; r dr + \int_0^1 f'(u) \phi \; r dr, \tag{6.10}$$

$\forall \phi \in H^1_{rad}(B)$ *and almost all* $t \in [0,T]$.

*Proof.* We will use a Galerkin method to approximate equations (6.1)-(6.4), using a finite number of elements from a countable basis of $H^1_{\text{rad}}(B)$. This will give us a sequence of approximating functions that solve a finite dimensional version of the original problem. Then, we will use radial Sobolev embeddings to get estimates, which will allow us to prove that there is a subsequence of the approximating functions that converges to a solution of the original problem with the previously stated regularity.

Let $\{\lambda_i\}_{i\in\mathbb{N}}$ be the ordered set of all eigenvalues of the radially symmetric Laplace operator with Neumann boundary conditions in the unitary disc, $\lambda_1 < \lambda_2 < \lambda_3 < \dots$, and let $\{\phi_i\}_{i\in\mathbb{N}}$ be an orthonormal basis for $H^1_{\text{rad}}(B)$ (see Remark 6.11) composed of the associated eigenfunctions, i.e.

$$-\frac{1}{r}\partial_r\left(r\partial_r\phi_i\right) = \lambda_i\phi_i \text{ in } (0,1), \text{ with } \partial_r\phi_i = 0 \text{ on } \{0,1\}, \tag{6.11}$$

and

$$\int_0^1 \phi_i\phi_j \; r dr = \delta_{ij}.$$

In particular, for $i = 1$ we have $\lambda_1 = 0$ and

$$\int_0^1 \partial_r\phi_1\partial_r v \; r dr = 0 \quad \forall v \in H^1_{\text{rad}}(B),$$

thus, after normalization, $\phi_1 \equiv \pm\sqrt{2}$, and we set $\phi_1 \equiv \sqrt{2}$. In fact, one can explicitly express each eigenfunction in terms of Bessel functions, but this is not needed for the proof. Although a priori $\phi_i \in H^1_{\text{rad}}(B)$, a bootstrap argument readily yields that $\phi_i \in C^\infty(B)$ for all $i \in \mathbb{N}$.

Moreover, let $v \in H^1_{\text{rad}}(B)$, if we multiply (6.11) by $v\,r$, integrate in space and use

integration by parts, then we obtain the following property

$$\int_0^1 \partial_r \phi_i \partial_r v \; r dr = \lambda_i \int_0^1 \phi_i v \; r dr. \tag{6.12}$$

In particular, this implies

$$\int_0^1 |\partial_r \phi_i|^2 \; r dr = \lambda_i \int_0^1 |\phi_i|^2 r dr. \tag{6.13}$$

**Remark 6.11.** *We can check that* $\{\phi_i\}_{i\in\mathbb{N}}$ *is indeed a basis for* $H^1_{rad}(B)$. *Note that since* $H^1_{rad}(B) \equiv H^1((0,1),r)$ *we only need to check that* $\{\phi_i\}_{i\in\mathbb{N}}$ *is a basis for* $H^1((0,1),r)$. *Now, the operator defined by* (6.11) *is self-adjoint and compact in* $H^1((0,1),r)$ *and since this space is separable and Hilbert, by Spectral Theory of Self-Adjoint operators (see for example Section 6.4. from [17]) there exists a basis made of the operator's eigenfunctions.*

Let $K \in \mathbb{N}$ and consider

$$u^K(t,r) = \sum_{i=1}^K c_i^K(t)\phi_i(r), \tag{6.14}$$

$$\mu^K(t,r) = \sum_{i=1}^K d_i^K(t)\phi_i(r), \tag{6.15}$$

where the functions $c_i^K$, $d_i^K$ are determined by the following equations

$$\int_0^1 \partial_t u^K \phi_j \; r dr = -\int_0^1 M_\delta(u^K)\partial_r \mu^K \partial_r \phi_j \; r dr, \quad \text{for } j = 1,\dots,K, \tag{6.16}$$

$$\int_0^1 \mu^K \phi_j \; r dr = \varepsilon^2 \int_0^1 \partial_r u^K \partial_r \phi_j \; r dr + \int_0^1 f'(u^K)\phi_j \; r dr, \quad \text{for } j = 1,\dots,K, \tag{6.17}$$

$$u^K(0) = \sum_{i=1}^K (u_0, \phi_i)_{L^2_{\text{rad}}(B)} \phi_i. \tag{6.18}$$

Note that for $j = 1$ we have

$$\sqrt{2}\int_0^1 \partial_t u^K \; r dr = \int_0^1 \partial_t u^K \phi_1 \; r dr = -\int_0^1 M_\delta(u^K)\partial_r \mu^K \partial_r \phi_1 \; r dr = 0. \tag{6.19}$$

We define the mean of $u^K$ as

$$\overline{u^K}(t) := \frac{1}{|B|}\int_B u^K(x,t)dx = \frac{1}{2\pi}\left(\int_0^{2\pi} d\theta\right)\int_0^1 u^K(r,t)\, r dr = \int_0^1 u^K(r,t)\, r dr,$$

Using (6.19) we obtain

$$\partial_t\left(\overline{u^K}\right)(t) = \int_0^1 \partial_t u^K(r,t)\, r dr = 0.$$

Hence $\overline{u^K}(t)$ is constant in time.

Taking the $L^2_{rad}(B)$ product between (6.18) and $\phi_1 = \sqrt{2}$ and using that $\{\phi_i\}_{i\in\mathbb{N}}$ is an orthonormal basis in $L^2_{rad}(B)$, we obtain

$$\overline{u^K}(t) = \int_0^1 u^K(t,r) r dr = \int_0^1 u_0(r) r dr = \mathrm{m}(0)$$

for all $K \in \mathbb{N}$, where $\mathrm{m}(0)$ is the mass function defined in (2.14) applied to the initial condition. This implies that the approximate solutions $u^K$ satisfy mass conservation.

Moreover, for $j = 1$ equation (6.17) becomes

$$\begin{aligned}\sqrt{2}\int_0^1 \mu^K \; r dr = \int_0^1 \mu^K \phi_1 \; r dr =& \varepsilon^2 \int_0^1 \partial_r u^K \partial_r \phi_1 \; r dr + \int_0^1 f'(u^K)\phi_1 \; r dr, \\ =& \sqrt{2}\int_0^1 f'(u^K) \; r dr.\end{aligned}$$

Thus

$$\int_0^1 \mu^K \; r dr = \int_0^1 f'(u^K) \; r dr.$$

Now, substituting the expressions for $u^K$ and $\mu^K$ given in (6.14) and (6.15) into

equations (6.16)-(6.18), we obtain the following system of ordinary differential equations:

$$\partial_t c_j^K(t) = -\sum_{k=1}^{K} d_k^K(t) \int_0^1 M_\delta \left( \sum_{i=1}^{K} c_i^K(t)\phi_i(r) \right) \partial_r \phi_k(r) \partial_r \phi_j(r)\ r dr, \tag{6.20}$$

$$d_j^K(t) = \varepsilon^2 \lambda_j c_j^K(t) + \int_0^1 f' \left( \sum_{i=1}^{K} c_i^K(t)\phi_i(r) \right) \phi_j(r)\ r dr, \tag{6.21}$$

$$c_j^K(0) = (u_0, \phi_j)_{L^2_{\text{rad}}(B)}, \tag{6.22}$$

for $j = 1, \ldots, K$. Since the right-hand side of (6.20) depends continuously on $c_1, \ldots, c_K$, it follows that the initial value problem has a local solution, i.e. there exists $T > 0$ and solutions $c_1, \ldots, c_K \in C^1([0,T))$. This also ensures the existence of functions $d_1, \ldots, d_K \in C^1([0,T))$ given by (6.21).

Let

$$E^K(t) = \int_0^1 \left( \frac{\varepsilon^2}{2} |\partial_r u^K|^2 + f(u^K) \right) r dr \tag{6.23}$$

be the energy associated with $u^K$. Then, because $c_1, \ldots, c_K \in C^1([0,T))$, we can differentiate in time

$$\begin{aligned} \frac{d}{dt} E^K(t) &= \int_0^1 \left( \varepsilon^2 \partial_r u^K \partial_r u_t^K + f'(u^K) u_t^K \right)\ r dr, \\ &= \int_0^1 \mu^K u_t^K\ r dr, \\ &= -\int_0^1 M_\delta(u^K) |\partial_r \mu^K|^2\ r dr, \\ &\leq 0. \end{aligned}$$

Integrating over the interval $[0,t]$, for $0 < t < T$, we obtain

$$E^K(t) - E^K(0) = -\int_0^t \int_0^1 M_\delta(u^K) |\partial_r \mu^K|^2\ r dr dt.$$

Substituting (6.23) we get

$$\begin{aligned}\int_0^1 \frac{\varepsilon^2}{2}|\partial_r u^K(t,r)|^2\ r dr + \int_0^1 f(u^K(t,r))\ r dr + \int_0^t\int_0^1 M_\delta(u^K)|\partial_r \mu^K|^2\ r dr dt,&\\ = \int_0^1 \frac{\varepsilon^2}{2}|\partial_r u^K(0,r)|^2\ r dr + \int_0^1 f(u^K(0,r))\ r dr,&\\ \leq \frac{\varepsilon^2}{2}\|u_0\|^2_{H^1_{\text{rad}}(B)} + \int_0^1 |f(u^K(0,r))|\ r dr,&\\ \leq \frac{\varepsilon^2}{2}\|u_0\|^2_{H^1_{\text{rad}}(B)} + \frac{1}{4}\int_0^1 \left(1-2|u^K(0,r)|^2+|u^K(0,r)|^4\right)\ r dr,&\\ \leq C\left(\|u_0\|^2_{H^1_{\text{rad}}(B)} + \|u_0\|^4_{L^4_{\text{rad}}(B)} + 1\right),&\\ \leq C\left(\|u_0\|^2_{H^1_{\text{rad}}(B)} + 1\right),&\end{aligned}$$

where we have used that $\{\phi_i\}_{i\in\mathbb{N}}$ is a basis for $H^1_{\text{rad}}(B)$ and $H^1_{\text{rad}}(B) \hookrightarrow L^4_{\text{rad}}(B)$ continuously. Since $u_0 \in H^1_{\text{rad}}(B)$ we obtain

$$\int_0^1 \frac{\varepsilon^2}{2}|\partial_r u^K(t,r)|^2\ r dr + \int_0^1 f(u^K(t,r))\ r dr + \int_0^t\int_0^1 M_\delta(u^K)|\partial_r \mu^K|^2\ r dr dt \leq C, \tag{6.24}$$

where $C$ is independent of $K$. Because $f(u), M_\delta(u^K) \geq 0$, then all the integrals on the left-hand side are non-negative. Thus, each of the integrals is bounded above by $C$. In particular,

$$\int_0^1 |\partial_r u^K(t,r)|^2\ r dr \leq C. \tag{6.25}$$

Moreover, recalling that $0 < m_1 \leq M_\delta(u)$, we obtain

$$\int_0^t\int_0^1 |\partial_r \mu^K|^2\ r dr dt \leq C. \tag{6.26}$$

Using Poincaré's inequality on (6.25) we get

$$\int_0^1 \left|u^K(t,r) - \overline{u^K}(t)\right|^2\ r dr \leq C\int_0^1 |\partial_r u^K|^2\ r dr \leq C.$$

Using that $a^2 - b^2 \leq |a^2 - b^2| \leq 2|a-b|^2$ for all $a$, $b \in \mathbb{R}$ we obtain

$$\int_0^1 \left|u^K(t,r)\right|^2 - \left|\overline{u^K}(t)\right|^2 \, rdr \leq 2 \int_0^1 \left|u^K(t,r) - \overline{u^K}(t)\right|^2 \, rdr \leq 2C.$$

In what follows we absorb the constant 2 into $C$. Now, since $\overline{u^K}$ does not depend on $r$, we deduce that

$$\int_0^1 \left|u^K(t,r)\right|^2 \, rdr - \left|\overline{u^K}(t)\right|^2 \int_0^1 rdr \leq C,$$

which implies

$$\int_0^1 \left|u^K(t,r)\right|^2 \, rdr \leq C + \frac{1}{2}\left|\overline{u^K}(t)\right|^2. \tag{6.27}$$

Adding (6.25) and (6.27), taking supremum in $t \in (0,T)$ and recalling that the mean of $u^K$ is constant in time, we obtain

$$\sup_{0<t<T} \|u^K(t)\|_{H^1_{\mathrm{rad}}(B)} \leq C. \tag{6.28}$$

Let $\phi \in L^2(0,T; H^1_{\mathrm{rad}}(B))$ and denote by $\Pi_K$ the orthogonal projection of $L^2_{\mathrm{rad}}(B)$ onto $\mathrm{span}\{\phi_1, \ldots, \phi_K\}$, then

$$\begin{aligned}
\left|\int_0^T \int_0^1 \partial_t u^K \phi \, rdrdt\right| &= \left|\int_0^T \int_0^1 \partial_t u^K \Pi_K \phi \, rdrdt\right|, \\
&= \left|\int_0^T \int_0^1 M_\delta(u^K) \partial_r \mu^K \partial_r \Pi_K \phi \, rdrdt\right|, \\
&\leq \left(\int_0^T \int_0^1 |M_\delta(u^K)\partial_r \mu^K|^2 \, rdrdt\right)^{\frac{1}{2}} \left(\int_0^T \int_0^1 |\partial_r \Pi_K \phi|^2 \, rdrdt\right)^{\frac{1}{2}}.
\end{aligned} \tag{6.29}$$

To bound the first term on the right-hand side of (6.29) we use that $0 < m_1 \leq M_\delta(u^K) \leq m_2$ and the fact that $|ab| \leq |a||b|$ for all $a$, $b \in \mathbb{R}$. To bound the second

term we denote the inner product of $L^2_{\text{rad}}(B)$ as $(\cdot,\cdot)_{L^2_{\text{rad}}(B)}$, thus

$$\begin{aligned}\partial_r \Pi_K \phi(t,r) =& \partial_r \left( \sum_{i=1}^{K} (\phi(t,\cdot),\phi_i)_{L^2_{\text{rad}}(B)} \phi_i(r) \right), \\ =& \sum_{i=1}^{K} (\phi(t,\cdot),\phi_i)_{L^2_{\text{rad}}(B)} \partial_r \phi_i(r).\end{aligned}$$

Using the orthogonality in $L^2_{\text{rad}}(B)$ of the basis $\{\phi_i\}_{i\in\mathbb{N}}$ we obtain

$$\begin{aligned}\|\partial_r \Pi_K \phi(t,\cdot)\|^2_{L^2_{\text{rad}}(B)} =& \sum_{i=1}^{K} |(\phi(t,\cdot),\phi_i)_{L^2_{\text{rad}}(B)}|^2 \|\partial_r \phi_i\|^2_{L^2_{\text{rad}}(B)}, \\ \leq& \sum_{i=1}^{\infty} |(\phi(t,\cdot),\phi_i)_{L^2_{\text{rad}}(B)}|^2 \|\partial_r \phi_i\|^2_{L^2_{\text{rad}}(B)}.\end{aligned}$$

We apply (6.12) to the inner product inside the sum (noting that the term for $i = 0$ is always 0), which yields

$$\|\partial_r \Pi_K \phi(t,\cdot)\|^2_{L^2_{\text{rad}}(B)} \leq \sum_{i=2}^{\infty} \frac{1}{\lambda_i^2} |(\partial_r \phi(t,\cdot), \partial_r \phi_i)_{L^2_{\text{rad}}(B)}|^2 \|\partial_r \phi_i\|^2_{L^2_{\text{rad}}(B)}.$$

Then,

$$\|\partial_r \Pi_K \phi(t,\cdot)\|^2_{L^2_{\text{rad}}(B)} \leq \sum_{i=2}^{\infty} \frac{1}{\lambda_i^2} \left| \left( \partial_r \phi(t,\cdot), \frac{\partial_r \phi_i}{\|\partial_r \phi_i\|_{L^2_{\text{rad}}(B)}} \right)_{L^2_{\text{rad}}(B)} \right|^2 \|\partial_r \phi_i\|^4_{L^2_{\text{rad}}(B)}.$$

Now, we note that from (6.13) we have that $\|\partial_r \phi_i\|^2_{L^2_{\text{rad}}(B)} = \frac{\lambda_i}{1+\lambda_i}$ for all $i \in \mathbb{N}$. Thus,

$$\begin{aligned}\|\partial_r \Pi_K \phi(t,\cdot)\|^2_{L^2_{\text{rad}}(B)} \leq& \sum_{i=2}^{\infty} \frac{1}{\lambda_i^2} \left| \left( \partial_r \phi(t,\cdot), \frac{\partial_r \phi_i}{\|\partial_r \phi_i\|_{L^2_{\text{rad}}(B)}} \right)_{L^2_{\text{rad}}(B)} \right|^2 \frac{\lambda_i^2}{(1+\lambda_i)^2}, \\ \leq& \sum_{i=2}^{\infty} \left| \left( \partial_r \phi(t,\cdot), \frac{\partial_r \phi_i}{\|\partial_r \phi_i\|_{L^2_{\text{rad}}(B)}} \right)_{L^2_{\text{rad}}(B)} \right|^2 \frac{1}{(1+\lambda_i)^2}.\end{aligned}$$

Since $0 < \lambda_i$ for all $i \geq 2$, then $\frac{1}{(1+\lambda_i)^2} < 1$, and

$$\begin{aligned}\|\partial_r \Pi_K \phi(t,\cdot)\|^2_{L^2_{\text{rad}}(B)} \leq & \sum_{i=2}^{\infty} \left| \left( \partial_r \phi(t,\cdot), \frac{\partial_r \phi_i}{\|\partial_r \phi_i\|_{L^2_{\text{rad}}(B)}} \right)_{L^2_{\text{rad}}(B)} \right|^2, \\ = & \|\partial_r \phi(t,\cdot)\|^2_{L^2_{\text{rad}}(B)},\end{aligned}$$

where the last equality is due to the fact that $\{\phi_i\}_{i\in\mathbb{N}}$ is an orthogonal basis of $H^1_{\text{rad}}(B)$, which implies that $\left\{ \frac{\partial_r \phi_i}{\|\partial_r \phi_i\|_{L^2_{\text{rad}}(B)}} \right\}_{i\in\mathbb{N}}$ is an orthonormal basis of $L^2_{\text{rad}}(B)$, which satisfies Parseval's Identity.

Finally, this implies

$$\begin{aligned}\left( \int_0^T \int_0^1 |\partial_r \Pi_K \phi|^2 \, r dr dt \right)^{\frac{1}{2}} = & \left( \int_0^T \|\partial_r \Pi_K \phi(t,\cdot)\|^2_{L^2_{\text{rad}}(B)} dt \right)^{\frac{1}{2}}, \\ \leq & \left( \int_0^T \|\partial_r \phi(t,\cdot)\|^2_{L^2_{\text{rad}}(B)} dt \right)^{\frac{1}{2}}, \\ \leq & \|\partial_r \phi\|_{L^2(0,T;L^2_{\text{rad}}(B))}.\end{aligned}$$

Thus, (6.29) becomes

$$\left| \int_0^T \int_0^1 \partial_t u^K \phi \, r dr dt \right| \leq m_2 \left( \int_0^T \int_0^1 |\partial_r \mu^K|^2 \, r dr dt \right)^{\frac{1}{2}} \|\partial_r \phi\|_{L^2(0,T;L^2_{\text{rad}}(B))},$$

and using (6.26) we obtain

$$\left| \int_0^T \int_0^1 \partial_t u^K \phi \, r dr dt \right| \leq C \|\partial_r \phi\|_{L^2(0,T;L^2_{\text{rad}}(B))}.$$

Therefore

$$\|\partial_t u^K\|_{L^2(0,T;H^{-1}_{\text{rad}}(B))} = \sup_{\phi \in L^2(0,T;H^1_{\text{rad}}(B))} \frac{\left| \int_0^T \int_0^1 \partial_t u^K \phi \, r dr dt \right|}{\|\partial_r \phi\|_{L^2(0,T;L^2_{\text{rad}}(B))}} \leq C. \tag{6.30}$$

Note that here we have also used the fact that

$$\|\partial_r \phi\|_{L^2(0,T;L^2_{\text{rad}}(B))} \leq \|\phi\|_{L^2(0,T;H^1_{\text{rad}}(B))}.$$

From (6.28) and (6.30) we have that $u^K$ is bounded in $L^\infty(0,T;H^1_{\text{rad}}(B))$ and $\partial_t u^K$ is bounded in $L^2(0,T;H^{-1}_{\text{rad}}(B))$. Using Lemma 6.6 with $X = H^1_{\text{rad}}(B)$, $Y = L^p_{\text{rad}}(B)$ with $p \in [1,\infty)$, and $Z = H^{-1}_{\text{rad}}(B)$ we obtain that the sequence $(u^K)_{K\in\mathbb{N}}$ has a subsequence, which we denote by the same name, such that:

$$u^K \rightharpoonup u \qquad \text{weakly-}* \text{ in} \quad L^\infty([0,T];H^1_{\text{rad}}(B)), \tag{6.31}$$

$$u^K \to u \qquad \text{strongly in} \quad L^2(0,T;L^p_{\text{rad}}(B)), \tag{6.32}$$

$$u^K \to u \qquad \text{strongly in} \quad C([0,T];L^2_{\text{rad}}(B)), \tag{6.33}$$

$$\partial_t u^K \rightharpoonup \partial_t u \qquad \text{weakly in} \quad L^2(0,T;H^{-1}_{\text{rad}}(B)). \tag{6.34}$$

From (6.24), with $f(u) \geq 0$ and the hypothesis on the mobility we get

$$\left\|\partial_r \mu^K(t,r)\right\|^2_{L^2(0,T;L^2_{\text{rad}}(B))} = \int_0^T \int_0^1 |\partial_r \mu^K|^2 \, r dr dt \leq C,$$

By Poincaré's inequality we have

$$\int_0^T \int_0^1 \left|\mu^K(t,r) - \overline{\mu}^K(t)\right|^2 \, r dr dt \leq C.$$

Then, applying the same arguments used to prove (6.27) we obtain

$$\int_0^T \int_0^1 \left|\mu^K(t,r)\right|^2 \, r dr dt - \int_0^1 \int_0^T \left|\overline{\mu}^K(t)\right|^2 \, r dr dt \leq C.$$

Recalling that $\overline{\mu}^K(t)$ does not depend on $r$ and integrating in this variable in the

second integral we have

$$\int_0^T \int_0^1 \left|\mu^K(t,r)\right|^2 \, r dr dt - \frac{1}{2}\int_0^T \left|\overline{\mu}^K(t)\right|^2 \, dt \leq C,$$

which implies

$$\int_0^T \int_0^1 \left|\mu^K(t,r)\right|^2 \, r dr dt \leq C\left(1 + \int_0^T \left|\overline{\mu}^K(t)\right|^2 \, dt\right),$$

where we have absorbed all constants into $C$.

Since $\int_0^1 \mu^K \, r dr = \int_0^1 f'(u^K) \, r dr$ and $|f'(u)| \leq 2\left(|u|^3 + |u|\right)$, we obtain

$$\begin{aligned}
\int_0^T \int_0^1 \left|\mu^K(t,r)\right|^2 \, r dr dt \leq & C\left(1 + \int_0^T \left|\overline{\mu}^K(t)\right|^2 \, dt\right), \\
\leq & C\left(1 + \int_0^T \left|\int_0^1 \mu^K(t,r) \, r dr\right|^2 dt\right), \\
\leq & C\left(1 + \int_0^T \left|\int_0^1 f'(u^K(t,r)) \, r dr\right|^2 dt\right), \\
\leq & C\left(1 + \int_0^T \int_0^1 \left(|u^K| + |u^K|^3\right)^2 \, r dr dt\right), \\
\leq & C\left(1 + \int_0^T \int_0^1 \left(|u^K|^2 + |u^K|^6\right) \, r dr dt\right), \\
\leq & C\Big(1 + \|u^K\|^2_{L^2(0,T;L^2_{\mathrm{rad}}(B))} \\
& \quad + \|u^K\|^6_{L^6(0,T;L^6_{\mathrm{rad}}(B))}\Big), \\
\leq & C,
\end{aligned}$$

where we used that $u^K \in L^2(0,T;L^2_{\mathrm{rad}}(B))$ and

$$L^\infty(0,T;H^1_{\mathrm{rad}}(B)) \hookrightarrow L^6(0,T;L^6_{\mathrm{rad}}(B))$$

continuously.

**Remark 6.12.** *Note that above we have also proved*

$$\|f'(u^K)\|^2_{L^2(0,T;L^2_{rad}(B))} := \int_0^T \int_0^1 |f'(u^K)|^2 \, r dr dt \leq C,$$

*i.e.* $f'(u^K)$ *is bounded in* $L^2(0,T;L^2_{rad}(B))$.

*In addition, at this stage we have shown that for all* $K \in \mathbb{N}$, *the functions* $\{c_i\}_{i=1}^{i=K}$ *and* $\{d_i\}_{i=1}^{i=K}$ *are globally bounded. This implies that there is a global in time solution to* (6.20)-(6.22).

Hence, for a subsequence of $(\mu^K)_{K\in\mathbb{N}}$ which we denote by the same name, we have

$$\mu^K \rightharpoonup \mu \quad \text{weakly in} \quad L^2(0,T;H^1_{\text{rad}}(B)). \tag{6.35}$$

Now we can pass to the limit in equations (6.16)-(6.17) and obtain equations (6.9)-(6.10). It is sufficient to prove that equations (6.9)-(6.10) hold for $\zeta = \varphi\psi$, where $\varphi \in L^2(0,T)$ and $\psi \in H^1_{\text{rad}}(B)$, because we can apply the $\pi$-$\lambda$ Theorem to indicator functions of rectangles in $B_T$ to extend the integrals in (6.9) to any $\zeta \in L^2(0,T;H^1_{\text{rad}}(B))$. Moreover, since $\{\phi_i\}_{i=1}^{\infty}$ is an orthonormal basis of $H^1_{\text{rad}}(B)$, it is sufficient to prove that equations (6.9)-(6.10) hold for

$$\zeta(r,t) = \phi_i(r)\varphi(t)$$

for all $i \in \mathbb{N}$.

Let $\varphi \in L^2(0,T)$, $i \in \mathbb{N}$ and $K \in \mathbb{N}$ such that $i \leq K$ (without loss of generality, as we can take $K$ sufficiently large). We multiply (6.16)-(6.17) by $\varphi$ and integrate in time from 0 to $T$ to obtain

$$\int_0^T \int_0^1 \partial_t u^K \phi_j \varphi \, r dr dt = -\int_0^T \int_0^1 M_\delta(u^K) \partial_r \mu^K \partial_r \phi_j \varphi \, r dr dt, \tag{6.36}$$

$$\int_0^T \int_0^1 \mu^K \phi_j \varphi \, r dr dt = \varepsilon^2 \int_0^T \int_0^1 \partial_r u^K \partial_r \phi_j \varphi \, r dr dt + \int_0^T \int_0^1 f'(u^K) \phi_j \varphi \, r dr dt, \tag{6.37}$$

for $j = 1, \ldots, K$. In particular, for $j = i$

$$\int_0^T \int_0^1 \partial_t u^K \phi_i \varphi \, r dr dt = - \int_0^T \int_0^1 M_\delta(u^K) \partial_r \mu^K \partial_r \phi_i \varphi \, r dr dt, \tag{6.38}$$

$$\int_0^T \int_0^1 \mu^K \phi_i \varphi \, r dr dt = \varepsilon^2 \int_0^T \int_0^1 \partial_r u^K \partial_r \phi_i \varphi \, r dr dt + \int_0^T \int_0^1 f'(u^K) \phi_i \varphi \, r dr dt. \tag{6.39}$$

Using the convergence obtained in (6.34) we have

$$\int_0^T \int_0^1 \partial_t u^K \phi_j \varphi \, r dr dt \to \int_0^1 \langle \phi_j \varphi, \partial_t u \rangle_{H^1_{\text{rad}}, H^{-1}_{\text{rad}}} dt,$$

as $K \to \infty$.

And, by (6.35) we have directly that

$$\int_0^T \int_0^1 \mu^K \phi_i \varphi \, r dr dt \to \int_0^T \int_0^1 \mu \phi_i \varphi \, r dr dt,$$

as $K \to \infty$.

Because of (6.31) we have that

$$\int_0^T \int_0^1 \partial_r u^K \partial_r \phi_i \varphi \, r dr dt \to \int_0^T \int_0^1 \partial_r u \partial_r \phi_i \varphi \, r dr dt,$$

as $K \to \infty$.

To see that $\int_0^T \int_0^1 f'(u^K) \phi_i \varphi \, r dr dt \to \int_0^T \int_0^1 f'(u) \phi_i \varphi \, r dr dt$ we need to proceed carefully as we only know that $f : \mathbb{R} \to \mathbb{R}$ is $C^1$ (and not $f \in C^2$ or $|f'| \leq C$, which would give us the result directly).

Since $u^K \to u$ strongly in $L^2(0, T; L^2_{\text{rad}}(B))$ there is a subsequence, which we

again denote $u^K$, such that $u^K \to u$ a.e. in $B_T$. Using the continuity of $f'$ we have that $f'(u^K) \to f'(u)$ a.e. in $B_T$. Moreover, because $f'(u^K)$ is uniformly bounded in $L^2(0,T;L^2_{\text{rad}}(B))$ we can apply Lemma 6.8 to deduce that $f'(u^K) \rightharpoonup f'(u)$ in $L^2(0,T;L^2_{\text{rad}}(B))$. In particular, we have

$$\int_0^T \int_0^1 f'(u^K)\phi_i\varphi \; r dr dt \to \int_0^T \int_0^1 f'(u)\phi_i\varphi \; r dr dt. \tag{6.40}$$

Now, to get the required convergence of the term with $M_\delta$ in (6.38) we note that $M_\delta$ is continuous and $u^K \to u$ strongly in $L^2(0,T;L^2_{\text{rad}}(B))$. Thus, using the same arguments as before we obtain a subsequence $u^K$ such that $M_\delta(u^K) \to M_\delta(u)$ a.e. in $B_T$. Since $|M_\delta| \leq m_2$ and we are in a bounded domain $B_T$, then we have that there is a subsequence such that $M_\delta(u^K) \to M_\delta(u)$ strongly in $L^2(0,T;L^2_{\text{rad}}(B))$. Because of the weak convergence proved in (6.35) and using Hölder's and triangle inequalities we obtain that $M_\delta(u^K)\partial_r\mu^K \rightharpoonup M_\delta(u)\partial_r\mu$ weakly in $L^1(0,T;L^1_{\text{rad}}(B))$, i.e.

$$\int_0^T \int_0^1 M_\delta(u^K)\partial_r\mu^K\partial_r\phi \; r dr dt \to \int_0^T \int_0^1 M_\delta(u)\partial_r\mu\partial_r\phi \; r dr dt,$$

for all $\phi \in L^\infty(0,T;L^\infty_{\text{rad}}(B))$.

Moreover, using again that $|M_\delta| \leq m_2$, we obtain that, in fact, $M_\delta(u^K)\partial_r\mu^K \rightharpoonup M_\delta(u)\partial_r\mu$ weakly in $L^2(0,T;L^2_{\text{rad}}(B))$. Thus,

$$\int_0^T \int_0^1 M_\delta(u^K)\partial_r\mu^K\partial_r\phi_j\varphi \; r dr dt \to \int_0^T \int_0^1 M_\delta(u)\partial_r\mu\partial_r\phi_j\varphi \; r dr dt,$$

as $K \to \infty$.

Finally, because of (6.33) and since $u^K(0) \to u_0$ in $L^2_{\text{rad}}(B)$, we obtain $u(0) = u_0$. Using the density of the eigenfunctions $\{\phi_j\}_{j\in\mathbb{N}}$ in $H^1_{\text{rad}}(B)$ and the fact that $\varphi \in L^2(0,T)$ is arbitrary, we can extend the result to all test functions $\zeta$ that live in $L^2(0,T;H^1_{\text{rad}}(B))$, concluding the proof.

□

**Lemma 6.13.** *Under the assumptions of Theorem 6.10, the regularity of the solution $u$ can be improved, namely $u \in L^2(0,T;H^2_{rad}(B))$ and $\nabla\Delta u \in L^2(0,T;L^2_{rad}(B))$. In addition, $f'(u) \in L^2(0,T;H^1_{rad}(B))$.*

*Proof.* Recall that

$$\int_0^1 \mu\phi \; r dr = \varepsilon^2 \int_0^1 \partial_r u \partial_r \phi \; r dr + \int_0^1 f'(u)\phi \; r dr, \tag{6.41}$$

for all $\phi \in H^1_{\mathrm{rad}}(B)$ and almost all $t \in [0,T]$. Moreover, we proved that this holds weakly against a test function $\varphi \in L^2(0,T)$. Since $\mu \in L^2(0,T;H^1_{\mathrm{rad}}(B))$, $f' \in C(\mathbb{R})$ and $u \in L^2(0,T;H^1_{\mathrm{rad}}(B))$, it follows that $u \in L^2(0,T;H^2_{\mathrm{rad}}(B))$. This may be seen directly by testing (6.17) with $\partial_r u^K$, integrating by parts and then taking limits as $K \to \infty$.

This gain in regularity allows us to integrate by parts in (6.41) and obtain that

$$\mu = -\varepsilon^2 \frac{1}{r}\partial_r(r\partial_r u) + f'(u) = -\varepsilon^2 \Delta u + f'(u)$$

weakly in $L^2_{\mathrm{rad}}(B)$ and almost all $t \in [0,T]$. Therefore,

$$\begin{aligned}\nabla\Delta u =& \frac{1}{\varepsilon^2}\left(\nabla f'(u) - \nabla\mu\right)\\ =& \frac{1}{\varepsilon^2}\left(f''(u)\nabla u - \nabla\mu\right) \in L^2(0,T;L^2_{\mathrm{rad}}(B)).\end{aligned}$$

In particular, this implies that $f'(u) \in L^2(0,T;H^1_{\mathrm{rad}}(B))$, which concludes our proof.

□

## 6.3 Existence and regularity for degenerate mobilities

In this section, we use the theorem proved in the previous section to obtain the existence of a weak solution for the degenerate mobility case. Thus, we consider problem (2.6)-(2.10) with

$$M_n(u) = [(1-u^2)_+]^n,$$

where $n > 0$. In particular, we note that $M_n \in C(\mathbb{R}, \mathbb{R})$ and $0 \leq M_n(u) \leq 1$.

Additionally, we define the entropy $\Phi : (-1, 1) \to \mathbb{R}^+$ by

$$\Phi(u) := \int_0^u \int_0^s \frac{1}{M_n(\ell)} d\ell \; ds$$

which satisfies

$$\begin{aligned} \Phi''(u) =& \frac{1}{M_n(u)}, \\ \Phi'(0) =& \Phi(0) = 0. \end{aligned}$$

**Theorem 6.14.** *Let $T > 0$. Suppose the initial condition $u_0 \in H^1_{rad}(B)$ is bounded $|u_0| \leq 1$ a.e. in $B$. And suppose there exists a constant $C > 0$ such that*

$$\int_0^1 \Phi(u_0) \; r dr \leq C. \tag{6.42}$$

*Then there exists a pair of functions $(u, j)$ such that*

*(a)* $u \in L^2([0,T]; H^2_{rad}(B)) \cap L^\infty(0,T; H^1_{rad}(B)) \cap C([0,T]; L^2_{rad}(B))$,

*(b)* $u_t \in L^2(0,T; H^{-1}_{rad}(B))$,

*(c)* $u(0) = u_0$ *a.e. on* $B$ *and* $\partial_r u = 0$ *on* $\{0,1\} \times (0,T)$,

*(d)* $|u| \leq 1$ *a.e. in* $B_T = B \times (0,T)$,

*(e)* $j \in L^2(B_T;\mathbb{R})$,

*which satisfy equations* (6.1)-(6.4) *in the following weak sense:*

$$\int_0^T \langle \zeta(t), \partial_t u(t) \rangle_{H^1_{rad}, H^{-1}_{rad}} \, dt = -\int_0^T \int_0^1 j \, \partial_r \zeta \; r dr dt, \tag{6.43}$$

*for all* $\zeta \in L^2(0,T;H^1_{rad}(B))$, *and*

$$\begin{aligned} \int_0^T \int_0^1 j \, \psi \; r dr dt = &-\varepsilon^2 \int_0^T \int_0^1 \frac{1}{r} \partial_r \left( r \partial_r u \right) \partial_r (M_n(u)\psi) \; r dr dt \\ &+ \int_0^T \int_0^1 (M_n f'')(u) \partial_r u \psi \; r dr dt, \end{aligned} \tag{6.44}$$

*for all* $\psi \in L^2(0,T;H^1_{rad}(B)) \cap L^\infty(B_T)$ *such that* $\frac{\psi}{r} \in L^2(0,T;L^2_{rad}(B))$ *which satisfy* $\psi = 0$ *on* $\{0,1\} \times (0,T)$.

We note that, in a way, this is a stronger definition of solution than in Theorem 6.10 as we are putting more spatial derivatives on $u$ instead of on the test function. This does not mean that we obtain the same or better regularity as in the positive mobility case as given by Lemma 6.13, since that lemma does not fully carry to the degenerate case, which is why we put it as a result separate from Theorem 6.10.

We also observe that we require $\frac{\psi}{r} \in L^2(0,T;L^2_{\text{rad}}(B))$. This is not in the original theorem by Elliott and Garcke [32], see Theorem 6.1. This constraint arises from the radial symmetry of the problem. In particular, it is required to obtain the convergence of the right-hand side of equation (6.44). This means that the test function has to behave well enough as $r \to 0$.

Before starting the proof we would like to remark that $u_0 \in H^1_{rad}(B)$ implies that

$$\int_0^1 f(u_0) \, r dr \leq C, \tag{6.45}$$

for some constant $C > 0$. Indeed,

$$\begin{aligned}\int_0^1 f(u_0) r dr =& \int_0^1 \frac{(1-u_0^2)^2}{2}\, r dr,\\ =& \frac{1}{2}\int_0^1 (1 - 2u_0^2 + u_0^4)\, r dr,\\ \leq& \frac{1}{4} + \|u_0\|^2_{L^2_{rad}} + \frac{1}{2}\|u_0\|^4_{L^4_{rad}},\\ \leq& C.\end{aligned}$$

*Proof.* Let $\delta > 0$. We approximate the degenerate mobility $M_n(u) = [(1-u^2)_+]^n$ by the positive mobilities treated in the previous section, namely

$$M_\delta(u) = \begin{cases} M_n(-1+\delta) & \text{for } u \leq -1+\delta,\\ M_n(u) & \text{for } |u| \leq 1-\delta,\\ M_n(1-\delta) & \text{for } u \geq 1-\delta,\end{cases}$$

where we have cut off the problematic parts of $M_n$. We use $M_\delta$ to define an approximating entropy

$$\Phi_\delta(u) := \int_0^u \int_0^s \frac{1}{M_\delta(\ell)} d\ell\, ds$$

which satisfies

$$\begin{aligned}\Phi_\delta''(u) =& \frac{1}{M_\delta(u)},\\ \Phi_\delta'(0) =& \Phi_\delta(0) = 0.\end{aligned}$$

We note that $\Phi_\delta(u) = \Phi(u)$ when $|u| \leq 1-\delta$.

Applying Theorem 6.10 and Lemma 6.13 to the problem with mobility $M_\delta$ we obtain the existence of an approximate pair $(u_\delta, \mu_\delta)$ such that

- $u_\delta \in L^2(0,T; H^2_{\text{rad}}(B)) \cap L^\infty(0,T; H^1_{\text{rad}}(B)) \cap C([0,T]; L^2_{\text{rad}}(B))$,

- $\nabla\Delta u_\delta \in L^2(0,T;L^2_{\text{rad}}(B))$ and $f'(u_\delta) \in L^2(0,T;H^1_{\text{rad}}(B))$,
- $\partial_t u_\delta \in L^2(0,T;H^{-1}_{\text{rad}}(B))$,
- $u_\delta(0) = u_0$ a.e. on $B$ and $\partial_r u_\delta = 0$ on $(0,T)\times\{0,1\}$,
- $\mu_\delta \in L^2(0,T;H^1_{\text{rad}}(B))$,

which satisfy

$$\int_0^T \langle \zeta(t), \partial_t u_\delta(t)\rangle_{H^1_{rad},H^{-1}_{rad}}\, dt = -\int_0^T\int_0^1 M_\delta(u_\delta)\partial_r\mu_\delta\partial_r\zeta\ r dr dt, \tag{6.46}$$

$\forall \zeta \in L^2(0,T;H^1_{\text{rad}}(B))$, and

$$\int_0^1 \mu_\delta\phi\ r dr = \varepsilon^2\int_0^1 \partial_r u_\delta\partial_r\phi\ r dr + \int_0^1 f'(u_\delta)\phi\ r dr, \tag{6.47}$$

$\forall \phi \in H^1_{\text{rad}}(B)$ and for almost all $t \in [0,T]$.

We record for later the definition of the associated flux

$$j_\delta := -M_\delta(u_\delta)\partial_r\mu_\delta.$$

Due to the regularity of $(u_\delta,\mu_\delta)$, improved by Lemma 6.13, we have that

$$\begin{aligned}-\int_0^T\int_0^1 \partial_r\mu_\delta\chi\ r dr dt =& \varepsilon^2\int_0^T\int_0^1 \partial_r\left(\frac{1}{r}\partial_r(r\partial_r u_\delta)\right)\chi\ r dr dt\\ &-\int_0^T\int_0^1 \partial_r(f'(u_\delta))\chi\ r dr dt,\end{aligned} \tag{6.48}$$

for all $\chi \in L^2(0,T;L^2_{\text{rad}}(B))$.

Let $\zeta \in L^2(0,T;H^1_{\text{rad}}(B))$ we can test (6.48) with $\chi = M_\delta(u_\delta)\partial_r\zeta$ and obtain

$$\begin{aligned}-\int_0^T\int_0^1 M_\delta(u_\delta)\partial_r\mu_\delta\partial_r\zeta\ r dr dt = &-\int_0^T\int_0^1 M_\delta(u_\delta)\partial_r\left(-\frac{\varepsilon^2}{r}\partial_r(r\partial_r u_\delta)\right.\\ &\left.+f'(u_\delta)\right)\partial_r\zeta\ r dr dt.\end{aligned} \tag{6.49}$$

Substituting (6.49) into (6.46) gives

$$\int_0^T \langle \zeta, \partial_t u_\delta \rangle_{H^1_{rad}, H^{-1}_{rad}} \, dt = -\int_0^T \int_0^1 M_\delta(u_\delta) \partial_r \left( -\frac{\varepsilon^2}{r} \partial_r (r \partial_r u_\delta) + f'(u_\delta) \right) \partial_r \zeta \; r dr dt, \tag{6.50}$$

$\forall \zeta \in L^2(0,T; H^1_{\text{rad}}(B))$. Again, because of the regularity noted in Lemma 6.13 we can test equation (6.50) with $\zeta = -\frac{\varepsilon^2}{r}\partial_r(r\partial_r u_\delta) + f'(u_\delta)$, yielding

$$\int_0^t \left\langle -\frac{\varepsilon^2}{r} \partial_r (r \partial_r u_\delta) + f'(u_\delta), \partial_t u_\delta \right\rangle_{H^1_{rad}, H^{-1}_{rad}} dt = -\int_0^t \int_0^1 M_\delta(u_\delta) |\partial_r \mu_\delta|^2 \; r dr dt, \tag{6.51}$$

for all $t \in [0,T]$.

As in the proof of Theorem 6.10 we need estimates on $u_\delta$ and $\mu_\delta$ to allow us to take subsequences that, due to compactness, converge in appropriate spaces in order to pass to the limit. Such estimates are given by the following lemma:

**Lemma 6.15.** *For $\delta_0 > 0$ sufficiently small, there exists a positive constant $C$ such that for all $0 < \delta \leq \delta_0$ the following estimates hold:*

$$\operatorname*{ess\,sup}_{0 \leq t \leq T} \int_0^1 \left( \frac{\varepsilon^2}{2} |\partial_r u_\delta(t)|^2 + f(u_\delta(t)) \right) \; r dr + \int_0^T \int_0^1 M_\delta(u_\delta) |\partial_r \mu_\delta|^2 \; r dr dt \leq C, \tag{6.52}$$

$$\operatorname*{ess\,sup}_{0 \leq t \leq T} \int_0^1 \Phi_\delta(u_\delta(t)) \; r dr + \int_0^T \int_0^1 \left( \varepsilon |\Delta u_\delta|^2 + f''(u_\delta) |\partial_r u_\delta|^2 \right) \; r dr dt \leq C, \tag{6.53}$$

$$\operatorname*{ess\,sup}_{0 \leq t \leq T} \int_0^1 [(|u_\delta| - 1)_+]^2 \; r dr \leq C \delta^n, \tag{6.54}$$

$$\int_0^T \int_0^1 |j_\delta|^2 \, r dr dt \leq C. \tag{6.55}$$

*Proof.* We will prove each inequality separately. To prove (6.52) we first prove that, for almost all $t \in [0,T]$, the following equality holds:

$$\begin{aligned}\int_0^t \left\langle -\frac{\varepsilon^2}{r}\partial_r(r\partial_r u_\delta) + f'(u_\delta), \partial_t u_\delta \right\rangle_{H^1_{rad},H^{-1}_{rad}} dt = \int_0^1 \left(\frac{\varepsilon^2}{2}|\partial_r u_\delta(t)|^2 + f(u_\delta(t))\right) \, r dr \\ - \int_0^1 \left(\frac{\varepsilon^2}{2}|\partial_r u_0|^2 + f(u_0)\right) \, r dr.\end{aligned} \tag{6.56}$$

For the remainder of this proof we use the notation $\langle \cdot, \cdot \rangle := \langle \cdot, \cdot \rangle_{H^1_{rad},H^{-1}_{rad}}$.

Let $h > 0$, we define

$$u_{\delta h}(t,r) := \frac{1}{h}\int_{t-h}^t u_\delta(\tau, r) d\tau,$$

where we set $u_\delta(\tau, \cdot) = u_0(\cdot)$ for $\tau \leq 0$. We observe that

$$\partial_t u_{\delta h}(t,r) = \partial_t \left(\frac{1}{h}\int_{t-h}^t u_\delta(\tau,r)d\tau\right) = \frac{u_\delta(t,r) - u_\delta(t-h,r)}{h} = \frac{1}{h}\int_{t-h}^t \partial_t u_\delta(\tau,r)d\tau.$$

Hence $\partial_t u_{\delta h} \in L^2(0,T; L^2_{\text{rad}}(B))$. Therefore, for almost all $t \in [0,T]$ we have that

$$\begin{aligned}\int_0^t \left\langle -\frac{\varepsilon^2}{r}\partial_r(r\partial_r u_{\delta h}) + f'(u_{\delta h}), \partial_t u_{\delta h} \right\rangle d\tau &= \int_0^t \int_0^1 \left(-\frac{\varepsilon^2}{r}\partial_r(r\partial_r u_{\delta h})\right. \\ &\quad \left. + f'(u_{\delta h})\right) \partial_t u_{\delta h} \, r dr d\tau, \\ &= \int_0^t \int_0^1 -\varepsilon^2 \partial_r(r\partial_r u_{\delta h})\partial_t u_{\delta h} \, dr d\tau \\ &\quad + \int_0^t \int_0^1 f'(u_{\delta h})\partial_t u_{\delta h} \, r dr d\tau, \\ &= \int_0^t \int_0^1 \frac{\varepsilon^2}{2}\partial_r u_{\delta h}\partial_r \partial_t u_{\delta h} \, r dr d\tau\end{aligned}$$

$$+\int_0^t\int_0^1 \partial_t(f(u_{\delta h}))\ r dr d\tau.$$

Hence, using Fubini's Theorem,

$$\begin{aligned}\int_0^t \left\langle -\frac{\varepsilon^2}{r}\partial_r(r\partial_r u_{\delta h}) + f'(u_{\delta h}), \partial_t u_{\delta h}\right\rangle d\tau =& \int_0^t\int_0^1 \partial_t\left(\frac{\varepsilon^2}{2}|\partial_r u_{\delta h}|^2 + f(u_{\delta h})\right)\ r dr d\tau,\\ =&\partial_t\int_0^t\int_0^1 \left(\frac{\varepsilon^2}{2}|\partial_r u_{\delta h}|^2 + f(u_{\delta h})\right)\ r dr d\tau.\end{aligned}$$

Thus, by the Fundamental Theorem of Calculus,

$$\begin{aligned}\int_0^t \left\langle -\frac{\varepsilon^2}{r}\partial_r(r\partial_r u_{\delta h}) + f'(u_{\delta h}), \partial_t u_{\delta h}\right\rangle d\tau =& \int_0^1 \left(\frac{\varepsilon^2}{2}|\partial_r u_{\delta h}(t)|^2 + f(u_{\delta h}(t))\right)\ r dr\\ &- \int_0^1 \left(\frac{\varepsilon^2}{2}|\partial_r u_0|^2 + f(u_0)\right)\ r dr. \quad (6.57)\end{aligned}$$

We need now to prove that in the limit $h \to 0$, the above equality remains valid.

First, we will prove that

$$\begin{aligned}-\frac{\varepsilon^2}{r}\partial_r(r\partial_r u_{\delta h}) &\to -\frac{\varepsilon^2}{r}\partial_r(r\partial_r u_\delta) && \text{strongly in } L^2(0,T;H^1_{\text{rad}}(B)),\\ f'(u_{\delta h}) &\to f'(u_\delta) && \text{strongly in } L^2(0,T;H^1_{\text{rad}}(B)),\\ \int_0^1 \frac{\varepsilon^2}{2}|\partial_r u_{\delta h}(t)|^2\ r dr &\to \int_0^1 \frac{\varepsilon^2}{2}|\partial_r u_\delta(t)|^2\ r dr && \text{for almost all } t\in[0,T],\\ \int_0^1 f(u_{\delta h}(t))\ r dr &\to \int_0^1 f(u_\delta(t))\ r dr && \text{for almost all } t\in[0,T].\end{aligned}$$

We note that due to Lebesgue's Differentiation Theorem we have that for all $g \in L^1(0,T)$,

$$\lim_{h\to 0}\frac{1}{h}\int_{t-h}^t g(s)ds = g(t), \quad \text{a.e. in } [0,T]. \quad (6.58)$$

We will apply this argument to obtain the desired convergences. First, we define

$$I = \left\|\frac{\varepsilon^2}{r}\partial_r(r\partial_r u_{\delta h}) - \frac{\varepsilon^2}{r}\partial_r(r\partial_r u_\delta)\right\|^2_{L^2(0,T;H^1_{\text{rad}}(B))}.$$

Then,

$$
\begin{aligned}
I =& \int_0^T \left\| \frac{\varepsilon^2}{r} \frac{1}{h} \int_{t-h}^{t} \partial_r(r\partial_r u_\delta(\tau))d\tau - \frac{\varepsilon^2}{r}\partial_r(r\partial_r u_\delta(t)) \right\|^2_{H^1_{\mathrm{rad}}(B)} dt, \\
=& \int_0^T \left\| \frac{\varepsilon^2}{r} \frac{1}{h} \int_{-h}^{0} \left(\partial_r(r\partial_r u_\delta(t+s)) - \partial_r(r\partial_r u_\delta(t))\right) ds \right\|^2_{H^1_{\mathrm{rad}}(B)} dt, \\
\leq& \frac{1}{h} \int_{-h}^{0} \int_0^T \left\| \frac{\varepsilon^2}{r} \left(\partial_r(r\partial_r u_\delta(t+s)) - \partial_r(r\partial_r u_\delta(t))\right) \right\|^2_{H^1_{\mathrm{rad}}(B)} dtds, \\
=& \frac{1}{h} \int_{-h}^{0} \left\| \frac{\varepsilon^2}{r} \left(\partial_r(r\partial_r u_\delta(\cdot+s)) - \partial_r(r\partial_r u_\delta(\cdot))\right) \right\|^2_{L^2(0,T;H^1_{\mathrm{rad}}(B))} ds, \\
\to& 0, \quad \text{as } h \to 0.
\end{aligned}
$$

To prove that $f'(u_{\delta h}) \to f'(u_\delta)$ strongly in $L^2(0,T;H^1_{\mathrm{rad}}(B))$ we first note that $u_{\delta h} \to u_\delta$ strongly in $L^2(0,T;H^2_{\mathrm{rad}}(B))$. Indeed,

$$
\begin{aligned}
\|u_{\delta h} - u_\delta\|^2_{L^2(0,T;H^2_{\mathrm{rad}}(B))} =& \int_0^T \left\| \frac{1}{h} \int_{t-h}^{t} u_\delta(\tau)d\tau - u_\delta(t) \right\|^2_{H^2_{\mathrm{rad}}(B)} dt, \\
=& \int_0^T \left\| \frac{1}{h} \int_{-h}^{0} \left(u_\delta(t+s) - u_\delta(t)\right) ds \right\|^2_{H^2_{\mathrm{rad}}(B)} dt, \\
\leq& \frac{1}{h} \int_{-h}^{0} \int_0^T \|(u_\delta(t+s) - u_\delta(t))\|^2_{H^2_{\mathrm{rad}}(B)} dtds, \\
=& \frac{1}{h} \int_{-h}^{0} \|(u_\delta(\cdot+s) - u_\delta(\cdot))\|^2_{L^2(0,T;H^2_{\mathrm{rad}}(B))} ds, \\
\to& 0, \quad \text{as } h \to 0.
\end{aligned}
$$

In addition, because of Lemma 6.13 we know that $f'(u_\delta) \in L^2(0,T;H^1_{\mathrm{rad}}(B))$, which implies that $f'(u_{\delta h}) \in L^2(0,T;H^1_{\mathrm{rad}}(B))$ since $u_{\delta h}$ has even more regularity in time. Using a similar argument as for (6.40) we have that $f'(u_{\delta h}) \rightharpoonup f'(u_\delta)$ weakly in $L^2(0,T;H^1_{\mathrm{rad}}(B))$. Moreover, due to the regularity of $f'(u_{\delta h})$ we can apply Dominated Convergence Theorem to show that $\|f'(u_{\delta h})\|_{L^2(0,T;H^1_{\mathrm{rad}}(B))} \to \|f'(u_\delta)\|_{L^2(0,T;H^1_{\mathrm{rad}}(B))}$.

Since we are in a Hilbert space, this implies strong convergence, i.e.

$$f'(u_{\delta h}) \to f'(u_\delta) \quad \text{strongly in } L^2(0,T;H^1_{\text{rad}}(B)).$$

Now, to prove that $\int_0^1 \frac{\varepsilon^2}{2}|\partial_r u_{\delta h}(t)|^2\ r dr \to \int_0^1 \frac{\varepsilon^2}{2}|\partial_r u_\delta(t)|^2\ r dr$ for almost all $t$ in $[0,T]$ we let $\varphi \in L^2(0,T)$ and define

$$J := \int_0^T \left| \int_0^1 |\partial_r u_{\delta h}(t,r)|^2\ r dr - \int_0^1 |\partial_r u_\delta(t,r)|^2\ r dr \right| \varphi dt.$$

Then

$$\begin{aligned}
J =& \int_0^T \left| \|\partial_r u_{\delta h}(t)\|^2_{L^2_{\text{rad}}(B)} - \|\partial_r u_\delta(t)\|^2_{L^2_{\text{rad}}(B)} \right| \varphi dt, \\
\leq& 2\int_0^T \left| \|\partial_r u_{\delta h}(t)\|_{L^2_{\text{rad}}(B)} - \|\partial_r u_\delta(t)\|_{L^2_{\text{rad}}(B)} \right|^2 \varphi dt, \\
\leq& 2\int_0^T \left| \|\partial_r u_{\delta h}(t) - \partial_r u_\delta(t)\|_{L^2_{\text{rad}}(B)} \right|^2 \varphi dt, \\
=& 2\int_0^T \|\partial_r u_{\delta h}(t) - \partial_r u_\delta(t)\|^2_{L^2_{\text{rad}}(B)} \varphi dt,
\end{aligned}$$

where we used that $|a^2 - b^2| \leq 2|a-b|^2$ for all $a$, $b \in \mathbb{R}$ and then applied the reverse triangle inequality.

Now, we substitute $u_{\delta h}$ to obtain

$$\begin{aligned}
J \leq& 2\int_0^T \left\| \frac{1}{h}\int_{t-h}^t \partial_r u_\delta(\tau) d\tau - \partial_r u_\delta(t) \right\|^2_{L^2_{\text{rad}}(B)} \varphi dt, \\
=& 2\int_0^T \left\| \frac{1}{h}\int_{-h}^0 (\partial_r u_\delta(t+s) - \partial_r u_\delta(t))\, ds \right\|^2_{L^2_{\text{rad}}(B)} \varphi dt, \\
\leq& 2\frac{1}{h}\int_{-h}^0 \int_0^T \|\partial_r u_\delta(t+s) - \partial_r u_\delta(t)\|^2_{L^2_{\text{rad}}(B)} \varphi dt\, ds, \\
\leq& 2\|\varphi\|_{L^2(0,T)} \frac{1}{h}\int_{-h}^0 \|\partial_r u_\delta(\cdot + s) - \partial_r u_\delta(\cdot)\|_{L^2(0,T;L^2_{\text{rad}}(B))}\ ds, \\
\to& 0 \quad \text{as } h \to 0.
\end{aligned}$$

due to (6.58). Since this is for all $\varphi \in L^2(0,T)$ we have the result for almost all $t$ in $[0,T]$.

An analogous argument in conjunction with the fact that $f \in C^1(\mathbb{R})$ can be used to obtain that $\int_0^1 f(u_{\delta h}(t))\ rdr \to \int_0^1 f(u_\delta(t))\ rdr$ for almost all $t$ in $[0,T]$.

In a similar fashion, we will now prove that $\partial_t u_{\delta h} \rightharpoonup \partial_t u_\delta$ weakly in $L^2(0,T;H^{-1}_{\text{rad}}(B))$. For any $\zeta \in L^2(0,T;H^1_{\text{rad}}(B))$ we have that

$$
\begin{aligned}
|\langle \zeta, \partial_t u_{\delta h} - \partial_t u_\delta \rangle_{L^2(H^1),L^2(H^{-1})}| &= \left| \int_0^T \left\langle \zeta, \frac{1}{h}\int_{t-h}^t \partial_t u_\delta(\tau)d\tau - \partial_t u_\delta(t) \right\rangle dt \right|, \\
&= \frac{1}{h}\left| \int_0^T \left\langle \zeta, \int_{-h}^0 (\partial_t u_\delta(t+s) - \partial_t u_\delta(t))ds \right\rangle dt \right|, \\
&\le \frac{1}{h}\int_{-h}^0 \left| \int_0^T \int_0^1 \partial_r \zeta(-(M_\delta \partial_r \mu_\delta)(t+s) + (M_\delta \partial_r \mu_\delta)(t))\ rdrdt \right| ds, \\
&\le C\frac{1}{h}\int_{-h}^0 \|(M_\delta \partial_r \mu_\delta)(\cdot + s) - (M_\delta \partial_r \mu_\delta)(\cdot)\|_{L^2(0,T;L^2_{\text{rad}}(B))} ds, \\
&\to 0 \qquad\qquad \text{as } h \to 0\,,
\end{aligned}
$$

where the last convergence is due to (6.58).

Lastly, taking $h \to 0$ in (6.57) we obtain (6.56). We use (6.51) in (6.56), and the fact that (6.45) implies that the terms depending on the initial condition are bounded, to get

$$
\int_0^1 \left( \frac{\varepsilon^2}{2}|\partial_r u_\delta(t)|^2 + f(u_\delta(t)) \right)\ rdr + \int_0^t \int_0^1 M_\delta(u_\delta)|\partial_r \mu_\delta|^2\ rdrdt \le C,
$$

a.e. in $[0,T]$. Taking $\operatorname{ess\,sup}_{0\le t\le T}$ we obtain inequality (6.52).

To prove (6.53) we note that $\Phi''_\delta(u_\delta)$ is bounded since $M_\delta$ is bounded from below, it follows that $\Phi'_\delta(u_\delta) \in L^2(0,T;H^1_{\text{rad}}(B))$. Let us take $\zeta := \Phi'_\delta(u_\delta)$ in (6.50),

$$
\int_0^T \langle \Phi'_\delta(u_\delta), \partial_t u_\delta \rangle\, dt = -\int_0^T \int_0^1 M_\delta(u_\delta)\partial_r \left( -\frac{\varepsilon^2}{r}\partial_r(r\partial_r u_\delta) + f'(u_\delta) \right) \partial_r(\Phi'_\delta(u_\delta))\ rdrdt.
$$

Then, using the same steps as in the proof of (6.56), we obtain

$$\int_0^t \langle \Phi'_\delta(u_\delta), \partial_t u_\delta \rangle \, dt = \int_0^1 \Phi_\delta(u_\delta(t)) r dr - \int_0^1 \Phi_\delta(u_0) r dr$$

for almost all $t \in [0, T]$. Also,

$$\begin{aligned}
\int_0^t \langle \Phi'_\delta(u_\delta), \partial_t u_\delta \rangle \, dt &= - \int_0^T \int_0^1 M_\delta(u_\delta) \partial_r \mu_\delta \partial_r (\Phi'_\delta(u_\delta)) \; r dr dt, \\
&= - \int_0^T \int_0^1 M_\delta(u_\delta) \partial_r \left( \Delta u_\delta + f'(u_\delta) \right) \partial_r (\Phi'_\delta(u_\delta)) \; r dr dt, \\
&= - \int_0^T \int_0^1 M_\delta(u_\delta) \Phi''_\delta(u_\delta) \partial_r u_\delta \left( -\varepsilon^2 \partial_r \Delta u_\delta + f''(u_\delta) \partial_r(u_\delta) \right) \; r dr dt, \\
&= - \int_0^T \int_0^1 \partial_r u_\delta \left( -\varepsilon^2 \partial_r \Delta u_\delta + f''(u_\delta) \partial_r(u_\delta) \right) \; r dr dt, \\
&= \varepsilon^2 \int_0^T \int_0^1 r \partial_r u_\delta \partial_r \Delta u_\delta \; dr dt - \int_0^T \int_0^1 f''(u_\delta) |\partial_r(u_\delta)|^2 \; r dr dt, \\
&= - \int_0^T \int_0^1 \left( \varepsilon^2 |\Delta u_\delta|^2 + f''(u_\delta) |\partial_r(u_\delta)|^2 \right) \; r dr dt.
\end{aligned}$$

Therefore,

$$\int_0^1 \Phi_\delta(u_\delta(t)) r dr + \int_0^T \int_0^1 \left( \varepsilon^2 |\Delta u_\delta|^2 + f''(u_\delta) |\partial_r(u_\delta)|^2 \right) \; r dr dt = \int_0^1 \Phi_\delta(u_0) r dr.$$

We note that (6.42) ensures that the terms depending on the initial condition are bounded. Taking the supremum in time, we obtain (6.53).

To prove (6.54) we will use that, from (6.53), we have

$$\operatorname*{ess\,sup}_{0 \le t \le T} \int_0^1 \Phi_\delta(u_\delta(t)) \; r dr \le C.$$

Let $z > 1$ and $\delta < 1$. Using the definitions of $M_\delta$, $\Phi$, $\Phi_\delta$ and the fact that $z > 1 - \delta$

yields

$$\begin{aligned}
\Phi_\delta(z) =& \int_0^z \int_0^s \frac{1}{M_\delta(\ell)} d\ell ds, \\
=& \int_0^{1-\delta} \int_0^s \frac{1}{M_\delta(\ell)} d\ell ds + \int_{1-\delta}^z \int_0^s \frac{1}{M_\delta(\ell)} d\ell ds, \\
=& \Phi(1-\delta) + \int_0^{z-(1-\delta)} \int_0^{k+(1-\delta)} \frac{1}{M_\delta(\ell)} d\ell dk, \\
=& \Phi(1-\delta) + \int_0^{z-(1-\delta)} \left[ \int_0^{1-\delta} \frac{1}{M_\delta(\ell)} d\ell + \int_{1-\delta}^{k+(1-\delta)} \frac{1}{M_\delta(\ell)} d\ell \right] dk,
\end{aligned}$$

thus

$$\begin{aligned}
\Phi_\delta(z) =& \Phi(1-\delta) + \int_0^{z-(1-\delta)} \left[ \Phi'(1-\delta) + \int_{1-\delta}^{k+(1-\delta)} \frac{1}{M_\delta(\ell)} d\ell \right] dk, \\
=& \Phi(1-\delta) + \Phi'(1-\delta)(z-(1-\delta)) + \frac{1}{M(1-\delta)} \int_0^{z-(1-\delta)} \int_{1-\delta}^{k+(1-\delta)} d\ell dk, \\
=& \Phi(1-\delta) + \Phi'(1-\delta)(z-(1-\delta)) + \frac{1}{2}\Phi''(1-\delta)(z-(1-\delta))^2.
\end{aligned}$$

Then, since $\Phi(1-\delta)$, $\Phi'(1-\delta)$, $(z-(1-\delta)) \geq 0$ and $z-1>0$, we have

$$\begin{aligned}
\Phi_\delta(z) =& \Phi(1-\delta) + \Phi'(1-\delta)(z-(1-\delta)) + \frac{1}{2}\Phi''(1-\delta)(z-(1-\delta))^2, \\
\geq& \frac{1}{2}\Phi''(1-\delta)\left((z-1)^2 + 2\delta(z-1) + \delta^2\right), \\
\geq& \frac{1}{2}\Phi''(1-\delta)(z-1)^2, \\
=& \frac{1}{2}\frac{1}{\delta^n(2-\delta)^n}(z-1)^2, \\
\geq& \frac{1}{2^{n+1}}\frac{1}{\delta^n}(z-1)^2.
\end{aligned}$$

Thus, $(z-1)^2 \leq 2^{n+1}\delta^n \Phi_\delta(z)$. Using the same argument with $z<-1$ we obtain

$$(|z|-1)^2 \leq 2^{n+1}\delta^n \Phi_\delta(z).$$

Integrating in space and taking $\operatorname{ess\,sup}_{0\le t\le T}$ we obtain (6.54).

One can obtain (6.55) directly from (6.52) by recalling that $j_\delta = M_\delta(u_\delta)\partial_r\mu_\delta$ and noting that $0 \le |M_\delta| \le 1$ and thus $|M_\delta|^2 \le |M_\delta|$.

□

Using the estimates from Lemma 6.15 and the fact that $f$ and $M$ are non-negative, we obtain the necessary bounds which allow us to apply Lemma 6.6 with $X = H^2_{\text{rad}}(B)$, $Y = H^1_{\text{rad}}(B)$, $Z = H^{-1}_{\text{rad}}(B)$ and obtain a subsequence, which we still denote $(u_\delta)_{\delta>0}$, such that

$$u_\delta,\ \partial_r u_\delta \to u,\ \partial_r u \quad \text{strongly in} \quad L^2(0,T;L^2_{\text{rad}}(B)) \text{ and a.e. in } B_T, \tag{6.59}$$

$$\partial_t u_\delta \rightharpoonup \partial_t u \quad \text{weakly in} \quad L^2(0,T;H^{-1}_{\text{rad}}(B)), \tag{6.60}$$

$$\Delta u_\delta \rightharpoonup \Delta u \quad \text{weakly in} \quad L^2(0,T;L^2_{\text{rad}}(B)), \tag{6.61}$$

$$j_\delta \rightharpoonup j \quad \text{weakly in} \quad L^2(0,T;L^2_{\text{rad}}(B)), \tag{6.62}$$

where $j = -M(u)\partial_r\mu$.

We note that taking $\delta \to 0$ in (6.54) yields $|u| \le 1$ a.e. in $B_T$.

With (6.60) and (6.62) we can pass to the limit in equation (6.46) and obtain

$$\int_0^T \langle \zeta(t), \partial_t u_\delta(t)\rangle_{H^1_{rad},H^{-1}_{rad}}\, dt = \int_0^T \int_0^1 j\,\partial_r\zeta\ r dr dt$$

for all $\zeta \in L^2(0,T;H^1_{\text{rad}}(B))$.

Let $\psi \in L^2(0,T;H^1_{\text{rad}}(B)) \cap L^\infty(B_T)$ such that $\psi = 0$ on $\{0,1\}\times[0,T]$. We can test (6.48) with $\chi = M_\delta(u_\delta)\psi$ and obtain

$$-\int_0^T \int_0^1 j_\delta\,\psi\ r dr dt = \int_0^T \int_0^1 M_\delta(u_\delta)\partial_r\left(-\frac{\varepsilon^2}{r}\partial_r(r\partial_r u_\delta) + f'(u_\delta)\right)\psi\ r dr dt.$$

It follows that

$$-\int_0^T\int_0^1 j_\delta\,\psi\;rdrdt=\varepsilon^2\int_0^T\int_0^1\frac{1}{r}\partial_r(r\partial_r u_\delta)\partial_r(rM_\delta(u_\delta)\psi)\;drdt + \int_0^T\int_0^1 f''(u_\delta)M_\delta(u_\delta)\partial_r u_\delta\psi\;rdrdt.$$

Thus,

$$\begin{aligned}-\int_0^T\int_0^1 j_\delta\,\psi\;rdrdt=&\varepsilon^2\int_0^T\int_0^1\frac{1}{r}\partial_r(r\partial_r u_\delta)M_\delta(u_\delta)\psi\;drdt\\&+\varepsilon^2\int_0^T\int_0^1\frac{1}{r}\partial_r(r\partial_r u_\delta)M_\delta(u_\delta)\partial_r\psi\;rdrdt\\&+\varepsilon^2\int_0^T\int_0^1\frac{1}{r}\partial_r(r\partial_r u_\delta)M'_\delta(u_\delta)\partial_r u_\delta\psi\;rdrdt\\&+\int_0^T\int_0^1 f''(u_\delta)M_\delta(u_\delta)\partial_r u_\delta\psi\;rdrdt,\\=:&I_1+I_2+I_3+I_4.\end{aligned}$$

Because of (6.62) the left-hand side converges, i.e.

$$\int_0^T\int_0^1 j_\delta\,\psi\;rdrdt\to\int_0^T\int_0^1 j\,\psi\;rdrdt.$$

Next, we focus on the right-hand side and rewrite $I_1$ as

$$I_1=\varepsilon^2\int_0^T\int_0^1\Delta u_\delta M_\delta(u_\delta)\left(\frac{\psi}{r}\right)\;rdrdt.$$

Using that $\psi/r\in L^2(0,T;L^2_{\mathrm{rad}}(B))$, the convergence obtained in (6.61) and the argument we used to prove (6.40) (which uses the boundedness and continuity of $M_\delta$ and $M_n$) we get

$$I_1\to\varepsilon^2\int_0^T\int_0^1\frac{1}{r}\partial_r(r\partial_r u)M_n(u)\psi\;drdt.$$

With similar reasoning we have

$$I_2 \to \varepsilon^2 \int_0^T \int_0^1 \frac{1}{r}\partial_r(r\partial_r u) M_n(u)\partial_r\psi \; r dr dt.$$

In $I_3$ we want $M'_\delta(u_\delta)\partial_r u_\delta$ to converge to $M'_n(u)\partial_r u$ weakly in $L^1(0,T;L^1_{\text{rad}}(B))$, but $M'_n(u)$ is discontinuous at $|u|=1$. Thus, we first focus on

$$\begin{aligned}\int_{B_T} |M'_\delta(u_\delta)\partial_r u_\delta - M'_n(u)\partial_r u|^2 \; r dr dt = &\int_{B_T\cap\{|u|<1\}} |M'_\delta(u_\delta)\partial_r u_\delta - M'_n(u)\partial_r u|^2 \; r dr dt \\ &+ \int_{B_T\cap\{|u|=1\}} |M'_\delta(u_\delta)\partial_r u_\delta - M'_n(u)\partial_r u|^2 \; r dr dt,\end{aligned}$$

where we used the previously defined notation of $B_T = (0,1)\times(0,T)$.

Noticing that $\partial_r u = 0$ on $\{|u|=1\}$ we obtain

$$\begin{aligned}\int_{B_T\cap\{|u|=1\}} |M'_\delta(u_\delta)\partial_r u_\delta - M'_n(u)\partial_r u|^2 \; r dr dt = &\int_{B_T\cap\{|u|=1\}} |M'_\delta(u_\delta)\partial_r u_\delta|^2 \; r dr dt \\ \leq &C \int_{B_T\cap\{|u|=1\}} |\partial_r u_\delta|^2 \; r dr dt \\ \to &C \int_{B_T\cap\{|u|=1\}} |\partial_r u|^2 \; r dr dt = 0,\end{aligned}$$

as $\delta \to 0$, and where $C$ is a constant.

On the other hand, we have that $M'_\delta(u_\delta) \to M'_n(u)$ a.e. in $\{B_T \cap \{|u|<1\}\}$. The a.e. convergence of $\partial_r u_\delta$ from (6.59) gives us that $M'_\delta(u_\delta)\partial_r u_\delta \to M'_n(u)\partial_r u$ a.e. in $B_T$. Using that $M'_\delta(u_\delta)$ is bounded on the set $\{B_T\cap\{|u|<1\}\}$, we can apply Lemma 6.8 to obtain that

$$\int_{B_T\cap\{|u|<1\}} |M'_\delta(u_\delta)\partial_r u_\delta - M'_n(u)\partial_r u|^2 \; r dr dt \to 0$$

as $\delta \to 0$. Hence, $M'_\delta(u_\delta)\partial_r u_\delta$ converges to $M'_n(u)\partial_r u$ weakly in $L^1(0,T;L^1_{\text{rad}}(B))$. Moreover, the convergence in (6.61) implies that the product $\frac{1}{r}\partial_r(r\partial_r u_\delta)M'_\delta(u_\delta)\partial_r u_\delta$

converges to $\frac{1}{r}\partial_r(r\partial_r u)M_n'(u)\partial_r u$ weakly in $L^1(0,T;L^1_{\mathrm{rad}}(B))$, i.e.

$$I_3 \to \varepsilon^2 \int_0^T \int_0^1 \frac{1}{r}\partial_r(r\partial_r u)M_n'(u)\partial_r u\psi \; r dr dt.$$

Now, to pass to the limit in $I_4$ we note that $f''(u) = 2 - 6u^2$ is continuous in $u$ so we can apply the argument from (6.40) again. Then, because of (6.62) we have that $M_\delta(u_\delta)\partial_r u_\delta \rightharpoonup M_\delta(u)\partial_r u$ weakly in $L^2(0,T;L^2_{\mathrm{rad}}(B))$ which implies

$$I_4 \to \int_0^T \int_0^1 f''(u)M_n(u)\partial_r u\psi \; r dr dt.$$

Finally, note that $u_\delta \in L^\infty(0,T;H^1_{\mathrm{rad}}(B))$ and $\partial_t u_\delta \in L^2(0,T;H^{-1}_{\mathrm{rad}}(B))$. Applying Lemma 6.6 with $X = H^1_{\mathrm{rad}}(B)$, $Y = L^p_{\mathrm{rad}}(B)$ with $p \in [1,\infty)$, and $Z = H^{-1}_{\mathrm{rad}}(B)$ we obtain that $u_\delta \to u$ strongly in $C([0,T];L^2_{\mathrm{rad}}(B))$. It follows that $u \in C([0,T],L^2_{\mathrm{rad}}(B))$ and $u(\cdot,0) = u_0(\cdot)$, concluding the proof.

□

# Chapter 7

# Conclusion

While the spontaneous appearance of touchdown, that is, the emergence of points $\{x \in \Omega : M(u) = 0\}$ for the degenerate Cahn-Hilliard equation is a well-known phenomenon in the development of numerical algorithms for these types of partial differential equations, so far, they have been addressed by ad-hoc measures such as adding a small positive constant to the mobility, see for example [68]. In this study, we systematically investigate how such points of vanishing mobility arise in the particular case of radially symmetric solutions in the 2-dimensional unitary ball, which yields the following system of equations

$$\partial_t u = \frac{1}{r}\partial_r \left(r M_n(u)\partial_r \mu\right), \text{ for } (r,t) \in (0,1)\times(0,\infty), \tag{7.1}$$

$$\mu = -\varepsilon^2 \frac{1}{r}\partial_r \left(r\partial_r u\right) + f'(u), \text{ for } (r,t) \in (0,1)\times(0,\infty), \tag{7.2}$$

where $M_n(u) = [(1-u^2)_+]^n$, $f(u) = \frac{(1-u^2)^2}{2}$, accompanied by the boundary conditions (2.8)-(2.11).

The first results of this work are twofold. In Chapter 2 we showed via an informal argument that small energy solutions (in the sense stated in (A.1)) to the degenerate Cahn-Hilliard problem (7.1)-(7.2) touch down, either in finite or infinite time. Moreover, for $n \geq 1$, we proved in Chapter 3 that if touchdown occurs in finite time, then

it leads to singularity formation (in the sense of Proposition 3.1).

The second set of results, from Chapters 4 and 5, focuses on $n > 1/2$ and tanh-like initial data, which are relevant for applications (as it was explained in Chapter 1). We showed, using numerical results and matched asymptotics, that numerical solutions to our degenerate Cahn-Hilliard equation converge as $t \to \infty$ to a profile that touches down in infinite time. This outcome persists under variations of the initial data and the $\varepsilon$ parameter, which suggests that for $n > 1/2$, finite time touchdown does not typically occur.

Our asymptotic analysis also revealed that $n = 2$ itself is an interesting case where a transition in the profile of the infinite time touchdown occurs and, thus, the values of $1/2 < n < 2$ and $2 < n$ require separate investigations. We have shown that asymptotic approximations for infinite time touchdown solutions can be found for both ranges, but they become increasingly fragile as $n$ approaches $1/2$.

To leading order, the asymptotic approximations are divided into three main regions: central, touchdown and annular. The first two have the following self-similar profiles

$$v_{central} \sim t^{\alpha}\psi_0(r), \quad v_{touchdown} \sim t^{\beta}\varphi_0(\eta), \quad \eta := \frac{r - r_*}{t^{\gamma}},$$

where $r_*$ denotes the radius at which infinite time touchdown is expected to occur, and

$$\alpha(n) = \begin{cases} -\frac{1}{n}, & 1/2 < n < 2, \\ -\frac{1}{n-1}, & n > 2, \end{cases} \qquad \beta(n) = \begin{cases} -\frac{2(n+1)}{n(2n-1)}, & 1/2 < n < 2, \\ -\frac{1}{2(n-1)}, & n > 2, \end{cases}$$

$$\gamma(n) = \begin{cases} -\frac{(n+1)}{n(2n-1)}, & 1/2 < n < 2, \\ -\frac{1}{(n-1)}, & n > 2. \end{cases}$$

The solution in the third region is almost stationary and coincides, to leading order,

with the stationary solution obtained in Lee et al. [49].

Based on our numerical results we believe that for $n = 2$, the solution has the same asymptotic behaviour as in the case $1/2 < n < 2$; but that the matching between the central and touchdown regions is linear in space, as in the case $n > 2$.

Inside a spherically symmetric phase domain during the late stages of phase separation, the degenerate Cahn-Hilliard equation with Neumann and no-flux boundary conditions is closely related to the thin film equation with pressure boundary conditions [13], and hence the points with vanishing mobility can be analysed in a similar way.

In [13], Bertozzi et al. studied the thin film problem introduced in (1.10)-(1.11) coupled with fixed pressure boundary conditions, i.e.

$$\begin{aligned} \partial_t h + \partial_x(h^n \partial_{xxx} h) =& 0, \quad \text{in } (-1,1) \times (0,\infty), \\ & h(x,\cdot) = 1, \quad \partial_{xx} h(x,\cdot) = p, \quad p \in \mathbb{R},\, x = -1, 1, \end{aligned}$$

where $n > 0$. The authors found that infinite time touchdown was possible for $n > 1/2$, where the structure of the leading order expansion (as $t \to \infty$) could be described in terms of three regions: central, pinch-off and outer. For $n > 2$, the matching between the expansions in the central and pinch-off regions was linear and the matching between the expansions in the pinch-off and outer regions was quadratic in terms of the inner variable $\eta := \frac{x - x_c(t)}{\xi(t)}$, where $\xi$ is a function of time and $x_c(t) = \lim_{t\to\infty} \operatorname{argmin}_{x\in[0,1]} h(x,t)$. For $1/2 < n < 2$, the matching between the expansion in the pinch-off and outer regions was also quadratic in terms of the same variable. While they eliminate the possibility of a linear matching between the solutions in the central and pinch-off regions, they do not proceed further to complete the matching.

Additionally, the solution in [13] could be approximated in the central and pinch-

off regions, respectively, by

$$h_0(x) = t^{p(n)}C(x), \quad h_{min}(x) = t^{q(n)}H(\eta),$$

where $C(x)$ is a polynomial, $H(\eta)$ is a solution to an ordinary differential equation, and the exponents $p(n)$ and $q(n)$ are given by

$$q(n) = \begin{cases} -\frac{1}{n}, & 1/2 < n < 2, \\ -\frac{1}{n-1}, & n > 2, \end{cases} \qquad p(n) = \begin{cases} -\frac{2(n+1)}{n(2n-1)}, & 1/2 < n < 2, \\ -\frac{1}{2(n-1)}, & n > 2. \end{cases}$$

In the formulation from [13], the physical assumptions that in our framework lead the solution to touch down, i.e. the use of $f(u) = \frac{(1-u^2)^2}{2}$ and $M(u) = [(1-u^2)_+]^n$, is replaced by an external pressure condition at the boundary. Nevertheless, the exponents of the self-similar leading order behaviour in the pinch-off and outer regions are the same as in our touchdown (i.e. $p = \beta$) and central (i.e. $q = \alpha$) regions, respectively. This is true for both ranges, $1/2 < n < 2$ and $n > 2$. However, our system of equations is in a radially symmetric setting which changes the behaviour in the central region drastically; this is compounded by the imposition of different boundary conditions.

Our third main result, presented in Chapter 6, establishes the existence of a radially symmetric weak solution to our degenerate Cahn-Hilliard problem. Specifically, for a final time $T > 0$, we proved that there exists a weak solution $u \in L^2([0,T]; H^2_{\text{rad}}(B)) \cap L^\infty(0,T; H^1_{\text{rad}}(B)) \cap C([0,T]; L^2_{\text{rad}}(B))$ with $u_t \in L^2(0,T; H^{-1}_{\text{rad}}(B))$ such that $|u| \leq 1$ a.e. in $B_T$. This result leads to the following question: If we strengthen our assumptions, could we ensure that the solution remains strictly bounded, i.e. $|u| < 1$ for all time? We believe that we can apply a similar approach as for results about the positivity of thin-film solutions by Bertozzi et. al. [13] and Dal Passo et. al. [29], which involve entropy methods. In particular, if Bertozzi et.

al.'s proof [13] for positivity can be adapted to our case, it would imply that a smooth solution cannot become singular in finite time. In combination with Proposition 3.1, this implies that smooth solutions must touch down in infinite time, giving us a better understanding of how the type of degenerate mobilities studied here determine touchdown formation in Cahn-Hilliard equations in the 2-dimensional radially symmetric case.

As the connection to [13] illustrates, our work is closely related to results in the thin film literature. For example, the argument that a touchdown has to occur, either in finite or infinite time, was introduced in [22] for a Hele-Shaw cell, then generalised to thin film type equations for higher orders of degeneracy in [13] and rigorously proved in [23]. Moreover, for $n < 1/2$, Beretta et al. [6] proved that the solution to the thin film equation with pressure boundary conditions always vanishes in finite time. In contrast, for $n \geq 4$ Bertozzi et al. [13] showed that finite time touchdown cannot occur for the thin film equation with pressure boundary conditions and smooth positive initial data, based on an argument used by Bernis and Friedman [9] for the thin film equation with Neumann boundary conditions.

Furthermore, the rigorous existence result by Bernis and Friedman [9] has been repeatedly used to understand Cahn-Hilliard equations, but, as we have illustrated here, there is a whole range of formal and rigorous results from the thin film literature that have not been applied to Cahn-Hilliard models. One of the main achievements of this thesis has been to use the insight gained from thin film and lubrication theory to tackle the degeneracy in Cahn-Hilliard equations directly, rather than circumvent it.

Future work could study the $n = 2$ case and the strict boundedness of solutions $|u| < 1$. Going further, we could investigate fully 2-dimensional situations and non-convex interfaces between the phases, and the impact of touchdown regions on the sharp interface evolution. For finite time touchdown, once the solution has reached

$|u| = 1$, further questions arise about how to continue the solution, noting that already more than one weak solution concept has been considered in the literature, see [32, 28]. Also, thin film theory could provide insight into how to construct numerical schemes that maintain $|u| < 1$, e.g. [72, 36]. Moreover, one could explore the occurrence of finite time touchdown in numerical solutions for degrees of degeneracy $0 < n < 1/2$, which were not studied in the present work. Another avenue of research could be to introduce another parameter by taking $f(u) = (1 - u^2)^{2m}$ with $m \in \mathbb{N}$, and explore singularity formation depending on both the degeneracy degree $n$ and the free energy power $m$, which could lead to a parameter plane for $(m, n)$ with an additional interesting structure. Similar studies have been done for solutions of thin film equations [15, 34, 41]. Also left to be explored are the transitional regimes in time seen in Figure 4.5, where one could study how the ratio $\varepsilon/\delta$ affects the evolution of the solution.

In particular, the combination of different methods used in this work has allowed us to gain insight into touchdown formation that we could not have achieved by using each method separately. Summarising, we started our analysis by giving a heuristic argument that a touchdown must occur and proving that finite time touchdown leads to singularity formation for $n \geq 1$. Then, we showed numerical evidence that for certain initial conditions and $n$'s infinite time touchdown occurs. In practice, the numerical solution always runs into a finite time touchdown. We countered this observation by refining the spatial grid and showing that the time of touchdown increases as the grid is refined and, moreover, the numerical results become more accurate. Still, we needed further evidence of infinite time touchdown, which is why we analysed the solution, identified its asymptotic structure and constructed an approximate solution as $t \to \infty$ using matched asymptotics. This approximation touches down in infinite time and is very close to the numerical solution of the partial differential equation at long times. This makes for a stronger argument of infinite time touch-

down than anything we could have achieved using only the numerical solution of the partial differential equation, which can only rule out finite time touchdown without necessarily confirming infinite time touchdown. It could still be the case that the solution to the partial differential equation is unstable and further evidence could be found via a stability analysis. In addition, we complemented our analysis with a rigorous argument on the existence and regularity of weak radially symmetric solutions. This result, if used to prove the strict boundedness of weak solutions, could lead to a stronger argument for the infinite time touchdown results obtained with the previous methods.

More generally, our study underscores the close connection between degenerate Cahn-Hilliard equations and thin film models, and the still untapped potential for using not only the rigorous proofs, but also the asymptotic results from thin film theory to understand singularity formation in degenerate Cahn-Hilliard models. This opens up a rich source of analytical tools, both asymptotic and rigorous, that we can apply to degenerate Cahn-Hilliard problems in the future [22, 23, 6, 12].

# Appendix A

# Stationary solutions

## A.1 Small energy problem

In [56], Niethammer studies radially symmetric minimizers of the functional

$$I_\varepsilon(U) := \int_\Omega f(U) + \frac{\varepsilon^2}{2}|\nabla U|^2,$$

subject to a mass constraint

$$\int_\Omega U = M^*|\Omega|,$$

for given $M^* \in (-1, 1)$, $\Omega \subset \mathbb{R}^N$. Here $U$ represents the density of a fluid contained in the domain $\Omega$, $f(U)$ is the same double-well homogeneous free energy from (1.8) and $\varepsilon$ is a small positive parameter. Niethammer considers only solutions with small energy, i.e.

$$\frac{1}{\varepsilon} I_\varepsilon(U) \leq C, \tag{A.1}$$

for some given constant $C > 0$. The Euler-Lagrange equations associated with $I_\varepsilon$ subject to the mass constraint, for $\Omega = B_1(0)$, are

$$\varepsilon^2 \left( U'' + \frac{N-1}{r} U' \right) = 2U(U^2 - 1) - \eta_\varepsilon \quad r \in (0, 1), \tag{A.2}$$

$$U'(0) = 0,\ U'(1) = 0, \tag{A.3}$$

$$N\int_0^1 U(r)r^{N-1}dr = M^*, \tag{A.4}$$

where $\eta_\varepsilon \in \mathbb{R}$ is an unknown integration constant.

Niethammer proves the existence of exactly two solutions, which are monotone in the radial direction and converge to two possible radially symmetric single interface minimizers of $I_0$ as $\varepsilon \to 0$. In what follows we state the original result from her paper [56].

**Theorem A.1.** *Given $M^* \in (-1, 1)$, there is an $\varepsilon_0(M^*) > 0$, such that for all $\varepsilon \in (0, \varepsilon_0(M^*)]$ there exists $\eta_\varepsilon \in \mathbb{R}$ and a strictly decreasing function $U(r)$ satisfying (A.2)-(A.4). As $\varepsilon \to 0$, $U$ converges in $L_1(0,1)$ to*

$$u^*(r) = \begin{cases} 1 & r \in (0, r_0^*), \\ -1 & r \in (r_0^*, 1), \end{cases}$$

*where $-1 + 2(r_0^*)^N = M^*$, i.e. $u^*$ satisfies the mass constraint. Furthermore,*

$$\sup_{t\in(0,1)} \left| U(r) + \tanh\left(\frac{r - r(\varepsilon, M^*)}{\varepsilon}\right)\right| \leq \varepsilon C,$$

*where $r(\varepsilon, M^*)$ is defined by $U(r(\varepsilon, M^*)) = 0$, and*

$$\left|\frac{\eta_\varepsilon}{\varepsilon} - \frac{2(N-1)}{3r(\varepsilon, M^*)}\right| \leq C\varepsilon^2.$$

Her proof uses the asymptotic approximation as an ansatz, which reduces the problem to one of finding a corrective remainder such that adding it to the approximation solves the original equation. Then, by means of a fixed point argument, one can prove that for a good enough approximation such a remainder exists. The method used by Niethammer is originally credited to Berger and Fraenkel [7].

## A.2 Free boundary problem

Now, we study the case in which we set $u = U_*(r)$ in (2.6)-(2.10). Thus, we take the time derivative in (2.6) to be zero, yielding

$$\begin{aligned} 0 &= \partial_r \left( r M_n(U_*) \partial_r \mu \right), \quad r \in (0,1), \\ \mu &= -\varepsilon^2 \frac{1}{r} \partial_r \left( r \partial_r U_* \right) + f'(U_*), \quad r \in (0,1), \end{aligned}$$

with boundary conditions

$$\begin{aligned} &\partial_r U_*(1) = 0, \quad M_n(U_*(1)) \partial_r \mu(1,t) = 0, \\ &\partial_r U_*(0) = 0, \quad \partial_r \mu(0) = 0. \end{aligned}$$

We can then integrate once in $r$ and, using the no-flux boundary condition at $r = 1$, get

$$0 = r M_n(U_*) \partial_r \mu, \quad r \in (0,1). \tag{A.5}$$

One can use this equation and boundary conditions to study the case when the mobility is allowed to degenerate in an interval $(0, r_*)$, i.e. $M_n(U_*)(r) \equiv 0$ for $r \in (0, r_*]$ and $M_n(U_*)(r) > 0$ for $r \in (r_*, 1)$, where $r_* = r_*(\varepsilon) > 0$ is such that $U_*(r_*) = 1$, thus defining a free boundary. Then we only need to solve the equation in $(r_*, 1)$. Since the solution does not degenerate for $r \in (r_*, 1)$, we can divide by the mobility in equation (A.5), integrate again and substitute the chemical potential $\mu$, obtaining

$$\frac{\varepsilon^2}{r} \partial_r \left( r \partial_r U_* \right) - 2U_*(U_*^2 - 1) + \sigma = 0, \quad r \in (r_*, 1), \tag{A.6}$$

$$U_*(r_*) = 1, \quad \partial_r U_*(r_*) = 0 \tag{A.7}$$

$$\partial_r U_*(1) = 0, \tag{A.8}$$

where $\sigma \in \mathbb{R}$ is an unknown integration constant.

This particular free boundary steady state problem was studied by Lee, Münch and Süli in [49], where they included the specification of the interface position at a radius $r_0 \in (r_*, 1)$ such that

$$U_*(r_0) = 0. \tag{A.9}$$

This condition can also be replaced by a mass constraint, which is what we do in Section 4.2.3 to solve numerically the leading order equation in the annular region. Their paper not only covers the axially symmetric case, but also the general one where they obtain important formal results on the sharp interface limit. However, in this sub-section we only focus on the radial problem (A.6)-(A.8) with condition (2.18). In [49] the authors obtain asymptotic approximations in three main regions, an annular outer region about $r = 1$, an interface region around $r_0$ and a free boundary region around $r = r_*$. In what follows we summarise their results as we use them throughout our analysis.

*Outer region.* The asymptotic expansion in the region near $r = 1$ is given by:

$$\hat{u} = \hat{u}_0 + \varepsilon\hat{u}_1 + \varepsilon^2\hat{u}_2 + O(\varepsilon^3), \tag{A.10}$$

where $\hat{u}_0$, $\hat{u}_1$ and $\hat{u}_2$ are constants determined by matching to the touchdown layer about the interface. Thus

$$\hat{u}_0 = -1, \quad \hat{u}_1 = \frac{1}{6r_0}, \quad \hat{u}_2 = \frac{7}{144r_0^2}.$$

One can also obtain an approximation to the integration constant, i.e.

$$\hat{\sigma} = \hat{\sigma}_0 + \varepsilon\hat{\sigma}_1 + \varepsilon^2\hat{\sigma}_2 + O(\varepsilon^3), \tag{A.11}$$

where $\hat{\sigma}_0$, $\hat{\sigma}_1$ and $\hat{\sigma}_2$ are constants set by the matching between the touchdown layers about the interface and the boundary, thus $\hat{\sigma}_0 = 0$, $\hat{\sigma}_1 = \frac{2}{3r_0}$ and $\hat{\sigma}_2 = \frac{1}{36r_0^2}$. Moreover,

in this region, one can approximate the chemical potential by

$$\hat{\mu} = \hat{\mu}_0 + \varepsilon\hat{\mu}_1 + O(\varepsilon^2), \tag{A.12}$$

where $\hat{\mu}_0 = 0$ and $\hat{\mu}_1 = \frac{2}{3r_0}$.

*Interface region.* In the layer near $r_0$ one obtains the following asymptotic expansion

$$\tilde{u}(\rho) = \tilde{u}_0(\rho) + \varepsilon\tilde{u}_1(\rho) + \varepsilon^2\tilde{u}_2(\rho) + O(\varepsilon^3), \tag{A.13}$$

where $\rho := \frac{r-r_0}{\varepsilon}$ is an touchdown variable centered around the interface and

$$\begin{aligned}
\tilde{u}_0(\rho) =& -\tanh(\rho)\\
\tilde{u}_1(\rho) =& -\frac{(\hat{\sigma}_1 r_0 + 2)}{16r_0}\mathrm{sech}(\rho)^2 + \frac{(3\hat{\sigma}_1 r_0 - 2)}{3r_0}\mathrm{sech}(\rho)^2\left(\frac{3\rho}{8} + \frac{1}{4}\sinh(2\rho) + \frac{1}{32}\sinh(4\rho)\right)\\
&+ \frac{(2-\hat{\sigma}_1 r_0)}{8r_0} + \frac{(2-3\hat{\sigma}_1 r_0)}{48r_0}(2\cosh(2\rho) - 5\mathrm{sech}(\rho)^2),\\
\tilde{u}_2(\rho) =& -\frac{\hat{\sigma}_2}{8} - \frac{\rho}{4r_0^2} - \left(\frac{\hat{\sigma}_2}{8} + \frac{\rho}{12r_0^2}\right)\cosh(\rho)^2 + \left(\frac{5\hat{\sigma}_2}{16} + \frac{23\rho}{96r_0^2} - \frac{2\rho^2}{16r_0^2}\right)\mathrm{sech}(\rho)^2\\
&+ \left(\frac{\rho^2}{4r_0^2} - \frac{\log(2)\rho}{4r_0^2}\right)\mathrm{sech}(\rho)^2 + \frac{1}{8r_0^2}\mathrm{sech}(\rho)^2\mathrm{Li}_2(-e^{2\rho})\\
&- \left(\frac{1}{288r_0^2} - \frac{\log(\cosh(\rho))}{12r_0^2}\right)\sinh(2\rho)\\
&- \left(\frac{1}{96r_0^2} - \frac{\log(\cosh(\rho))}{4r_0^2} - \frac{\mathrm{sech}(\rho)^2}{36r_0^2}\right)\tanh(\rho) + \frac{(\pi^2 - 6\hat{\sigma}_2 r_0^2)}{96r_0^2}\mathrm{sech}(\rho)^2\\
&+ \left(\frac{1 + 24\log(2) + \hat{\sigma}_2 36r_0^2}{1152r_0^2}\right)(12\rho + 8\sinh(2\rho) + \sinh(4\rho)).
\end{aligned}$$

Here $\mathrm{Li}_2$ is Spence's function, also known as dilogarithm.

*Free boundary region.* In the touchdown layer near $r$ one obtains the following asymptotic expansion

$$\check{u}(z) = \check{u}_0(z) + \varepsilon\check{u}_1(z) + \varepsilon^2\check{u}_2(z) + O(\varepsilon^3), \tag{A.14}$$

where $z := \frac{r-r_*}{\varepsilon}$ is an inner variable centered around the free boundary and

$$\begin{aligned}
\check{u}_0(z) =& 1, \\
\check{u}_1(z) =& \frac{\hat{\sigma}_1}{4}(1-\cosh(2z)), \\
\check{u}_2(z) =& \frac{1}{(12r_0)^2}\left(\cosh(4z) + 3e^{-2z}(1+4z) - 9\right) + \frac{1}{(12r_0)^2}e^{2z} \\
&+ \frac{1}{(6r_0)^2}e^{-2z} + \frac{\hat{\sigma}_2}{4}(1-\cosh(2z)).
\end{aligned}$$

Thus, up to leading order, we have

$$\check{u}(z) = 1 + \frac{\hat{\sigma}_1}{4}(1-\cosh(2z)) + O(\varepsilon^2).$$

It is important to note that this can be expanded for $r \sim r_*$, $r > r_*$, i.e. for $z \to 0$ as

$$\check{v}(z) := 1 - \check{u}(z) = \frac{\hat{\sigma}_1}{2}z^2 + O(\varepsilon^2) + O(z^4),$$

where we have used the Taylor expansion of $\cosh(\cdot)$ near $z = 0$. The expansion, in terms of $r$, is

$$\check{v}(r) = \frac{\hat{\sigma}_1}{2\varepsilon^2}(r-r_*)^2 + O(\varepsilon^2). \tag{A.15}$$

The takeaway from this is the fact that we have, from Lee et al. [49], explicit asymptotic approximations of second order accuracy in $\varepsilon$ for the stationary free boundary problem.

# Appendix B

# Numerical Method

In this section, we outline the numerical scheme used to solve the following problem

$$\partial_t u = \frac{1}{r}\partial_r \left( r M_n(u) \partial_r \mu \right), \text{ for } (r,t) \in (0,1) \times (0,T), \tag{B.1}$$

$$\mu = -\varepsilon^2 \frac{1}{r}\partial_r \left( r \partial_r u \right) + f'(u), \text{ for } (r,t) \in (0,1) \times (0,T), \tag{B.2}$$

where $M_n(u) = [(1-u^2)_+]^n$, $f(u) = \frac{(1-u^2)^2}{2}$, $T > 0$ is sufficiently large, namely $T = O(10^{15})$ and with the boundary conditions

$$\partial_r u(1,t) = 0, \quad t \in (0,T), \tag{B.3}$$

$$M_n(u(1,t))\partial_r \mu(u(1,t)) = 0, \quad t \in (0,T), \tag{B.4}$$

$$\partial_r u(0,t) = 0, \quad t \in (0,T), \tag{B.5}$$

$$\partial_r \mu(0,t) = 0, \quad t \in (0,T). \tag{B.6}$$

**Remark B.1.** *Observe that it is infeasible to impose the radial boundary condition at $r = 0$ numerically because of the $\frac{1}{r}$ term appearing in $\mu$. Thus we cut our domain at some $0 < \tilde{r} \ll 1$ where we can evaluate the condition.*

Let $i \in \{0, \dots, m\}$, $j \in \{0, \dots, s\}$ define a grid of points $(r_i, t_j)$ with spacing

$\Delta r = \frac{1}{m}$ and $\Delta t = \frac{1}{s}$, where $(r_0, t_0) = (\tilde{r}, 0)$ and $(r_m, t_s) = (1, t)$. Let $u_i^j = u(r_i, t_j)$, $\mu_i^j = \mu(r_i, t_j)$. Then we can discretise problem (B.1)-(B.6) as follows: We want to find $u_i^j$ and $\mu_i^j$ such that

$$F_1(u_i^j, \mu_i^j) = 0, \quad i = 1, \dots, m-1,\ j = 1, \dots, s, \tag{B.7}$$

$$F_2(u_i^j, \mu_i^j) = 0, \quad i = 1, \dots, m-1,\ j = 1, \dots, s, \tag{B.8}$$

where

$$\begin{aligned} F_1(u_i^j, \mu_i^j) :=& \frac{u_i^j - u_i^{j-1}}{\Delta t} - \frac{1}{r_i}\frac{1}{\Delta r}\left[\frac{r_{i+1} + r_i}{2} M_n\left(\frac{u_{i+1}^j + u_i^j}{2}\right)\frac{(\mu_{i+1}^j - \mu_i^j)}{\Delta r}\right. \\ & \left. - \frac{r_i + r_{i-1}}{2} M_n\left(\frac{u_i^j + u_{i-1}^j}{2}\right)\frac{(\mu_i^j - \mu_{i-1}^j)}{\Delta r}\right], \\ F_2(u_i^j, \mu_i^j) :=& \mu_i^j - \varepsilon^2\left(\frac{u_{i+1}^j - 2u_i^j + u_{i-1}^j}{(\Delta r)^2} + \frac{1}{r_i}\frac{u_{i+1}^j - u_{i-1}^j}{2\Delta r}\right) + f'(u_i^j), \end{aligned}$$

and boundary conditions

$$\begin{aligned} \frac{u_m^j - u_{m-1}^j}{\Delta r} =& 0, \\ M_n(u_m^j)\frac{\mu_m^j - \mu_{m-1}^j}{\Delta r} =& 0, \\ \frac{u_1^j - u_0^j}{\Delta r} =& 0, \\ \frac{\mu_1^j - \mu_0^j}{\Delta r} =& 0, \end{aligned}$$

for $j = 1, \dots, s$. Here we are applying a Backward Euler finite difference scheme of first order in time and second order in space. In particular, we are using a one-sided approximation for $\partial_t u$, a one-sided approximation at midpoints for $\partial_r(rM_n(u)\partial_r\mu)$ and centered approximations for $\partial_{rr}u$ and $\partial_r u$.

We do not solve problem (B.7)-(B.8) directly, instead we implement a Newton

scheme. The method is initialised with the solution at the previous time step

$$(\boldsymbol{u}_0^j, \boldsymbol{\mu}_0^j)^T = (\boldsymbol{u}^{j-1}, \boldsymbol{\mu}^{j-1})^T,$$

here $()^T$ is the transpose of a vector, and at the $k$-th iteration we solve

$$F(\boldsymbol{u}_k^j, \boldsymbol{\mu}_k^j) + \nabla F(\boldsymbol{u}_k^j, \boldsymbol{\mu}_k^j) \begin{pmatrix} \boldsymbol{u}_{k+1}^j - \boldsymbol{u}_k^j \\ \boldsymbol{\mu}_{k+1}^j - \boldsymbol{\mu}_k^j \end{pmatrix} = \begin{pmatrix} 0 \\ 0 \end{pmatrix}.$$

where $F = (F_1, F_2)^T$. We continue until certain tolerances $tol_1$ and $tol_2$ are reached, i.e.

$$\|(u^{j+1} - u^j, \mu^{j+1} - \mu^j)^T\| \leq tol_1, \text{ or } \|F(u^{j+1}, \mu^{j+1})\| \leq tol_2,$$

where $\|\cdot\|$ denotes the Euclidean norm and $tol_1$, $tol_2$ are chosen to be small. If the algorithm does not converge satisfactorily then it is stopped after a certain amount of iterations.

## B.1 Numerical scheme convergence

Let $u$ and $\mu$ be smooth solutions of the continuous problem $G(u, \mu) = 0$, where

$$G(u, \mu) := \begin{pmatrix} G_1(u, \mu) \\ G_2(u, \mu) \end{pmatrix} := \begin{pmatrix} \partial_t u - \frac{1}{r}\partial_r \left(r M_n(u) \partial_r \mu\right) \\ \mu - \varepsilon^2 \frac{1}{r}\left(r \partial_r \tilde{u}\right) + f'(u) \end{pmatrix}.$$

We will compute $G(u, \mu) - F(u, \mu)$ at $(r_i, t_j)$, i.e. the difference between the continuous and the discrete operators applied to the continuous solution. For this, we use the

following Taylor expansions

$$
\begin{aligned}
u_i^{j+1} &= u_i^j + \Delta t \partial_t u_i^j + O(\Delta t^2), \\
u_{i+1}^j &= u_i^j + \Delta r \partial_r u_i^j + \frac{\Delta r^2}{2} \partial_{rr} u_i^j + O(\Delta r^3), \\
u_{i-1}^j &= u_i^j - \Delta r \partial_r u_i^j + \frac{\Delta r^2}{2} \partial_{rr} u_i^j + O(\Delta r^3),
\end{aligned}
$$

thus

$$
\begin{aligned}
M_n\left(\frac{u_{i+1}^j + u_i^j}{2}\right) =& M_n\left(u_i^j + \frac{\Delta r}{2}\partial_r u_i^j + \frac{\Delta r^2}{4}\partial_{rr} u_i^j + O(\Delta r^3)\right), \\
=& M_n\left(u_i^j\right) + M_n'\left(u_i^j\right)\left(\frac{\Delta r}{2}\partial_r u_i^j + \frac{\Delta r^2}{4}\partial_{rr} u_i^j + O(\Delta r^3)\right) \\
&+ \frac{1}{2} M_n''(u_i^j)\left(\frac{\Delta r}{2}\partial_r u_i^j + \frac{\Delta r^2}{4}\partial_{rr} u_i^j + O(\Delta r^3)\right)^2 + O(\Delta r^3), \\
=& M_n\left(u_i^j\right) + \frac{\Delta r}{2} M_n'\left(u_i^j\right)\partial_r u_i^j + \frac{\Delta r^2}{4} M_n'\left(u_i^j\right)\partial_{rr} u_i^j \\
&+ \frac{\Delta r^2}{8} M_n''(u_i^j)\partial_r u^2(r_i, t_j) + O(\Delta r^3).
\end{aligned}
$$

**Remark B.2.** *We note that by using these Taylor's expansions we are assuming that $M_n$ is smooth, i.e. the method works as long as the solution does not touch down. Once it touches down, the numerical method is not reliable.*

There is an analogous expression for $M_n\left(\frac{u_i^j + u_{i-1}^j}{2}\right)$. We substitute both expressions into $F_1$ and obtain

$$
\begin{aligned}
F_1(u, \mu_i^j) =& u_t - \frac{1}{r}\frac{1}{\Delta r}\left[\left(r + \frac{\Delta r}{2}\right)\left(M_n(u) + \frac{\Delta r}{2} M_n'(u)\partial_r u\right.\right. \\
&\left. + \frac{\Delta r^2}{4} M_n'(u)\partial_{rr} u + \frac{\Delta r^2}{8} M_n''(u)\partial_r u^2\right)\left(\partial_r \mu + \frac{\Delta r}{2}\partial_{rr}\mu + \frac{\Delta r^3}{6}\partial_{rrr}\mu\right) \\
&- \left(r - \frac{\Delta r}{2}\right)\left(M_n(u) - \frac{\Delta r}{2} M_n'(u)\partial_r u + \frac{\Delta r^2}{4} M_n'(u)\partial_{rr} u\right. \\
&\left.\left. + \frac{\Delta r^2}{8} M_n''(u)\partial_r u^2\right)\left(\partial_r \mu - \frac{\Delta r}{2}\partial_{rr}\mu + \frac{\Delta r^3}{6}\partial_{rrr}\mu\right)\right] + O(\Delta t) + O(\Delta r^2).
\end{aligned}
$$

Note that since everything is evaluated at the same point $(r_i, t_j)$ we have dropped the indices. Then, expanding, most terms cancel out leaving only

$$\begin{aligned} F_1(u,\mu) =& u_t - \frac{1}{r}(\partial_r \mu r M_n'(u)\,\partial_r u + \partial_r \mu M_n(u) + \partial_{rr}\mu r M_n(u)) + O(\Delta t) + O(\Delta r^2), \\ =& G_1(u,\mu) + O(\Delta t) + O(\Delta r^2), \end{aligned}$$

and for $F_2$ we have

$$\begin{aligned} F_2(u,\mu) =& w - \varepsilon^2\left(\frac{2u + \Delta r^2 \partial_{rr}u + O(\Delta r^4) - 2u}{\Delta r^2} + \frac{2\Delta r \partial_r u + O(\Delta r^3)}{2r\Delta r}\right) + f'(u), \\ =& \mu - \varepsilon^2\left(\partial_{rr}u + \frac{1}{r}\partial_r u\right) + f'(u) + O(\Delta r^2), \\ =& G_2(u,\mu) + O(\Delta r^2). \end{aligned}$$

So we conclude that the scheme has order of convergence $O(\Delta t) + O(\Delta r^2)$.

## B.2 Initial condition change

Because we want to study the late stages of the phase separation process we would like the initial condition to be close to the profile of a stationary solution but far enough away so that we can see the dynamics evolve over a long time interval. A sensible choice is

$$u_{init}(r) = u_{tanh}(r) := -0.95 \tanh\left(\frac{r - 0.5}{\varepsilon}\right),$$

where we have chosen the value 0.95 so that the initial condition satisfies $|u_{init}(r)| < 1$ for all $r \in (0,1)$ but still remains close to $u = \pm 1$.

We note that initial conditions based on a hyperbolic tangent have been used for Cahn-Hilliard and thin film equations regularly in, for example, rigorous results (see

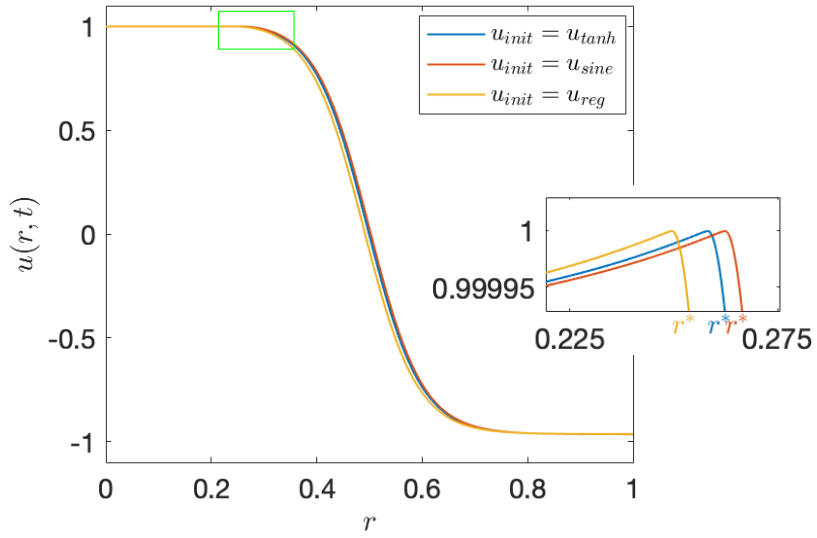



Figure B.1: $u(r,t)$ versus $r$ for $t = 10^{15}$, $n = 4$, $\varepsilon = 0.1$ for three different initial conditions. Inset is a zoom of the region enclosed by the green rectangle.

[2]), computational studies (see [27, 38]) and material science (see [68, 67]). Different initial conditions will affect the outcome of the system, but profiles such as $u_{tanh}$ are the most relevant if we only wish to study the very late stages of a binary phase field under the assumptions of the homogeneous free energy $f$.

We tested the algorithm with three different initial conditions: $u_{tanh}$,

$$u_{sine} = \begin{cases} 0.95 & \text{if } r < \frac{1}{4} \\ 0.95\sin(-\pi(2r-1)) & \text{if } \frac{1}{4} \leq r \leq \frac{3}{4} \\ -0.95 & \text{if } r > \frac{3}{4} \end{cases}$$

and

$$u_{reg} = \chi * u_{tanh}(r),$$

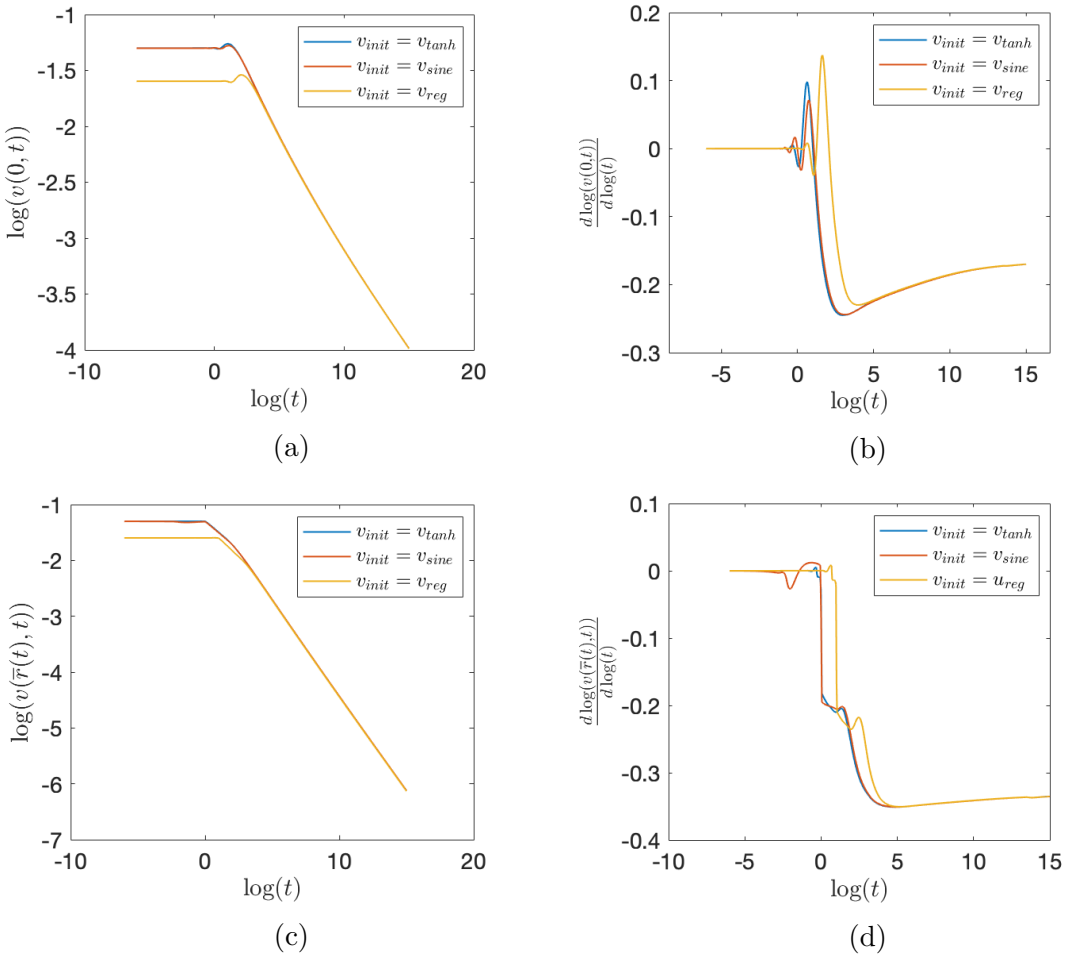



Figure B.2: (a) Log-log plot of $v(0,t)$. (b) Slope of (a). (c) Log-log plot of $v(\bar{r},t)$. Recall $\bar{r}$ =(d) Slope of (c). For $n = 4$, final time $10^{15}$, $\varepsilon = 0.1$ and the different initial conditions.

where $\chi$ is the following mollifier

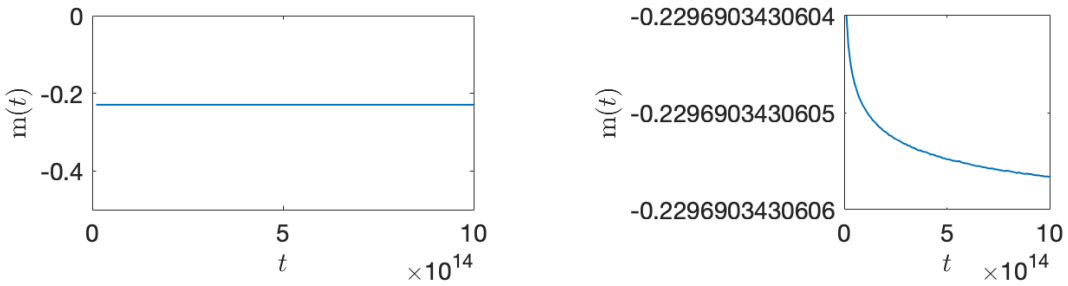
$$\chi(r) := \frac{c}{\lambda} e^{\frac{-1}{1-\left(\frac{r}{\lambda}\right)^2}},$$

$c = 3.08$ is a normalising constant and $\lambda \ll 1$ is a regularising parameter, chosen here as $\lambda = 0.01$. Note that the initial condition $u_{tanh}$ is smooth but does not satisfy the boundary conditions exactly.

We set $v_{tanh} := 1 - u_{tanh}$, $v_{sine} := 1 - u_{sine}$ and $v_{reg} := 1 - u_{reg}$ and plot the figures for the self-similar coefficients as done in section 4.1. From Figure B.1 we can see that the value of $r_*$ varies with the initial conditions. Additionally, from Figure B.2 we can observe that at an early stage the value of $v$ at $r_*$ and 0 is different for each initial condition and the transition region is also quite different with regard to the time it starts and the value of the self-similar exponent. However, the eventual long time regime is the same for all. Thus, all three initial conditions produce the same final profile with the same overall touchdown shape and a slight translation of $r_*$. Moreover, looking at the value at which the curves in Figure B.2(c) converge as time grows we can infer that in all three cases we obtain the same approximation to the long time similarity coefficients. This allows us to infer that small deviations in the initial condition do not change the long time self-similar profile of the numerical solution.

## B.3 Conservation of mass

We check that the algorithm satisfies the mass conservation of the analytical equation by computing the integral $\int_0^1 u(r,t) r dr$ numerically using the trapezoid rule. Note that in Figure B.3 $\mathrm{m}(t)$ is constant up to an error of $O(10^{-13})$, which is very small in comparison with $\Delta r = 10^{-6}$.




(a) (b)

Figure B.3: (a) Mass over a long time interval. (b) Zoom of (a). For $n = 4$, $\Delta r = 10^{-6}$, $T = 10^{15}$ and $\varepsilon = 0.1$.

## B.4 Epsilon

An important issue in our analysis is how $\varepsilon$ affects the similarity exponents. In Figure B.4 we have plotted the numerical solution to the partial differential equation for $\varepsilon = 0.025, 0.05, 0.075, 0.1$. We can see in Figure B.4 that at very long times, i.e. $\log(t) \sim 15$, varying $\varepsilon$ does not change the value at which $\frac{d\log(v(\bar{r},t))}{d\log(t)}$ and $\frac{\log(v(0,t))}{d\log(t)}$ converge to as $t \to 10^{15}$. This implies that the numerical approximations to the similarity coefficients $\alpha$ and $\beta$ do not change. Thus we can study the long time behaviour using any $\varepsilon$ of these four values. On the other hand, the transitional regime, where $\frac{d\log(v(\bar{r},t))}{d\log(t)}$ and $\frac{\log(v(0,t))}{d\log(t)}$ dip to a transitional value, seems to depend strongly on $\varepsilon$. The relation between the time when the transition starts and $\varepsilon$ should be studied in the future. This type of transitional behaviour can also be seen in other fourth order degenerate parabolic equations, for example when studying the saturation function (ratio between the measure of the set of points that achieve touchdown and the measure of the whole domain) for solutions of the deep quench obstacle free boundary problem, see Banas et. al. [3].

We note that in Figure B.4 the numerical solution for $\varepsilon = 0.025$ exists only until $\log(t) \sim 13$, due to the mobility crossing 0 because the grid size is too large to capture changes in the mobility. Since our computers cannot run with grid sizes less than $10^{-6}$ in a reasonable amount of time, we cannot obtain solutions at longer times for $\varepsilon$ less

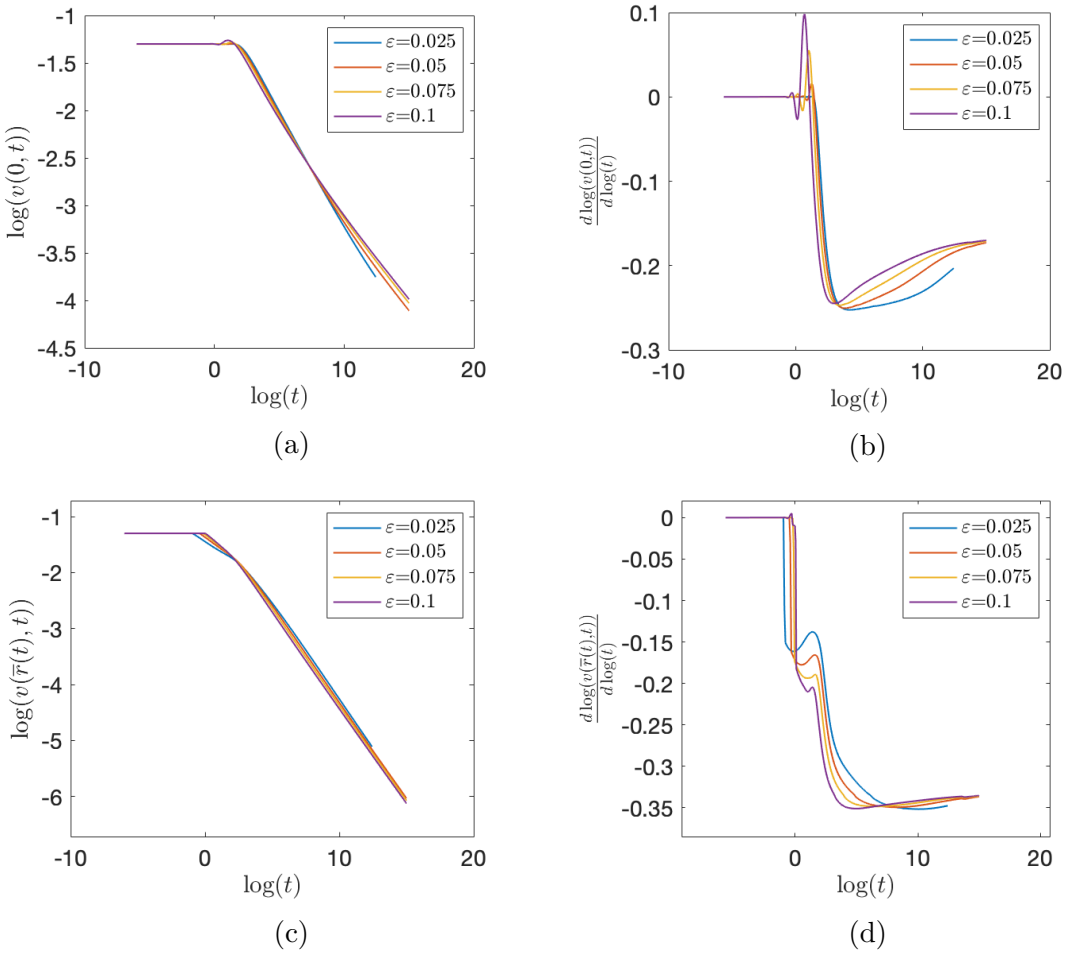



Figure B.4: (a) Log-log plot of $v(0,t)$. (b) Slope of (a). (c) Log-log plot of $v(\bar{r},t)$. Recall $\bar{r} = \bar{r}(t)$ is where $v$ achieves its minimum at time $t$. (d) Slope of (c). For $n = 4$, final time $10^{15}$ and four different values of $\varepsilon$.

than 0.05. This issue is also remarked upon in Section 4.1.

## B.5 Grid spacing convergence study

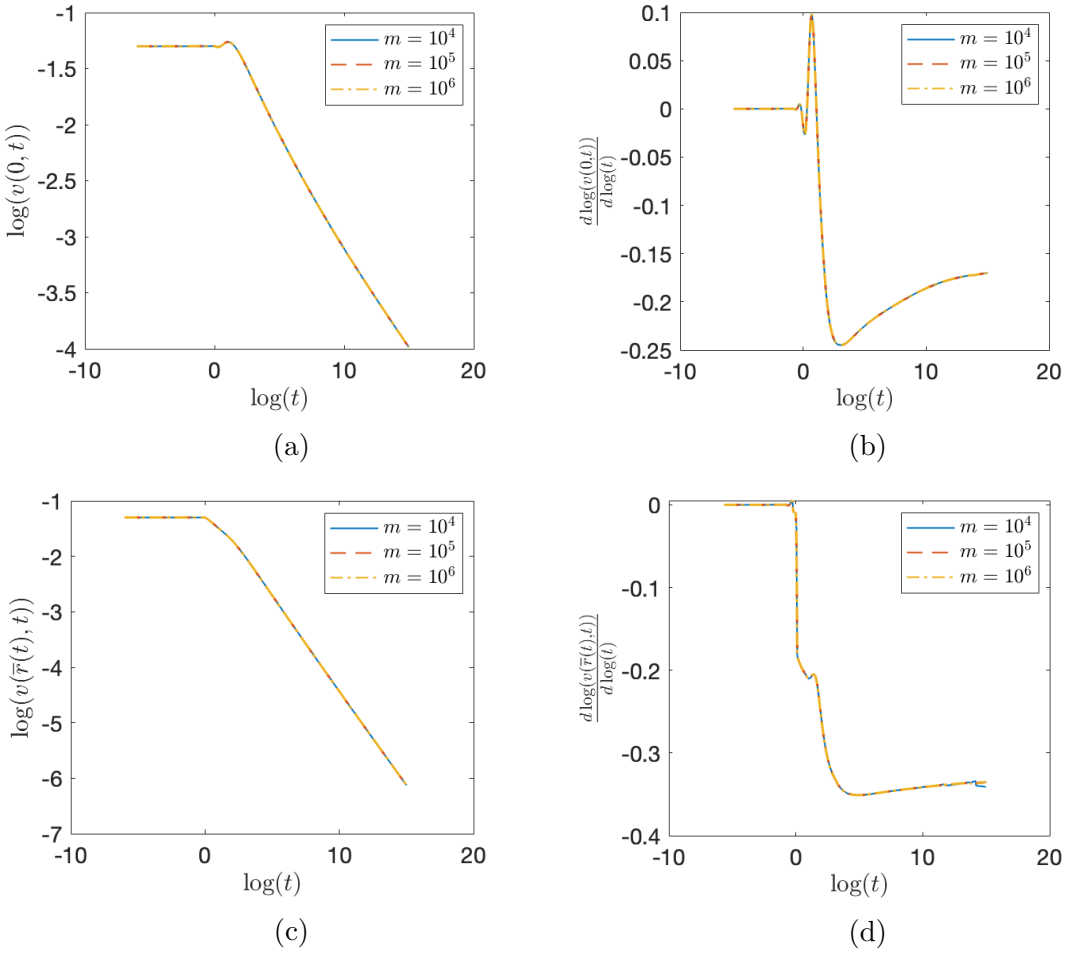
To check the robustness of the algorithm we increased the number of grid points, $m$, and compared $\frac{d\log(v(\bar{r},t))}{d\log(t)}$ and $\frac{\log(v(0,t))}{d\log(t)}$, which approximate the similarity exponents $\alpha$ and $\beta$ numerically. We can see in Figure B.5 that increasing $m$ does not change the profile of $\frac{d\log(v(\bar{r},t))}{d\log(t)}$ and $\frac{\log(v(0,t))}{d\log(t)}$, although it can diminish the oscillations in long time, which are due to the solution approaching touchdown with bad spatial resolution, as seen in Figure B.5(d) for the end of the curve $\frac{d\log(v(r_*,t))}{d\log(t)}$.

## B.6 Time tolerance

One can also check how the time tolerance, i.e. the bound on the maximum error possible of the solution at each time step, affects the outcome. The default time tolerance that we used is $tol = 0.01$. Here, we vary it between $tol = 0.01, 0.005, 0.0025$. In Figure B.6 we can see that the tolerance does not affect the similarity coefficients visibly.

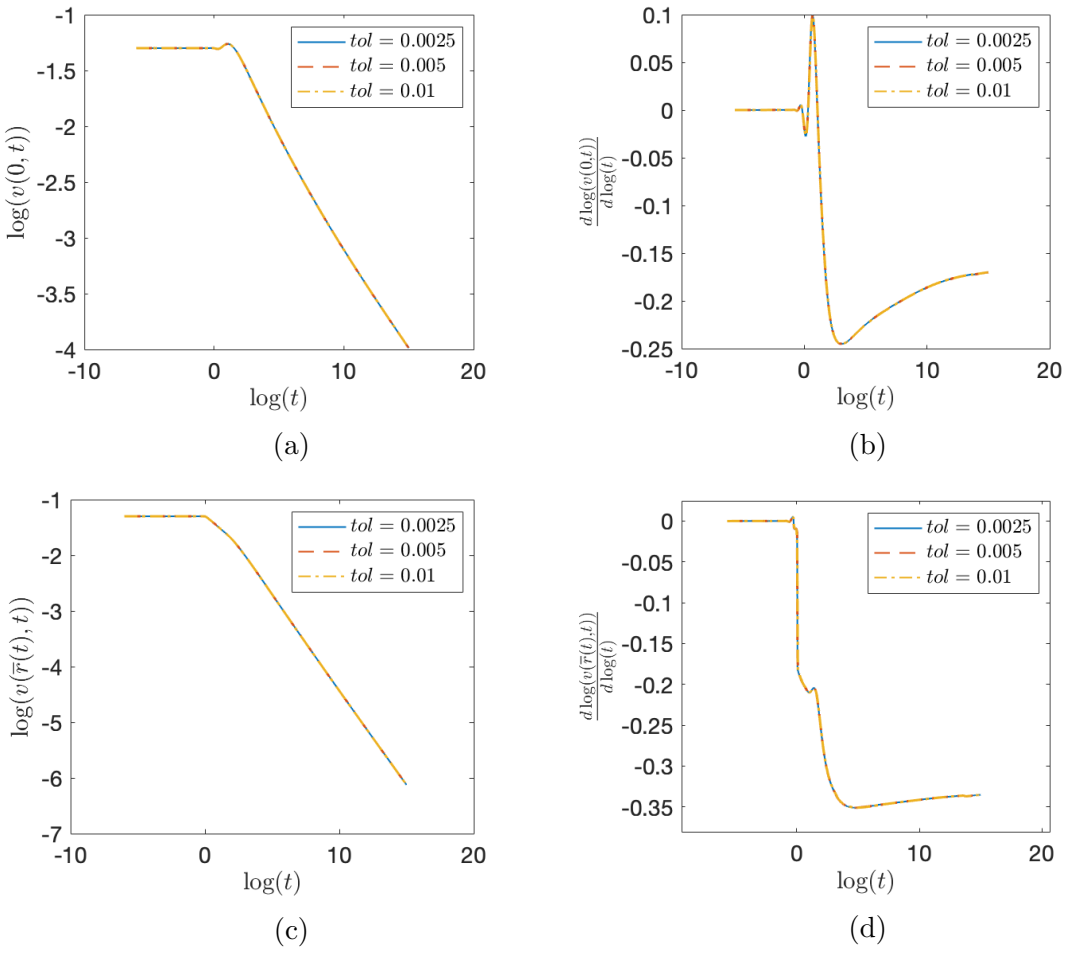
## B.7 Comparison with free boundary expansion

In Lee et al. [49] the authors obtain an approximation to problem (A.6)-(A.9), which is described in detail in section A.2 of the Appendix. Here we compare it to the numerical solution of the partial differential equation (B.1)-(B.6), which we denote by $u$. Note that since this is a stationary solution it is independent of the degeneracy degree of the mobility, as long as it remains strictly bounded between $\pm 1$ in the interior of the domain. In Figure B.7 (a) we can see that the difference between the expansions $\hat{u}$ (A.10), $\tilde{u}$ (A.13), $\check{u}$ (A.14) and the numerical solution of the partial



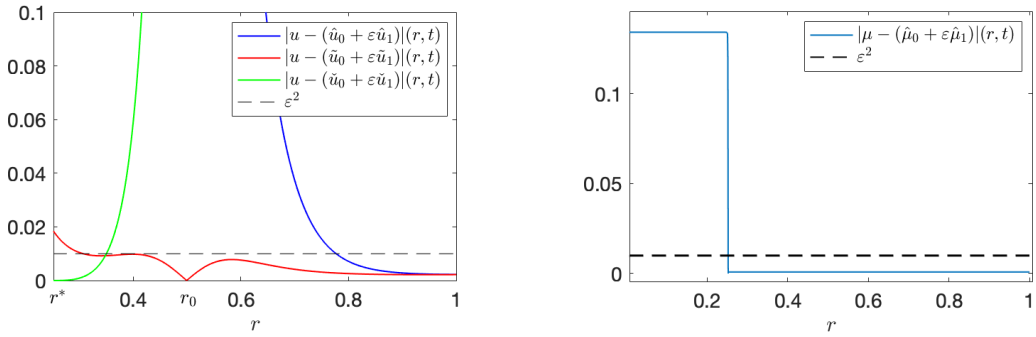

(a) (b) (c) (d)

Figure B.5: (a) Log-log plot of $v(0,t)$. (b) Slope of (a). (c) Log-log plot of $v(\bar{r},t)$. (d) Slope of (c). For $n = 4$, final time $10^{15}$ and different amount of grid points.




(a) (b) (c) (d)

Figure B.6: (a) Log-log plot of $v(0,t)$. (b) Slope of (a). (c) Log-log plot of $v(\bar{r},t)$. (d) Slope of (c). For $n = 4$, final time $10^{15}$ and different time tolerances.




(a) (b)

Figure B.7: (a) Error between numerical partial differential equation solution $u$ and Lee et. al. approximations. (b) Error between numerical chemical potential $\mu$ and Lee et al. annular approximation. For $n = 4$, $m = 10^6$, $t = 10^{15}$, $\varepsilon = 0.1$.

differential equation for $n = 4$, $u$, is $O(\varepsilon^2)$ in the outer, interface and free boundary layers, respectively. Analogously, from Lee et al. [49], we have that the chemical potential can be approximated in the annular region by $\hat{\mu}$ given by (A.12). We confirm in Figure B.7 (b) that this approximation is very good in the outer region near $r = 1$.

# Appendix C

# Frobenius method for fourth order ODEs

In several parts of our asymptotic analysis of the case $n < 2$ we use the Frobenius method, which is usually discussed for second order linear ordinary differential equations in the literature, see for example these course notes for Differential Equations II [46]. Here we describe the method for a specific type of fourth order equation which is useful in Chapter 5.

Suppose we are trying to find $y = y(x)$ as $x \to x_0$, where $x_0$ is a regular singular point of the equation, such that

$$\mathcal{L}(y) := y'''' + \frac{p(x)}{(x-x_0)}y''' + \frac{q(x)}{(x-x_0)^2}y'' + \frac{l(x)}{(x-x_0)^3}y' + \frac{m(x)}{(x-x_0)^4}y = 0, \qquad \text{(C.1)}$$

where $p$, $q$, $l$ and $m$ are analytic functions which can be expressed as

$$p(x) = \sum_{k=0}^{\infty} p_k (x-x_0)^k, \qquad q(x) = \sum_{k=0}^{\infty} q_k (x-x_0)^k,$$
$$l(x) = \sum_{k=0}^{\infty} l_k (x-x_0)^k, \qquad m(x) = \sum_{k=0}^{\infty} m_k (x-x_0)^k,$$

where $p_k, q_k, l_k, m_k \in \mathbb{R}$. The idea is to seek a solution in the form of a Frobenius series

$$y(x) = y(x;\lambda) := \sum_{k=0}^{\infty} a_k (x - x_0)^{\lambda+k},$$

for some $\lambda \in \mathbb{R}$.

Plugging all the expansions into equation (C.1), we obtain

$$\begin{aligned}
0 = &\sum_{k=0}^{\infty} (\lambda+k)(\lambda+k-1)(\lambda+k-2)(\lambda+k-3) a_k (x-x_0)^{\lambda+k-4} \\
&+ \sum_{k=0}^{\infty}\sum_{j=0}^{\infty} (\lambda+k)(\lambda+k-1)(\lambda+k-2) a_k p_j (x-x_0)^{\lambda+k+j-4} \\
&+ \sum_{k=0}^{\infty}\sum_{j=0}^{\infty} (\lambda+k)(\lambda+k-1) a_k q_j (x-x_0)^{\lambda+k+j-4} \\
&+ \sum_{k=0}^{\infty}\sum_{j=0}^{\infty} (\lambda+k) a_k l_j (x-x_0)^{\lambda+k+j-4} \\
&+ \sum_{k=0}^{\infty}\sum_{j=0}^{\infty} a_k m_j (x-x_0)^{\lambda+k+j-4}.
\end{aligned}$$

At the lowest order, i.e. $(x - x_0)^{\lambda-4}$, we have

$$\left[\lambda(\lambda-1)(\lambda-2)(\lambda-3) + \lambda(\lambda-1)(\lambda-2)p_0 + \lambda(\lambda-1)q_0 + \lambda l_0 + m_0\right] a_0 = 0$$

which we call the indicial equation as it will determine us the index $\lambda$. Let

$$F(\lambda) := \lambda(\lambda-1)(\lambda-2)(\lambda-3) + \lambda(\lambda-1)(\lambda-2)p_0 + \lambda(\lambda-1)q_0 + \lambda l_0 + m_0.$$

Let $\lambda_1$, $\lambda_2$, $\lambda_3$, $\lambda_4$ be the solutions to $F(\lambda) = 0$ which have been ordered as follows $\mathrm{Re}(\lambda_1) \geq \mathrm{Re}(\lambda_2) \geq \mathrm{Re}(\lambda_3) \geq \mathrm{Re}(\lambda_4)$. To equate powers of $(x - x_0)$ we need to rewrite all the double sums. First we change $j \to j - k$, which yields

$$0 = \sum_{k=0}^{\infty} (\lambda+k)(\lambda+k-1)(\lambda+k-2)(\lambda+k-3) a_k (x-x_0)^{\lambda+k-4}$$

$$
\begin{aligned}
&+\sum_{k=0}^{\infty}\sum_{j=k}^{\infty}(\lambda+k)(\lambda+k-1)(\lambda+k-2)a_k p_{j-k}(x-x_0)^{\lambda+j-4}\\
&+\sum_{k=0}^{\infty}\sum_{j=k}^{\infty}(\lambda+k)(\lambda+k-1)a_k q_{j-k}(x-x_0)^{\lambda+j-4}\\
&+\sum_{k=0}^{\infty}\sum_{j=k}^{\infty}(\lambda+k)a_k l_{j-k}(x-x_0)^{\lambda+j-4}\\
&+\sum_{k=0}^{\infty}\sum_{j=k}^{\infty}a_k m_{j-k}(x-x_0)^{\lambda+j-4}.
\end{aligned}
$$

Then, we interchange the roles of $k$ and $j$ and note that $\sum_{j=0}^{\infty}\sum_{k=j}^{\infty}=\sum_{k=0}^{\infty}\sum_{j=0}^{k}$,

$$
\begin{aligned}
0=&\sum_{k=0}^{\infty}(\lambda+k)(\lambda+k-1)(\lambda+k-2)(\lambda+k-3)a_k(x-x_0)^{\lambda+k-4}\\
&+\sum_{k=0}^{\infty}\sum_{j=0}^{k}(\lambda+j)(\lambda+j-1)(\lambda+j-2)a_j p_{k-j}(x-x_0)^{\lambda+k-4}\\
&+\sum_{k=0}^{\infty}\sum_{j=0}^{k}(\lambda+j)(\lambda+j-1)a_j q_{k-j}(x-x_0)^{\lambda+k-4}\\
&+\sum_{k=0}^{\infty}\sum_{j=0}^{k}(\lambda+j)a_j l_{k-j}(x-x_0)^{\lambda+k-4}\\
&+\sum_{k=0}^{\infty}\sum_{j=0}^{k}a_j m_{k-j}(x-x_0)^{\lambda+k-4},\\
=&\sum_{k=0}^{\infty}\Bigg[F(\alpha+k)a_k+\sum_{j=0}^{k-1}\left((\lambda+j)(\lambda+j-1)(\lambda+j-2)p_{k-j}\right.\\
&\left.+(\lambda+j)(\lambda+j-1)q_{k-j}+(\lambda+j)l_{k-j}+m_{k-j}\right)a_j\Bigg](x-x_0)^{\lambda+k-4}.
\end{aligned}
$$

Hence for all $k\in\mathbb{N}_0$

$$
\begin{aligned}
F(\lambda+k)a_k=&-\sum_{j=0}^{k-1}\left((\lambda+j)(\lambda+j-1)(\lambda+j-2)p_{k-j}\right.\\
&\left.+(\lambda+j)(\lambda+j-1)q_{k-j}+(\lambda+j)l_{k-j}+m_{k-j}\right)a_j.
\end{aligned}
$$

Since $\lambda_1$ is the largest root, then $F(\lambda_1 + k) \neq 0$ for all $k > 1$; thus we can obtain an expression for $a_k$ given by

$$\begin{aligned} a_k = &- \frac{1}{F(\lambda + k)} \sum_{j=0}^{k-1} ((\lambda + j)(\lambda + j - 1)(\lambda + j - 2)p_{k-j} \\ &+ (\lambda + j)(\lambda + j - 1)q_{k-j} + (\lambda + j)l_{k-j} + m_{k-j})\, a_j, \quad \forall k \in \mathbb{N}, \end{aligned}$$

and $a_0 \in \mathbb{R}$ is left free.

By denoting

$$\begin{aligned} Q(\lambda, j) :=&(\lambda + j)(\lambda + j - 1)(\lambda + j - 2)p_{k-j} \\ &+ (\lambda + j)(\lambda + j - 1)q_{k-j} + (\lambda + j)l_{k-j} + m_{k-j}. \end{aligned}$$

We obtain a first solution

$$y_1(x) = \sum_{k=0}^{\infty} a_k (x - x_0)^{\lambda_1 + k},$$

where

$$a_k = - \frac{1}{F(\lambda_1 + k)} \sum_{j=0}^{k-1} Q(\lambda_1, j) a_j \tag{C.2}$$

for $k \geq 1$ and $a_0 \in \mathbb{R}$ is a free constant.

We can now obtain second, third and fourth solutions, whose form depends on the relationship between the roots of the indicial equation. We will focus on specific cases, as they pertain to our asymptotic analysis of the Cahn-Hilliard equation.

**Case $\boldsymbol{\lambda_i - \lambda_j \notin \mathbb{Z}, i, j = 1, 2, 3, 4, i \neq j}$:** In this case $F(\lambda_2 + k), F(\lambda_3 +$

$k), F(\lambda_4 + k) \neq 0$ for all $k \geq 1$ and we obtain three linearly independent solutions

$$\begin{aligned} y_2(x) &= \sum_{k=0}^{\infty} b_k (x - x_0)^{\lambda_2 + k}, \\ y_3(x) &= \sum_{k=0}^{\infty} c_k (x - x_0)^{\lambda_3 + k}, \\ y_4(x) &= \sum_{k=0}^{\infty} d_k (x - x_0)^{\lambda_4 + k}, \end{aligned}$$

whose coefficients are given by

$$b_k = -\frac{1}{F(\lambda_2 + k)} \sum_{j=0}^{k-1} Q(\lambda_2, j) b_j, \quad k \in \mathbb{N}, \tag{C.3}$$

$$c_k = -\frac{1}{F(\lambda_3 + k)} \sum_{j=0}^{k-1} Q(\lambda_3, j) c_j, \quad k \in \mathbb{N}, \tag{C.4}$$

$$d_k = -\frac{1}{F(\lambda_4 + k)} \sum_{j=0}^{k-1} Q(\lambda_4, j) d_j, \quad k \in \mathbb{N}, \tag{C.5}$$

and $b_0, c_0, d_0 \in \mathbb{R}$ are free constants.

**Case $\boldsymbol{\lambda_1 = \lambda_2, \lambda_3 = \lambda_4, \lambda_1 - \lambda_3 \in \mathbb{Z}}$:** Suppose we solve (C.2) for arbitrary $\lambda$, i.e. such that $F(\lambda)$ is not necessarily zero. With this we can define a general function $y$ where each coefficient $a_k$ depends on $\lambda$, i.e.

$$y(x; \lambda) := \sum_{k=0}^{\infty} a_k(\lambda)(x - x_0)^{\lambda + k}.$$

We note that (C.2) ensures that

$$\mathcal{L}\left(y(x; \lambda)\right) = (x - x_0)^{\lambda - 4} F(\lambda),$$

thus $y_1(x) = y(x; \lambda_1)$ (since $F(\lambda_1) = 0$). We can now show that given $\lambda_1 = \lambda_2$, i.e. $\lambda_1$ is a double root of $F(\lambda) = 0$, we can find a second solution by differentiating the

first solution with respect to $\lambda$,

$$\begin{aligned}\mathcal{L}\left(\frac{d}{d\lambda}y(x;\lambda)\right) =& \frac{d}{d\lambda}\mathcal{L}\left(y(x;\lambda)\right)\\ =& \frac{d}{d\lambda}\left[(x-x_0)^{\lambda-4}F(\lambda)\right]\\ =& (x-x_0)^{\lambda-4}\left[\ln(x-x_0)F(\lambda)+F'(\lambda)\right]\end{aligned}$$

If $\lambda_1$ is a double root, then $F(\lambda_1) = F'(\lambda_1) = 0$, thus

$$\mathcal{L}\left(\frac{d}{d\lambda}y(x;\lambda)\bigg|_{\lambda=\lambda_1}\right) = 0.$$

This allows us to compute the form of this second solution as

$$\begin{aligned}y_2(x) = \frac{d}{d\lambda}y(x;\lambda)\bigg|_{\lambda=\lambda_1} =& \sum_{k=0}^{\infty}(a_k\ln(x-x_0)+b_k)(x-x_0)^{\lambda_1+k},\\ =& y_1(x)\ln(x-x_0)+\sum_{k=0}^{\infty}b_k(x-x_0)^{\lambda_1+k}\end{aligned} \tag{C.6}$$

where $a_k = a_k(\lambda_1)$ and the coefficients $b_k$ can be obtained by either differentiating the original coefficients with respect to $\lambda$, $b_k = a_k'(\lambda_1)$, or by substituting (C.6) into the original equation and equating coefficients. The former requires us to have a closed and explicit form for $a_k$ in terms of $\lambda$, and the latter requires a long computation, though we note that all terms which include the factor $\ln(x-x_0)$ drop because $y_1$ is a solution.

To obtain a third and fourth solution, we set $\lambda_3 = \lambda_1 + K$ where $K > 0$ is an integer. However a problem may arise with equation (C.2) for $k = K$, i.e. when

$$F(\lambda_1+K)a_K = -\sum_{j=0}^{K-1}Q(\lambda_1,j)a_j.$$

Because $\lambda_3$ is also a solution of $F(\lambda) = 0$ we have that

$$0 = -\sum_{j=0}^{K-1} Q(\lambda_1, j) a_j. \tag{C.7}$$

- If the right-hand side of (C.7) is not zero then we have a contradiction, but we can construct an additional solution like $y_2$, i.e.

$$y_3(x) = y_1(x)\ln(x - x_0) + \sum_{k=0}^{\infty} c_k (x - x_0)^{\lambda_3 + k},$$

  where the $c_k$'s are determined as before.

- If the right-hand side of (C.7) is zero, then we obtain the solution

$$y_3(x) = \sum_{k=0}^{\infty} c_k (x - x_0)^{\lambda_3 + k},$$

  where the $c_k$'s are determined with a recurrence as before, but now any $c_K \in \mathbb{R}$ will satisfy the equation, adding a free constant.

Now, the fourth solution, which arises from a double root, is given by the addition of log terms; thus

$$y_4(x) = y_3(x)\ln(x - x_0) + \sum_{k=0}^{\infty} d_k (x - x_0)^{\lambda_4 + k},$$

where the $d_k$'s are determined as before.

**Case $\boldsymbol{\lambda_3 = \lambda_4, \lambda_i - \lambda_3 \notin \mathbb{Z}}$, $\boldsymbol{i = 1, 2}$:** This case is a mixture of the previous two cases. We can get the second and third solutions as

$$y_2(x) = \sum_{k=0}^{\infty} b_k (x - x_0)^{\lambda_2 + k},$$
$$y_3(x) = \sum_{k=0}^{\infty} c_k (x - x_0)^{\lambda_3 + k},$$

where $b_k$ and $c_k$ are given by (C.3) and (C.4), respectively. The fourth solution arises from the double root,

$$y_4(x) = y_3(x)\ln(x - x_0) + \sum_{k=0}^{\infty} d_k(x - x_0)^{\lambda_4 + k},$$

where the $d_k$'s are determined as before.

**Case $\boldsymbol{\lambda_1 - \lambda_2 \in \mathbb{Z}}$, $\boldsymbol{\lambda_2 - \lambda_3}$, $\boldsymbol{\lambda_3 - \lambda_4 \notin \mathbb{Z}}$:** As earlier, the second solution can be obtained by letting $\lambda_2 = \lambda_1 + K$, where $K > 0$ is an integer, and we note that

$$F(\lambda_1 + K)a_K = -\sum_{j=0}^{K-1} Q(\lambda_1, j)a_j.$$

- If the right-hand side is not zero then we may set

$$y_2(x) = y_1(x)\ln(x - x_0) + \sum_{k=0}^{\infty} b_k(x - x_0)^{\lambda_2 + k},$$

  where the $b_k$'s are set as before.

- If the right-hand side is zero, then we can use

$$y_2(x) = \sum_{k=0}^{\infty} b_k(x - x_0)^{\lambda_2 + k},$$

  as a second independent solution, but now any $b_K \in \mathbb{R}$ will satisfy the equation.

We obtain the third and fourth solutions as

$$y_3(x) = \sum_{k=0}^{\infty} c_k(x - x_0)^{\lambda_3 + k},$$
$$y_4(x) = \sum_{k=0}^{\infty} d_k(x - x_0)^{\lambda_4 + k},$$

where $c_k$ and $d_k$ are given by (C.4) and (C.5), respectively.

# Bibliography


[1] H. Abels and M. Wilke. Convergence to equilibrium for the Cahn–Hilliard equation with a logarithmic free energy. *Nonlinear Analysis: Theory, Methods and Applications*, 67(11):3176–3193, 2007.

[2] N. Alikakos, P. Bates, and X. Chen. Convergence of the Cahn-Hilliard equation to the Hele-Shaw model. *Archive for Rational Mechanics and Analysis*, 128(2):165–205, 1994.

[3] L. Banas, A. Novick-Cohen, and R. Nürnberg. The degenerate and non-degenerate deep quench obstacle problem: A numerical comparison. *Networks and Heterogeneous Media*, 8(1):37–64, 2013.

[4] J. Barrett and J. Blowey. Finite Element Approximation of a Degenerate Allen–Cahn/Cahn–Hilliard System. *SIAM Journal on Numerical Analysis*, 39(5):1598–1624, 2002.

[5] J. Barrett, J. Blowey, and H. Garcke. Finite Element Approximation of the Cahn–Hilliard Equation with Degenerate Mobility. *SIAM Journal on Numerical Analysis*, 37(1):286–318, 1999.

[6] E. Beretta, M. Bertsch, and R. Dal Passo. Nonnegative solutions of a fourth-order nonlinear degenerate parabolic equation. *Archive for Rational Mechanics and Analysis*, 129(2):175–200, 1995.

[7] M. Berger and L. Fraenkel. On the asymptotic solution of a nonlinear Dirichlet problem. *Journal of Mathematics and Mechanics*, 19:553–585, 1970.

[8] F. Bernis. Nonlinear parabolic equations arising in semiconductor and viscous droplet models. *Nonlinear Diffusion Equations and Their Equilibrium*, 3:77–88, 1992.

[9] F. Bernis and A. Friedman. Higher order nonlinear degenerate parabolic equations. *Journal of Differential Equations*, 83(1):179–206, 1990.

[10] F. Bernis, L. Peletier, and S. Williams. Source type solutions of a fourth order nonlinear degenerate parabolic equation. *Nonlinear Analysis: Theory, Meth. & Appl.*, 18(3):217–234, 1992.

[11] A. Bernoff and T. Witelski. Linear stability of source-type similarity solutions of the thin film equation. *Applied Mathematics Letters*, 15:599–606, 2002.

[12] A. Bertozzi. Symmetric singularity formation in lubrication-type equations for interface motion. *SIAM Journal on Applied Mathematics*, 56(3):681–714, 1996.

[13] A. Bertozzi, M. Brenner, T. Dupont, and L. Kadanoff. Singularities and similarities in interface flows. In *Trends and Perspectives in Applied Mathematics*, Applied Mathematical Sciences, pages 155–208. Springer, New York, NY, 1994.

[14] A. Bertozzi and M. Pugh. The lubrication approximation for thin viscous films: The moving contact line with a porous media cut-off of van der waals interactions. *Nonlinearity*, 7(6):1535–1564, 1994.

[15] A. Bertozzi and M. Pugh. Long-wave instabilities and saturation in thin film equations. *Communications on Pure and Applied Mathematics: A Journal Issued by the Courant Institute of Mathematical Sciences*, 6(51):625–661, 1998.

[16] S. Boatto, L. Kadanoff, and P. Olla. Traveling-wave solutions to thin-film equations. *Physical Review E*, 48(6):4423–4431, 1993.

[17] H. Brezis. Functional analysis, sobolev spaces and partial differential equations. *Springer, New York, NY*, 2011.

[18] J. Cabral, J. Higgins, N. Yerina, and S. Magonov. Topography of phase-separated critical and off-critical polymer mixtures. *Macromolecules*, 35:1941–1950, 2002.

[19] J. Cahn. On spinodal decomposition. *Acta Metallurgica*, 9(9):795–801, 1961.

[20] J. Cahn, C. Elliott, and A. Novick-Cohen. The Cahn-Hilliard equation with a concentration dependent mobility: Motion by minus the Laplacian of the mean curvature. *European Journal of Applied Mathematics*, 7(3):287–301, 1996.

[21] J. Cahn and J. Hilliard. Free energy of a nonuniform system. I. interfacial free energy. *J. Chem. Phys.*, 28(2):258, 1958.

[22] P. Constantin, T. F. Dupont, R. Goldstein, L. Kadanoff, M. Shelley, and S.-M. Zhou. Droplet breakup in a model of the Hele-Shaw cell. *Phys. Rev. E*, 47(6):4169–4181, 1993.

[23] P. Constantin, T. Elgindi, H. Nguyen, and V. Vicol. On singularity formation in a Hele-Shaw Model. *Communications in Mathematical Physics*, 363(1):139–171, 2018.

[24] R. Craster and O. Matar. Dynamics and stability of thin liquid films. *Archive for Rational Mechanics and Analysis*, 129:175–200, 1995.

[25] S. Dai and Q. Du. Motion of interfaces governed by the Cahn–Hilliard equation with highly disparate diffusion mobility. *SIAM Journal on Applied Mathematics*, 72(6):1818–1841, 2012.

[26] S. Dai and Q. Du. Coarsening mechanism for systems governed by the Cahn–Hilliard equation with Degenerate Diffusion Mobility. *Multiscale Modeling and Simulation*, 12(4):1870–1889, 2014.

[27] S. Dai and Q. Du. Computational studies of coarsening rates for the Cahn–Hilliard equation with phase-dependent diffusion mobility. *Journal of Computational Physics*, 310:85–108, 2016.

[28] S. Dai and Q. Du. Weak solutions for the Cahn–Hilliard equation with degenerate mobility. *Archive for Rational Mechanics and Analysis*, 219(3):1161–1184, 2016.

[29] R. Dal Passo, H. Garcke, and G. Grün. On a fourth-order degenerate parabolic equation: Global entropy estimates, existence, and qualitative behavior of solutions. *SIAM Journal of Mathematical Analysis*, 29:321–34, 1998.

[30] R. Dal Passo, L. Giacomelli, and A. Novick-Cohen. Existence for an Allen-Cahn/Cahn-Hilliard system with degenerate mobility. *Interfaces and Free Boundaries*, 1(2):199–226, 1999.

[31] R. Dal Passo, L. Giacomelli, and A. Shishkov. The thin film equation with nonlinear diffusion. *Communications in Partial Differential Equations*, 26:1509–1557, 2001.

[32] C. Elliott and H. Garcke. On the Cahn–Hilliard Equation with Degenerate Mobility. *SIAM Journal of Mathematical Analysis*, 27(2):404–423, 1996.

[33] C. Elliott and Z. Songmu. On the Cahn–Hilliard equation. *Archive for Rational Mechanics and Analysis*, 96:339–357, 1986.

[34] V. Galaktionov. Very singular solutions for thin film equations with absorption. *Studies in Applied Mathematics*, 1(124):39–63, 2010.

[35] H. Greenspan. On the motion of a small viscous droplet that wets a surface. *Journal of Fluid Mechanics*, 84(01):125–143, 1978.

[36] G. Grün and M. Rumpf. Nonnegativity preserving convergent schemes for the thin film equation. *Numerische Mathematik*, 87(1):113–152, 2000.

[37] D. Guedes de Figueiredo, E. Moreira dos Santos, and O. Hiroshi Miyagaki. Sobolev spaces of symmetric functions and applications. *Journal of Functional Analysis*, 261:2735–3770, 2011.

[38] C. Gugenberger, R. Spatschek, and K. Kassner. Comparison of phase-field models for surface diffusion. *Physical Review E*, 78(016703), 2008.

[39] M. Gurtin. Generalized Ginzburg-Landau and Cahn–Hilliard equations based on a microforce balance. *Physica D*, 92:178–192, 1996.

[40] P. Haley and J. Miksis. The effect of contact line on droplet spreading. *Journal of Fluid Mechanics*, 223:57–81, 1991.

[41] H. Ji and T. Witelski. Finite-time thin film rupture driven by modified evaporative loss. *Physica D: Nonlinear Phenomena*, 342:1–15, 2017.

[42] W. Jihui and S. Wang. On the degenerate Cahn-Hilliard equation: Global existence and entropy estimates of weak solutions. *Asymptotic Analysis*, 114:1–38, 2020.

[43] J. King and M. Bowen. Moving boundary problems and non-uniqueness for the thin film equation. *European Journal of Applied Mathematics*, 12(03):321–356, 2001.

[44] R. Kohn and F. Otto. Upper bound on coarsening rates. *Communications in Mathematical Physics*, 229:375–395, 2002.

[45] A. Lacey. The motion with slip of a thin viscous droplet over a solid-surface. *Studies in Applied Mathematics*, 67(3):217–230, 1982.

[46] R. Lambiotte. Differential equations II. *Lecture notes for the course Differential Equations II at the University of Oxford*, 2020.

[47] A. Lee, A. Münch, and E. Süli. Degenerate mobilities in phase field models are insufficient to capture surface diffusion. *Applied Physics Letters*, 107(8):081603, 2015.

[48] A. Lee, A. Münch, and E. Süli. Response to "Comment on 'Degenerate mobilities in phase field models are insufficient to capture surface diffusion'" [Appl. Phys. Lett. 108, 036101 (2016)]. *Applied Physics Letters*, 108(3):036102, 2016.

[49] A. Lee, A. Münch, and E. Süli. Sharp-interface limits of the Cahn–Hilliard equation with degenerate mobility. *SIAM Journal of Mathematical Analysis*, 76(2):433–456, 2016.

[50] D. Lee, J. Huh, D. Jeong, J. Shin, A. Yun, and J. Kim. Physical, mathematical, and numerical derivations of the Cahn–Hilliard equation. *Journal of Computational Material Science*, 81:216–225, 2014.

[51] M. Mahadevan and R. Bradley. Phase field model of surface electromigration in single crystal metal thin films. *Journal of Physics D*, 126:201–213, 1999.

[52] A. Miranville. Generalized Cahn–Hilliard equations based on a microforce balance. *Journal of Applied Mathematics*, 4:165–185, 2003.

[53] W. Mullins and R. Sekerka. Morphological stability of a particle growing by diffusion or heat flow. *Journal of Applied Physics*, 34:323–329, 1963.

[54] J. Murray. Mathematical Biology. I. An Introduction. *Springer, New York, NY. Interdisciplinary Applied Mathematics*, 2002.

[55] J. Murray. Mathematical Biology. II. Spatial Models and Biomedical Applications. *Springer, New York, NY. Interdisciplinary Applied Mathematics*, 2003.

[56] B. Niethammer. Existence and uniqueness of radially symmetric stationary points within the gradient theory of phase transitions. *European Journal of Applied Mathematics*, 6(01), 1995.

[57] A. Novick-Cohen and L. Segel. Nonlinear aspects of the Cahn-Hilliard equation. *Physica D: Nonlinear Phenomena*, 10(3):277–298, 1984.

[58] A. Novick-Cohen and A. Shishkov. The thin film equation with backwards second order diffusion. *Interfaces and free boundary*, 12:463–496, 2010.

[59] R. Pego. Front Migration in the Nonlinear Cahn-Hilliard Equation. *Proceedings of the Royal Society A: Mathematical and Physical Sciences*, 422(1863):261 –278, 1989.

[60] C. Pesce and A. Münch. How do degenerate mobilities determine singularity formation in Cahn-Hilliard equations? *Multiscale Modeling and Simulation*, 19:1143–1166, 2021.

[61] S. Puri and K. Binder. Surface-directed phase separation with off-critical composition: Analytical and numerical results. *Physical Review E*, 66(061602), 2002.

[62] S. Puri and H. Frisch. Surface-directed spinodal decomposition: modelling and numerical simulations. *Journal of Physics: Condensation Matter*, 9:2109–2133, 1997.

[63] A. Rätz, A. Ribalta, and A. Voigt. Surface evolution of elastically stressed films under deposition by a diffuse interface model. *Journal of Computational Physics*, 214(1):187–208, 2006.

[64] J. Robinson. Infinite-dimensional dynamical systems. *Cambridge University Press*, 2001.

[65] P. Rybka and K.-H. Hoffmann. Convergence of solutions to Cahn-Hilliard equation. *Communications in Partial Differential Equations*, 24(5-6):1055–1077, 1998.

[66] J. Simon. Compact sets in the space $L^p(0,T;B)$. *Annali di Matematica Pura ed Applicata*, 146:65–96, 1987.

[67] S. Torabi and J. Lowengrub. Simulating interfacial anisotropy in thin-film growth using an extended Cahn–Hilliard model. *Physical Review E*, 72(041603), 2012.

[68] S. Torabi, J. Lowengrub, A. Voigt, and S. Wise. A new phase-field model for strongly anisotropic systems. *Proceedings of the Royal Society A: Mathematical and Physical Sciences*, 465(2105):1337–1359, 2009.

[69] S. van Gemmert, G. Barkema, and S. Puri. Phase separation driven by surface diffusion: A monte carlo study. *Physical Review E*, 72(046131), 2005.

[70] A. Voigt. Comment on "Degenerate mobilities in phase field models are insufficient to capture surface diffusion" [Appl. Phys. Lett. 107, 081603 (2015)]. *Applied Physics Letters*, 108(3):036101, 2016.

[71] J. Wolterink, G. Barkema, and S. Puri. Spinodal decomposition via surface diffusion in polymer mixtures. *Physical Review E*, 74(1):011804, 2006.

[72] L. Zhornitskaya and A. Bertozzi. Positivity-Preserving Numerical Schemes for Lubrication-Type Equations. *SIAM Journal on Numerical Analysis*, 37(2):523–555, 2000.